ELIMINATING OXYGEN SUPPLY LIMITATIONS FOR TRANSPLANTED MICROENCAPSULATED ISLETS IN THE TREATMENT OF TYPE I DIABETES

by

Amy Suzanne Lewis

Bachelor of Science in Chemical Engineering
Northwestern University, 2002

Masters of Science in Chemical Engineering Practice
Massachusetts Institute of Technology, 2004

Submitted to the Department of Chemical Engineering
in Partial Fulfillment of the Requirements for the Degree of
Doctor of Philosophy in Chemical Engineering

at the

Massachusetts Institute of Technology

June 2008

Author……
Department of Chemical Engineering
May 19, 2008

Certified by……
Clark K. Colton
Professor of Chemical Engineering
Thesis Supervisor

Accepted by……...
William M. Deen
Professor of Chemical Engineering
Chairman, Committee for Graduate Students

ABSTRACT

Eliminating Oxygen Supply Limitations for Transplanted Microencapsulated Islets in the Treatment of Type I Diabetes

by Amy Suzanne Lewis

Submitted to the Department of Chemical Engineering
on May 19, 2008 in partial fulfillment of
the requirements for the degree of
Doctor of Philosophy in Chemical Engineering

Type I diabetes is a disease that results from a person's impaired ability to produce insulin, a protein that regulates the blood glucose concentration. Insulin is produced by β-cells in the Islets of Langerhans, which are aggregates of cells averaging about 150 μm in diameter and constituting about 1 to 2% of the pancreas volume. The efficacy of islet transplantation as a treatment for diabetes has been demonstrated in humans by the Edmonton Protocol, but obstacles remain for wide scale application. One major issue is that successful islet transplantation requires permanent use of multiple immunosuppressive agents. These agents may have serious side effects as well as a substantial financial burden. Microencapsulation is used for full or partial protection of transplanted islets from immune rejection. However, the microcapsule prevents islet revascularization and creates an additional mass transfer resistance for oxygen transport to islets. This reduced oxygen transfer can lead to a hypoxic core within the islet that results in tissue death and reduced function. We have studied two approaches to enhance microencapsulated islet survival and function by reducing oxygen transport limitations. The first method involves incorporating a perfluorocarbon emulsion into alginate microcapsules to enhance oxygen permeability in order to protect islets from hypoxia. The second method involves dispersing the islets into single cells and allowing them to reaggregate into cell clusters smaller than the original islet. The smaller aggregates are less prone to the development of a necrotic core and can function normally because of adequate oxygen supply and the presence of cell to cell contacts.

A theoretical reaction-diffusion model was developed to predict the oxygen partial pressure profile, extent of cell death, and rate of insulin secretion in alginate microcapsules or planar diffusion chambers containing an islet, islet cell aggregates, and dispersed single cells exposed to specified external P_{O2} values, with or without PFC. Results show that hypoxic conditions are reduced, therefore enhancing islet viability and substantially maintaining insulin secretion when PFC emulsion is incorporated in the encapsulation material or when smaller islet cell aggregates are used.

Methods were developed to assess encapsulated tissue through nuclei counting, DNA quantification, and oxygen consumption rate measurements. Experiments with islets and islet cell aggregates were performed to assess whether the benefits predicted by the theoretical model

can be observed experimentally. After two days of culture in a limited oxygen environment comparisons were made between islets and islet cell aggregates within normal alginate and islets within PFC alginate microcapsules in their viability by measurement of oxygen consumption rate, function by measuring glucose stimulated insulin secretion (only tissue in normal alginate capsules), and total tissue content by measuring DNA or performing nuclei counts. The PFC emulsion formulation that was used was toxic to islets and we were not conclusively able to demonstrate that it enhances survival in low oxygen. Islet cell aggregates survive and function better in low oxygen environments during *in vitro* experiments than intact islets. Encapsulated rat islet cell aggregates are also found to more effectively cure diabetes in mice than encapsulated islets.

Thesis Supervisor: Clark K. Colton
Title: Professor of Chemical Engineering

Acknowledgements

The completion of my thesis would not have been possible without help from so many different people. First of all I would like thank my advisor Clark Colton for all of us help and guidance throughout the years. I would also like to thank the members of my thesis committee - William Deen for his helpful insights with the modeling work, Gordon Weir for all of his help and assistance in the field of islet microencapsulation, and Klearchos Papas and Robert Fisher for providing insight and assistance in getting my thesis work off the ground.

From the Department of Chemical Engineering of MIT I would like to thank all the members of the Colton Lab throughout the years especially Michelle Miller, Anna Pisania, Daryl Powers, and Mike Rappel for being great friends and making the lab a fun place to work along with giving useful research insights. I would also like to thank the two undergraduate students that assisted me with my research – Laura D'Aoust and Kenneth Yan.

Over the course of completing my PhD I actually had two labs and I would like to thank everyone in the Islet Transplantation and Cell Biology Lab for letting me work in their lab also. I would most importantly like to thank Esther O'Sullivan who I worked so closely with for all of the experiments that were performed with aggregates. She was a great collaborator and a great friend. I would also like to thank Abdulkadir Omer for helping me with transplantation experiments and passing on his knowledge of islet microencapsulation. I would like to thank Susan Bonner-Weir for all of her assistance with the histology sections. Jennifer Hollister-Lock for being patient and teaching an engineer how to isolate islets and with all of her assistance in the isolations I needed for completion of this work. I would also like to acknowledge the rest of the islet isolation core – Vaja Tchipasvilli and Vassileios Kostaras for their assistance in isolating islets.

Finally I would like to thank all of my friends and family that have supported me throughout the years. My parents have always supported me no matter what path I have chosen and I have always appreciated their love and support. My sisters Cindy and Catherine have also always supported me even though they might have had no idea about what it was that I was working on. Ginger Chao and Mark Styczynski were also great friends and room mates throughout my years at MIT, without them I would not have survived my first year at MIT. Finally I would like to acknowledge my fiancé Jared Johnson he has been there for me during the up and downs over the past six years at MIT and I love him dearly.

TABLE OF CONTENTS

LIST OF FIGURES

LIST OF TABLES

Chapter 1 Introduction

1.1 BACKGROUND

1.1.1 Type 1 Diabetes

Type 1 diabetes is a disease that results from a person's impaired ability to produce insulin, a protein that regulates blood glucose concentration. Insulin is produced by β-cells in the Islets of Langerhans, which are aggregates of cells averaging about 150 μm in diameter and constituting about 1 to 2% of the pancreas volume. Type 1 diabetes is caused by autoimmune attack and destruction of the β-cells, which compose about 60% of the islet by volume. Diabetes has a serious impact on the health care system. In 2005, there were an estimated 14.6 million people diagnosed (and about 50% more undiagnosed) with diabetes in the U.S. This number is expected to double by 2050 [1, 2]. Type 1 (insulin-dependent) diabetes patients represent 5-10% of the total number of diabetes cases [1]. The increased blood sugar level puts diabetic patients at a greater risk for various complications, including blindness, gangrene, stroke, ketoacidosis, and heart, kidney, nervous system, and periodontal disease. Diabetes was the sixth leading cause of death in the United States in 2002, and the risk of death among people with diabetes is about 2 times greater than that of people without diabetes[1]. The cost associated with diabetes in the U.S. was $174 billion dollars in 2007 and represented 1 out of every 5 dollars spent on health care [2].

Conventional treatment for type 1 diabetes involves one or two daily insulin injections and daily monitoring of blood glucose but without adjustments of insulin dosage. Insulin injections under these conditions are not optimal because blood glucose levels fluctuate incorrectly when there is no feedback control like that provided by β-cells in healthy patients [3]. In a recent clinical trial, intensive insulin therapy (three or more times daily by injection or

external pump, adjusted according to results of self-monitoring of glucose at least four times per day) improved blood glucose control and substantially decreased occurrences of long term complications in comparison to conventional therapy [4]. The chief adverse event associated with intensive therapy was a two- to three-fold increase in severe hypoglycemia, a major concern because hypoglycemic unawareness can be life threatening and tends to occur when hypoglycemic episodes are more frequent.

Alternative methods of insulin delivery have been investigated to deliver insulin in a pain free manner, thereby increasing patient compliance and more effectively regulate blood glucose levels. Externally worn pumps that continuously deliver insulin subcutaneously are safe and effective with fewer hypoglycemic episodes and lower levels of glycosylated hemoglobin [5]. Methods are being developed to deliver insulin transdermally and through the pulmonary system and to measure blood glucose without the use of a needle, for example by permeabilizing the skin with ultrasound, extracting interstitial fluid, and correlating the glucose concentration to blood glucose concentration [6-8]. Implantable glucose sensors would be the best way to measure blood glucose, in real-time, but they have been limited by a need for frequent recalibration as a result of changes in transport properties of the tissue surrounding the sensor from fibrotic overgrowth [9-13]. Methods of administering insulin that do not provide feedback control do not usually produce normal glucose control, which make patients vulnerable to complications.

More advanced insulin delivery systems under study would provide feedback-controlled insulin delivery without patient intervention. One example is an implantable glucose sensor placed in a feedback control loop that controls the delivery of insulin from a reservoir with a pump [12, 13]. Another example is implantation of a polymer that changes permeability in

response to glucose. For example, glucose oxidase is immobilized on pH-responsive polyacrylic acid, which is grafted onto a porous support. When glucose concentration increases, its oxidation is accompanied by a decrease in pH that causes acrylic acid to assume a more compact conformation, thereby opening pores for insulin release [14].

1.1.2 Current State of Human Islet Transplantation

Islet transplantation gives promise of normoglycemia. The islets provide physiological feedback controlled insulin release and are capable of continuously producing insulin. In humans, this procedure involves implanting islets isolated from a cadaver donor into the recipient's liver via the portal vein. Islet transplantation would allow patients to be free of daily insulin injections and have tighter blood glucose control, thus eliminating many of the secondary complications of diabetes [3]. After several decades of frustration, a dramatic improvement in efficacy was reported in July of 2000 by a group from the University of Alberta, Edmonton that renewed interest throughout the medical community in islet transplantation research [15]. Seven consecutive patients with type 1 diabetes were freed from the need for exogenous insulin with excellent metabolic control for 1 year or more. There were three new features in the work: (1) Islet isolation from a human pancreas was followed by immediate (no more than 4 hr) implantation in the recipient to prevent islet damage that may occur during culture. (2) Patients received islets from two or more donors (until normoglycemia was achieved). (3) Patients were treated with a glucocorticoid-free immunosuppressive therapy, consisting of tacrolimus, sirolimus, and daclizumab, that protected the islets from autoimmune and alloimmune reactivity [15]. In further clinical studies with the Edmonton protocol, 87% of patients are insulin free one year after implantation [16]. Long term function of clinical islet transplantation has yet to be

achieved, after a five year follow-up of patients treated by the Edmonton protocol only 10% are insulin independent after receiving islets from up to three donor pancreases [17].

The efficacy of islet cell transplantations has been demonstrated in humans, but obstacles remain for wide scale application [18, 19]. This first obstacle is that there is a lack of available tissue for transplantation procedures. In the U.S. there are 1 million people with type 1 diabetes, and about 30,000 new cases per year. By contrast, there are currently about 5,000 cadaver pancreases available. Even if all other problems were eliminated, islet transplantation would be limited to a small fraction of those who can benefit from it. Expansion to a much larger patient population requires identification and development of new sources of islets or glucose responsive insulin-secreting tissue. The second issue is that successful islet transplantation requires permanent use of multiple immunosuppressive agents that may have serious side effects as well as a substantial financial burden. Protecting the islets from immune attack with a semipermeable membrane barrier is the basic notion behind a wide variety of immunoisolation device constructs that have been investigated.

1.1.3 Immune Destruction of Islets

Type 1 diabetes is an autoimmune disease, and islet transplantation will trigger an immune attack by the same mechanisms that caused the patient to become diabetic in the first place. Additionally, if the transplant is an allograft or a xenograft, the immune system will recognize it as non-self and mount an additional response. The reaction to the xenograft is generally more intense because the immune system will also recognize the transplant as being from another species [20]. The final component that can elicit an immune response is an immunobarrier material surrounding the islets. Successful islet transplantations require that the

immune system be blocked from attacking the transplant or responding deleteriously to the implanted material. The immune system can be blocked with drugs administered systemically or by encapsulation of the islets in a semipermeable material that will allow for glucose, insulin, and oxygen transport while blocking the transport of large immune reactive molecules. Other approaches, such as inducing immune tolerance, immunomodulation, and local immunosuppression are also under study.

1.1.4 Encapsulation Device Types

Various approaches have been investigated to impose a semipermeable barrier to immune system components between islets and the blood stream or surrounding tissue. These approaches can be usefully categorized into three approaches [21, 22].

(1) Intravascular devices are shunts between an artery and a vein. Blood flows through the lumen of a cylindrical membrane with islets surrounding the outer surface. This type of device is beneficial because islets come into close proximity with arterial blood, which has high oxygen content, thereby somewhat ameliorating the problem of oxygen supply limitations. This approach is the most successful to date in terms of long-term xenotransplantation (porcine islets transplanted into the dog), which have been successful for more than a year [22]. Human clinical trials were in the planning stages but were stopped by the FDA several years ago because a mechanical failure of the cannula leading from the device, and the studies never went forward for economic and safety reasons.

(2) Extravascular devices contain many islets in a device that is implanted into a cavity of the body. This type of device may be limited by the amount of oxygen that can be provided

to islets if diffusion distances for oxygen are large, thus preventing adequate oxygen transfer to maintain islets without vascularization of the device. This problem can be enhanced by the fibrotic tissue that can grow around implanted devices [23], but developments in improved interfacing materials can improve vascularization.

(3) Islet microcapsules are spheres of a biomaterial that contain usually one or sometimes more islets and have a diameter as low as 200-300 μm in the case of a conformal coating to as much as 1 to 2 mm (sometimes called macrobeads) with many islets encapsulated. The most common material used is alginate. A large number of these small capsules containing islets are usually implanted into the peritoneal cavity. This approach has been found effective in rodents even when there is only a minimal acute insulin secretory response to glucose stimulation [24].

Among the characteristics of the ideal microcapsule for islets are the following: (1) non cytotoxic to encapsulated cells, (2) biocompatible in transplantation location, (3) adequate permeability for oxygen, glucose and insulin, (4) impermeable to antibodies and complement proteins, (5) creates a physical barrier to prevent contact of transplanted tissue an immune cells (6) chemically and mechanically stable, (7) high purity materials, and (8) minimal shrinking/swelling after transplantation [25, 26]. Various materials have been studied as potential encapsulating materials. The most common is alginate, derived from seaweed and considered safe for human use, which is used alone or in combination with other materials such as poly-L-lysine, chitosan, cellulose sulfate, aminopropyl silicate, or polytheylene glycol [27-29].

Alginate and Poly L-Lysine

Alginate and poly L-lysine (PLL) microcapsules were first shown to provide immunoprotection in 1980 [30], and over twenty years later it is still the most widely used system. Alginate has remained the most common material used for microencapsulation because the encapsulation procedure is simple, and purified alginate is biocompatibile. Alginate is a polysaccharide made up of blocks of mannuronic (M) and guluronic (G) acid. Alginate beads are formed by dropwise addition of alginate into a solution of a bivalent cation, typically calcium chloride or barium chloride. The cation crosslinks the monomers of alginate and rapidly forms a gel bead. Beads crosslinked with barium ions have a greater mechanical stability than those crosslinked with calcium ions [31].

Alginate is a biocompatible material, but virtually all materials induce some foreign body response by the immune system. The foreign body response inhibits transport to the islets and causes an increase in central islet necrosis because the tissue attached to the outside of the capsule is consuming oxygen and creating a diffusion barrier [32]. Purification of alginate and smoother capsules greatly improve its biocompatibility, and, as a result, increases the survival of encapsulated islets [32-35]. In studies of purified alginate PLL microcapsules *in vivo*, the responses against intermediate-G alginate capsules are always less severe than against high-G alginate capsules [36]. Ninety percent of empty capsules, with intermediate-G content, implanted in the peritoneal cavity remain free of fibrotic overgrowth after 24 months, as compared to unpurified alginate capsules which are completely overgrown within a month [37].

Alginate Alone

Alginate has been used alone to encapsulate islets in order to maximize biocompatibility by eliminating the use of PLL or other polycations that produce a surface immunobarrier and

cause immune reactions. Highly purified barium alginate microcapsules protected islets against allorejection and autoimmunity in mice for up to 400 days [38]. Cytokines could still permeate the gel, but islet survival was not impaired because of the lack of a cellular response to the implant [38]. Barium alginate provided immune protection for porcine neonatal pancreatic cell clusters in streptozotocin induced diabetic mice against xenorejection for over 20 weeks [39, 40]. The neonatal pancreatic cell clusters were able to survive and mature within the microcapsule.

1.1.5 Mass Transfer Limitations

Islets contained within the pancreas are very well vascularized with blood at arterial P_{O2}. When islets are removed from the pancreas and implanted elsewhere, they loose their blood supply and must rely on diffusion for nutrient delivery and oxygen transport. In the case of naked islet transplantations, over time the islets are revascularized and regain their blood supply. Even then, transplanted islets may be exposed to a lower P_{O2} than in the pancreas (5 mmHg compared to 40 mmHg) [41]. Islets contained within devices never become revascularized and must rely on diffusion through the device for nutrient supply, insulin removal, and waste removal. Fibrotic tissue formation around an implant increases the diffusion distance of nutrients to islets and consumes nutrients, which worsens the mass transfer problem and decreases the survival of transplanted islets [42]. Hypoxic conditions can have deleterious effects on islet function and viability.

Hypoxic conditions *in vitro* allow for normal basal insulin secretion rates, but lower insulin secretion rates in response to glucose stimulation [43-46]. Viability of encapsulated islets *in vitro* is reduced as a result of necrosis associated with depletion of ATP and to some extent apoptosis caused by hypoxia [19, 47]. Hypoxia is associated with increased expression of

inducible iNOS (inducible nitric oxide synthase) mRNA in the islets, which likely leads to increased secretion of NO (nitric oxide) by the islets themselves and to increased expression of monocyte chemoattractant protein mRNA, suggesting that islets contribute to their own graft failure by attracting cytokine-producing macrophages [47].

Successful outcomes for islet transplantations will require prolonged survival of islets after implantation. If the islets can be adequately protected from the immune system, they will still have to be properly nourished in devices that have been engineered to provide the necessary amount of oxygen and nutrients. In order for immunobarrier devices to be successful, the transplanted cells must remain viable and functional post-transplantation.

1.1.6 Methods to enhance oxygen mass transfer

Methods have been studied to enhance mass transfer to immunoisolated tissue, most specifically transport of oxygen, by using vascularizing membranes, *in situ* oxygen generation, thinner microcapsules, smaller islet cell aggregates, and enhancing the oxygen carrying capacity of immunoisolating materials. Mass transfer of oxygen to an immunoisolated device can be enhanced if the vasculature is brought in very close contact with the device. The vasculature can not come into direct contact with the tissue itself, which would be a breach of the immunobarrier but vessels in close proximity to the device are beneficial. The Theracyte™ (Baxter Healthcare) planar diffusion chamber has two membranes: (1) an exterior vascularizing membrane that has an optimal pore size (5μm) so that cells can penetrate the layer and vascularization is induced, and (2) an immunoisolating membrane, pore size 0.45μm, both made from PTFE [48]. The Theracyte™ device can be preimplanted in order to induce vascularization of the device prior to transplantation which aids in islet survival post-transplantation [49].

An alternative approach to overcome oxygen limitations is to supply implanted tissue with oxygen generated *in situ* adjacent to or within the immunobarrier device [50, 51]. One method for *in situ* oxygen generation can occur by the electrolytic decomposition of water in an electrolyzer [51]. The electrolyzer is in the form of a thin, multilayer sheet, within which electrolysis reactions take place on the anode and the cathode to form oxygen and hydrogen respectively [51]. On one side of the device oxygen is generated and on the other side, the exterior of the device is exposed to either culture medium for *in vitro* studies or the host tissue for *in vivo* conditions. *In vitro* studies with βTC3 cells in the electrolytic *in situ* oxygen generation device show that the thickness of viable tissue increases with oxygen generation [51]. Another *in situ* oxygen generation system consists of photo-synthetic algae co-encapsulated with islets [50]. The algae require a light source in order to produce oxygen. Under anoxic conditions islets secreted insulin normally only when there was a light source to induce oxygen generation by the algae demonstrating that the photosynthetic algae can produce oxygen to support islet function [50].

Oxygen transport to encapsulated islets can be enhanced by reducing the diffusion distance through the use of smaller capsules or thinner membranes. There are drawbacks to reducing the diffusion distance because free radicals that are released from immune system effector cells may not become inactivated prior to reaching the encapsulated tissue and the amount of shed antigens from the encapsulated tissue can be increased, thereby enhancing the recipient's immune response to the transplant. Alginate capsules made using an electronic droplet generator as opposed to an air-driven droplet generator can be made to be <500 μm instead of ~800 μm. There are also techniques in which only a thin coherent membrane is used to coat the islets. Examples are the use of an emulsion procedure to form calcium alginate PLO

(poly L-ornithine) microcapsules [52] or by centrifuging an islet alginate cell suspension in a discontinuous gradient that contains a barium chloride layer [53].

Another way to enhance oxygen transport is that instead of using thin capsules is to use smaller islet cell aggregates. Aggregates that are smaller in size will have a shorter internal diffusion distance and thus the tissue on average should experience higher oxygen levels than an intact islet. Transplanted islet cell aggregates (50-150 μm) can reverse hyperglycemia as effectively as islets [54]. Normal insulin secretion was shown to be maintained at lower oxygen levels for perfused unencapsulated aggregates with a diameter of 37 μm (above bulk perfuasate P_{O2} of 20 mmHg) compared to intact islets (above bulk perfusate P_{O2} 60 mmHg) [55]. Also recent studies with rat and human islets have shown that small islets survive better than large islets in transplantation [56, 57].

A final approach that can be employed to enhance oxygen delivery to encapsulated tissue is to enhance the oxygen carrying capacity of the material and thus increase the rate at which oxygen can be delivered to the tissue. Components that can be used for this purpose are organic compounds with high oxygen solubility such as perfluorocarbons or silicone or soybean oils. Perfluorocarbon emulsions have been developed as blood substitutes and could be incorporated into the encapsulation material to increase its oxygen permeability. Perfluorocarbons and silicone oils have been used to enhance oxygen transfer in bioreactors [58, 59]. There are reports in the literature that including a perfluorocarbon emulsion in islet culture medium enhances islet function [60]. Perfluorocarbons have also been used in the storage of the pancreas prior to islet isolation to increase islet yield and storage time [61]. Culture of islets at the interface of a perfluorocarbon and cell culture media (two layer method) has been studied and was not shown to be beneficial in improving islet survival [62]. There are two potential

reasons for the lack of improvement (1) the culture system probably did not have any oxygen limitations for the islets cultured without PFC and (2) the two layer method is beneficial for short periods of time when the PFC can act as a source of oxygen, but as it is not exposed to the air directly it does not have an effect after its oxygen store has been depleted. Inclusion of hemoglobin in alginate microcapsules increases the length of islet survival after transplantation [63], but this enhancement likely results from trapping of nitric oxide by hemoglobin.

1.2 OBJECTIVES

The central hypothesis of this thesis is that a higher viability and better function of transplanted microencapsulated islets will be maintained when the local dissolved oxygen level is increased. I have studied two approaches to enhance microencapsulated islet survival and function by reducing oxygen transport limitations. The first method incorporates a perfluorocarbon (PFC) emulsion into alginate microcapsules to enhance oxygen permeability. The second method involves dispersing islets into single cells and allowing them to reaggregate into smaller cell clusters, which are then encapsulated instead of whole islets. In order to evaluate the two oxygen enhancement strategies the following tasks needed to be accomplished and are described in the subsequent chapters.

1.3 OVERVIEW

Chapter 2: Quantitative Assessment of Encapsulated Islets.

This chapter describes the quantitative methods that were adapted and developed for encapsulated tissue quality and quantity assessment similar to those used in the lab for

unencapsulated islet tissue. Tissue quality is assessed by oxygen consumption rate (OCR) measurements. Tissue quantity is determined by measuring DNA content or counting nuclei. Capsule quantity is measured by measuring alginate or PFC emulsion content.

Chapter 3: Theoretical Analysis of Methods to Enhance Oxygen Transport to Encapsulated Tissue

This chapter describes the calculations that were performed to predict oxygen profiles, fractional viability and fraction of normal insulin secretion for single cells, smaller aggregates, and islets. The three different types of tissue were analyzed in both microcapsules and planar diffusion chambers with and without a PFC emulsion in the alginate phase. These calculations assess the oxygen diffusion limitations for islets in immunoisolation devices and evaluate the benefits of the two strategies to enhance oxygen transport: smaller islet cell aggregates and a PFC emulsion.

Chapter 4: Encapsulated islet cell aggregates are superior to intact islets in terms of in vitro survival and function in low oxygen and ability to reverse diabetes in rodents

This chapter will discuss the experimental work that was done in collaboration with Esther O'Sullivan from Joslin Diabetes Center at Harvard Medical School with encapsulated aggregates. Theoretical predictions of encapsulated aggregate and islet survival and function in culture were calculated to determine oxygen levels for experiments. *In vitro* culture experiments were carried out for 2 days in 0.5%, 2% or 20% oxygen. OCR recovery, nuclei recovery, insulin to DNA ratios, and glucose stimulated insulin secretion were measured before and after culture. Two different types of transplantation experiments were also performed: (1) syngeneic transplants with non-diabetic recipients to assess tissue survival *in vivo* without the stresses of

immune reactions or diabetes and (2) xenogeneic transplants with diabetic recipients to assess effectiveness of encapsulated aggregates to treat diabetes.

Chapter 5: Evaluation of a perfluorocarbon emulsion within alginate capsules

This chapter will discuss the work that was done with PFC containing alginate capsules. Theoretical predictions of encapsulated islet survival and function in culture were calculated for microcapsules with and without PFC to determine oxygen levels for experiments. OCR measurements were performed after two days of culture in low oxygen (0.5% or 1%) for islet capsules with and without PFC. Histological sections were prepared to observe potential toxicity of the PFC emulsion and its components to islets. Empty capsule transplantation experiments were performed to assess the biocompatibility of the PFC containing alginate microcapsules.

Chapter 2 Quantitative Assessment of Encapsulated Islets in Alginate

2.1 INTRODUCTION

Microcapsules can be used to transplant islets to treat type 1 diabetes without the use of immunosuppressive drugs. Microcapsules are the most extensively studied encapsulation system and are the system that is under study in our lab. Microcapsules are hydrogels, most commonly made of alginate, that contain one to two islets. The tissue within a microcapsule relies on diffusion of nutrients through the hydrogel to the tissue and diffusion of waste products and secreted proteins away from the tissue. The cells are protected from the immune system because the hydrogel keeps immune system effector cells, such as T cells and macrophages, from coming in contact with the transplanted tissue along with preventing or minimizing access of some large immune molecules such as antibodies and complement components.

The most commonly used methods to characterize islet preparations have been reviewed previously [64, 65]. Most of the commonly used techniques to characterize islet preparations are found to be flawed because they are operator dependent, rely on the microscopic analysis in two dimensions of an irregularly shaped three dimensional spheroid, and tend to overestimate islet number and viability. Islet numbers are typically assessed by counting islet equivalents (IE), the volume of tissue equal to one 150 μm diameter sphere, in which tissue diameters are estimated using a microscope; only islet tissue that is stained with dithizone is counted. Dithizone is a zinc binding dye that specifically stains islet β cells. Islet equivalent counts typically overestimate the amount of tissue in an islet preparation by a factor of two [65]. Islet viability is typically determined by membrane integrity measurements using live/dead stains containing two fluorescent dyes. One commonly used dye is FDA (fluorescein diacetate) which stains live cells.

The second, propidium iodide (PI) will only stain cells with permeabilized membranes (a sign of cell death) and thus the fraction of cells stained with PI represent the dead cells in the tissue sample. The relative fraction of dead cells is estimated visually and no systematic counting procedure is typically performed. Thus this method of assessing cell viability is rather qualitative and very operator dependent.

Improved methods for accurately determining the total number of cells in an islet preparation and by assessing tissue viability have been developed in our lab for use with unencapsulated islets [64, 65]. The total number of cells in an islet preparation can be accurately determined by nuclei counting or DNA measurements [64, 65]. The viability of islet tissue can be assessed by the mitochondrial function assay for oxygen consumption rate (OCR) measurements in a stirred chamber [66]. It is preferred to perform mitochondrial function assays as opposed to membrane integrity assays as mitochondrial function is disrupted earlier than loss of membrane integrity during the cell death process [65].

Assessment of encapsulated tissue quantity and quality are commonly performed using similar methods as those used for free islets. Membrane integrity measurements are commonly performed to assess encapsulated cell and islet viability [47, 67, 68], but as these methods have limited value for unencapsulated islets they are also of limited value for encapsulated tissue. A two dimensional representation of an even more complex three dimensional system is being used to estimate tissue viability with FDA and PI. OCR measurements have been performed on encapsulated cells, but have been done so using a perfusion system which is complex to operate and time consuming to use [69].

Due to the complicated nature of assessing encapsulated islets much of the literature in the field of islet microencapsulation has focused on the results of transplantation studies. For the

purpose of my thesis I wanted to be able to carry out meaningful *in vitro* experiments and thus desired to adapt the nuclei counting, DNA measurements, and oxygen consumption rate measurements for use with encapsulated cells and islets. In order to improve oxygen transport to encapsulated tissue in some experiments a perfluorocarbon (PFC) emulsion was incorporated into the capsule. The PFC emulsion further complicated tissue assessment as the emulsion made the capsule opaque such that the tissue inside could not be visualized within the microcapsules using a standard microscope and the emulsion particles effected and interfered with certain measurements. In this paper the methods developed for quantitative assessment of encapsulated cells and islets will be described in detail and data verifying that the techniques are accurate will be presented.

2.2 METHODS

2.2.1 Islets and Cells

Rat islets were isolated from male Sprague-Dawley rats weighing 200-250 g using standard techniques [70]. Islets were cultured in tissue culture flasks at a density of up to 30 islets/cm^2 and a medium depth of 1.3 mm in RPMI 1640 supplemented with 10% fetal bovine serum (FBS), penicillin 100 units/ml and 100 μg/ml streptomycin (Mediatech, Herndon, VA). Rat insulinoma INS-1 cells were cultured in tissue culture flasks in cell medium further supplemented with 2 mM L-glutamine, 1mM sodium pyruvate (Mediatech), and 50 μM 2-mercaptoethanol (Sigma-Aldrich, St. Louis, MO). INS-1 cells were detached from flasks by incubation with 0.05% (w/v) trypsin in 0.52 mM EDTA (Mediatech) for 3 min at 37^{o}C.

2.2.2 PFC Emulsion Preparation

A PFC emulsion made from perfluorodecalin (Fluoromed, Round Rock, TX) and 20% (w/v) Intralipid® (Baxter, Deerfield, IL) (a soybean oil emulsion composed of 20% (w/v) soybean oil, 1.2% (w/v) egg yolk phospholipids, 2.3% (w/v) glycerin with balance water) was prepared as previously described [71]. A 40-ml volume of Intralipid was added to the inlet reservoir of an M110Y Microfluidizer (Microfluidics, Newton, MA) and recirculated for 2 min at an operating pressure of 14,500 psi through the interaction chamber and cooling coil and back to the reservoir. During recirculation, 11.25 ml of perfluorodecalin was added dropwise over 3 min to the reservoir. The system sat without running for 5 min to cool, and the ice bath surrounding the coil was changed. An additional 11.25 ml perfluorodecalin was added dropwise to the reservoir over 3 min with recirculation, followed by additional recirculation for 5 min. The final PFC content of the emulsion was 70% (w/v), equivalent to 36% (v/v).

2.2.3 Microencapsulation

Microcapsules were produced using highly purified alginate (FMC Polymer, Norway). For normal alginate capsules, 2% (w/v) LVG alginate was used with INS-1 cells and 1.5% (w/v) SLG100 alginate with islets both in 0.9% (w/v) NaCl. For PFC alginate, LVG alginate with INS-1 cells and SLG100 alginate with islets was dissolved into a 70% (w/v) PFC emulsion to a final concentration of 1.5% and 0.5% (w/v), respectively. Cells or islets were washed with calcium-free Krebs buffer (135 mM NaCl, 4.7 mM KCl, 1.2 mM KH_2PO_4, 1.2 mM $MgSO_4$, 25 mM HEPES, pH 7.4), resuspended in alginate (or PFC alginate) to form a tissue-alginate suspension, and microencapsulated by extrusion through a needle using an electrostatic droplet generator (Pronova Polymer, Norway) or a needle using an air droplet generator into 20 mM $BaCl_2$. Microcapsules made with the electronic droplet generator ranged from 350 μm to

600 μm diameter with an average for each batch between 400 μm and 500 μm. Microcapsules made with the air droplet generator ranged from 1000 μm to 2000 μm diameter. After sequential washes in HEPES buffer (132 mM NaCl, 4.7 mM KCl, 1.2 mM $MgCl_2$, 25 mM HEPES, pH 7.4) and Krebs buffer (133 mM NaCl, 4.7 mM KCl, 1.2 mM KH_2PO_4, 1.2 mM $MgSO_4$, 25 mM HEPES, 2.5 mM $CaCl_2$, pH 7.4) the microcapsules were analyzed for OCR, nuclei or DNA, and alginate or PFC content.

2.2.4 Oxygen Consumption Rate (OCR)

Microcapsules containing islets or cells resuspended in DMEM without phenol red (to avoid interference with absorbance in subsequent measurement of alginate content) containing 4.5 g/l glucose supplemented with 0.6 g/l L-glutamine, 100 units/ml penicillin, 100 μg/ml streptomycin, and 10 mM HEPES (all from Mediatech Inc.) without serum (to avoid formation of bubbles) were placed in a 200-μl stirred titanium chamber (Micro Oxygen Uptake System FO/SYSZ-P250, Instech Laboratories, Plymouth Meeting, PA) maintained at 37°C and equipped with a fluorescence-based oxygen sensor (Ocean Optics, Dunedin, FL), as previously described [66]. The time dependent P_{O2} within the chamber was recorded, and data yielding the highest slope of P_{O2} greater than 60 mm Hg of P_{O2} versus time were fit to a straight line. The OCR was evaluated from

$$OCR=V_{ch}\alpha_s\left(\frac{\Delta P_{O2}}{\Delta t}\right) \qquad (2\text{-}1)$$

where V_{ch} is the chamber volume, and α_s is the volumetric average Bunsen solubility coefficient of oxygen in the entire sample evaluated from

$$\alpha_s = \alpha_w \phi_w + \alpha_c \phi_c \quad (2\text{-}2)$$

where α_i and ϕ_i are the volumetric average oxygen solubility and volume fraction of the ith component in the sample, w is water, and c is capsule. For PEC alginate, α_c was evaluated from

$$\alpha_c = \alpha_j \phi_j \quad (2\text{-}3)$$

where ϕ_j is the volume fraction of the jth component in the capsule, and the components are water, PFC, soybean oil and tissue (or cells). Parameters used to calculate α_s are summarized in Table 2-1 and Table 2-2 and the calculations are presented in detail in Section 6.1. For further assays, the capsule suspension was removed and stored in a tube together with three consecutive 350-µl washes of the chamber. The capsules were allowed to settle, and 1.0 ml supernatant was removed, leaving a 250-µl suspension.

2.2.5 Capsule Dissolution

Quantitative assays of nuclei counts, DNA content, alginate content, and PFC emulsion content required that the capsule first be completely dissolved by adding 800 µl of 100 mM tetrasodium EDTA (pH = 8) to the 250 µl capsule suspension. Samples were incubated at 37^{o}C for 1 hr and vortex mixed every 30 min. Because dissolution of barium alginate was much more difficult than calcium alginate, tetrasodium EDTA was used instead of sodium citrate.

2.2.6 Nuclei Counts

Nuclei were prepared from naked islets or cells as previously described [65]. For encapsulated cell and islet suspensions with dissolved alginate, a 100-µl volume of sample was added to an equal volume of lysis solution (0.1 M citric acid and 1%, 2%, or 10% (v/v) Triton X-100 (Sigma Aldrich)) and incubated for 5 min (encapsulated cells) or 15 min (encapsulated islets) with

vortex mixing three times during incubation. For encapsulated islets, the sample was resuspended in 100 µl PBS prior to adding lysis buffer to remove EDTA because it interfered with nuclei liberation. Suspensions of encapsulated tissue were sheared through a 26G x 3/8-in needle (Becton Dickinson) after incubation in the lysis buffer to liberate all nuclei, and 100 µl of 100 mM tetrasodium EDTA was then added to the encapsulated islet nuclei suspension to prevent any alginate gelling. Liberated nuclei were stained with 0.8 µM LDS 751 and 0.2 µM Sytox Orange (Invitrogen,) in D-PBS and counted using a benchtop flow cytometer (Guava Personal Cell Analyzer, Guava Technologies, Hayward, CA) as previously described [65]. Nuclear membrane permeabilization by 10% Triton X-100 led to much brighter nuclei, and flow cytometer settings were adjusted accordingly.

2.2.7 DNA Analysis

DNA concentration was quantified by fluorospectrophotometry using the CyQUANT® Cell Proliferation Assay Kit and λ DNA standard (Invitrogen), which is based on the strong fluorescence enhancement that the CyQUANT GR dye undergoes when bound to cellular nucleic acids, as previously described [65]. Pre-treating the samples with DNAse-free RNAse (Sigma) eliminated fluorescence resulting from CyQUANT dye binding to RNA. Fluorescence intensity was measured with 480 nm excitation and 520 nm emission wavelengths in a plate reader (FLUOstar/POLARstar Galaxy, BMG Labtechnologies, Inc., Durham, NC) and was linearly related to DNA concentration. The presence of EDTA and dissolved alginate had no effect, but light scattering by the PFC emulsion droplets prevented use of this assay.

2.2.8 Alginate Content

The assay for alginate content of samples was adapted from a previously-described method using dimethyl methylene blue (DMMB) (Sigma Aldrich), a cationic dye that binds to polyanions

such as alginate [72]. Samples of SLG100 alginate were diluted to between 0. 5-3 mg/l with 100mM tetrasodium EDTA. A standard curve using samples created from the alginate solution originally used for preparation of the microcapsules diluted to different concentrations of alginate was prepared with each batch of unknown samples. To individual wells of a 96 well plate in triplicate 100 µl of each sample and standard were added, and 100 µl of 120 µM aqueous dye solution. After incubation for 15 min, the ratio of the absorbance of a sample at the wavelengths of 520 nm and 650 nm was measured using a plate reader (VERSAmax tunable microplate reader, Molecular Device, Sunnyvale, CA). For LVG alginate a DMMB dye concentration of 40 µM and an alginate standard of 3 g/l were used.

2.2.9 PFC Emulsion Content

The PFC emulsion content in dissolved capsule samples was assessed by absorbance. As prepared, the original 70% (w/v) PFC emulsion was opaque, but the absorbance of a sample at any wavelength increased linearly with increasing emulsion concentration at very high dilution, as determined by preparation of a standard curve from samples diluted 200- to 1000-fold. Each unknown sample was diluted so as to fall into this range. A series of standard samples and 100 µl of each unknown sample were added to wells of a 96 well plate in triplicate. We chose to measure the absorbance at 620 nm in a plate reader (FLUOstar/POLARstar Galaxy, BMG Labtechnologies, Inc., Durham, NC).

2.2.10 Statistics

Data are expressed as average ± standard deviation. Statistical significance ($p < 0.05$) was determined by a two-way Student t-test.

2.3 RESULTS

2.3.1 OCR Measurements to Assess Encapsulated Tissue Viability

Nothing about the way that OCR measurements are typically performed with naked islets or cells needed to be changed in order to perform OCR measurements of encapsulated tissue. However several conditions needed to be met to ensure that the data that was collected accurately reflected the rate of oxygen consumption of tissue and not diffusion of oxygen through the microcapsule and are discussed further in Section 2.5. Example OCR data for encapsulated INS-1 cells is shown in Figure 2-1. Even though the slopes of the two data sets are quite different, when the OCR is calculated in units of nmol/min the oxygen consumption rate of the two samples are found to be equal. The rate of decrease of P_{O2} with time is less in the sample that contained PFC because there was initially a greater concentration of oxygen in the chamber due to the higher sample solubility.

2.3.2 Nuclei Counting of Encapsulated Islets or Cells

In our lab a method had previously been developed for nuclei counting of islets in order to accurately assess the number of cells in an islet preparation. We desired to adapt this method for the measurement of nuclei from encapsulated cells or islets in barium alginate with and without PFC. It was first necessary to assess whether the PFC emulsion particles interfered with nuclei measurements using a bench top flow cytometer (Figure 2-2). Nuclei counts were performed with INS-1 cells that had not been encapsulated but had an emulsion volume fraction in the sample of 0, 4 or 10% (v/v). The nuclei counts were the same with and without emulsion ($p>0.05$) and thus PFC emulsion particles do not interfere when counting nuclei using a bench top flow cytometer.

In order to effectively dissolve the barium alginate capsules a new protocol had to be developed that required the use of 100 mM tetrasodium EDTA at a pH of 8. Nuclei samples from unencapsulated single cells only require vortex mixing and incubation with a 1% Triton X-100 lysis buffer in order to effectively liberate all nuclei in the sample [65]. It was desired to evaluate whether the presence of EDTA interfered with the liberation of nuclei, if the concentration of Triton X-100 could be increased without loss of nuclei, and if passing the sample through a needle more efficiently liberate nuclei (Figure 2-3). In the presence of EDTA at any concentration of Triton X-100 tested there were fewer nuclei detected than the control sample in PBS when only vortex mixing was used to liberate the nuclei. When any of the samples containing EDTA were sheared through a needle after vortex mixing there was no difference in the number of nuclei counted to the sample that contained only PBS. There were no differences in the nuclei concentration counted based on what concentration of Triton X-100 was used. Samples that contain EDTA should be sheared through a needle after vortex mixing to ensure all the nuclei are liberated and any concentration of Triton X-100 up to 10% (v/v) can be used in the lysis buffer.

To verify that the capsules were effectively dissolved and all nuclei were counted measurements of pg DNA per cell were performed after dissolution of INS-1 cells in calcium alginate or barium alginate (Figure 2-4). Comparisons were made between calcium and barium alginate because calcium does not bind as strongly to alginate as barium [73]. Calcium alginate capsules are easier to dissolve and prior methods developed for capsule dissolution are for calcium alginate capsules. Additionally, we compared the DNA content of the sample to the number of nuclei in the sample to ensure all of the nuclei were counted. DNA measurements can be performed on capsules without first dissolving the capsules since sonication alone breaks up

the alginate microcapsule [40]. Measurements of pg DNA per cell were the same for INS-1 cells liberated from calcium alginate with a lysis buffer of 1% or 10% Triton X-100 and for INS-1 cells in barium alginate capsules using a lysis buffer with 10% Triton X-100. The DNA content per cell was slightly higher (although not statistically significant $p=0.36$) for INS-1 cells in barium alginate capsules using a lysis buffer with 1% Triton X-100 indicating that all nuclei in the sample were not counted. Based on these observations we chose to use a lysis buffer with 10% Triton X-100 to liberate the nuclei from barium alginate capsules that contain INS-1 cells.

In order to liberate nuclei from naked islet samples the extra step of shearing the sample through a needle is required which is not necessary for an unencapsulated single cell suspension [65]. When it came to measuring the number of nuclei in an islet sample after the tissue was removed from a capsule it was found that a few extra steps were required in order to obtain accurate nuclei measurements. Prior to incubation with the lysis buffer the sample was resuspended in PBS because EDTA interferes with nuclei liberation, the sample was incubated in lysis buffer for 15 instead of 5 minutes, and after the sample was sheared through a needle and the nuclei were liberated 100 µl of EDTA was added to the sample to keep any trace amounts of alginate from gelling. Following the methods described we have been able to demonstrate that nuclei measurements are accurate for INS-1 cells, rat islets and human islets in barium alginate capsules as there is no difference in the measured pg DNA per cell compared to each unencapsulated tissue type (Table 2-5).

DNA measurements can not be performed in the presence of PFC emulsion as the emulsion particles interfere with the fluorescence reading that is used to quantify DNA. Measurements of pg DNA per cell could not be performed to verify that nuclei counting is accurate in PFC containing microcapsules. However, lower alginate concentrations are used to

make the PFC capsules and PFC capsules were always observed to more easily dissolve than normal alginate capsules. We thus assume that since the method is accurate for normal alginate capsules and the PFC emulsion particles do not interfere with nuclei counts the nuclei counting method is accurate for islets or cells in PFC capsules.

2.3.3 Capsule Quantification

The methods that were developed to assess either alginate content of a sample in grams or PFC emulsion volume fraction were determined to effectively measure the quantity of capsules in a sample. Standard curves for either assay were generated and they were both found to linearly increase with increases in alginate (Figure 2-5) or PFC emulsion content (Figure 2-6). The volume of alginate capsules can be calculated by dividing the number of grams of alginate in a sample by the concentration of the alginate solution used to make the capsules. Depending on the type of alginate that was used, different dye and alginate concentrations were required to generate a standard curve that is a straight line. PFC emulsion particles interfere with the alginate assay and thus measurements of alginate content could only be performed on dissolved normal alginate samples. Either assay method can be used to normalize a sample by the capsule content in order to reduce errors due to differences in capsule sampling. This is critical to measurements performed with PFC containing capsules. The density of PFC is approximately twice the density of water and thus the high density of PFC containing capsules make it impossible to sample from a uniform suspension.

2.4 DISCUSSION

The quantitative measurements for the assessment of islet quantity and quality that have been developed in our lab for use with naked islets have been effectively adapted to be used with

encapsulated cells or islets. OCR measurements of small capsules can be performed to assess mitochondrial function. Nuclei measurements can be performed to assess tissue quantity in normal alginate or PFC alginate capsules. DNA measurements can be performed to quantify tissue in normal alginate capsules.

It was determined by scaling approximations that OCR measurements can effectively measure the kinetics of oxygen consumption in small capsules (~500 μm). OCR measurements are also an effective means of measuring the mitochondrial function of tissue encapsulated in PFC containing alginate capsules. However, the PFC emulsion content of the chamber must be measured and the effective solubility of the contents of the chamber must be used in the calculation of oxygen consumption rate.

Nuclei measurements can be performed on tissue in alginate or PFC alginate capsules after the capsules have been dissolved with 100 mM tetrasodium EDTA. PFC emulsion particles do not interfere with nuclei measurements quantified with the Guava PCA bench top flow cytometer. In the presence of EDTA, shearing of a cell suspension through a needle is required to effectively liberate all nuclei. Higher concentrations of Triton X-100 in the lysis buffer result in more effective liberation of nuclei from INS-1 cells in barium alginate. Nuclei measurements of encapsulated islets require removal of EDTA prior to incubation in the lysis buffer in order to effectively liberate all nuclei in a sample. The final verification that the nuclei counting method is effective is that the measurement of pg DNA per cell for naked cells or islets to cells or islets in barium alginate capsules were the same.

The use of OCR, nuclei, DNA, alginate content, and PFC emulsion content measurements for the assessment of encapsulated islet tissue quantity and quality will allow for quantitative measurements of results from *in vitro* experiments. These methods will allow for

accurate determinations of tissue quality that should allow for one to observe the effects of culture under low oxygen and evaluation of methods to enhance oxygen transport to increase tissue survival in low oxygen.

2.5 Supplementary Material: Validity of Equation (2-1) for Measuring OCR

The oxygen consumption rate N within the chamber is assumed to be related to P_{O2} changes within the medium (measured P_m) and capsule (P_{cap}) by

$$N = v_{cap}\alpha_{cap}\frac{dP_{cap}}{dt} + v_m\alpha_m\frac{dP_m}{dt} \qquad (2\text{-}4)$$

where v_{cap} and v_m are the volumes of capsules and medium, respectively, and α_{cap} and α_m are the volume averaged oxygen solubility in capsules and medium, respectively. At high P_{O2} where OCR is constant and independent of P_{O2}, N is related to volumetric consumption rate expressed in different forms by

$$N = v_{cap}V_{max,cap} = v_tV_{max,t} = n_{cell}v_{cell}V_{max,cell} \qquad (2\text{-}5)$$

where $V_{max,cap}$, $V_{max,t}$, and $V_{max,cell}$ are the maximal consumption rates expressed per unit volume of capsule, islet tissue, or cell, v_t and v_{cell} are the volume of total tissue in the chamber and of an individual cell, respectively, and n_{cell} is the number of cells in the chamber.

If P_{cap} and P_m are equal, Equation (2-4) reduces to Equation (2-1) and (2-2). These assumptions are reasonable if (1) quasi-steady conditions exist within the capsules, and (2) P_{O2} differences within the capsule and across the boundary layer around the capsule are small compared to P_m. Following the development for a similar problem [74], the species conservation equations for oxygen diffusion in a capsule with a constant, uniformly distributed oxygen sink (e.g. encapsulated cells) is

$$\alpha_{cap}\frac{\partial P_{cap}}{\partial t} = (\alpha D)_{cap}\frac{1}{r^2}\frac{\partial}{\partial r}\left(r^2\frac{\partial P_{cap}}{\partial r}\right) - V_{max,cap} \qquad (2\text{-}6)$$

By equating the transient term to the diffusion term, the time scale for relaxation of diffusion gradients within the sphere is

$$\tau_D \sim \frac{R_{cap}^2}{D_{cap}} \tag{2-7}$$

Assuming that P_m=P_{cap}, Equations (2-2), (2-4), and (2-5) may be combined to yield

$$v_{ch}\alpha_s \frac{dP_m}{dt} = v_{cap}V_{max,cap} \tag{2-8}$$

from which the time scale of the experiment may be estimated as

$$\tau_E \sim \frac{v_{ch}\alpha_s P_m(0)}{v_{cap}V_{max,cap}} \tag{2-9}$$

The transient term in Equation (2-6) may be neglected if $\tau_D \ll \tau_E$, which leads to

$$\frac{R_{cap}^2 v_{cap} V_{max,cap}}{\alpha_s D_{cap} P_m(0) v_{ch}} \ll 1 \tag{2-10}$$

This may be rewritten using Equation (2-5) as

$$\frac{R_{cap}^2 V_{max,ch}}{\alpha_s D_{cap} P_m(0)} \ll 1 \tag{2-11}$$

where $V_{max,ch} = N/v_{ch}$ is the measured OCR per unit chamber volume.

Gradients within the capsule are small enough to be neglected if the rate of oxygen consumption is small relative to its rate of diffusion. Comparing the two terms on the right hand side of Equation (2-6) leads to

$$\frac{R_{cap}^2 V_{max,cap}}{\alpha_{cap} D_{cap} P_m(0)} \ll 1 \tag{2-12}$$

which has the same form as Equation (2-11) but is slightly more restrictive.

The P_{O2} drop across the boundary layer surrounding the capsule can be obtained directly from the boundary conditions at the surface of the capsules:

$$k\alpha_m\left[P_m - P\left(R_{cap}\right)\right]4\pi R_{cap}^2 = V_{max,cap}\frac{4}{3}\pi R_{cap}^3 \tag{2-13}$$

The most conservative estimate for the mass transfer coefficient k corresponds to the case of a sphere in a stagnant medium,

$$\frac{k\left(2R\right)}{D} = 2 \tag{2-14}$$

so that

$$k = D_m / R_{cap} \tag{2-15}$$

and the resulting limit on the boundary layer P_{O2} difference $\Delta P_m = P_m - P\left(R_{cap}\right)$ becomes

$$\frac{\Delta P_m}{P_m\left(0\right)} = \frac{R_{cap}^2 V_{max,cap}}{3\alpha_m D_m P_m\left(0\right)} \ll 1 \tag{2-16}$$

which is slightly less restrictive than Equation (2-12).

For the case of an islet at the center of the capsule, Equation (2-16) remains the same, since the right side of Equation (2-13) remains the same when it is replaced by N. Additionally, the condition that diffusion through the capsule to the islet is not limiting, the P_{O2} drop within the capsule can be estimated from the boundary conditions written at the islet surface ($r = R_I$):

$$\frac{4\pi\left(\alpha D\right)_c}{\frac{1}{R_I} - \frac{1}{R_{cap}}}\left[P_{cap}\left(R_{cap}\right) - P_{cap}\left(R_I\right)\right] = V_{max,t}\left(\frac{4}{3}\pi R_I^3\right) = N \tag{2-17}$$

where α_c and D_c apply to the continuous phase of the capsule without tissue, leading to

$$\frac{P_{cap}\left(R_{cap}\right) - P_{cap}\left(R_I\right)}{P_m\left(0\right)} = \frac{R_{cap}^2 V_{max,cap}\left[\frac{R_{cap}}{R_I} - 1\right]}{3\left(\alpha D\right)_c P_m\left(0\right)} \ll 1 \tag{2-18}$$

To evaluate these dimensionless groups, solubilities were taken from Table 2-1 and Table 2-2. Effective diffusivities of heterogeneous phases were evaluated by successive application of Maxwell's equation [75].

$$\frac{(\alpha D)_{eff}}{(\alpha D)_c} = \frac{2\text{-}2\phi_d+\rho(1+2\phi_d)}{2+\phi_d+\rho(1-\phi_d)} \qquad (2\text{-}19)$$

Where $\rho=(\alpha D)_d/(\alpha D)_c$, c is the continuous phase, d is the dispersed phase, and ϕ_d is the volume fraction of the dispersed phase. Additional details of the calculation are described elsewhere (Chapter 6.1). Effective diffusivities of various combinations of materials are given in Table 2-2. Additional parameters for calculations are in Table 2-3.

Estimates of dimensionless parameters for typical conditions of interest in this study are summarized in Table 2-4. The condition that the diffusion rates are faster than reaction rates within the capsules (Equation (2-12)) and diffusion through the capsules to the islet does not limit reaction (Equation (2-18)) are more restrictive for normal alginate capsules than PFC containing capsules and are the most stringent conditions that need to be satisfied. The condition that quasi-steady state exists within the capsule (Equation (2-11)) is more restrictive for PFC containing capsules than normal alginate capsules. The condition of the external boundary layer being negligible (Equation (2-18)) is unaffected by capsule type. In general, validity criteria for validity of Equation (2-1) were satisfied with 500-μm diameter capsules but not with 2000-μm diameter capsules.

Contributions: Rat islet isolations were performed with the assistance of Jennifer Hollister-Lock, Vaja Tchipasvilli, and Vassileios Kostaras from Joslin Diabetes Center. Human islets were received from the Islet Cell Resource Consortium.

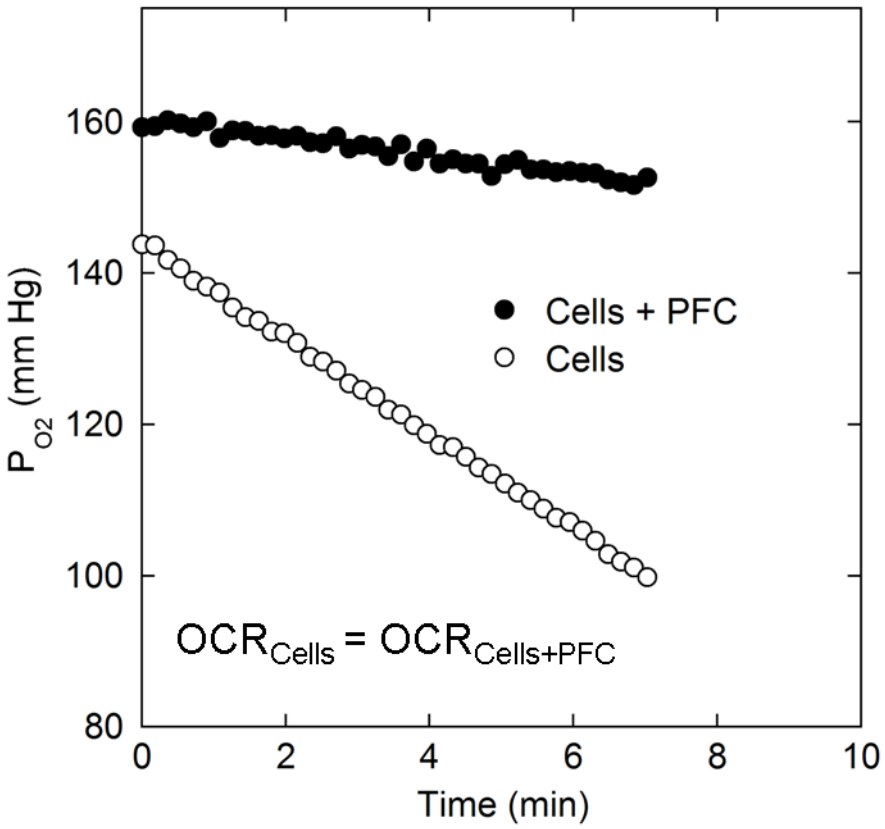

Figure 2-1: Example OCR data for INS-1 cells in normal alginate or PFC alginate microcapsules. The slopes of the data from the two samples are quite different, but after calculating OCR in units of nmol/min and thus correcting for differences in the solubility of the chamber contents of the two measurements, the OCRs of the two samples were determined to be equal.

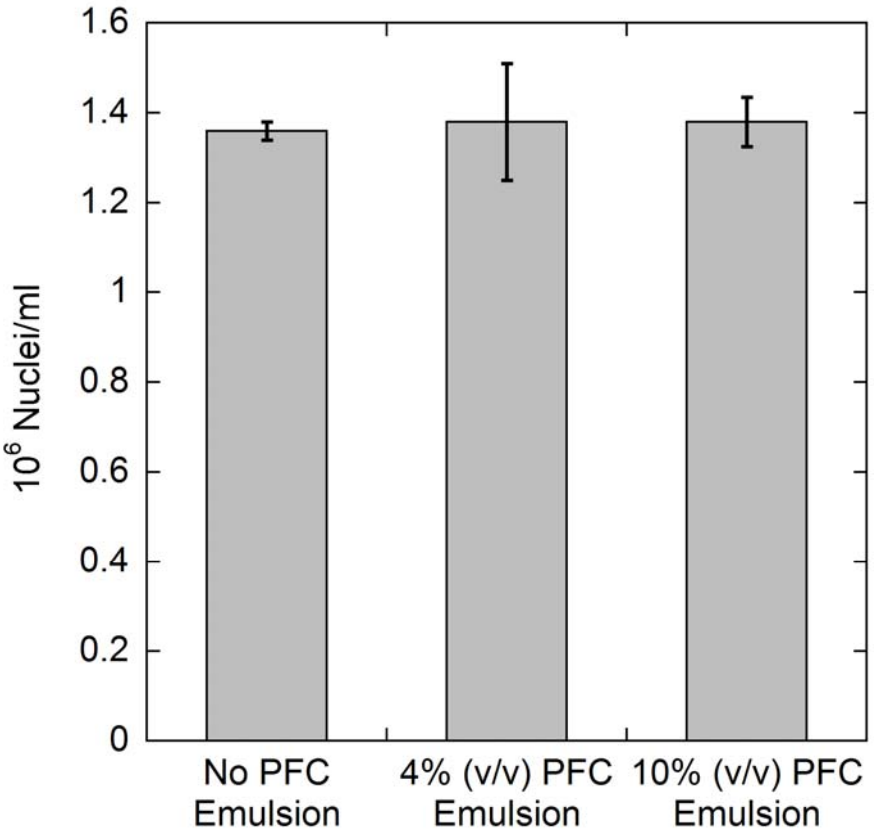

Figure 2-2: Nuclei counts of INS-1 cells performed without or with PFC emulsion. PFC emulsion volume fraction (4 or 10% (v/v)) in the sample. Each bar represents the average of triplicate samples from the same experiment. Nuclei counts were not affected by the presence of PFC emulsion particles ($p>0.05$).

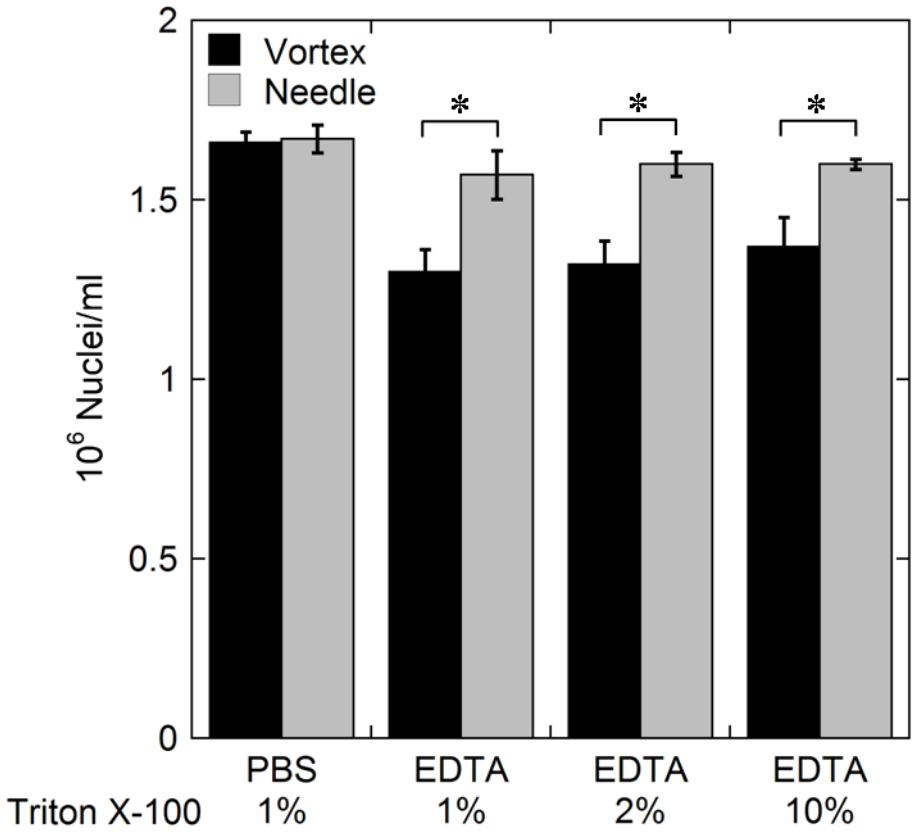

Figure 2-3: Nuclei counts of INS-1 cells in either PBS or 100mM tetrasodium EDTA (pH = 8). The lysis buffer that was used to liberate the nuclei contained 1% (v/v), 2% (v/v), or 10% (v/v) Triton X-100. Nuclei were liberated by vortex mixing only or vortex mixing followed by shearing through a needle. In the presence of EDTA shearing through a needle was required to effectively liberate nuclei ($p<0.05$ by Student t-test). There were no differences between any of the samples that were sheared through a needle ($p>0.05$). Each bar represents the average of triplicate samples from the same experiment.

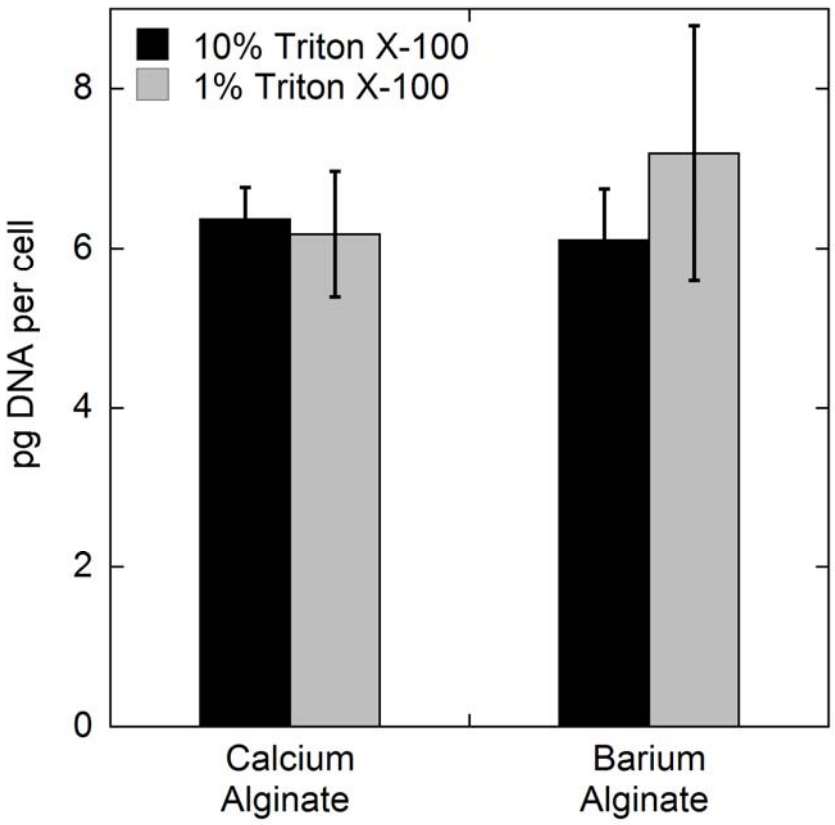

Figure 2-4: Nuclei counts and DNA content measurements were performed for encapsulated INS-1 cells.

INS-1 cells in calcium alginate or barium alginate capsules after capsule dissolution with 100mM tetrasodium EDTA (pH = 8). The lysis buffer that was used to liberate the nuclei contained 1% (v/v) or 10% (v/v) Triton X-100. Each bar represents the average of triplicate samples from the same experiment. There was no difference in pg DNA per cell for cells in calcium alginate with nuclei liberated with 1% or 10% Triton X-100 ($p=0.80$). There was no difference in DNA per cell for cells in calcium or barium alginate with nuclei liberated with 10% Triton X-100 ($p=0.59$). There appears to be a difference in the lysis buffer used for barium alginate capsules but this is not statistically significant ($p=0.36$).

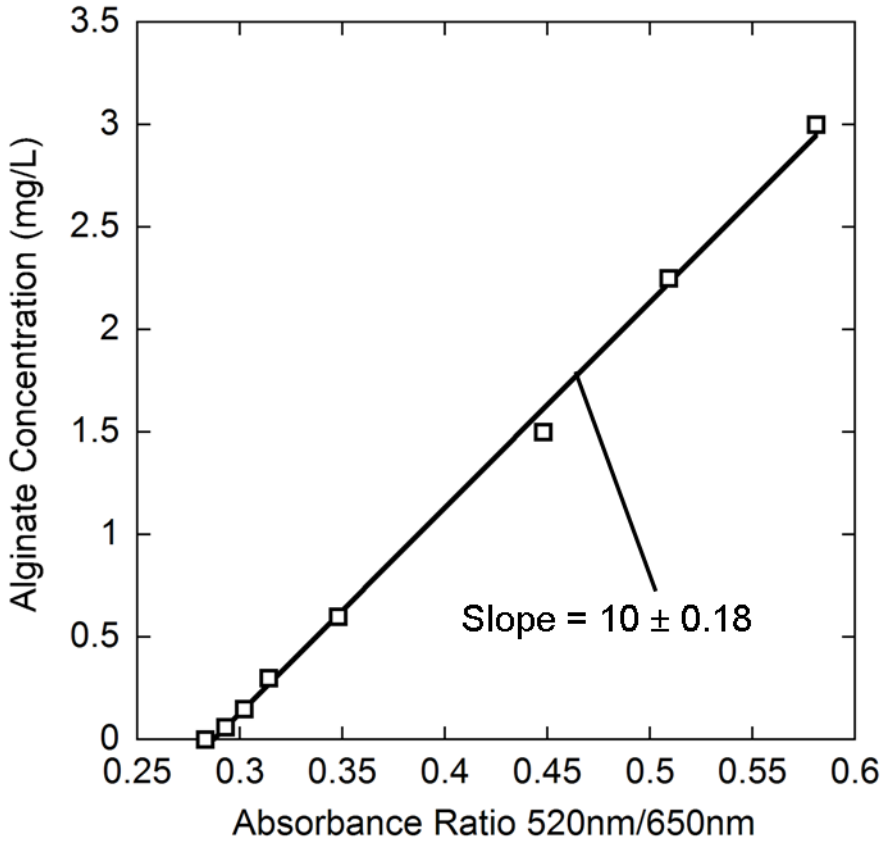

Figure 2-5: Example standard curve for alginate assay.

Ratio of Absorbance at 520 nm to 650 nm was plotted versus alginate concentration for a standard curve of 8 samples with known alginate concentrations.

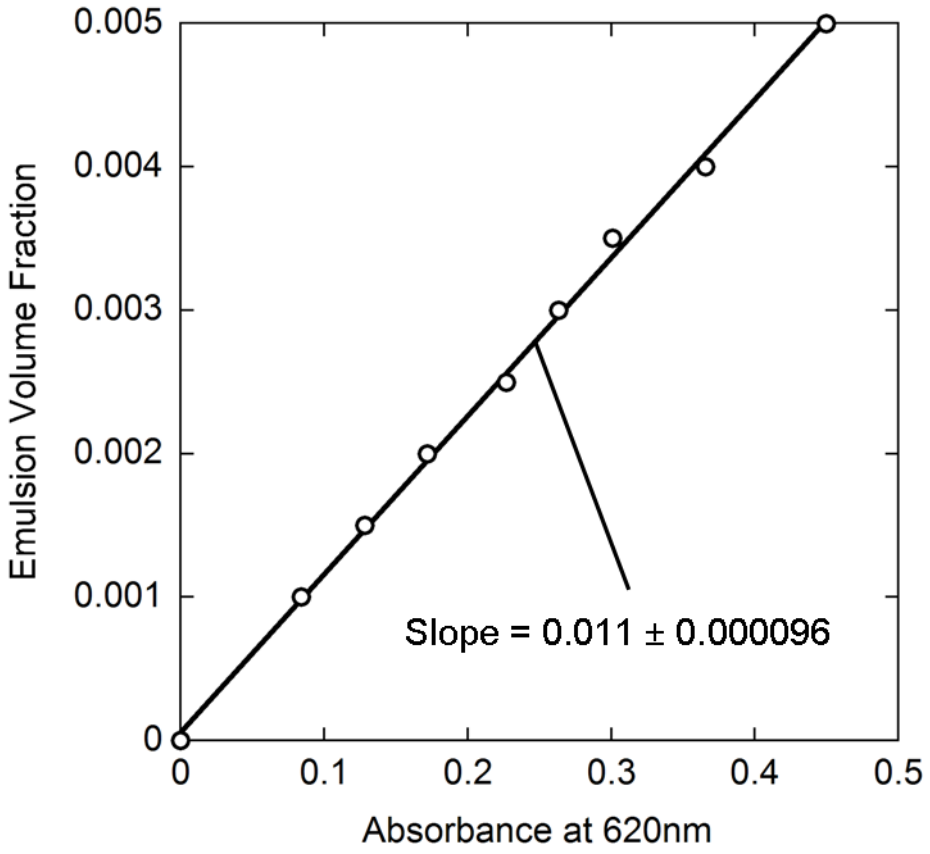

Figure 2-6: Example standard curve for PFC emulsion content assay.

Absorbance at 620 nm was plotted versus emulsion volume fraction for a standard curve of 9 samples with known emulsion volume fractions.

Table 2-1: Volume fraction (ϕ) of phases in capsules.

Capsules contained $2.4x10^7$ cells/ml or the pure PFC emulsion contained 70% (w/v) PFC.

Component	Cells + Alginate	PFC Emulsion	Cells + Alginate + PFC
Tissue	0.023	0	0.023
Alginate	0.02	0	0.02
PFC	0	0.36	0.36
Soybean Oil	0	0.12	0.12
Water	0.957	0.52	0.477

Table 2-2: Diffusion coefficient (D), Bunsen solubility coefficient (α) or permeability coefficient (αD) for oxygen in all pure components and composite phases in OCR measurements.

Parameters are from the literature or calculated. The cell concentration in the microcapsules is 2.4×10^7 cells/ml.

	D (cm^2/s)	α (mol/mmHg/ml)	αD (mol/cm/mmHg/s)	Source
Water	2.78×10^{-5}	1.27×10^{-9}	3.53×10^{-14}	[23]
PFC	5.61×10^{-5}	2.54×10^{-8}	1.42×10^{-12}	[76]
Soybean Oil	2.13×10^{-5}	6.84×10^{-9}	1.46×10^{-13}	[77, 78]
Tissue	1.24×10^{-5}	1.00×10^{-9}	1.24×10^{-14}	[23]
Alginate	0	0	0	[23]
2% (v/v) Alginate	2.77×10^{-6}	1.24×10^{-9}	3.43×10^{-14}	Ch. 6.1
Cells Normal Alginate	2.73×10^{-5}	1.23×10^{-9}	3.36×10^{-14}	Ch. 6.1
70% (w/v) PFC Emulsion	9.36×10^{-6}	1.06×10^{-8}	9.92×10^{-14}	Ch. 6.1
70% (w/v) PFC Emulsion in 2% (v/v) Alginate	9.08×10^{-6}	1.06×10^{-8}	9.63×10^{-14}	Ch. 6.1
Cells 70% (w/v) PFC Alginate	8.83×10^{-6}	1.06×10^{-8}	9.36×10^{-14}	Ch. 6.1

Table 2-3: Other parameters used for OCR feasibility calculations

Description	Variable	Equation	Value	Units
Experimentally measured OCR per cell (4 fmol/min/cell)	OCR		6.67×10^{-17}	mol/s/cell
Volume of an islet with a diameter of 150 μm	v_I		1.77×10^{-6}	cm^3
Volume of a capsule with a diameter of 500 μm	$v_{500capsule}$		6.54×10^{-5}	cm^3
Maximum oxygen consumption rate for solid tissue	V_{max_tissue}	$OCR \frac{1560\,cells/IE}{v_I}$	5.89×10^{-8}	$mol/(cm^3*s)$
Maximum oxygen consumption rate for capsules containing cells	$V_{max\_capsule}$	$V_{max\_tissue} * \frac{v_I}{v_{500cap}}$	1.59×10^{-9}	$mol/(cm^3*s)$
Initial partial pressure of oxygen in chamber	P_o		160	mmHg
Volume fraction capsules in chamber	ϕ_{caps}		0.1	

Table 2-4: Calculation of conditions that need to be met in order for OCR measurements to be valid.

Calculations were performed for alginate and PFC capsules of either 500-µm or 2000-µm in diameter. The volume fraction of capsules in the chamber was assumed to be 0.1.

	Equation (2-11)	Equation (2-12)	Equation (2-16)	Equation (2-18)
2% (v/v) Alginate 500µm	0.02	0.18	0.06	0.14
2% (v/v) Alginate 2000µm	0.29	2.96	0.94	11.91
70% (w/v) PFC 2% (v/v) Alginate 500µm	0.03	0.07	0.06	0.05
70% (w/v) PFC 2% (v/v) Alginate 2000µm	0.51	1.06	0.94	4.24

Table 2-5: Summary of measurements of pg DNA per cell for naked cells or islets or cells or islets in barium alginate

	Unencapsulated	Barium Alginate
INS-1 Cells	6.0 ± 0.8 (n=25)	6.5 ± 0.8 (n=5)
Rat Islets (n=7)	6.5 ± 0.8	6.1 ± 1.1
Human Islets (n=6)	6.2 ± 0.8	7.3 ± 3.0

Chapter 3 Theoretical Analysis of Methods to Enhance Oxygen Transport to Encapsulated Tissue

3.1 INTRODUCTION

Immunoisolation devices can be used to transplant cells to treat a variety of human diseases without the use of immunosuppressive drugs. An immunoisolation device consists of cells that are entrapped within a perrmselective membrane. The tissue relies on diffusion of nutrients through the device membrane to the tissue and diffusion of waste products and secreted proteins of interest away from the tissue. The cells are protected from the immune system by a membrane that keeps immune system effector cells, such as T cells and macrophages, from coming in contact with the transplanted tissue along with preventing or minimizing access of some large immune molecules such as antibodies and complement components. Immunoisolation devices could possibly be used to treat a large variety of human diseases that result from the body's inability to produce a required protein. Some diseases that might be treated by immunoisolation include diabetes [79], hemophilia [80], anemia [81], parathyroid disease [82], chronic pain [83], Parkinson's disease [84], Huntington's disease [85], and amyotrophic lateral sclerosis [86]. The work in our lab is focused on the use of immunoisolation devices for the treatment of diabetes. For all of the diseases listed above diabetes is probably the hardest to treat by the transplantation of immunoisolated cells as it requires more cells to be transplanted - about 10^9 cells to be transplanted into a patient compared to 10^6-10^7 for diseases of the central nervous system [22]. Also when the number of cells needed to be transplanted is large, the size of an immune device that can support efficient oxygen transport can in some cases becomes infeasible [87].

There are three main types of immunoisolation devices: (1) intravascular devices, (2) extravascular devices, and (3) microcapsules [21, 22]. Intravascular devices are inserted as a vascular shunt between an artery and a vein. Theses devices are typically hollow fibers in which blood flows through the lumen of the device. This type of device was extensively studied and is probably the best design for effective oxygen delivery since oxygenated blood flows through the device lumen, but due to the threat of thrombosis within the device lumen it is no longer being evaluated for the transplantation of immunoisolated tissue. The second type of device is an extravascular macrocapsule which is most commonly a planar diffusion chamber or a hollow fiber. Both types of macrocapsules have encapsulated cells within their interior surrounded by an immunoisolating membrane. One advantage of this type of device is that due to its large size it can, depending on the circumstances, be retrieved after transplantation. Many researchers working in the field of islet encapsulation have been working with planar diffusion chambers. Planar diffusion chambers are typically implanted into the subcutaneous tissue or the peritoneal cavity. Recent work by Gianello and Dufrane where encapsulated pig islets were transplanted into non-immunosuppressed monkeys has even further invigorated research in this area [88]. The final type of immunoisolation device is a microcapsule. Microcapsules are small spherical gels that range in size from 200 μm to 2 mm. Microcapsules are the most extensively studied encapsulation system and are under study in our lab. Microcapsules are hydrogels that contain one to two islets. The most common implantation site is the peritoneal cavity.

Islets within the native pancreas are heavily vascularized, and during islet isolation procedures the vascular network of the islet is destroyed, collapses during culture and does not regenerate when the islets are transplanted within an immunoisolating device [89-91]. Tissue within an immunoisolation device must rely on delivery of oxygen and other nutrients by

diffusion from the exterior of the device. Oxygen diffusion is much more limited than glucose diffusion because glucose concentrations *in vivo* are much higher than oxygen [92]. The oxygen level will be studied as the critical nutrient that determines encapsulated tissue survival and function. For oxygen to reach the encapsulated tissue it must diffuse from the vasculature to the device exterior, through the device to the tissue and through the islet while being consumed to reach the cells at the center. Oxygen delivery is even further hampered when an immune reaction to the transplanted cells or immunoisolating material results in cells adhering to the outside of the device consuming oxygen before it is able to reach the cell in the device interior [23].

Reduced oxygen levels have been shown to reduce islet insulin secretion below what was observed under normoxic conditions [44, 47]. In the work by Dionne et al. [44] islets were perfused with media that was equilibrated with air at various oxygen levels, at gas phase P_{O2} values below 60 mmHg there was a reduction in insulin secretion. The ability of an islet to effectively secrete insulin following transplantation is essential for transplantation success. Thus, since reduced oxygen levels have been shown to decrease islet survival and function, effective oxygen delivery is critical for successful transplantation of immunoisolated islets to treat type 1 diabetes. Previous theoretical analysis of oxygen limitations to immunoisolated tissue have been studied and have shown that depending on the transplantation conditions these problems can be quite serious [23, 93].

In this work we expand on previous models to evaluate what the oxygen limitations are for islets in either microcapsules or planar diffusion chambers over a range of external oxygen levels. We chose to look at these two types of devices because they are the two most commonly studied in the field of islet immunoisolation. We will also evaluate the use of two different

methods to reduce oxygen transport limitations to encapsulated tissue: (1) increasing the permeability of the immunoisolating material through the use of a perfluorocarbon emulsion and (2) dispersing the islets into single cells and allowing them to reaggregate into aggregates with a smaller diameter than an intact islet. Perfluorocarbons are highly desirable materials for enhancing oxygen transport, due to their very high oxygen solubility, approximately 25 times that of water, on a volumetric basis. Enhanced solubility will lead to enhanced permeability because the permeability is a product of the solubility and diffusivity. Perfluorocarbon emulsions have been developed as a blood substitute and can be incorporated into encapsulation materials. There are reports in the literature that including a perfluorocarbon emulsion in islet culture enhances function [60]. Perfluorocarbons are also used during pancreas storage prior to islet isolation [61]. Culture of islets at the interface of a perfluorocarbon and cell culture media (two layer method) has been studied and was not shown to be beneficial in improving islet survival [62]. There are two potential reasons for the lack of improvement (1) the culture system probably did not have any oxygen limitations for the islets cultured without PFC and (2) the two layer method is beneficial for short periods of time when the PFC can act as a source of oxygen, but as it is not exposed to the air directly it does not have an effect after its oxygen store has been depleted. All of these facts taken together indicate that the incorporation of perfluorocarbons into an encapsulating material is likely to be beneficial, and in this work we evaluate the theoretical benefits perfluorocarbons can have on increasing oxygen levels experienced by encapsulated tissue along with improving fractional viability and fraction of normal insulin secretion after transplantation. We are interested in studying aggregates because it is likely that for an intact islet with a diameter of 150-μm all oxygen is consumed prior to reaching the cells at the center of the islet. However, with aggregates, by reducing the internal

diffusion distance within the tissue there are potential benefits to tissue survival and function. Normal insulin secretion was shown to be maintained at lower oxygen levels for perfused unencapsulated aggregates with a diameter of 37 μm (above bulk perfuasate P_{O2} of 20 mmHg) compared to intact islets (above bulk perfusate P_{O2} 60 mmHg) [55]. Also recent publications have suggested that smaller islets are superior to larger islets in terms of survival in low oxygen and transplantation outcome [56, 57].

In this work a theoretical model was developed to assess the oxygen level, fractional viability, and fraction of normal insulin secretion for islets, single cells and aggregates ranging in size from 37.5 to 125 μm. The different tissue sizes were analyzed in two types of immunoisolation devices – microcapsules and planar diffusion chambers with and without a perfluorocarbon emulsion at varying tissue loadings and over a range of external oxygen environments. The theoretical analysis in this paper can be used to determine which oxygen enhancement strategy is most beneficial under a particular transplantation situation and is worth further investigation.

3.2 MODELING

To assess the benefits of aggregate and PFC-containing immunoisolation devices, a theoretical model has been developed to predict the local partial pressure of oxygen, which, in turn, is used to assess tissue viability and fraction of normal insulin secretion for encapsulated islets, aggregates, and single cells in microcapsules and planar diffusion chambers. For most calculations the microcapsules have a diameter of 500 μm and the planar diffusion chambers have a thickness of 500 μm. A few calculations were performed for device sizes of 250, 1000 and 2000-μm for microcapsules and diffusion chambers. For both device types the immunoisolating material will be 2% (v/v) alginate as this is the most commonly used material

for microcapsules and is sometimes used in planar diffusion chambers. We chose to use the same immunoisolating material for both types of devices so that any differences observed in the calculations are due to differences in device geometry and not to the selection of different immunoisolating materials.

3.2.1 Model Geometry

Sketches of example geometries that were analyzed are presented in Figure 3-1A for microcapsules and Figure 3-1B for planar diffusion chambers. All aggregate and islet tissue are assumed to be spheres. Tissue in a microcapsule was arranged four different ways: (A1) a single tissue sphere which is a centrally located 150-μm diameter islet or smaller aggregate, (A2) aggregates or islets arranged in a cubic array where the tissue lies throughout the capsule diameter and the length of the side of the cube is equal to the capsule diameter, (A3) aggregates in a cubic array where the cube fits entirely within the capsule, and (A4) homogenously distributed tissue which is meant to approximate single cells. Comparisons between capsule and device loadings will be made using islet equivalents. An islet equivalent (IE) is a volume of tissue equal to that of a 150-μm sphere. For the aggregate case, calculations were performed for five different sizes of aggregates – 37.5, 50, 75, 100 and 125-μm diameter at many different capsule loadings starting with one single centrally located aggregate to about 2-10 IE of encapsulated tissue. Calculations were only performed for arrangement model geometry (A2) with an odd number of aggregates across the capsule diameter such that an aggregate was always placed at the center of the capsule, and calculations were performed with increased capsule tissue loading up to the point where the aggregates filled the capsule diameter. For each capsule, with the origin placed at the center of the capsule, there are three planes of symmetry perpendicular to

each axis through the origin, thus the model can be solved for only one eighth of the capsule in order to reduce the number of degrees of freedom.

Calculations were performed for three different types of tissue in a planar diffusion chamber – islets, aggregates and single cells. Sketches of the geometries studied are presented in Figure 3-1B. (B1) For a single layer of islets or any size aggregate, the tissue spheres were placed at the central plane of the device arranged in a cubic array. The unit cell that was analyzed for a monolayer of tissue is sketched in Figure 3-1B for the monolayer planar device that contains islets and represents one quarter of an islet. (B2) When multiple layers of tissue were modeled the bottom and top tissue layers were nearly touching the device membrane. The positions of the alternating layers are offset to create a body centered cubic configuration. An example unit cell that was analyzed for many tissue layers is shown in Figure 3-1B2 for a multilayer planar device where one quarter of an aggregate from each layer is modeled. (B3) In the homogenously distributed tissue planar device cells were modeled as a homogenous phase of tissue equally distributed throughout the device.

3.2.2 Material and Tissue Properties

The effective permeability in subdomains containing several components was determined from theoretical relationships. The ratio of the effective permeability $(\alpha D)_{eff,i}$ for layer i consisting of a dispersed (d) phase and a continuous (c) phase (as occurs in the alginate subdomains of the model system) to the permeability of the continuous phase $(\alpha D)_c$ was calculated from Maxwell's relationship [75]

$$\frac{(\alpha D)_{eff,i}}{(\alpha D)_c} = \frac{2-2\phi+\rho(1+2\phi)}{2+\phi+\rho(1-\phi)} \tag{3-1}$$

where αD is the effective permeability of the material (mol/cm/mmHg/s), $\rho=(\alpha D)_d/(\alpha D)_c$ is the ratio of the permeability of the dispersed phase to the permeability of the continuous phase, and ϕ is the volume fraction of the dispersed phase. For the multiple dispersed phases employed in our model system, Maxwell's relationship was used sequentially, starting with the phase with the smallest particle size and ending with the phase with the largest particle size. For particle types of the same size, Maxwell's relationship was used for one particle, then the other (and in the reverse order), and the two results were averaged.

The perfluorocarbon emulsion that we have been studying in the lab consists of 70% (w/v) perfluorodecalin and 20% (w/v) Intralipid® (Baxter), a soybean oil emulsion, and a PFC emulsion of this composition is used in all model simulations that contain PFC alginate [71]. In the final PFC alginate composite phase, there were perfluorodecalin and soybean oil droplets of approximately the same size (0.4 μm); the alginate polymer itself was treated as an impermeable dispersed in water. The pure component material transport properties are given in Table 3-1 and the effective properties for different alginate types are given in Table 3-2. A detailed description of the calculation of effective solubility, permeability and diffusivity for the different composite materials used in the model can be found in Section 6.1.

3.2.3 Model Equations

The three-dimensional species conservation equation for reaction and diffusion at steady state was used to predict the oxygen profile within the different tissue and material subdomains in the immunoisolation device:

$$D_i \nabla^2 C_i = V_i \qquad (3\text{-}2)$$

where D_i (cm^2/s) is the effective diffusivity of oxygen in subdomain i, C_i (mol/cm^3) is the concentration of oxygen in subdomain i, and V_i ($mol/cm^3/s$) is the local oxygen consumption rate per unit volume in subdomain i. For convenience, since partial pressures are equal across interfaces of different materials, we make use of oxygen partial pressure instead of concentration, which are related by

$$C = \alpha P \tag{3-3}$$

where α ($mol/cm^3/mmHg$) is the effective Bunsen solubility coefficient in subdomain i and P is the partial pressure of oxygen. Combining Eq. (1) and Eq. (2) gives

$$(\alpha D)_i \nabla^2 P_i = V_i \tag{3-4}$$

The oxygen consumption rate is assumed to follow Michaelis-Menten kinetics for all tissue,

$$V_i = \frac{V_{max} \varepsilon_i P_i}{K_m + P_i} \tag{3-5}$$

where V_{max} is the maximum oxygen consumption rate for the tissue, ε_i is the tissue volume fraction in subdomain i, and K_m is the Michaelis-Menten constant. For the immunoisolation devices that contain an islet or aggregates, no oxygen is consumed in the alginate subdomain; therefore V_i is equal to zero, and the tissue volume fraction in the islet or aggregate subdomains is equal to one. For the case of an immunoisolation device containing dispersed single cells, the model consists of only one subdomain and the tissue volume fraction (ε) is less than one and is calculated based on the particular tissue density used. The equations for each subdomain are written out in detail in Section 6.2.

The boundary conditions for these problems are as follows. For the microcapsule there are planes of symmetry where the capsule was cut to create the unit cells and thus zero flux of oxygen across these surfaces for both the alginate and tissue subdomains

at x=0, y=0 or z=0

$$n\bullet\left(-D\alpha\nabla P\right)_i=0 \tag{3-6}$$

At the boundary between a tissue subdomain (t) and the alginate subdomain (a) there is continuity and thus the partial pressure of oxygen and the flux of oxygen across the boundary are both equal.

At $r=R_{tissue}$

$$P_t=P_a \tag{3-7}$$

$$n\bullet\left[\left(-D\alpha\nabla P\right)_t-\left(-D\alpha\nabla P\right)_a\right]=0 \tag{3-8}$$

The final boundary condition that is required to solve the problem is the assumption that the external partial pressure of oxygen is specified at the capsule surface (s),

at $r=R_{capsule}$

$$P_a=P_s \tag{3-9}$$

We chose to assume a value of the exterior surface P_{O2} rather than model external oxygen diffusion because within the peritoneal cavity oxygen levels vary greatly and have been measured to be anywhere between near 0 and 38 mmHg [94]. Therefore, as microcapsules in the peritoneal cavity are likely to move and thus likely to experience wide ranges of oxygen levels it is important to know how tissue survival and function will be affected over the range of oxygen levels likely to be experienced.

For the planar device there are planes of symmetry where the device was cut to create the unit cells and thus zero flux of oxygen across these surfaces for both the tissue and alginate subdomains

$$n\bullet\left(-D\alpha\nabla P\right)_i=0 \tag{3-10}$$

At the boundary between a tissue subdomain (t) and the alginate subdomain (a) there is continuity and thus the partial pressure of oxygen and the flux of oxygen across the boundary are both equal.

At $r=R_{tissue}$

$$P_t = P_a \tag{3-11}$$

$$n \cdot \left[\left(-D\alpha \nabla P \right)_t - \left(-D\alpha \nabla P \right)_a \right] = 0 \tag{3-12}$$

The final boundary condition that is required to solve the problem is the assumption that the external partial pressure of oxygen is specified at the device surface (s),

at $z = \pm h/2$ where h is the device thickness

$$P_a = P_s \tag{3-13}$$

The model was solved by the finite element method using the commercially available software package COMSOL Multiphysics in combination with MATLAB and using the model parameters in Table 3-1, Table 3-2, and Table 3-3. Equation (3-4) was solved simultaneously for all subdomains of the immunoisolation devices subject to the boundary conditions stated above. The mesh size that was chosen for each calculation was verified to be fine enough when on further decreases in mesh size the solution did not change.

The fractional viability of the encapsulated tissue was estimated by determining the volume fraction of tissue where $P>P_C$. P_C is the critical oxygen partial pressure below which tissue dies and the value of P_C is assumed to be 0.1 mmHg. The fractional viability was calculated using the following equation:

$$\text{Fractional Viability} = \frac{V_{Viable}}{V_{Tissue}} \tag{3-14}$$

where V_{Viable} is the volume of tissue where P is greater that 0.1 mmHg and V_{Tissue} is the total encapsulated tissue volume.

The relationship used to predict the local fraction (F_I) of normal insulin secretion rate as a function of local oxygen partial pressure within the islet was developed from data on the effect of hypoxia on islet insulin secretion, estimating the oxygen partial pressure profile within the islet in the experimental system, and then determining the simplest model type and parameters(s) that best predict the insulin secretion level [44, 93]. The result for a value of $V_{max} = 4x10^{-8}$ mol/cm^3/s is

$$\begin{aligned} P < 5.1 \text{ mmHg} \quad & F_I = \frac{P}{5.1} \\ P \geq 5.1 \text{ mmHg} \quad & F_I = 1.0 \end{aligned} \tag{3-15}$$

The fraction of normal insulin secretion averaged over all tissue within the microcapsule or planar device was determined by evaluating the volume integral of F_I in all tissue containing subdomains

$$F_S = \frac{\int_{Viable} F_I dV}{V_{Tissue}} \tag{3-16}$$

where F_S is the fraction of normal insulin secretion averaged over all of the encapsulate tissue.

3.3 RESULTS

3.3.1 Estimation of Oxygen Diffusion Limitations in Microcapsules and Planar Diffusion Chambers

To begin our analysis of the benefits of using smaller islet cell aggregates or a permeability enhancer we first performed a scaling analysis to determine if and under what circumstances either strategy would be beneficial to enhancing oxygen transport. The first scaling

approximation that was studied was to compare the rate of reaction to the rate of diffusion for solid spheres of tissue also known as the Damkohler number.

$$Da=\frac{V_{max,t}R_t^2}{\left(K_m+P_{s,t}\right)\left(\alpha D\right)_t} \tag{3-17}$$

where Da is the Damkohler number and $P_{s,t}$ is the given partial pressure of oxygen at the tissue surface. The calculation of the Damkohler number is only an approximation of relative rates of oxygen diffusion and reaction because oxygen gradients do exist within the islet and as a result not all tissue is respiring at the same rate. In many cases the oxygen consumption rate by the tissue is being over estimated as the oxygen level decreases.

One would want the Damkohler number to be small for a given tissue size and oxygen level such that oxygen consumption would not be limited by diffusion. The Damkohler number was calculated for tissue that has a diameter of 37.5, 50, 75, 100, 125, and 150 μm over a range of 1-40 mmHg (Figure 3-2). Only for the smallest tissue sizes (37.5 and 50 μm) is the Damkohler less that 1 and then only when the surface oxygen level is greater than 20 mmHg. COMSOL models were also solved for the six different tissue sizes over a range of specified tissue surface oxygen levels. Lines are drawn across the family of curves to show at which point the tissue no longer remains functional or viable. The Damkohler number at which these cutoffs occur is greater than one as some gradients within the tissue can be tolerated as long as the oxygen level at the tissue center does not get below 0.1 or 5.09 mmHg for either maintenance of tissue viability or insulin secretion respectively. The value of the Damkohler number for the fraction of normal insulin secretion cutoff increases with increasing tissue diameter and occurs at higher oxygen levels for the larger tissue sizes. The value of the Damkohler number for the fractional viability cutoff has some dependence on tissue size and the external oxygen level for

which it occurs increases with tissue size and always occurs for lower oxygen levels than the fraction of normal insulin secretion cutoff. From the simple analysis of the Damkohler we were able to show that oxygen gradients within smaller aggregates can be greatly reduced compared to intact islets over the entire range of oxygen levels likely to be experienced by transplanted tissue. Aggregates should be beneficial in allowing tissue to maintain function and viability in lower oxygen environments. Since the Damkohler number is only ever less than one for 37.5 or 50-μm aggregates these size aggregates should be the most beneficial in reducing oxygen transport limitations to encapsulated tissue.

The next scaling approximation that was performed was to estimate the pressure drop through the alginate phase of a microcapsule that contains a centrally located tissue of diameter 37.5 to 150-μm or through the alginate phase of a planar device to a layer of tissue located in the central plane of the device. For the case of a centrally located sphere of tissue at the center of a microcapsule the pressure drop within the capsules can be estimated from the boundary conditions written at the tissue surface:

$$\frac{4\pi(\alpha D)_{cap}}{\frac{1}{R_t}-\frac{1}{R_{cap}}}\left[P_{s,cap}-P_{cap}(R_t)\right]=\frac{V_{max,t}P_s}{K_m+P_s}\left(\frac{4\pi}{3}R_t^3\right) \qquad (3\text{-}18)$$

where R_t is the radius of the tissue sphere and R_{cap} is the radius of the capsule. Rearranging to determine the scaled capsule pressure drop:

$$\frac{\Delta P_{cap}}{P_s}=\frac{V_{max,t}R_t^2\left(1-R_t/R_{cap}\right)}{3(\alpha D)_{cap}(K_m+P_s)} \qquad (3\text{-}19)$$

To determine a similar expression for the pressure drop through the encapsulating material to a layer of tissue at the center of the device a few assumptions needed to be made. First, the tissue

within the device could not be approximated as discrete spheres and therefore was assumed to be a slab with a tissue volume fraction of $\pi/6$ and thus $V_{max,t}$ was multiplied by this value. Second, this assumed tissue volume fraction is therefore approximating the case where the monolayer of tissue within the device consists of spheres that are touching and therefore does not represent the case where lower tissue loadings are used. The pressure drop within the device can be estimated from the boundary conditions written at the tissue surface:

$$\frac{A(\alpha D)_{dev}}{z_{dev}-z_t}\left[P_{s,dev}-P_{dev}(R_t)\right]=\frac{\frac{\pi}{6}V_{max,t}P_s}{K_m+P_s}(A^*z_t) \tag{3-20}$$

where A is the device surface area, z_{cap} is the device half thickness, z_t is the tissue half thickness, dev refers to the device. Rearranging to determine the scaled device pressure drop:

$$\frac{\Delta P_{dev}}{P_s}=\frac{\frac{\pi}{6}V_{max,t}z_t(z_{dev}-z_t)}{(\alpha D)_{dev}(K_m+P_s)} \tag{3-21}$$

It is desirable that the expression on the right hand side of both equation (3-19) for microcapsules and (3-21) for planar devices is small such that the encapsulating material does not impose a large mass transfer resistance. Comparing the two equations a couple of interesting observations can be made. First by examining Equation (3-19)

$$\frac{\Delta P_{cap}}{P_s}\propto R_t^{\,2}\left(1-R_t/R_{cap}\right) \tag{3-22}$$

when $R_t<<R_{cap}$ equation (3-22) becomes

$$\frac{\Delta P_{cap}}{P_s}\propto R_t^{\,2} \tag{3-23}$$

the pressure drop through the microcapsule loses any sort of dependence on capsule size and thus after a certain point there is no further detriment to the tissue of using a larger capsule. By examinging Equation (3-21)

$$\frac{\Delta P_{dev}}{P_s} \propto z_t \left(z_{dev} - z_t \right) \tag{3-24}$$

when $z_t << z_{dev}$ Equation (3-24) becomes

$$\frac{\Delta P_{dev}}{P_s} \propto z_t z_{dev} \tag{3-25}$$

The pressure drop through the device always gets worse with increasing device thickness. The fact that the pressure drop is proportional to the square of the tissue size for microcapsules and is only linearly proportional to pressure drop for a planar device indicates that tissue size is going to have a greater impact in microcapsules. For either type of device the scaled pressure drop is inversely proportional to the effective permeability of the encapsulating material. Thus the benefits that will be observed by incorporating a permeability enhancer such as the 70% (w/v) PFC emulsion which has 2.8 times the permeability of normal alginate is to decrease the pressure drop by approximately one third. The spherical geometry should also be better for oxygen transport compared to planar device because the expressions for the pressure drop are quite similar except the microcapsule expression has a factor of three in the denominator.

The scaled pressure drop for capsules and planar diffusion devices was calculated for tissue sizes of 37.5 to 150-μm over a range of capsule or device surface P_{O2} for a device or capsule diameter of 500 μm (Figure 3-3) with the encapsulating material being normal alginate or 70% (w/v) PFC alginate. The predicted pressure drop is always less for the microcapsules (Figure 3-3A,B) compared to the planar device (Figure 3-3C,D) at all oxygen levels and for the smaller tissue at the higher oxygen levels the pressure drop through the microcapsule is

negligible. The curves for the planar device are much close together for the various tissue sizes compared to the microcapsules indicating that the aggregates have a greater effect in the microcapsules.

The scaled pressure drop for capsule and planar diffusion devices was calculations for a tissue sizes of 37.5 to 150-μm over a range of capsule or device sizes at a surface P_{O2} of 40 mmHg (Figure 3-4). The predictions for the microcapsule suggest that above a capsule diameter of 500 μm there will be a minimal effect of increasing the capsule diameter (Figure 3-4A,B). The degree of the pressure drop varies greatly with tissue size and the presence of PFC in the encapsulating material reduces the pressure drop. The predictions for the planar device are that the pressure drop always increases with increasing device size there are less differences between different tissue sizes and the magnitude of the pressure drop is several order of magnitude higher in the planar device (Figure 3-4C,D). The spherical geometry of the microcapsule is much more favorable to oxygen transport than the planar slab geometry of the planar diffusion chamber.

In some of the scaling calculations for pressure drop through the encapsulating material the predictions are greater than one which is not actually feasible unless negative partial pressure of oxygen can be obtained. The pressure drop being greater than one is a result of the fact that the oxygen levels within the tissue are low enough that the oxygen consumption rate is less than the value that we approximate by using the oxygen level at the tissue surface due to entrance into the first order regime of Michaelis-Menten kinetics where oxygen consumption is dependent on oxygen level and decreases with decreasing oxygen level.

Although in this section very simple expressions were used to represent a very complex problem many very useful insights were gained. The microcapsule is the more ideal geometry for oxygen delivery. Aggregates have a greater impact in a microcapsule than in a planar

diffusion chamber. Increasing device size is always detrimental but increasing microcapsule size is not. Incorporation of a permeability enhancer is always going to decrease the pressure drop through the encapsulating material and the overall benefits of the permeability enhancer will depend on if you are within a regime where decreasing the pressure drop through the encapsulating material is going to impact viability or insulin secretion.

3.3.2 Microcapsules

Oxygen profiles were calculated for a centrally located 150-μm diameter islet with and without PFC emulsion in a 500-μm microcapsule at a capsule surface P_{O2} of 40 mmHg. Comparing the oxygen profiles for the capsules containing a single centrally located intact islet with (Figure 3-5B) and without PFC emulsion (Figure 3-5A), the oxygen level at the outer surface of the islet is higher when PFC emulsion is incorporated into the alginate phase of the microcapsule (P_{O2} = 25 versus 35 mmHg at r = R_{tissue}). The oxygen gradient in the capsule subdomain is greater for a normal alginate capsule compared to a 70% (w/v) PFC alginate capsule. The minimum oxygen level at the islet center is greater for an islet within PFC alginate (5.5 versus 0.15 mmHg at r=0).

Oxygen profiles were also calculated for a 500-μm capsule containing many 50-μm diameter aggregates with a total tissue volume of 1.2, 4.6 or 9.5 islet equivalents at a capsule surface P_{O2} of 40 mmHg (Figure 3-6). The aggregates were arranged in a cubic array that extended over the entire capsule diameter (model geometry A2). Comparing the oxygen profile in a normal alginate capsule that contains an islet (Figure 3-5A) or aggregates (Figure 3-6A) of approximately the same total tissue volume, the minimum oxygen level that the tissue experiences in the microcapsule is significantly increased for the aggregates (P_{min} = 30 mmHg)

compared to the islet where the minimum oxygen level is low enough to cause reduced function and almost low enough to cause tissue death (P_{min} = 0.15 mmHg). The oxygen gradients within the alginate subdomain are also greatly reduced for the a capsule with 1.2 islet equivalents of tissue. The minimum oxygen level experienced by tissue in capsules containing aggregates that also contain PFC emulsion (Figure 3-6B) is even further increased (P_{min} = 34 mmHg). Increasing the tissue loading for 50-µm aggregates in a 500-µm normal alginate capsule to 4.6 IE (Figure 3-6C) and then 9.5 IE (Figure 3-6E) results in increased gradients within the capsule and lower oxygen levels within the tissue at the center of the capsule (16 mmHg and <0.1 mmHg, respectively). The same capsule loadings of 4.6 IE (Figure 3-6D) and 9.5 IE (Figure 3-6F) in PFC alginate have less oxygen gradients and higher oxygen levels are maintained for tissue at the center of the capsule (29 and 13 mmHg respectively). The minimum oxygen levels experienced in the PFC containing capsules are similar to those in normal alginate at the tissue loading that is one step lower (Figure 3-6A and D are similar and Figure 3-6F and C are similar). The permeability enhancement of the PFC is beneficial because it reduces the oxygen gradients within the alginate subdomain allowing for a greater oxygen level at the tissue surface and thus greater oxygen delivery to the encapsulated tissue.

Oxygen profiles were also calculated for a 1000-µm capsule containing many 50-µm diameter aggregates with a total tissue volume of 1.2 or 9.5 islet equivalents at a capsule surface P_{O2} of 40 mmHg (Figure 3-7). The oxygen gradients within all four oxygen profiles are less in Figure 3-7 for 1000-µm capsules compared to the oxygen profiles in Figure 3-6 for the exact same total encapsulated tissue volume and encapsulating material. In fact the tissue actually does better in the larger capsules because there is greater spacing between individual aggregates.

Oxygen profiles were calculated for a variety of tissue sizes, tissue configurations, and capsule surface oxygen levels. The oxygen profiles were then used to make predictions of fractional viability and fraction of normal insulin secretion. The predictions allow one to assess the benefits of both methods of enhancing oxygen delivery to microencapsulated tissue: smaller islet cell aggregates and incorporating PFC emulsion into the microcapsule. The first comparisons of tissue viability and insulin secretion were for a centrally located intact islet and one islet equivalent of tissue homogenously distributed throughout the entire capsule to approximate the case of encapsulated single cells (Figure 3-8). The homogenous case represents the limit of the best case for uniform tissue distribution in a microcapsule; both tissue viability and insulin secretion are maintained in lower oxygen environments in capsules containing a homogenously distributed islet compared to intact islets. Adding 70% (w/v) PFC emulsion to the capsules containing homogeneously distributed tissue has essentially no benefit. Adding PFC emulsion to microcapsules containing an intact islet results in a modest improvement in the oxygen environments where islets maintain viability and insulin secretion. For the rest of the calculations for microencapsulated tissue only the predictions for fraction of normal insulin secretion will be presented since oxygen effects on insulin secretion are seen at higher oxygen levels than reductions in tissue viability, but the predictions of fractional viability can be found in Section 6.4 of the Appendix.

The next comparison was to examine the effect of breaking up a 150-μm islet into 37.5, 50, or 75-μm diameter aggregates and comparing microcapsules that all contain a total tissue volume equal to one islet equivalent (Figure 3-9). The aggregate tissue for these calculations was arranged in a cube that fit entirely within the capsule (Model Geometry A3). The predictions for normal insulin secretion show that the use of aggregates allows for the tissue to

secrete insulin normally in much lower external oxygen environments than an islet and are quite similar to the homogeneous case. It is very beneficial to use smaller aggregates in order to have the tissue function in lower oxygen environments while keeping the total tissue volume within the capsule constant. Decreasing the tissue diameter to at least half of an intact islet significantly improves tissue function in low oxygen environments.

The predictions for fraction of normal insulin secretion for homogeneously distributed tissue (total encapsulated tissue volume of 1 islet equivalent) and an intact islet (1 islet equivalent (IE)) were compared to 50-μm aggregates with a total capsule tissue loading of 1.2 or 9.5 islet equivalents all in a 500-μm capsule (Figure 3-10A). The tissue for these calculations and all subsequent calculations was arranged in a cube that was the same size as the capsule (model geometry A2). This type of cubic arrangement was more desirable than model geometry A3 because it allowed for greater capsule tissue loadings but does result in numbers of islet equivalents that were not whole numbers. For the case of 1.2 islet equivalents of aggregate tissue, function was maintained at lower oxygen than an intact islet and the effects of reduced oxygen were similar to those seen for single cells. Increasing the capsule tissue loading to 9.5 islet equivalents of aggregates, the predicted fraction of normal insulin secretion was similar to one intact islet over the range of oxygen levels examined. Much higher capsule tissue loadings can be achieved for 50-μm aggregates with similar losses in function as an intact islet which could lead to a reduction in total transplant volume assuming the current effectiveness of intact islets is considered satisfactory. It is advantageous to reduce the total transplant volume as the large volume of microcapsules required to treat diabetic patients is a drawback for the use of microcapsules [87].

Predictions for fraction of normal insulin secretion were also made for microcapsules containing 50-μm aggregates with a total tissue volume of 1.2 or 9.5 islet equivalents with 70% (w/v) PFC emulsion incorporated into the alginate phase of the microcapsule (Figure 3-10B). Marginal improvements in insulin secretion were predicted for capsules containing 70% (w/v) PFC emulsion with an aggregate loading of 1.2 islet equivalents. However, incorporating PFC into capsules at high tissue loadings (9.5 islet equivalents) offers a significant improvement in the ability for the tissue to function in lower oxygen environments. Increased permeability of the alginate phase of the microcapsules is beneficial in improving insulin secretion of 50-μm aggregate containing capsules at high tissue loadings.

The minimum capsule surface P_{O2} at which all of the encapsulated tissue remained fully functional can be used to compare the oxygen effects for all microencapsulated tissue calculations that were performed for 500-μm capsules. Calculations were performed at various capsule loadings for single cells; 37.5-μm, 50-μm, 75-μm, 100-μm, and 125-μm aggregates; and 150-μm islets with (Figure 3-11B) and without PFC emulsion (Figure 3-11A). The minimum surface P_{O2} for fully functional tissue is always the lowest in either capsule type for capsules that contain single cells at all capsule loadings studied. As the size of the aggregate increases, the minimum surface P_{O2} for fully functional tissue increases at a specified capsule tissue loading. For any size tissue in normal alginate the minimum surface P_{O2} increases as the capsule tissue loading increases. The results for capsules that contain 70% (w/v) PFC emulsion in the alginate phase (Figure 3-11B) are shifted down slightly compared to the results for the same tissue size in normal alginate in Figure 3-11A. The increase in minimum surface P_{O2} for fully functional tissue, as tissue loadings increase, is not as steep for the capsules that contain PFC as compared to those without. In both types of capsules the smaller aggregates (37.5 and 50-μm) come

closest to the theoretical homogenous limit represented by the single cells, 75-µm aggregates are quite beneficial in maintaining tissue function in low oxygen environments compared to normal intact islets, and even aggregates of 100 and 125-µm aggregates provide some assistance in reducing oxygen limitations compared to the predictions for a 150-µm islet.

Predictions for fraction of normal insulin secretion for a centrally located islet in different size microcapsules (250, 500, 1000 and 2000-µm) were made in order to determine the effects that decreasing or increasing the capsule size has on oxygen transport (Figure 3-12). Increasing the capsule size above 500-µm had small effects in normal alginate capsules and nearly no effect in PFC alginate capsules. Decreasing the capsule size in normal alginate capsules had almost the same benefit as incorporating a PFC emulsion into a 500-µm microcapsule. There was a slight benefit of decreasing the size of a PFC containing microcapsule. All of these predictions are in keeping with the analysis of scaled pressure drop in section 3.3.1; there would be some benefit in lowering the capsule size below 500-µm but there would be nearly no effect of increasing the capsule size above 500-µm.

The effects of increasing the capsule size from 500-µm to 1000-µm for 50-µm aggregates in alginate capsules and a total tissue loading of 1.2 or 9.5 IE (Figure 3-13A) were assessed by calculating the fraction of normal insulin secretion for capsules with a specified capsule surface P_{O2} of 0-40mmHg. The same amount of total encapsulated tissue can maintain normal levels of insulin secretion in lower oxygen environments in the larger capsule, due to the increased spacing between aggregates. 1.2 IE in a 500-µm capsule and 9.5 IE in a 1000-µm capsule have the same tissue density in the capsule on a volumetric basis. The tissue at the same density does better in the smaller capsule since oxygen has to travel a shorter distance and through less tissue to reach the aggregates located at the center of the capsule. Predictions of fraction of normal

insulin secretion were also made for 500 and 1000-μm capsules containing 50-μm aggregates in which PFC emulsion was incorporated into the alginate phase of the microcapsule (Figure 3-13B). For all three tissue configurations presented, the incorporation of PFC into the alginate microcapsule is beneficial to promoting tissue function in lower oxygen environments. The predicted fraction of normal insulin secretion was identical for 1.2 IE in 500-μm normal alginate (solid red curve) and 9.5 IE in 1000-μm (dashed blue curve). These two cases have the same tissue density and the negative effects that are observed for increasing the capsule size while the spacing between the aggregates is kept constant is negated by the incorporation of a permeability enhancer into the alginate phase of the microcapsule.

In summary we have calculated oxygen profiles in microcapsules containing homogeneously distributed tissue, aggregates, and islets. The oxygen profiles are then used to predict tissue fractional viability and fraction of normal insulin secretion. The model predictions demonstrate that using smaller aggregates as opposed to intact islets greatly improves the ability of encapsulated tissue to function in lower oxygen environments. Incorporating a PFC emulsion into the microcapsule, to increase the material's permeability to oxygen, allows for intact islets to function in lower oxygen environments and is most beneficial to capsules containing aggregates at high tissue loadings.

3.3.3 Planar Device

Oxygen profiles and predictions of fractional viability and fraction of normal insulin secretion were made for single cells, aggregates, and islets in planar devices. For most calculations device thickness was 500-μm. These calculations were performed because we also wanted to investigate the effectiveness of both methods, the use of aggregates and incorporation

of a PFC emulsion into an immunoisolating device, to enhance oxygen transport to encapsulated islets in the other commonly used immunoisolation system – an extravascular planar device. It is important to assess that the benefits of each method to enhance oxygen transport that were observed in microcapsules also translate to different geometries, and to assess under what circumstances in a planar diffusion chamber each type of oxygen enhancement strategy is the most beneficial. A planar device is typically implanted in a location (such as the subcutaneous space) in which the exterior of the device will be in close contact with the vasculature. There are even some planar diffusion chambers that have been developed in which the external membrane of the device becomes vascularized [48]. The close proximity to the vasculature results in a partial pressure of oxygen at the device surface similar to that of venous blood as long as no foreign body reaction occurs. The first set of calculations performed assumed that the device surface P_{O2} was 40 mmHg, the oxygen level in venous blood.

Oxygen profiles were calculated for a range of tissue sizes – 37.5, 50, 75, 100 and 125-μm aggregates and 150-μm islets in one centrally located monolayer of tissue with a device surface oxygen level of 40 mmHg at either a tissue surface density of 500 (Figure 3-14) or 2000 IE per cm^2 (Figure 3-15). At 500 IE per cm^2 the portion of the tissue that is blue and is thus severely oxygen limited increases with increasing tissue size in normal alginate devices (Figure 3-14A) and PFC alginate devices (Figure 3-14B). The oxygen gradient within the alginate subdomain is greater in the normal alginate devices showing that PFC alginate is an effective permeability enhancer in a planar device by reducing oxygen gradients within the encapsulating material. At 2000 IE per cm^2 (Figure 3-15A) for the smallest tissue presented, 75-μm aggregates, in normal alginate it is observed that because the tissue spheres are so close together the oxygen profile begins to approximate that of a slab. Even though the overall tissue densities

are the same, the fractional surface coverage is higher (0.7) for the 75-µm aggregates compared to the fractional surface coverage of a 150-µm islet (0.35) and thus neighboring tissue spheres have a greater influence over each others oxygen profile. At this higher tissue surface density the oxygen gradients outside the tissue are significant with and without PFC present but they are reduced in the presence of PFC alginate. The minimum oxygen level experienced by the tissue is always lower in normal alginate devices. Observing these oxygen profiles it becomes apparent that there are different length scales that are important in different regimes – the tissue diameter, spacing between capsules and the distance the tissue is from the capsule surface.

The predictions of fractional viability and fraction of normal insulin secretion as a function of tissue surface density in islet equivalents per centimeter squared, center to center tissue spacing, and fractional surface coverage for a range of tissue sizes – 37.5, 50, 75, 100 and 125-µm aggregates and 150-µm islets in one centrally located monolayer of tissue with a device surface oxygen level of 40 mmHg are shown in Figure 3-16. The maximum tissue surface density that can be achieved depends on the tissue diameter. The maximum tissue surface density is lower for 50-µm aggregates (1400 IE/cm^2) in a cubic array where the spheres are touching compared to 4400 IE/cm^2 for 150-µm islets. 37.5 and 50-µm aggregates are fully viable and functional at all tissue loadings achievable with a monolayer of tissue. Tissue with a diameter of 150-µm arranged in a monolayer is not fully functional even at very low densities but it is fully viable. The predicted fractional viability is always better for the smaller aggregates at any loading density. As the tissue diameter decreases from 125 to 100 to 75-µm the tissue remains fully functional up to a surface density of 500, 1000, and 1200 IE/cm^2 respectively. However, with decreasing tissue diameter, at the surface density where oxygen limitations begin to effect insulin secretion the decrease in function is steeper with increased tissue loading. The

steeper decrease in predicted fraction of normal insulin secretion is because the smaller the tissue is, the closer the tissue spheres are together and thus they have more interaction and greater decreases in the oxygen profile. Aggregates arranged in a monolayer within a planar diffusion chamber are able to maintain function at higher tissue surface densities than a 150-µm islet, but the predictions show that one should be cautious to not enter the regime where oxygen limitations do occur for the smaller aggregates as the aggregates could secrete insulin less effectively than an intact islet. Instead of plotting the predictions of fractional viability and fraction of normal insulin secretion versus tissue density in IE/cm^2 the results were plotted as a function of the center to center spacing in number of tissue diameters (Figure 3-16C,D) and fractional surface coverage (Figure 3-16E,F). The results plotted in this fashion demonstrate that the smaller the tissue diameter is the closer the tissue spheres can be brought to each other before there are detrimental effects on viability and insulin secretion (Figure 3-16C,D). Additionally the smaller tissue can cover a greater fraction of the device surface before there is loss of viability or function (Figure 3-16E,F).

Figure 3-17 is a plot of the predicted fraction of normal insulin secretion versus the device tissue surface density in islet equivalents per square centimeter for 50-µm aggregates, 75-µm aggregates, or 150-µm islets in a planar device of alginate with or without 70% (w/v) PFC emulsion at a device surface P_{O2} of 40 mmHg. The calculations were performed for three to ten layers of 50-µm aggregates, 1,3-6 layers of 75-µm aggregates, and 1 or 3 layers of 150-µm islets arranged in a body centered cubic array. Devices made from normal alginate maintained 100% insulin secretion for tissue densities up to 2,500-3,000 IE/cm^2 for 50-µm or 75-µm aggregates (3-6 layers) depending on the number of tissue layers within the device. Full insulin secretion capacity is maintained in PFC alginate devices that contain 50-µm or 75-µm aggregates

at surface densities up to 6,000 IE/cm^2. At a particular tissue surface density the results are quite similar for all numbers of tissue layers for 50-μm aggregates in normal alginate devices as all the results fall within one serpentine band. The reason that the serpentine behavior is observed is that the aggregates are discrete entities throughout the device thickness and the undulations occur as an additional aggregate is effected by experiencing reduced insulin secretion. For the maximum number of layers that can be observed for 50-μm aggregates the serpentine behavior is not observed as the tissue layers are close enough together that they behave as a continuous phase. The results for different numbers of layers are indistinguishable from each other for devices that contain 50 or 75-μm aggregates in 70% (w/v) PFC emulsion. At a device surface P_{O2} of 40 mmHg it is very beneficial to incorporate PFC emulsion into the alginate phase of a device that contains 50 or 75-μm aggregates in order to maintain tissue function at higher tissue densities. Although the tissue surface densities at which function is lost are similar for 75-μm aggregates there appears to be a transition in the normal alginate devices that above this level the results are not the same for the different number of layers. The serpentine behavior is not observed most likely because the oxygen transport within the aggregate has become more limiting. The predictions of fraction of normal insulin secretion are quite different for an islet containing planar device than they are for the aggregates (Figure 3-17C). There is a larger difference between having 1 and 3 layers of tissue within the device and there are still large differences in the number of layers when PFC emulsion is used. The incorporation of PFC emulsion into a planar device with any size tissue or number of layers is very beneficial in order to improve tissue function at higher loading densities.

Prediction of fractional viability and fraction of normal insulin secretion were made for the homogeneously distributed tissue in a planar device with increasing tissue loading and

compared to the predicted results for 13 layers of 37.5-μm aggregates and 3 layers of 150-μm islets (Figure 3-18). For predictions of fractional viability and insulin secretion there are conditions under which the homogeneously distributed tissue does worse than either 37.5-μm aggregates or islets in either normal alginate or PFC alginate planar devices. This indicates that Maxwell's Equation and the homogenous assumption are not an accurate approximation to model single cells at high tissue loadings especially in the presence of PFC alginate. The inaccuracies are greater in the PFC containing devices because there is a greater difference between the permeability of PFC alginate and tissue compared to normal alginate and tissue. When the tissue is modeled as discrete elements within PFC alginate a greater permeability enhancement can be obtained and increasing the tissue density does not decrease the effective permeability of the alginate phase.

The predictions of fraction of normal insulin secretion as a function of device tissue surface density for an external device oxygen level of 40 mmHg over a range of tissue sizes and for a device with and without PFC that containing the maximum number of layers that would fit within in a 500-μm thick device are shown in Figure 3-19. This corresponds to 13, 10, 6, 5, 4, and 3 layers of tissue for 37.5, 50, 75, 100, 125 and 150-μm diameter tissue respectively. It is predicted that the smallest aggregate sizes (37.5 and 50-μm) behave nearly identical when the tissue surface density is increased. As the tissue diameter increases above 50-μm the tissue begins to have slightly worse function at similar tissue densities. The tissue is no longer fully functional at loadings of 2000, 1500, and 750 IE/cm^2 for 75, 100, and 125-μm aggregates respectively compared to being fully functional at up to 2500 IE/cm^2 for 37.5 and 50-μm aggregates. As the tissue surface density gets higher, above 4000 IE/cm^2, the results for all tissue sizes become quite similar in normal alginate devices. There is a shift of all curves for all

tissue sizes for devices that contain 70% (w/v) PFC emulsion such that the incorporation of PFC into the device allows for function at much higher tissue densities.

Following the analysis of oxygen effects on tissue function at different surface densities at a given device surface oxygen level of 40 mmHg, the effects of lowering the device surface oxygen level below 40 mmHg were examined. Theses calculations were performed for a tissue surface density of 150, 1000, 2000, and 7272 IE/cm^2 for all tissue sizes (37.5, 50, 75, 100, 125-μm aggregates and 150-μm islets) using the maximum number of tissue layers for each tissue size as used for the predictions in Figure 3-19. Plots of the predictions of insulin secretion as a function of device surface P_{O2} for all tissue sizes are shown in Figure 3-20. At the lowest device loading (150 IE/cm^2 Figure 3-20A) the use of smaller aggregates had the largest effect on improving insulin secretion in low oxygen environments. As the tissue density increased to 1000 and 2000 IE/cm^2 (Figure 3-20B,C) there were still benefits of using smaller aggregates but they were not as great. At the very high tissue density of 7272 IE/cm^2 (Figure 3-20D) there were nearly no benefits of using aggregates as the predictions of fractional viability were low even at 40 mmHg and there were nearly no differences in the predictions for different tissue sizes. Aggregates can be beneficial to increasing tissue function in low oxygen environments, but within normal alginate devices they have the greatest impact at low tissue densities.

The same calculations as shown in Figure 3-20 were repeated with the addition of PFC emulsion into the alginate phase of the device. The predictions of insulin secretion for select tissue sizes (37.5, 75, and 150-μm) with and without PFC are shown in Figure 3-21 as a function of device surface P_{O2} for device with a tissue surface density of 150, 1000, 2000, and 7272 IE/cm^2. At all tissue densities there are similar benefits to incorporating PFC emulsion into planar devices that contain 150-μm islets. It is predicted for the smaller tissue sizes (37.5 and

75-μm) there are always benefits to adding PFC emulsion to the device in order to maintain function in low oxygen environments. As the loading density increases for 37.5 or 75-μm aggregates the curves for predicted levels of insulin secretion shift to the right indicating the function is not maintained in as low of oxygen environments. PFC emulsion has the biggest impact in improving insulin secretion at low oxygen at the intermediately high tissue density of 2000 IE/cm^2 by shifting the curves to the greatest extent. PFC has the biggest impact at intermediate loadings where the tissue is relatively close together such that reduction in external gradients is very beneficial but when the gradients are too severe, there is only so much that a permeability enhancer can do.

Up until this point only a planar device that has a thickness of 500-μm has been examined, it also desirable to see what effects decreasing and increasing the device thickness can have on predictions of fraction of normal insulin secretion. Predictions for fraction of normal insulin secretion were made for 50-μm aggregates in a 250, 500, and 1000-μm device consisting of 5, 10 and 20 layers of tissue respectively (Figure 3-22). Predictions for fraction of normal insulin secretion were made for the three different device sizes as a function of increasing tissue density at a device surface P_{O2} of 40 mmHg (Figure 3-22A) or over a range of device surface P_{O2} at a tissue surface density of 1000 IE/cm^2 (Figure 3-22B). The smaller the device thickness the higher the tissue density that can be achieved before tissue function begins to be lost and there are always benefits to incorporating PFC emulsion into the device. Similarly the thinner device is able to maintain tissue function in lower oxygen environments than the larger device when normal alginate is the encapsulating material. There are benefits to incorporation of a PFC emulsion into the planar device for all thicknesses but it has the largest impact for the 1000-μm

device. It is always detrimental to increase the device thickness of a planar device but PFC emulsion can help to improve oxygen transport when the use of thicker device is necessary.

3.3.4 Comparison of Microcapsules and Planar Devices

Thus far the analysis has focused on microcapsules and planar devices individually and it has been demonstrated that aggregates and PFC emulsion are beneficial in promoting tissue survival and function at higher densities and in lower oxygen environments. It also desirable to compare the results for microcapsules and planar devices at similar tissue loadings in order to assess under what situations aggregates and increased encapsulating material permeability are going to have the biggest impact on improving tissue function. Predictions of fraction of normal insulin secretion were made for one centrally located 150-μm islet in a 500-μm microcapsule and 1.2 and 9.5 IE of 50-μm aggregates which corresponds to a tissue volume fraction (ϕ_t) in the device of 0.03, 0.03, and 0.3 respectively (Figure 3-23A). Similar calculations were also performed for 150-μm islets arranged in 3 layers and 50-μm aggregates arranged in 10 layers in a 500-μm thick planar device (Figure 3-23B) at a tissue loading of 764 IE/cm^2 which corresponds to a tissue volume fraction of 0.03. Additionally calculations were performed with 10 layers of 50-μm aggregates at a loading of 2000 and 7272 IE/cm^2 which corresponds to a tissue volume fraction of 0.07 and 0.3 respectively. The predictions for the fraction of normal insulin secretion for the islet cases are very similar in Figure 3-23A and B. Aggregates at a tissue volume fraction of 0.03 or 0.3 in normal alginate do better in a microcapsule and the predictions for fraction of normal insulin secretion are much lower in a planar device at tissue volume fraction of 0.3 than the islet predictions compared to being quite similar in a microcapsule. The planar device does not allow for the achievement of such high tissue loadings through the use of aggregates. Predicted fraction of normal insulin secretion for the aggregate

cases with PFC incorporated into the encapsulating material are shown in Figure 3-23C and D respectively. PFC is always beneficial to improving aggregate function, but the benefits at the a tissue volume fraction of 0.3 are greatest in a microcapsule. The greatest benefit of PFC for the planar device is at an intermediate tissue volume fraction of 0.07.

3.4 DISCUSSION

This chapter has studied the effects of oxygen diffusion limitations to immunoisolated islets and the benefits that two methods: (1) incorporation of a perfluorocarbon emulsion into an immunoisolation device to enhance encapsulation material permeability to oxygen and (2) use of aggregates that have a smaller tissue diameter than an intact islet have on eliminating oxygen diffusion limitations. Severe oxygen limitations can occur for islets encapsulated in microcapsules and planar diffusion chambers. The use of either strategy to enhance oxygen transport, a perfluorocarbon emulsion or smaller aggregates, has beneficial effects in either type of device geometry, but there are certain configurations or conditions in which one oxygen enhancing strategy is the most beneficial.

Following the transplantation of microcapsules into the peritoneal cavity many of the capsules are likely to experience surface oxygen levels below that of the vasculature due to the likelihood of capsules being located large distances away from the vasculature. Islets within the microcapsule will likely experience oxygen levels low enough to result in tissue death and loss of insulin secretion capabilities. When single cells (the homogenous case) are encapsulated in microcapsules the cells are able to maintain function and viability in much lower oxygen environments than intact 150-μm islets. The use of smaller islet cell aggregates (37.5-75 μm) with one islet equivalent of total encapsulated tissue volume are predicted to maintain tissue function in lower oxygen environments than an intact 150-μm islet and are quite similar to those

for the homogenous single cell case. If the oxygen effects on insulin secretion are considered to be satisfactory for an intact 150-μm islet then one is able to obtain similar results with aggregates at much higher capsule loadings. The incorporation of 70% (w/v) PFC emulsion into alginate microcapsules has modest effects on enhancing 150-μm islet survival and function over a range of oxygen levels. The benefits of incorporating a permeability enhancer for single cells or aggregates (37.5-75 μm) at tissue loadings around 1 IE are negligible in order to better maintain tissue function in lower oxygen environments. It is beneficial to incorporate a permeability enhancer into aggregate containing capsules at high capsule loadings (6-10 islet equivalents) in order to have tissue function in lower oxygen environments.

Calculations have been performed for 37.5, 50, 75, 100, and 125-μm aggregates and 150-μm islets in a planar device for various numbers of layers at a device surface P_{O2} of 40 mmHg over a range of surface densities and for a tissue surface density of 150, 1000, 2000 and 7272 IE/cm^2 at a device surface P_{O2} of 0-40 mmHg. The number of layers of tissue did not greatly affect the predicted tissue function for smaller tissue sizes at a given surface density. The smaller an aggregates is, the higher the surface density that can be achieved in which the tissue will remain fully functional. In all results shown, the addition of a permeability enhancer was very beneficial to maintaining function either at higher surface densities or in lower oxygen environments especially at intermediate loading densities.

The use of smaller islet cell aggregates and a permeability enhancer in the encapsulation matrix have both been shown to be beneficial in reducing oxygen limitations to immunoisolated islets in microcapsules and planar diffusion chambers based on theoretical calculations. The effects of the two methods on enhancing oxygen transport are greatest when used in combination. For microcapsules this is at high density, for example 9.5IE of 50-μm aggregates

microencapsulated in PFC alginate. For planar diffusion chambers this is a medium density where 50-μm aggregates are using in a planar device containing PFC alginate at 2000 IE/cm^2. In the calculations that were performed, aggregates were most beneficial for eliminating oxygen transport limitations and maintaining encapsulated tissue viability and function in the microcapsule geometry. When the device surface P_{O2} was 40 mmHg in a planar diffusion chamber twice the amount of tissue could be kept fully functional when 70% (w/v) perfluorocarbon is incorporated into the alginate matrix. When direct comparisons were made between microcapsules and planar diffusion chambers it was seen that the highest tissue densities could be achieved in microcapsules as they are a more ideal geometry for oxygen transport. However, this conclusion could be slightly misleading because the microcapsules were modeled individually and thus the potential effects of capsules stacking on top of each other during transplantation were not taken into account. Capsule stacking is likely to occur as large number of capsules would be transplanted into the peritoneal cavity, ~500,000 for human islet transplantation diabetes using current transplant doses and assuming 1 islet per capsule. Capsule stacking may actually make microcapsules less favorable under the transplant setting compared to a planar device where likely only one or a handful devices would be transplanted and interactions between devices would not be important.

It is critical that the necessary amount of oxygen be delivered to immunoisolated tissue after transplantation in order to maintain normal levels of insulin secretion. Without a solution that allows for effective oxygen delivery transplantation of immunoisolated tissue will never be successful as the tissue will not be capable of effectively delivering its protein of interest. Based on theoretical predictions it seems that both strategies hold the potential to improve oxygen delivery to immunoisolated tissue and improve the success rate of cell therapies with

immunoisolation devices. Both methods – incorporation of PFC emulsion and the use of islet cell aggregates should be further evaluated experimentally for their ability to enhance encapsulated tissue survival and function both *in vitro* and *in vivo*.

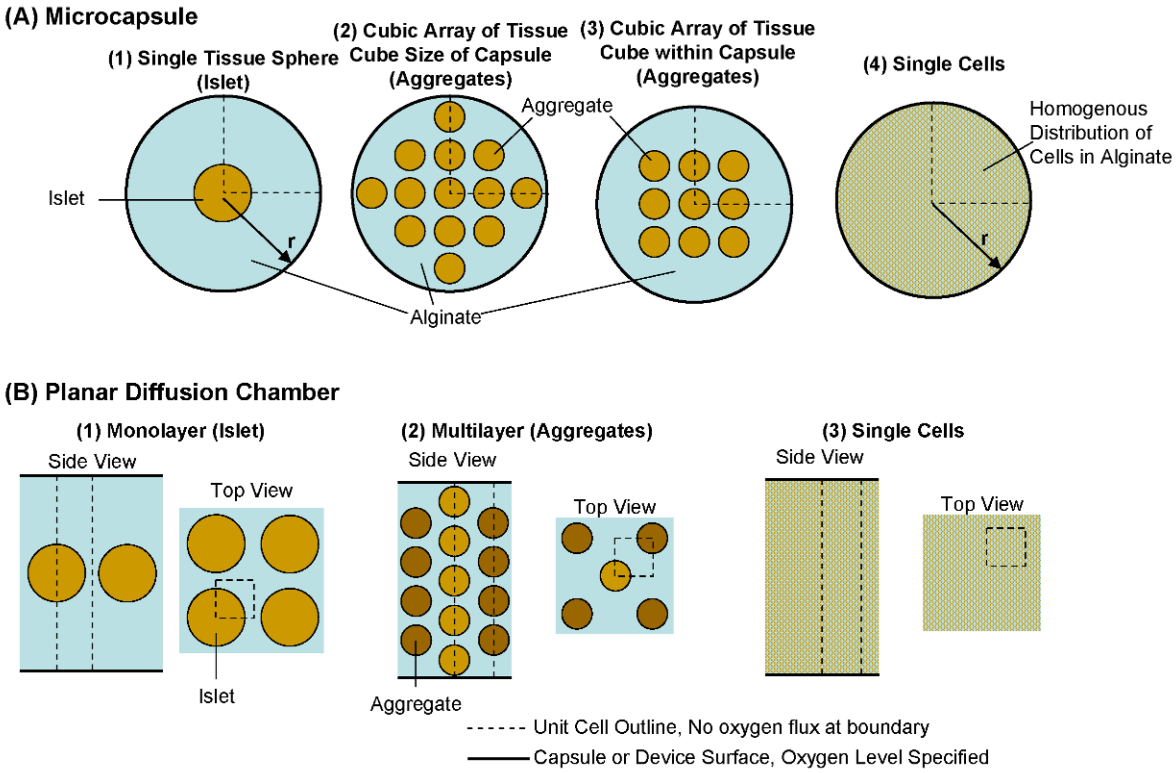

Figure 3-1: Sketches of example model geometries studied.

(A) for microcapsules and (B) for planar devices. In both A and B the geometries are sketched for an islet, many aggregates or islets, or for single cells. The dashed lines represent the unit cell that was analyzed for each geometry.

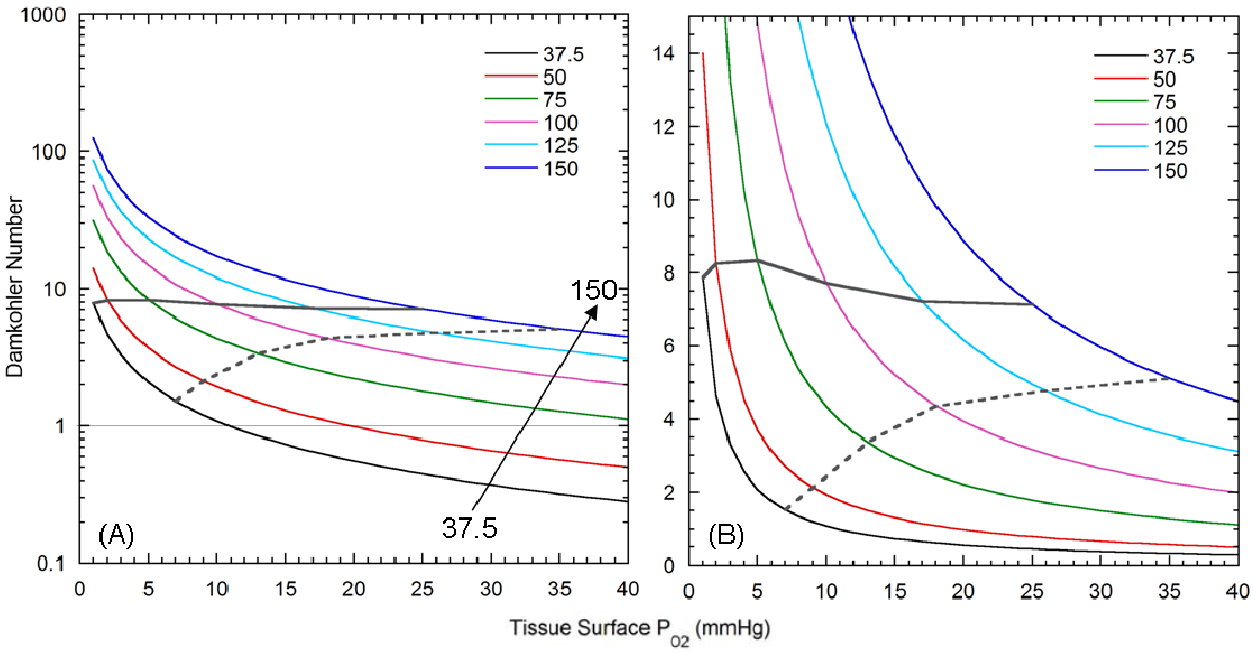

Figure 3-2: Predictions of the Damkohler number for different size tissue with a given P_{O2} at the tissue surface.

(A) predictions of the Damkohler number plotted on a semilog plot and (B) prediction of the Damkohler number plotted on a linear plot. The solid grey curve cutting across the family of curves represents the maximum value of the Damkolher number where all levels of P_{O2} are greater than P_c (0.1 mmHg) at all positions within the tissue. The dashed grey curve represents the cutoff for the Damkohler number above which all tissue is not fully functional.

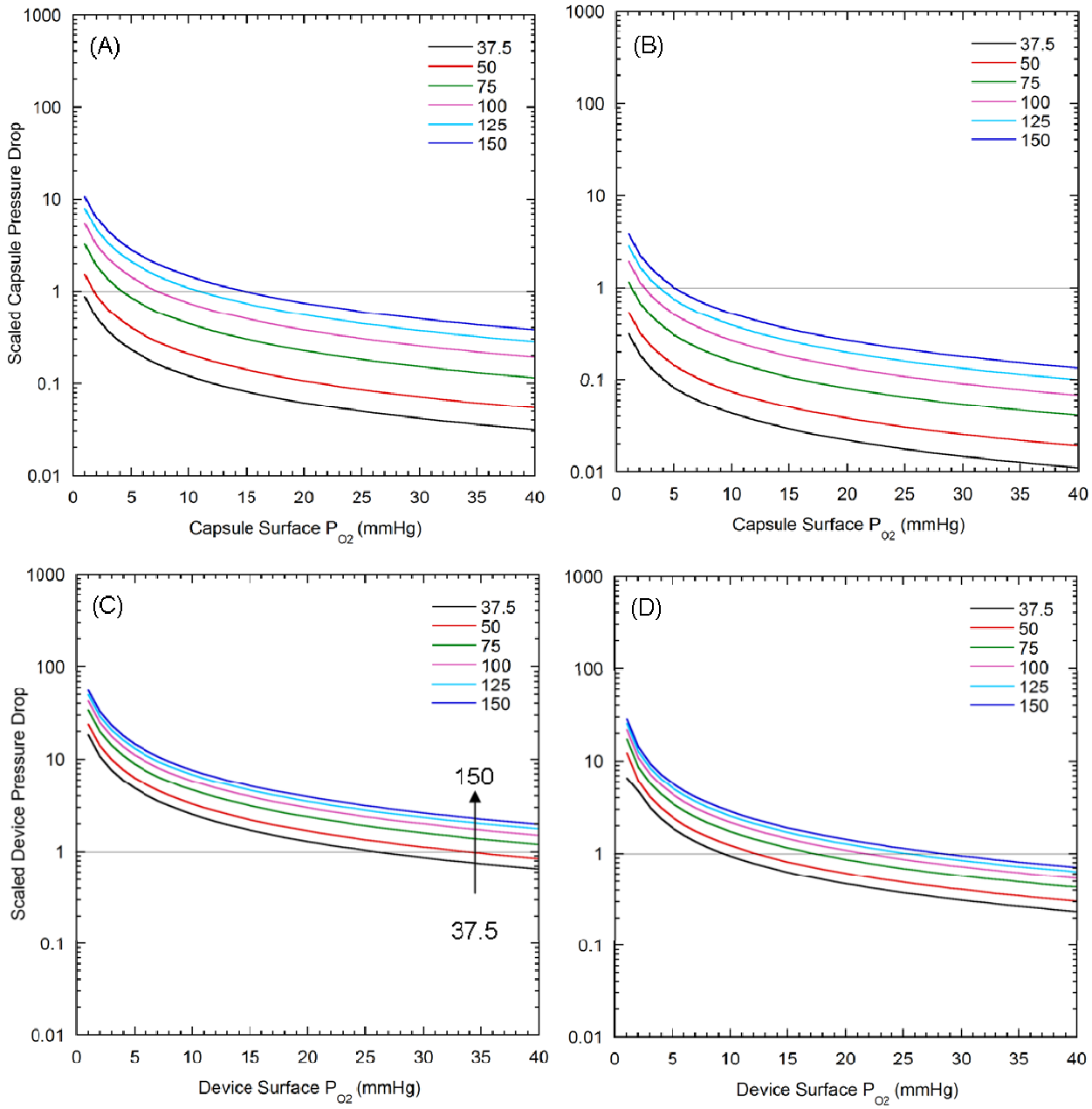

Figure 3-3: The scaled pressure drop within a capsule (A&B) or a planar device (C&D) to centrally located tissue was estimated for a range of surface P_{O2}.

A&C are the predictions for tissue in normal alginate, B&D are the predictions for tissue in PFC alginate. The predictions were made for tissue that has a diameter of 37.5, 50, 75, 100, 125, and 150-µm in a capsule or planar device of 500-µm.

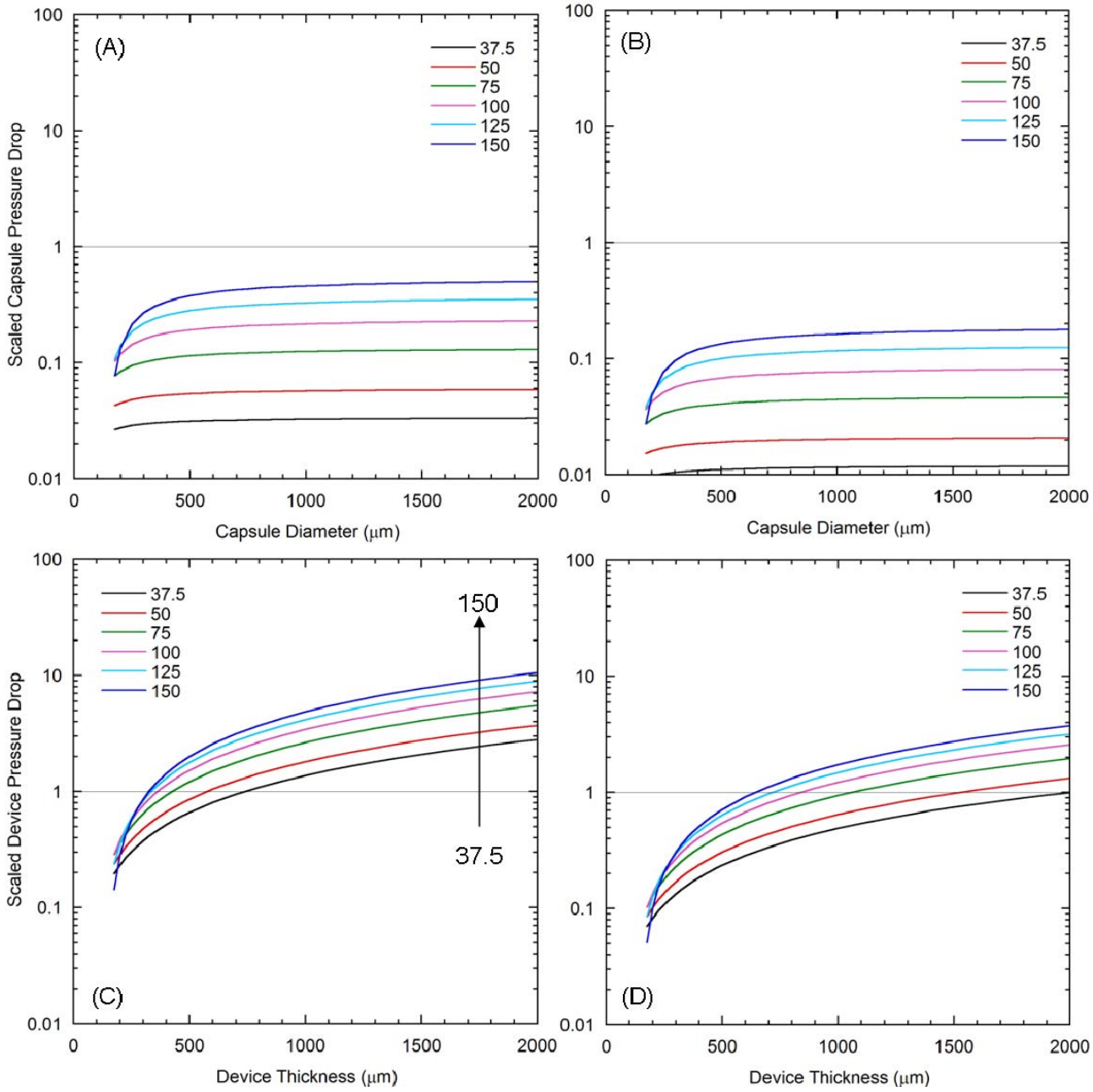

Figure 3-4: The sclaed pressure drop within a capsule (A&B) or a planar device (C&D) to centrally located tissue was estimated for a range capsule and device sizes.

A&C are the predictions for tissue in normal alginate, B&D are the predictions for tissue in PFC alginate. The predictions were made for tissue that has a diameter of 37.5, 50, 75, 100, 125, and 150-μm at a capsule or device surface P_{O2} of 40 mmHg.

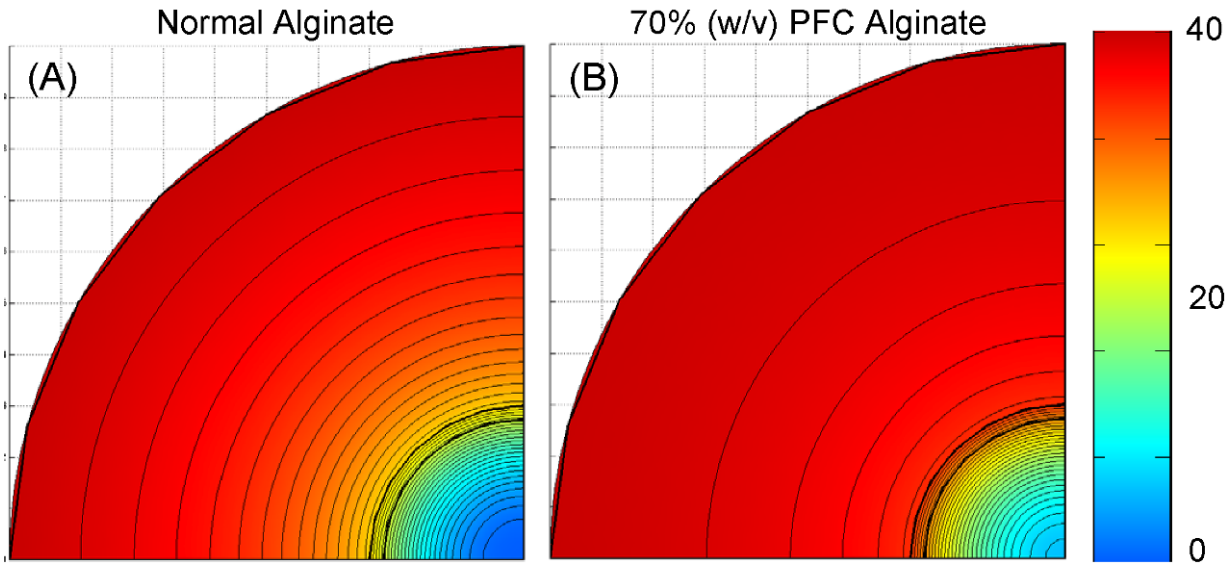

Figure 3-5: Plot of predicted oxygen profiles for a centrally located 150-µm diameter islet in 500-µm diameter microcapsules with a capsule surface P_{O2} equal to 40 mmHg.

(A) 150-µm islet in normal alginate (B) 150-µm islet in 70% (w/v) PFC alginate. Contours are drawn at 1-40 mmHg at 1 mmHg increments and at 0.1 mmHg.

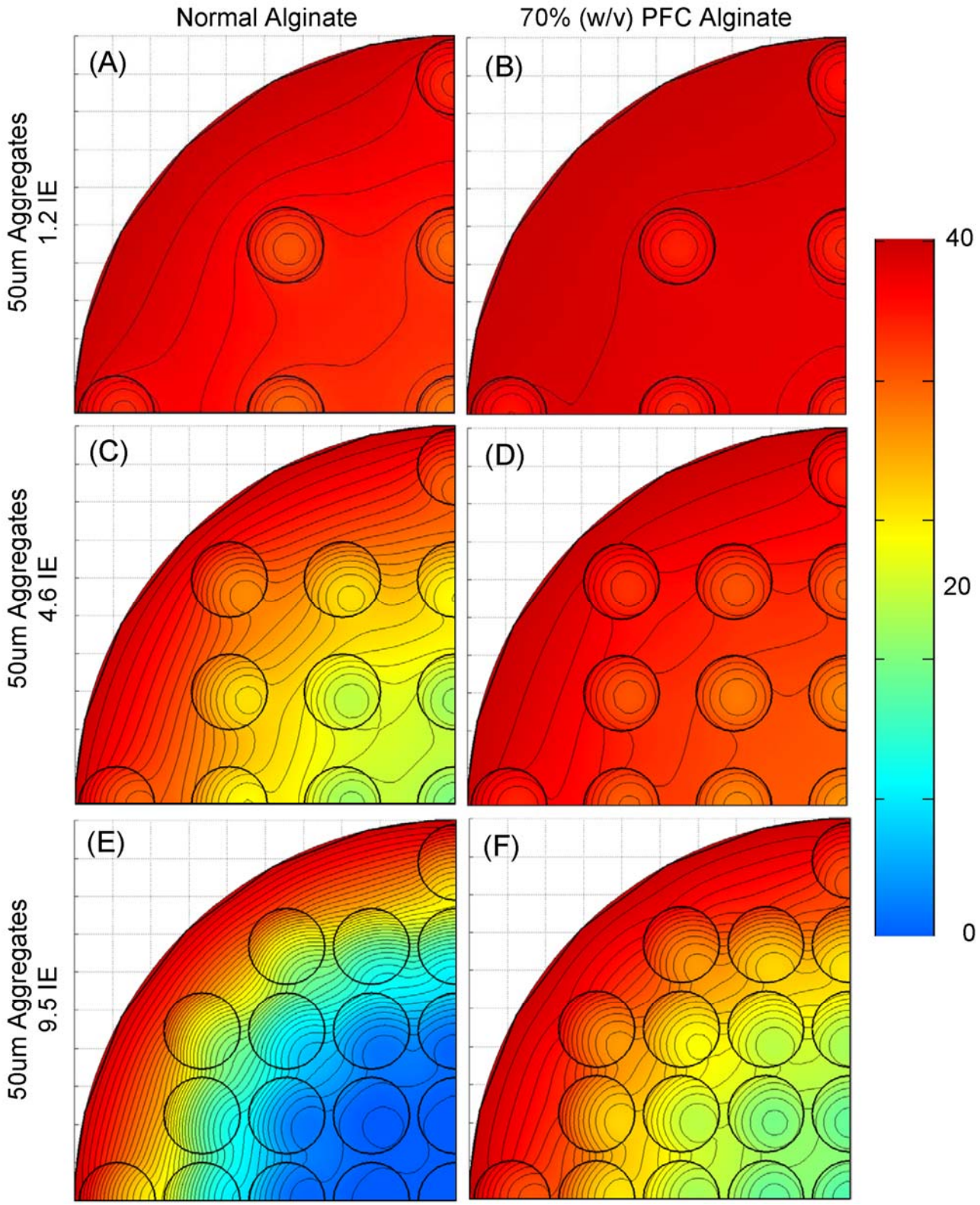

Figure 3-6: Plot of predicted oxygen profiles for 50-µm aggregates in 500-µm diameter microcapsules with a capsule surface P_{O2} equal to 40 mmHg.

(A) 1.2 IE in normal alginate (B) 1.2 IE in 70% (w/v) PFC alginate (C) 4.6 IE in normal alginate (D) 4.6 IE in 70% (w/v) PFC alginate (E) 9.5 IE in normal alginate (F) 9.5 IE in 70% (w/v) PFC alginate. IE (islet equivalents) is a volume of tissue equal to that of a 150-μm sphere. Contours are drawn at 1-40 mmHg at 1 mmHg increments and at 0.1 mmHg.

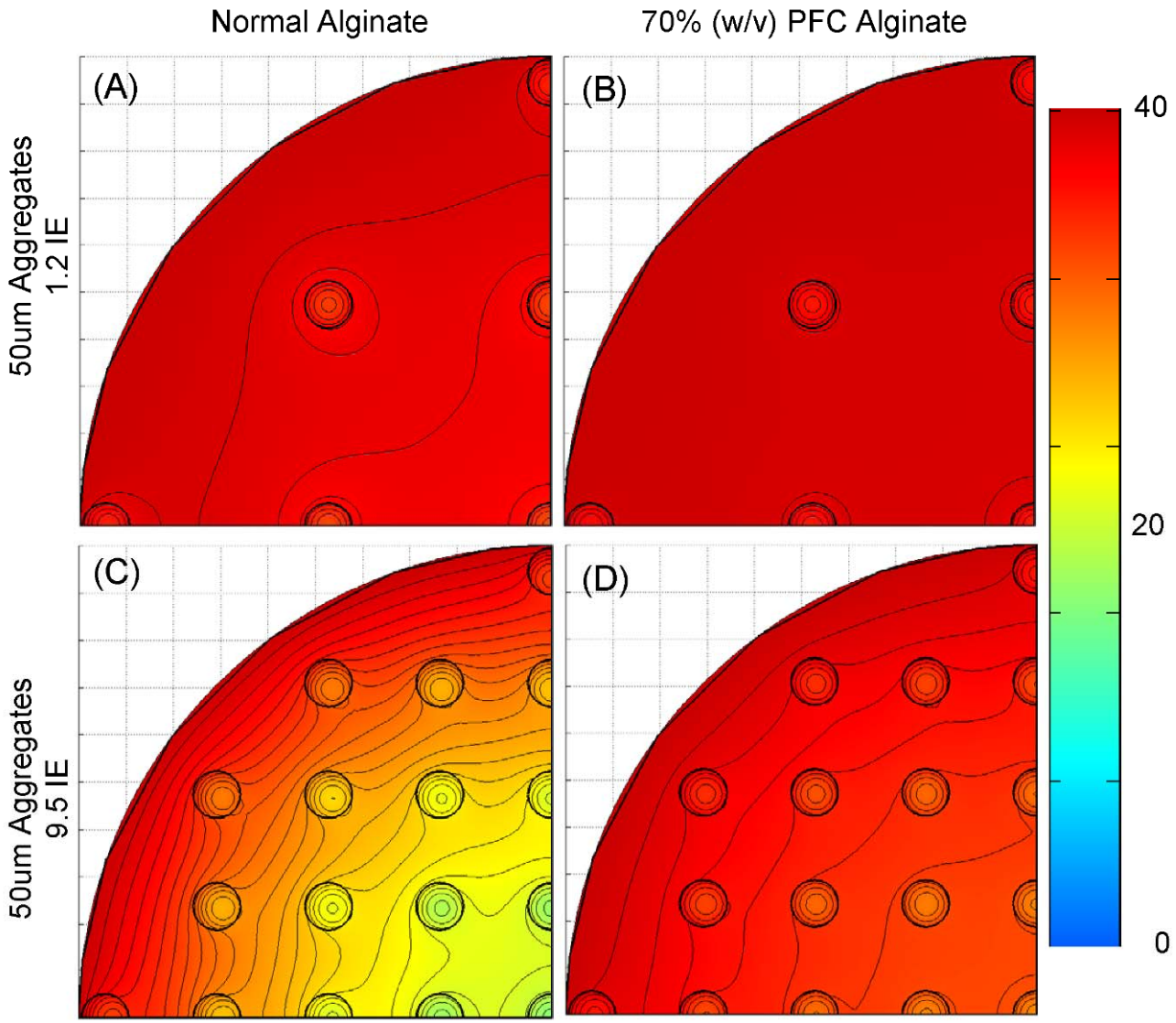

Figure 3-7: Plot of predicted oxygen profiles for 50-µm aggregates in 1000-µm diameter microcapsules with a capsule surface P_{O2} equal to 40 mmHg.

(A) 1.2 IE in normal alginate (B) 1.2 IE in 70% (w/v) PFC alginate (C) 9.5 IE in normal alginate (D) 9.5 IE in 70% (w/v) PFC alginate. IE (islet equivalents) is a volume of tissue equal to that of a 150-µm sphere. Contours are drawn at 1-40 mmHg at 1 mmHg increments and at 0.1 mmHg.

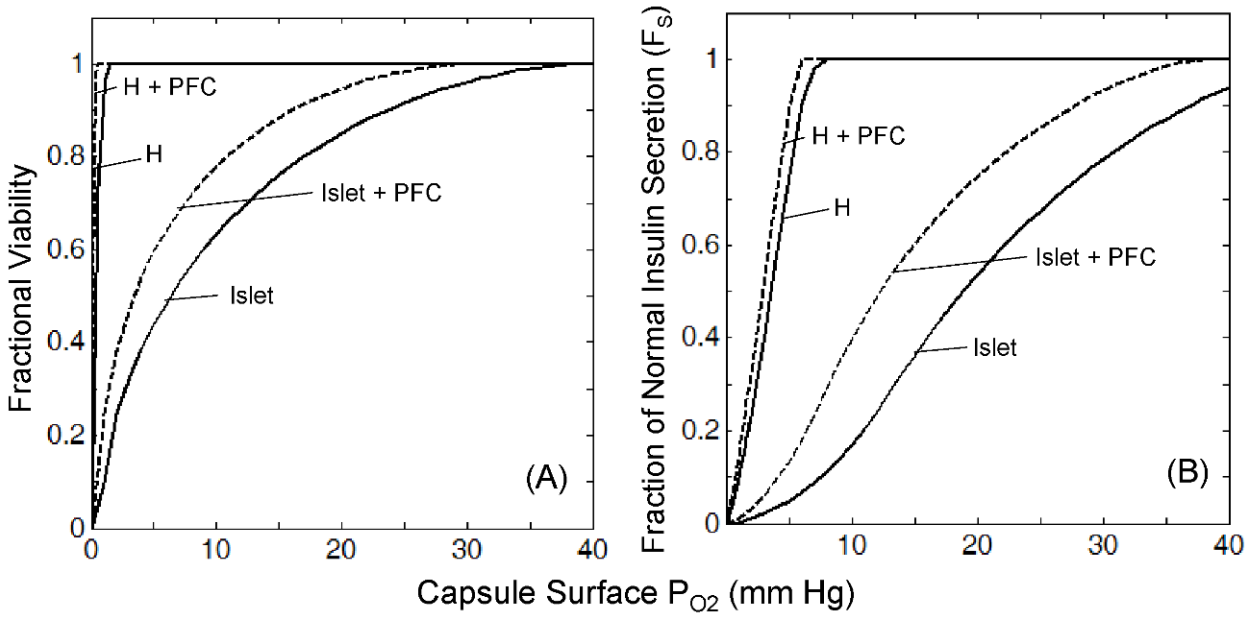

Figure 3-8: The predicted fractional viability (A) and insulin secretion (B) for an encapsulated islet or homogenously distributed tissue (H) in a 500-µm capsule.

Total encapsulated volume is one islet equivalent with and without 70% (w/v) PFC emulsion. The homogenous case is meant to be an approximation of the case for single cells distributed throughout the entire capsule.

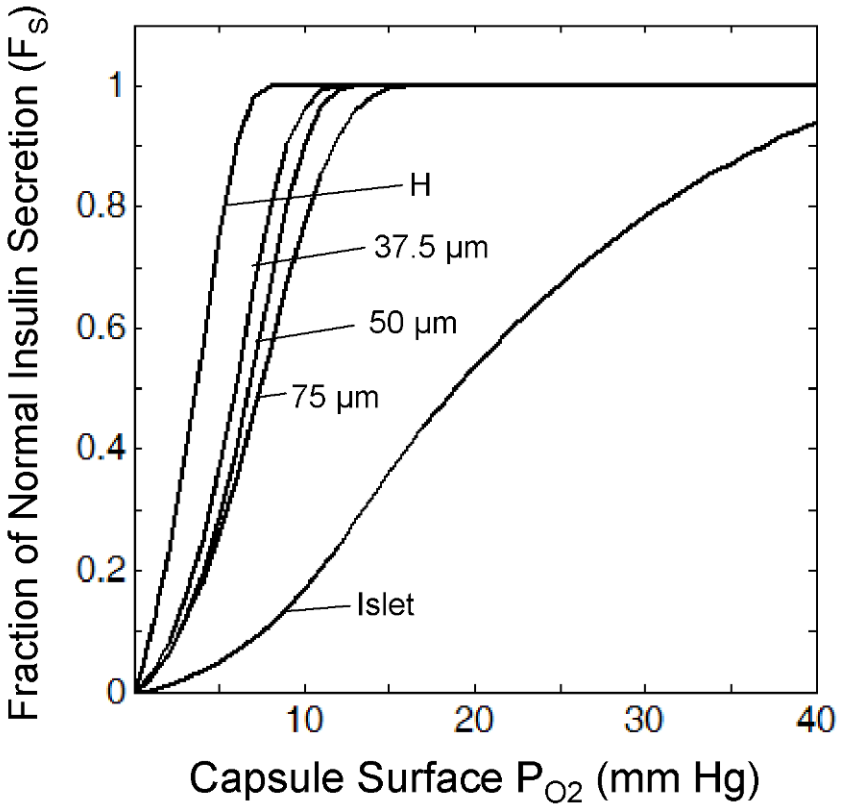

Figure 3-9: Predicted fraction of normal insulin secretion as a function of capsule surface P_{O2} for a 500-µm capsule that contains one islet equivalent - homogeneously distributed throughout the capsule (H), as 64 37.5-µm aggregates , 27 50-µm aggregates, 8 75-µm aggregates, or 1 150-µm islet.

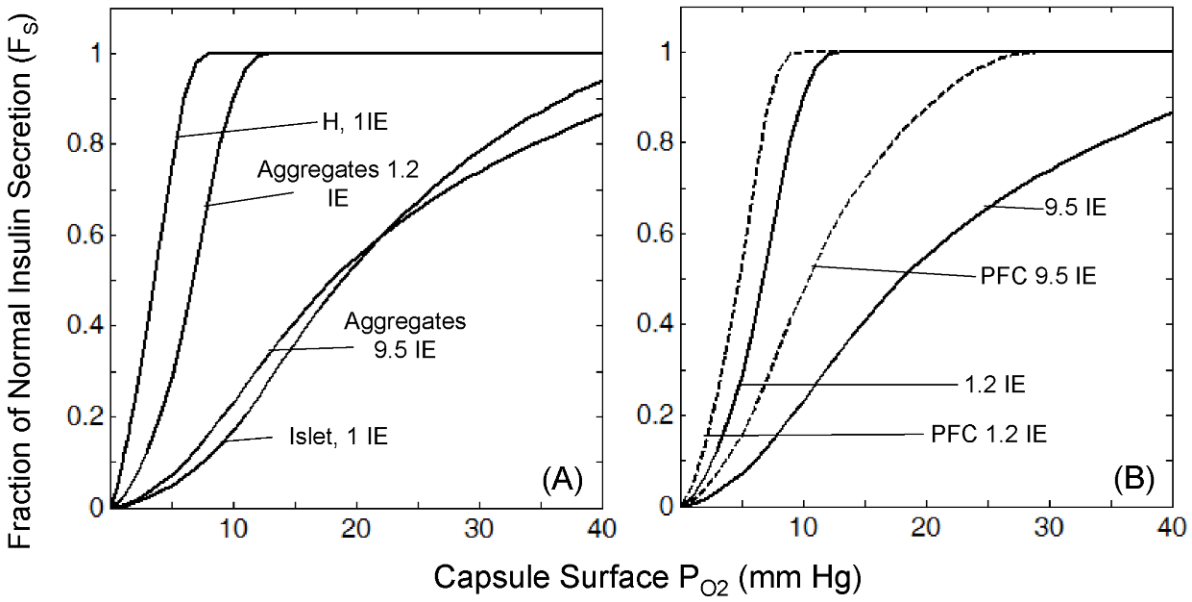

Figure 3-10: Predicted fraction of normal insulin secretion for single cells (H), an islet, and 50-µm aggregates at various loadings in a 500-µm capsule.

(A) Alginate capsules (B) 50-µm aggregates at various loadings in a capsule containing 70% (w/v) PFC emulsion. IE = islet equivalent

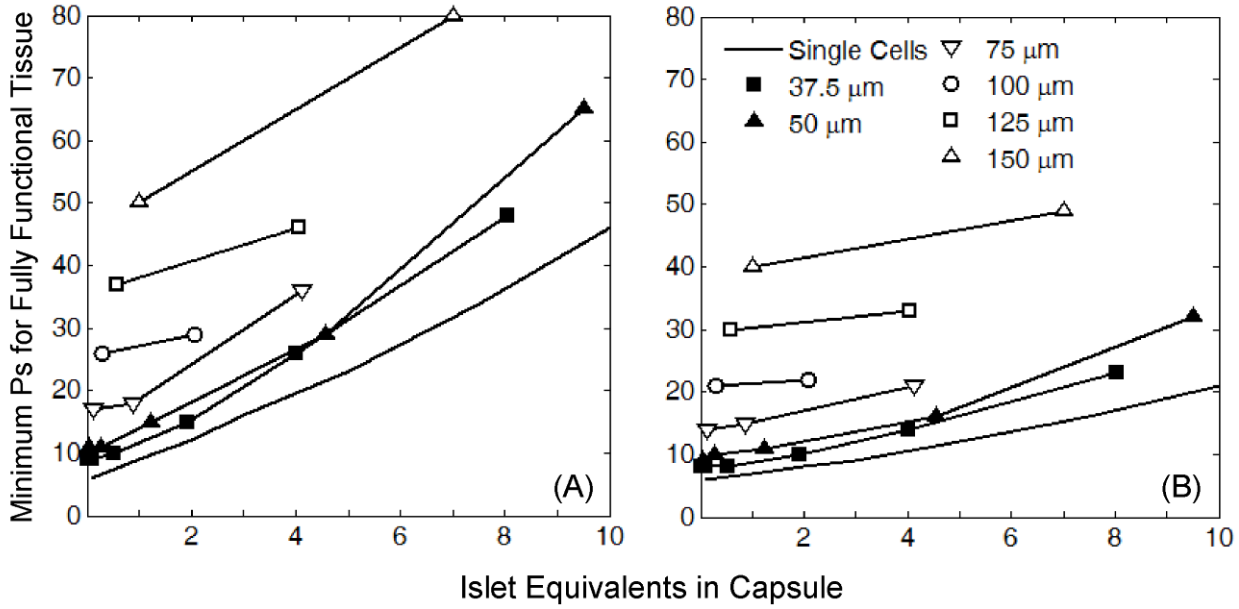

Figure 3-11: Predictions of the minimum capsule surface oxygen level that results in all encapsulated tissue being fully functional for a 500-μm capsule.

(A) Results for a variety of tissue sizes and capsule loadings for normal alginate capsules (B) results for a variety of tissue sizes and capsule loadings for 70% (w/v) PFC alginate capsules.

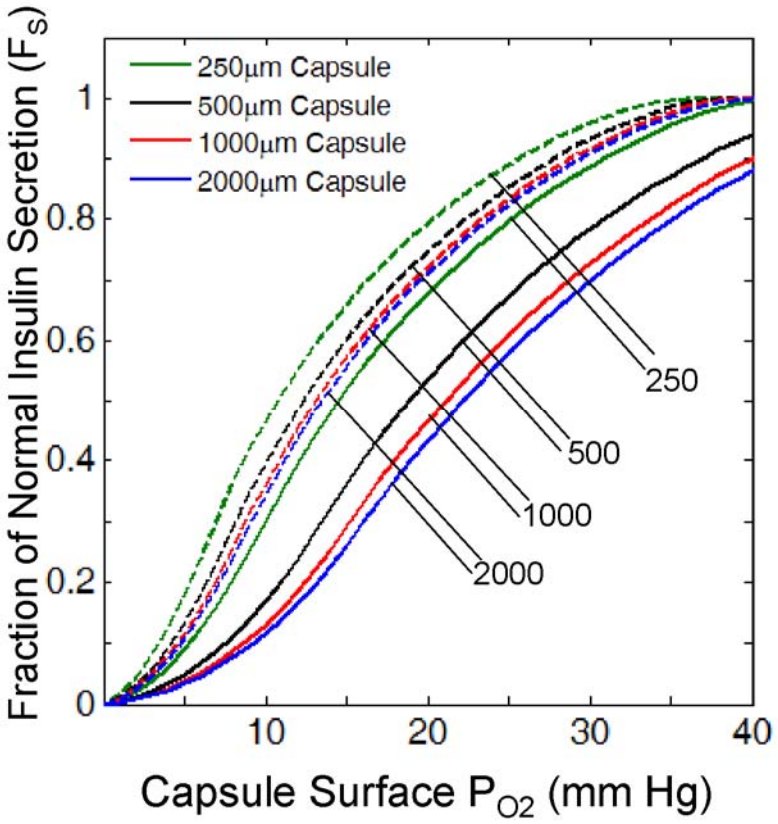

Figure 3-12: Predictions of fraction of normal insulin secretion for one centrally located islet in a 250, 500, 1000, or 2000-μm capsule with (dashed lines) and without (solid lines) 70% (w/v) PFC emulsion.

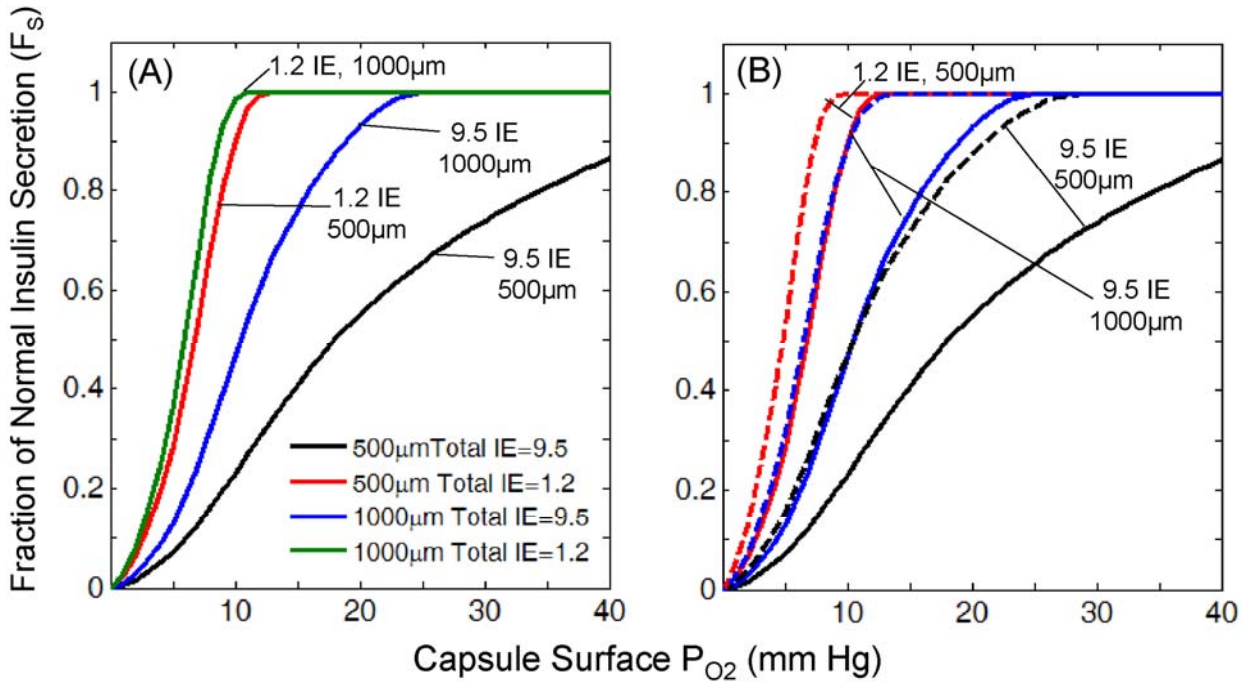

Figure 3-13: Predictions of fraction of normal insulin secretion for 50-µm aggregates in either a 500-µm or 1000-µm diameter capsule.

(A) Normal alginate capsule (B) normal alginate (solid curves) and 70% (w/v) PFC alginate (dashed curves).

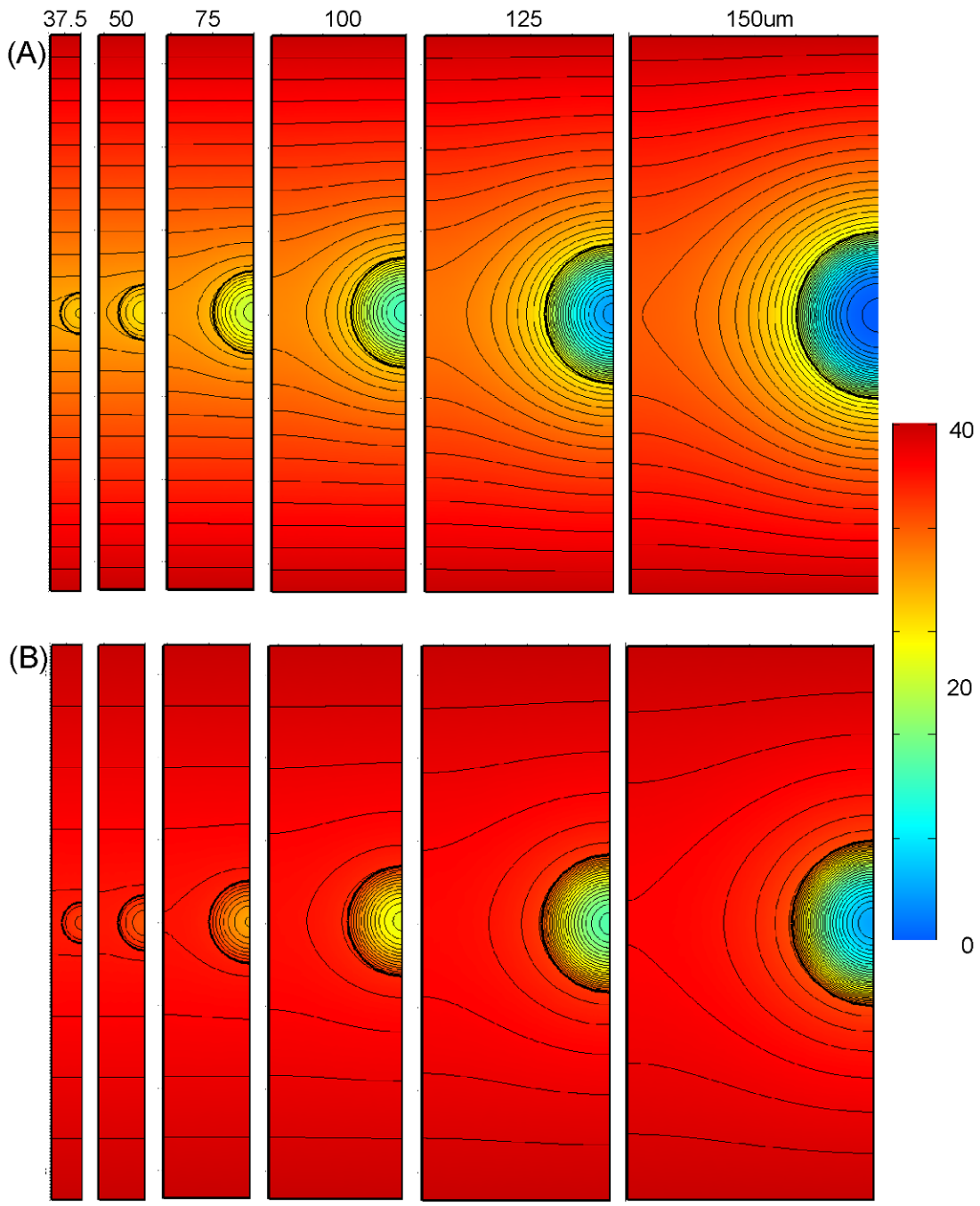

Figure 3-14: Predicted oxygen profiles in 500-µm planar devices with tissue of different sizes (37.5, 50, 75, 100, 125, 150 µm) arranged in a monolayer at the center of the device. The tissue surface density is 500 IE per cm^2, the device surface P_{O2} is 40 mmHg (A) normal alginate device and (B) 70% (w/v) PFC alginate device. Contours are drawn at 1-40 mmHg at 1 mmHg increments and at 0.1 mmHg.

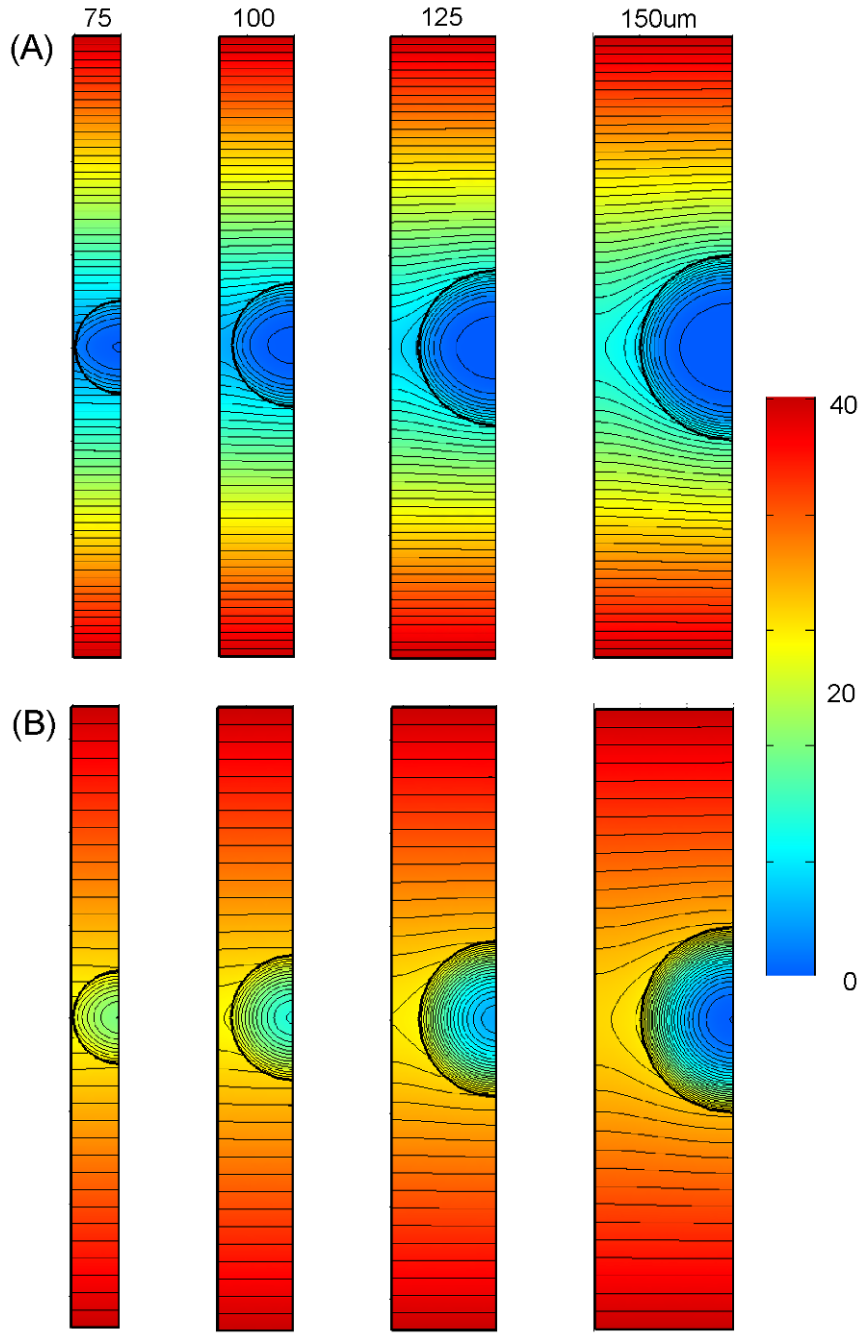

Figure 3-15: Predicted oxygen profiles in 500-μm planar devices with tissue of different sizes (75, 100, 125, 150 μm) arranged in a monolayer at the center of the device.

The tissue surface density is 2000 IE per cm^2, the device surface P_{O2} is 40 mmHg (A) normal alginate device and (B) 70% (w/v) PFC alginate device. Contours are drawn at 1-40 mmHg at 1 mmHg increments and at 0.1 mmHg.

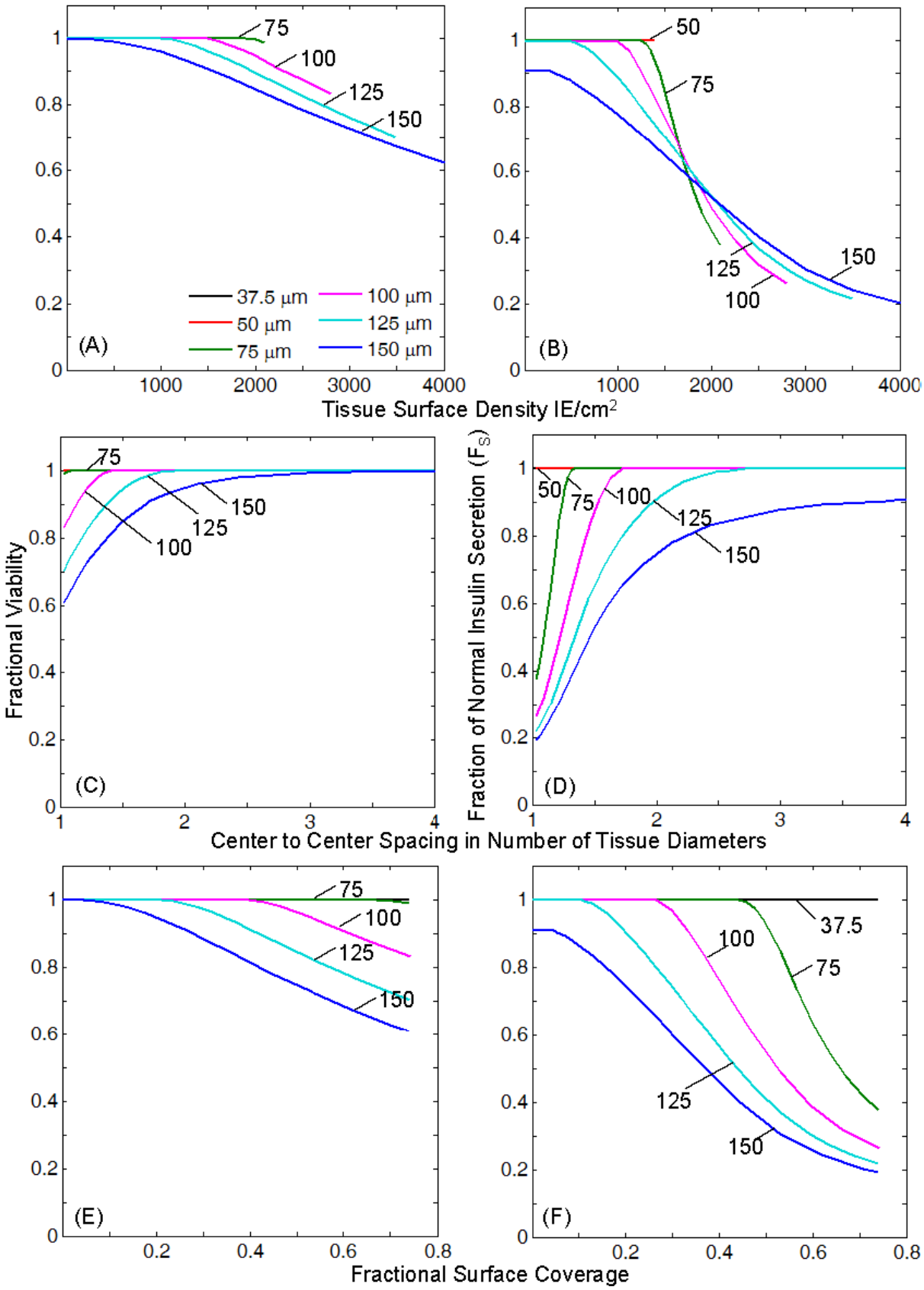
(A)
(B)
(C)
(D)
(E)
(F)
75
100
125
150
50
37.5 µm
50 µm
75 µm
100 µm
125 µm
150 µm
Tissue Surface Density IE/cm2
Fractional Viability
Fraction of Normal Insulin Secretion (FS)
Center to Center Spacing in Number of Tissue Diameters
Fractional Surface Coverage
37.5

Figure 3-16: Predictions of fractional viability (A,C,E) and fraction of normal insulin secretion (B,D,F) for tissue arrange in a monolayer in the central plane of a 500-μm device at varying densities.

Device surface oxygen level equals 40 mmHg. Encapsulation material is normal alginate. (A,B) device loading measured in IE/cm2 (C,D) device loading measured in center to center tissue spacing in number of tissue diameters (E,F) device loading measured by fractional surface coverage.

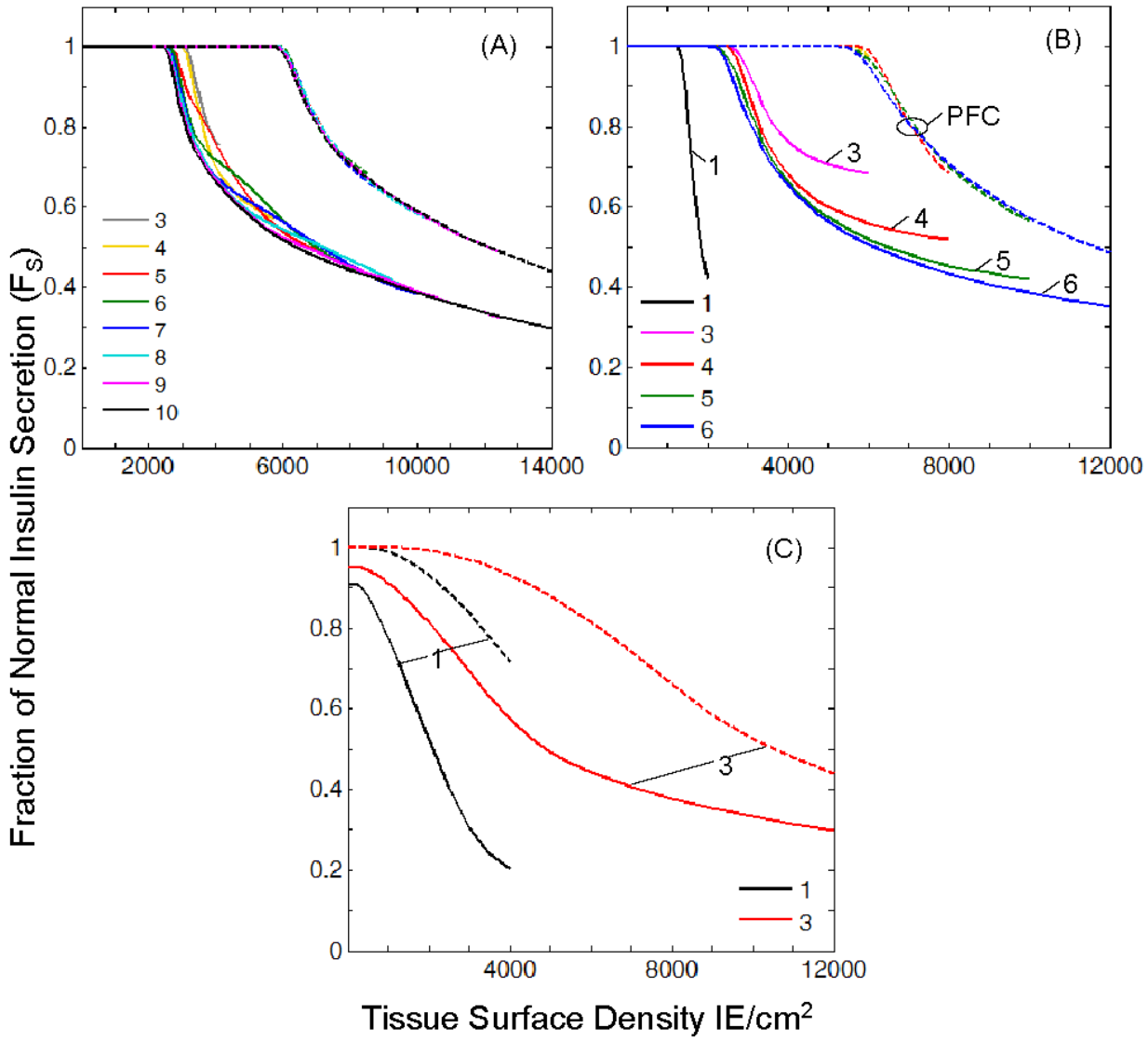

Figure 3-17: Predictions of the fraction of normal insulin secretion for 50-µm aggregates, 75-µm aggregates, and 150-µm islets in a 500-µm planar device.

The device surface oxygen level is 40 mmHg and the tissue within the device is arranged in multiple layers. (A) 50-µm aggregates in 3-10 layers (B) 75-µm aggregates in 1,3-6 layers (C) 150-µm islets in 1 and 3 layers The solid lines are for the predictions in normal alginate devices and the dashed lines are the predictions for 70% (w/v) PFC alginate devices.

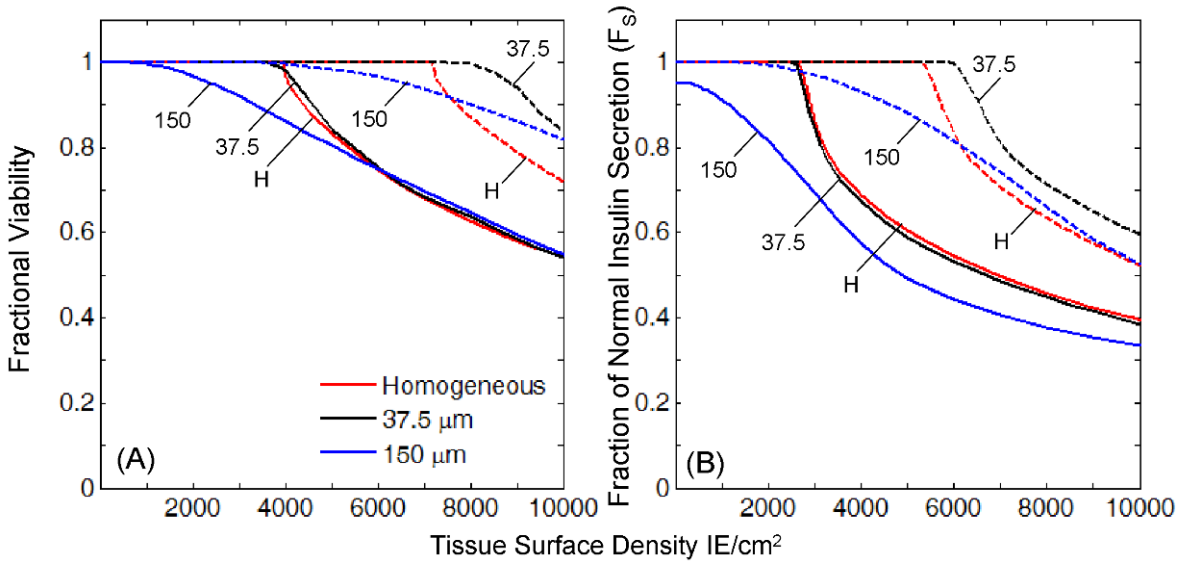

Figure 3-18: Predictions of fractional viability (A) and fraction of normal insulin secretion (B) for homogenously distributed tissue (H), 13 layers of 37.5-µm aggregates, and 3 layers of 150-µm islets in a 500-µm device made of normal alginate (solid curves) and 70% (w/v) PFC alginate (dashed curves) with a device surface P_{O2} of 40 mmHg.

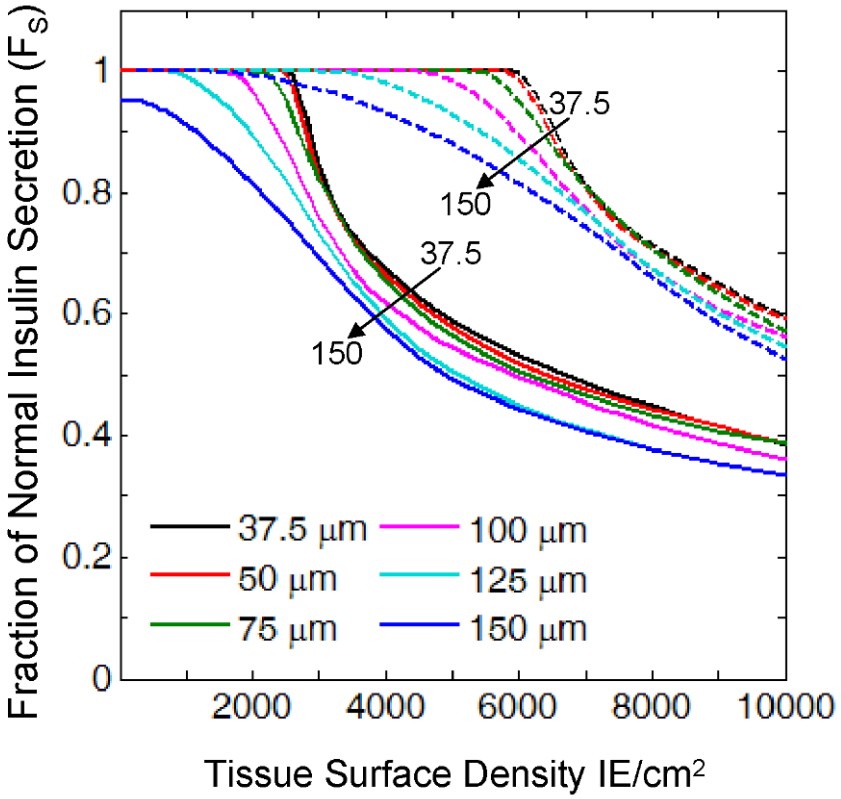

Figure 3-19: Fraction of normal insulin secretion as a function of tissue surface density for tissue of a variety of sizes with tissue arranged in multiple layers throughout the device thickness. The number of which being the maximum number that will fit for a particular size - 37.5-µm 13 layers, 50-µm 10 layers, 75-µm 6 layers, 100-µm 5 layers, 125-µm 4 layers, and 150-µm 3 layers. Device surface P_{O2} equals 40 mmHg and device thickness equals 500-µm. The solid lines are the predictions for normal alginate the dashed lines are the predictions for 70% (w/v) PFC alginate.

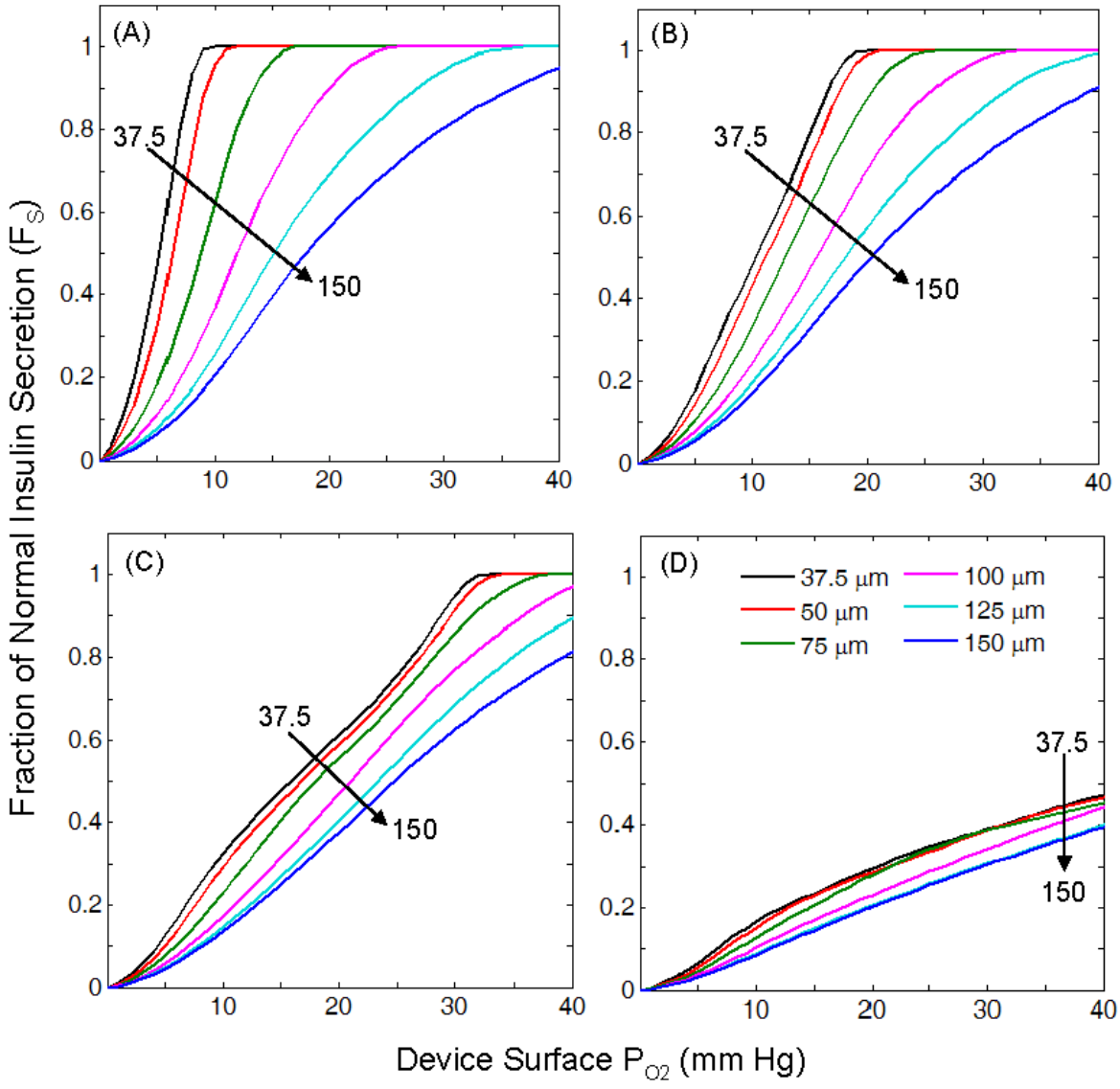

Figure 3-20: Predictions of fraction of normal insulin secretion over a range of device surface P_{O2} for tissue of a variety of sizes arranged in multiple layers within a planar diffusion chamber. The number of layers used is the maximum that would fit for a particular tissue size – 37.5-µm 13 layers, 50-µm 10 layers, 75-µm 6 layers, 100-µm 5 layers, 125-µm 4 layers, and 150-µm 3 layers. The device is 500-µm thick and made of normal alginate. The tissue device surface density was equal to (A) 150 IE/cm^2, (B) 1000 IE/cm^2, (C) 2000 IE/cm^2, and (D) 7272 IE/cm^2.

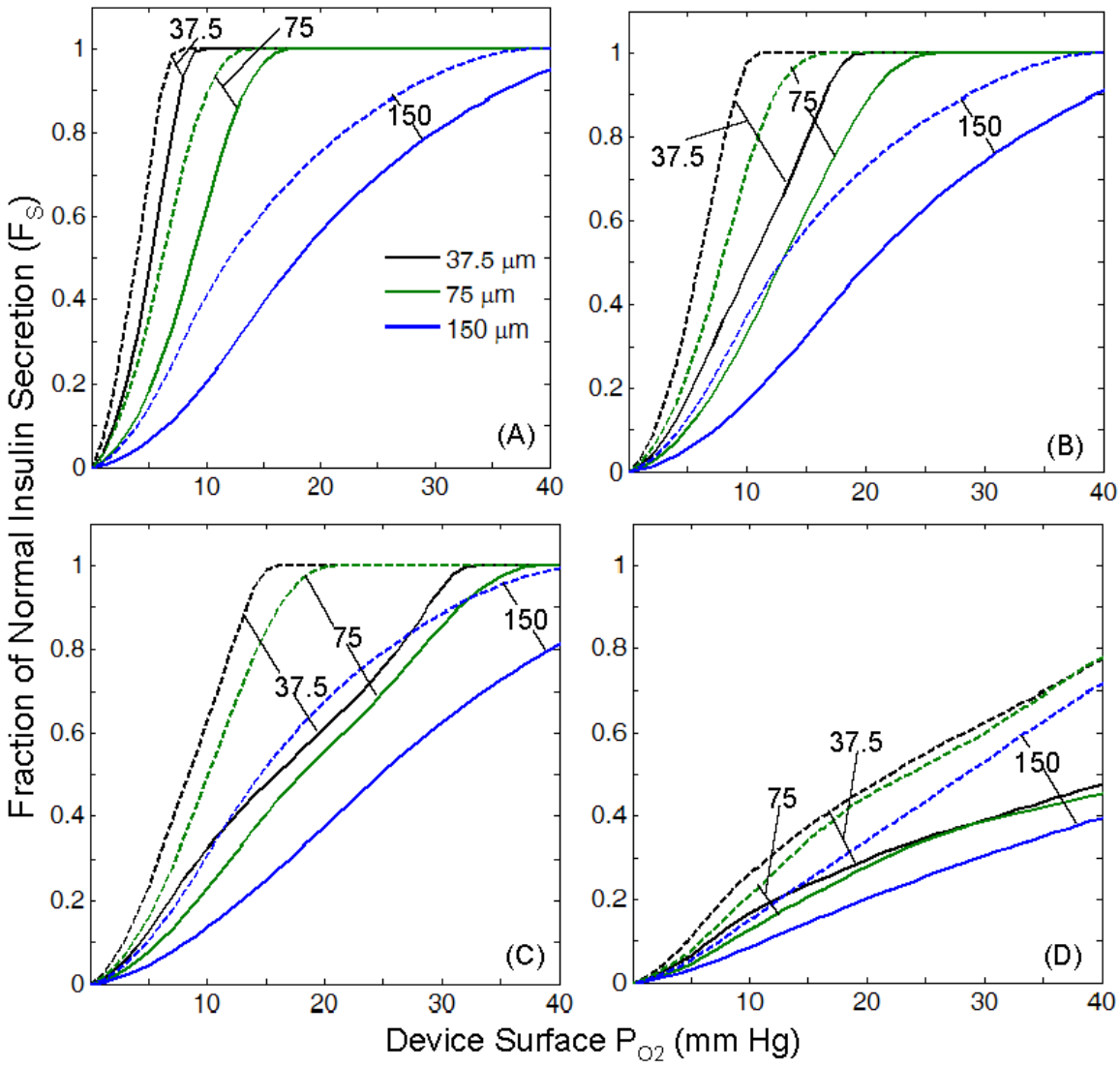

Figure 3-21: Predictions of fraction of normal insulin secretion over a range of device surface P_{O2} for tissue of a variety of sizes arranged in multiple layers within a planar diffusion chamber. The number of layers used is the maximum that would fit for a particular tissue size – 37.5-µm 13 layers, 75-µm 6 layers, and 150-µm 3 layers. The device is 500-µm thick and made of normal alginate (solid curves) and 70% (w/v) PFC alginate (dashed curves). The tissue device surface density was equal to (A) 150 IE/cm^2, (B) 1000 IE/cm^2, (C) 2000 IE/cm^2, and (D) 7272 IE/cm^2.

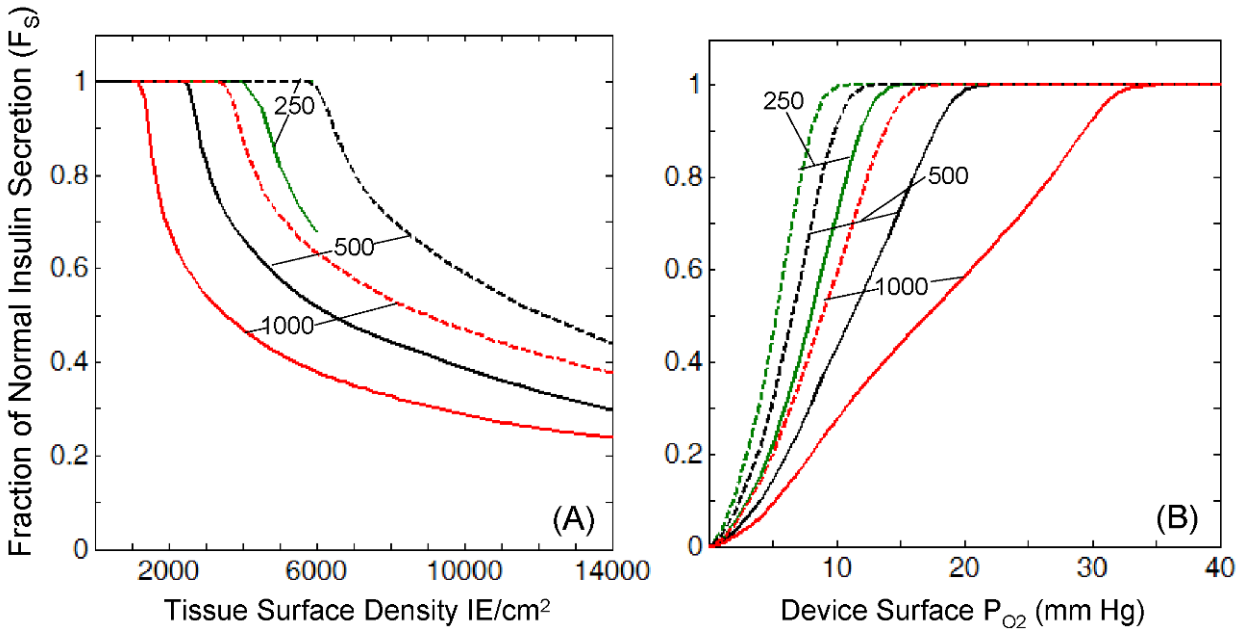

Figure 3-22: Effects of increasing device thickness on predictions of fraction of normal insulin secretion for 50-µm aggregates arranged in multiple layers.

250-µm device 5 layers, 500-µm device 10 layers, and 1000-µm device 20 layers made from normal alginate (solid curves) or 70% (w/v) PFC alginate (dashed curves). (A) The effects of varying surface density for a device surface P_{O2} of 40mmHg were investigates and (B) the effects of reducing the device surface P_{O2} at a tissue loading of 1000 IE/cm^2.

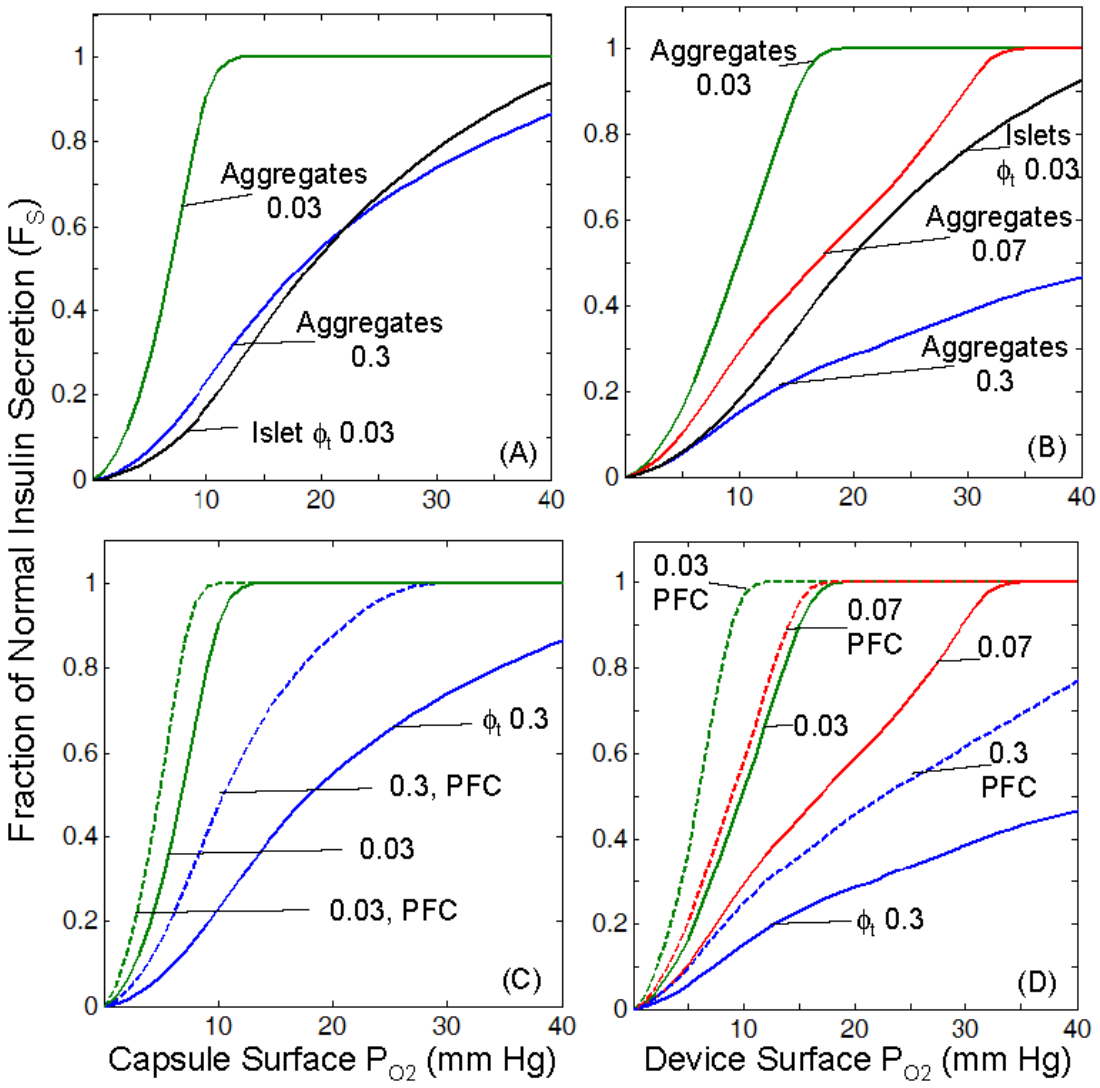

Figure 3-23: Comparison of the predictions of fraction of normal insulin secretion for 500-µm microcapsules (A,C) and 500-µm planar devices (B,D) that have similar loading of 50-µm aggregates and 150-µm based on the encapsulated tissue volume fraction (ϕ_t).

Comparisons between predictions in A & B examine the benefits of using aggregates in microcapsules and planar devices. Comparisons between predictions in C & D examine the benefits of using 70% (w/v) PFC emulsion (dashed lines) compared to normal alginate (solid lines) at different loadings in both types of encapsulation devices.

Table 3-1: Oxygen transport properties of materials in system

	D (cm^2/s)	**α (mol/mmHg/ml)**	**αD (mol/cm/mmHg/s)**	**Source**
H_20	$2.78x10^{-5}$	$1.27x10^{-9}$	$3.53x10^{-14}$	[23]
PFC	$5.61x10^{-5}$	$2.54x10^{-8}$	$1.42x10^{-12}$	[76]
Soybean Oil	$2.13x10^{-5}$	$6.84x10^{-9}$	$1.46x10^{-13}$	[77, 78]
Tissue	$1.24x10^{-5}$	$1.00x10^{-9}$	$1.24x10^{-14}$	[23]
Alginate	0	0	0	[23]

Table 3-2: Effective permeability of oxygen calculated using Maxwell's relationship. All capsules are composed of 2 vol% Alginate.

	αD (mol/cm/mmHg/s)
70% (w/v) PFC Emulsion	9.92×10^{-14}
70% (w/v) PFC Alginate	9.63×10^{-14}
Dispersed Cells 70% (w/v) PFC Alginate	9.31×10^{-14}
Pure Alginate	3.43×10^{-14}
Dispersed Cells Pure Alginate	3.35×10^{-14}

Table 3-3: Other Model parameters

Parameter	Symbol	Value	Units	Source
Maximum oxygen consumption rate	V_{max}	$4x10^{-8}$	$mol/cm^3/s$	[23]
Michaelis-Menten Constant	K_m	0.44	mmHg	[23]
Insulin Secretion Model Parameter	P*	5.1	mmHg	[93]
Critical P_{O2} for cell death	P_c	0.1	mmHg	[23]

Chapter 4 Encapsulated islet cell aggregates are superior to intact islets in terms of *in vitro* survival and function in low oxygen and ability to reverse diabetes in rodents

This chapter was written in collaboration with Esther O'Sullivan from Joslin Diabetes Center. The experiments were performed together using tissue from the same isolations. Due to the number of assessment methods that were performed on the tissue this effort was divided between the two of us. I performed the modeling portions of the work and the OCR and nuclei measurements. Esther performed the Insulin to DNA measurements, glucose stimulated insulin secretion measurements, and the transplantation experiments.

4.1 INTRODUCTION

Microencapsulation has been shown to effectively confer immunoprotection on transplanted islets, thereby potentially making the use of immunosuppressive therapy in clinical islet transplantation unnecessary [38, 79, 95]. Immunosuppressive drugs have undesirable side effects and have even been shown to have harmful effects on transplanted islet tissue [96]. If a clinically useful new *in vitro* source of beta cells can be found – either derived from adult or embryonic stem cells or otherwise [97-103] – it is likely that their immunogenicity will remain an obstacle to be overcome for their success in transplantation, and microencapsulation is an attractive means of protecting these beta cells from the host immune response. A further obstacle to successful islet cell transplantation is loss of the islets' normal vascularity and rich blood supply [104]. This limits the supply of oxygen and nutrients to the islet cells, leading to cell death and necrosis. In human islet transplant 50% or more of the islet tissue is lost in the 10 week period immediately following transplantation [105]. This is likely to be due in large part to hypoxia in the period prior to engraftment and delay in development of a vascular network [106]. Oxygen supply to encapsulated islets is limited in the long-term as they never become

revascularized, and the islet cells are completely dependant on diffusion of oxygen from their surroundings. It has been shown that small islets survive better than large islets in transplantation [56, 57]. This is because for larger islets oxygen must diffuse over a greater distance and cell number to reach cells at the core. Oxygen supplied in this way is not sufficient to keep up with demand, resulting in hypoxic beta cells and central necrosis. Furthermore hypoxic and necrotic islet cells are pro-inflammatory [47, 107], and the capsules containing them are permeable to the debris and pro-inflammatory factors produced. Once released it is likely that these act to elicit a host immune response. We hypothesize that well oxygenated healthy islet cells are better equipped to evade immune surveillance resulting in a more successful longer-lasting transplantation.

When islets are dispersed into single cell they tend to reaggregate to clusters [108] and if left long enough to islet-like structures. We know that transplanted islet cell aggregates (50-150 μm) can reverse hyperglycemia as effectively as islets [54]. It is clear that aggregates that are smaller than whole islets act as less of a barrier to oxygen diffusion, as there is a shorter distance, and fewer cells between the tissue surface and tissue core (Chapter 3). A further advantage to the use of islet cell aggregates is the potential for higher capsule packing density, which up to now has been limited by the problem of increasing oxygen demands. Higher capsule packing density is advantageous because a curative volume of beta cells could be provided in a lower capsule volume which is more amenable to transplantation to sites where space is limited, such as the intraportal site, subcutaneous site, and under the kidney capsule. Furthermore islet tissue that remains healthy even when densely packed is of use not only in microcapsules but in all encapsulation devices.

In this study we first showed that encapsulated islet cell aggregates survive and function better than encapsulated islets when cultured in low oxygen tensions to simulate the transplant setting. We then used diabetic and non-diabetic transplant models to show that encapsulated islet cell aggregates also prove to be superior to encapsulated islets on transplantation.

4.2 MODELING

To determine the culture conditions where the benefits of aggregate containing microcapsules will be observed in terms of enhanced tissue survival and function compared to intact islets, a theoretical model has been developed to predict the local partial pressure of oxygen, which, in turn, is used to assess tissue viability and fraction of normal insulin secretion for encapsulated islets and aggregates in culture. This model was adapted from the model for microcapsules containing islets and aggregates discussed in Chapter 3. For all calculations the microcapsules have a diameter of 500 μm and the microcapsule material will be 2% (v/v) alginate.

4.2.1 Model Geometry

Sketches of example geometries that were analyzed are presented in Figure 4-1A for microcapsules cultured on polystyrene which is assumed to have an oxygen impermeable bottom and Figure 4-1B for microcapsules cultured in silicone rubber bottom plates which are highly oxygen permeable. Two tissue configurations in microcapsules were analyzed: (1) one centrally located 150-μm diameter islet or (2) 1.2 islet equivalents of 50-μm aggregates arranged in a cubic array of spheres where the tissue lies throughout the capsule diameter. An islet equivalent (IE) is a volume of tissue equal to that of a 150-μm sphere. The capsules are arranged in a monolayer on the bottom of the culture dish in a cubic array. For each capsule, with the origin

placed at the center of the capsule, there are planes of symmetry perpendicular to the bottom of the culture dish, thus the model can be solved for only one quarter of the capsule in order to reduce the number of degrees of freedom.

4.2.2 Material and Tissue Properties

The effective permeability of the alginate microcapsule was determined from theoretical relationships assuming that alginate is the dispersed phase and has a permeability of zero. The ratio of the effective permeability $(\alpha D)_{eff,i}$ for layer i consisting of a dispersed (d) phase and a continuous (c) phase (as occurs in the alginate subdomains of the model system) to the permeability of the continuous phase $(\alpha D)_c$ was calculated from Maxwell's relationship [75]

$$\frac{(\alpha D)_{eff,i}}{(\alpha D)_c} = \frac{2-2\phi+\rho(1+2\phi)}{2+\phi+\rho(1-\phi)} \tag{4-1}$$

where αD is the effective permeability of the material (mol/cm/mmHg/s), $\rho=(\alpha D)_d/(\alpha D)_c$ is the ratio of the permeability of the dispersed phase to the permeability of the continuous phase, and ϕ is the volume fraction of the dispersed phase. The parameters used in the model are in Table 3-1.

4.2.3 Model Equations

The three-dimensional species conservation equation for reaction and diffusion at steady state was used to predict the oxygen profile within the different tissue, alginate, cell culture media, and silicone rubber membrane subdomains of the culture system:

$$D_i \nabla^2 C_i = V_i \tag{4-2}$$

where D_i (cm^2/s) is the effective diffusivity of oxygen in subdomain i, C_i (mol/cm^3) is the concentration of oxygen in subdomain i, and V_i ($mol/cm^3/s$) is the local oxygen consumption rate per unit volume in subdomain i. For convenience, since partial pressures are equal across interfaces of different materials, we make use of oxygen partial pressure instead of concentration, which are related by

$$C = \alpha P \tag{4-3}$$

where α ($mol/cm^3/mmHg$) is the effective Bunsen solubility coefficient in subdomain i and P is the partial pressure of oxygen. Combining Eq. (1) and Eq. (2) gives

$$(\alpha D)_i \nabla^2 P_i = V_i \tag{4-4}$$

The oxygen consumption rate is assumed to follow Michaelis-Menten kinetics for all tissue,

$$V_i = \frac{V_{max} \varepsilon_i P_i}{K_m + P_i} \tag{4-5}$$

where V_{max} is the maximum oxygen consumption rate for the tissue, ε_i is the tissue volume fraction in subdomain i, and K_m is the Michaelis-Menten constant. No oxygen is consumed in the alginate, cell culture media, or silicone rubber subdomains; therefore V_i is equal to zero in those subdomains, and the tissue volume fraction in the islet or aggregate subdomains is equal to one.

The model was solved by the finite element method using the commercially available software package COMSOL Multiphysics in combination with MATLAB and using the model parameters in Table 4-1. (4-4) was solved simultaneously for all subdomains of the culture system subject to the following conditions. There are planes of symmetry on the sides of the unit cell where the media or capsule was cut and thus zero flux of oxygen across these boundaries. At the boundary between a tissue subdomain and the alginate subdomain or the alginate

subdomain and culture media the partial pressure of oxygen and the flux of oxygen across the boundary are both equal. For the case of capsules cultured on polystyrene the bottom of the culture dish is assumed to be impermeable to oxygen and the flux across that boundary is zero. For the silicone rubber bottom culture condition, at the culture media and silicone rubber boundary the oxygen partial pressure and flux of oxygen across the boundary are equal. The bottom boundary of the silicone rubber membrane is at the partial pressure of oxygen in the gas phase. The external partial pressure of oxygen in the gas phase is specified and it is assumed that the top surface of the culture media is at the gas phase partial pressure of oxygen.

The fractional viability of the encapsulated tissue was estimated by determining the volume fraction of tissue where $P>P_C$. P_C is the critical oxygen partial pressure below which tissue dies and the value of P_C is assumed to be 0.1 mmHg [23]. The fractional viability was calculated using the following equation:

$$\text{Fractional Viability} = \frac{V_{Viable}}{V_{Tissue}} \tag{4-6}$$

where V_{Viable} is the volume of tissue where P is greater than 0.1 mmHg and V_{Tissue} is the total encapsulated tissue volume.

The relationship used to predict the local fraction (F_I) of normal insulin secretion rate as a function of local oxygen partial pressure within the islet was developed from data on the effect of hypoxia on islet insulin secretion, estimating the oxygen partial pressure profile within the islet in the experimental system, and then determining the simplest model type and parameter(s) that best predict the insulin secretion level [44, 93].

$$\begin{aligned} P < P^* \text{ mmHg} \quad & F_I = \frac{P}{P^*} \\ P \geq P^* \text{ mmHg} \quad & F_I = 1.0 \end{aligned} \tag{4-7}$$

When V_{max} is equal to $4x10^{-8}$ mol/cm^3/s, P* equals 5.1 mmHg and when V_{max} equals $6x10^{-8}$ mol/cm^3/s, P* equals 1.1 mmHg [93]. A value of V_{max} of $6x10^{-8}$ mol/cm^3/s was used for the predictions of encapsulated tissue viability and function in culture because it corresponds to an OCR per cell of 4 fmol/min/cell, within the range that was measured for the rat islets used in these experiments. The fraction of normal insulin secretion averaged over all tissue within the microcapsule was determined by evaluating the volume integral of F_I in all tissue containing subdomains

$$F_S = \frac{\int_{Viable} F_I dV}{V_{Tissue}} \tag{4-8}$$

where F_S is the fraction of normal insulin secretion averaged over all of the encapsulate tissue.

4.3 MODELING RESULTS

Traditional cell culture is carried out in polystyrene dishes which have a bottom that can be assumed to be impermeable to oxygen. We performed calculations to predict the fractional viability for islet and aggregate capsules cultured on polystyrene dishes over a range of oxygen levels. We performed these calculations in order to determine what gas phase oxygen level should be used for *in vitro* culture experiments in order to show that aggregate survival is enhanced compared to islet survival. The predictions for differences in fractional viability were not as great between the aggregate and islet conditions as we would have hoped based on previous theoretical predictions with a specified capsule surface P_{O2} (Chapter 3) and the predictions were very dependent on tissue surface density (Figure 4-2A-C). We also performed calculations in which the capsules were cultured in oxygen permeable silicone rubber bottom dishes (Figure 4-2D-F) which have been previously used to enhance oxygen transport to islets

cultured at P_{O2} of 142 mmHg and for better oxygen control during embryonic stem cell differentiation in low oxygen [109, 110]. Calculations predicted greater differences in encapsulated islet and aggregate survival, tissue could survive at lower gas phase oxygen levels for both tissue types, and the predicted viabilities had less of a dependence on surface density. The silicone rubber membranes allow for better oxygen control to the encapsulated tissue and maximize the predicted differences in tissue survival. Silicone rubber membranes were therefore used for *in vitro* experiments to demonstrate that aggregates will survive better than intact islets in low oxygen.

Calculations were performed to predict the fraction of normal insulin secretion and fractional viability of encapsulated islets and aggregates cultured on silicone rubber over a range of gas phase oxygen levels. These calculations were used to determine what gas phase oxygen level should be used during *in vitro* experiments to observe that aggregates function and survive better in low oxygen than intact islets. At a gas phase oxygen level of 3.5 mmHg (0.5%) aggregate survival is predicted to be greater than islet survival (60% versus 20% at low surface densities) (Figure 4-3A). Insulin secretion is significantly impaired for both tissue types (<20%) (Figure 4-3B). We chose to culture tissue at a gas phase P_{O2} of 3.5 mmHg in order to ensure that there would be loss of tissue in the islet capsules, but still greater survival rates in the aggregate capsules. We also wanted to show experimentally that at intermediately low oxygen levels the aggregates function and secrete insulin normally while function is impaired for intact islets. The intermediate oxygen level that we chose to study these effects at was a gas phase P_{O2} of 14 mmHg or 2% oxygen. In 2% oxygen when the aggregates and islets are cultured at a relatively low surface density all aggregate tissue is predicted to survive and nearly normal levels of insulin secretion (93%) are expected (Figure 4-3C & D). In comparison only 55% of

encapsulated islets are predicted to survive 2% O_2 culture and the fraction of normal insulin secretion will only be 40%.

4.4 METHODS

4.4.1 Animals

Male Lewis or Sprague-Dawley rats weighing 200-250 g (Harlan Sprague-Dawley) were used as islet donors. Lewis rats were used as recipients for syngeneic transplants. Hyperglycemic BALB/c mice (Taconic) were used as diabetic recipients. Diabetes was induced with an intraperitoneal injection of streptozotocin (Sigma Aldrich) at 250 mg/kg 10 to 14 days prior to transplantation. Mice having fed glucose levels higher than 350 mg/dl on two separate occasions were used as recipients. Normoglycemia was defined as two consecutive measurements on different days with non-fasting blood glucose levels below 200 mg/dl. All animal experiments were approved by the Joslin Animal Care Committee.

4.4.2 Islet Isolation

Rat islets were isolated according to standard techniques [70]. Briefly a laparotomy was performed under anesthesia with Ketamine/Xylazine. The common bile duct was cannulated and 8-10 ml of rodent Liberase RI ((Roche) 0.33 mg/ml) in M199 media was injected. Pancreas was then removed and incubated in a circulating water bath at 37^{o}C for 24.5 minutes. The digested pancreatic tissue was washed with M199 containing 10% newborn calf serum (Mediatech) and then strained through 400 μm wire mesh (Thomas Scientific). Islets were purified by centrifugation at 1750xg for 17 minutes through a discontinuous Hisotpaque 1077 gradient (Sigma Aldrich). Islets were handpicked under a dissecting microscope, counted, and then

cultured overnight at a density of up to 30 islets/cm^2 and a media height of 1.3 mm. Islet culture media was RPMI 1640 supplemented with 10% fetal bovine serum, penicillin 100 units/ml and 100 μg/ml streptomycin (Mediatech).

4.4.3 Islet Dispersion and Reaggregation

Islets were washed twice in PBS. A solution of bovine pancreas trypsin (Sigma Aldrich) 1 mg/ml and bovine pancreas DNAse 1 (Roche) 30 μg/ml in PBS was added. The islet suspension was incubated at 37^{o}C for 13.5 minutes with mixing by vortexing every 4.5 minutes. Cold islet culture media was added to stop the digestion. Cells were counted using a haemocytometer and then put in ultra low attachment dishes (Corning) at 500,000 cells per 60 mm dish. They were cultured overnight prior to encapsulation to allow for the cells to reaggregate. The size of the resulting aggregates were 39±25 μm.

4.4.4 Microencapsulation

Microcapsules were produced using purified alginate with high guluronic acid content (SLG 100, FMC Polymer, Norway) at a concentration of 1.5% (w/v) in 0.9% (w/v) NaCl. Whole islets or islet cell aggregates were washed with calcium free Krebs buffer (135 mM NaCl, 4.7 mM KCl, 1.2 mM KH_2PO_4, 1.2 mM $MgSO_4$, 25 mM HEPES, pH 7.4) and then resuspended in alginate to form a tissue-alginate suspension. Microcapsules were produced by extrusion of the tissue-alginate suspension through a needle using an electrostatic droplet generator (Pronova Polymer, Norway) into 20 mM $BaCl_2$ solution. Microcapsules ranged in size from 350 μm to 600 μm in diameter with an average for each batch between 400 μm and 500 μm. After sequential washes in HEPES buffer (132 mM NaCl, 4.7 mM KCl, 1.2mM $MgCl_2$, 25 mM HEPES, pH 7.4) and Krebs buffer (133 mM NaCl, 4.7 mM KCl, 1.2 mM KH_2PO_4, 1.2 mM

$MgSO_4$, 25 mM HEPES, 2.5 mM $CaCl_2$, pH 7.4) the encapsulated islet tissue was cultured in islet culture media.

4.4.5 Encapsulated Tissue Culture

Capsules that were cultured in 20% oxygen were placed in 100 cm^2 silicone rubber flasks (PR-AY-5-0017-5 from Wilson Wolf Manufacturing Inc., New Brighton, MN) in islet culture media at a depth of 2.5 mm, at a density of less than 30 IE/cm^2 where there should be no oxygen limitations, and placed in a standard humidified air incubator with 5% CO_2 at 37^{o}C. Capsules to be cultured at 0.5% or 2% oxygen were placed in 24 well plates that were custom made to contain silicone rubber bottoms (PR-AY-7-0004, from Wilson Wolf Manufacturing Inc., New Brighton, MN) in islet culture media at a depth of 10 mm at a density of 50-200 IE/cm^2 and then placed into a humidified incubator (Xvivo from Biospherix Ltd., Redfield, NY) where the gas levels were controlled to be at 5% CO_2, 0.5% O_2 or 2% O_2, and balance N_2. Capsules were cultured for two days under these conditions for the *in vitro* experiments.

4.4.6 Oxygen Consumption Rate (OCR)

The oxygen consumption rate measurements were performed as previously described (Chapter 2 and [66]). Islet or aggregate containing microcapsules were resuspended in DMEM without phenol red containing 4.5 g/l glucose supplemented with 0.6 g/l L-glutamine, 100 units/ml penicillin, 100 µg/ml streptomycin, 10 mM HEPES (Mediatech) without serum for OCR measurements. Phenol red free media was required such that the media would be colorless as to not interfere with the absorbance measurements associated with the alginate assay. The tissue microcapsule samples were added to a 200 µl stirred titanium chamber maintained (Micro Oxygen Uptake System FO/SYSZ-P250, Instech Laboratories, Plymouth Meeting, PA) at 37^{o}C [66]. After the samples equilibrated with air at 37^{o}C the chambers were sealed. The time

dependent P_{O2} within the chamber was recorded with a fluorescence-based oxygen sensor (Ocean Optics, Dunedin, FL), and the data at high P_{O2} was fit to a straight line. The maximal OCR was evaluated from $OCR=V_{ch}\alpha(\Delta P_{O2}/\Delta t)$, where V_{ch} is the chamber volume and α is the effective Bunsen solubility coefficient for the contents of the OCR chamber.

4.4.7 Capsule Dissolution

Many of the quantitative measures of encapsulated tissue - nuclei counts, DNA content, alginate content, or insulin content require that the capsule first be dissolved. After OCR measurements were complete the tissue was collected from the chamber and the tissue and capsule quantity were determined. Tissue was removed from microcapsules by adding 800 µl of 100 mM tetrasodium EDTA (pH=8) to approximately 300 µl of a capsule suspension. The samples were placed in an incubator at 37^{o}C for 1 hour and were vortex mixed every 30 minutes to dissolve the capsules.

4.4.8 Nuclei Counts

Nuclei suspensions were prepared and quantified as described in Chapter 2. 200 µl aliquot of islet tissue from dissolved capsules (~ 2.5 x 10^6 cells/ml or 125 IEQ/ml) was resuspended in 100 µl of PBS and then incubated in a lysis solution (0.1 M citric acid and 10% (v/v) Triton X-100 (Sigma Aldrich)) for 15 min with vortex mixing every 5 minutes. Next the nuclei samples was sheared through a needle to liberate all nuclei. 100 µl of 100 mM tetrasodium EDTA was added to the nuclei suspension to prevent alginate gelling prior to the nuclei counting. The liberated nuclei were stained with 0.8 µM LDS 751 and 0.2 µM Sytox Orange (Invitrogen,) in D-PBS and counted using a benchtop flow cytometer (Guava Personal Cell Analyzer, Guava Technologies, Hayward, CA).

4.4.9 DNA Analysis

DNA concentration was quantified by fluorospectrophotometry using the CyQUANT® Cell Proliferation Assay Kit (Invitrogen), which is based on the strong fluorescence enhancement that the CyQUANT GR dye undergoes when bound to cellular nucleic acids. Pre-treating the samples with DNAse-free RNAse eliminated fluorescence resulting from CyQUANT dye binding to RNA. The fluorescence intensity was linearly related to the concentration of nucleic acids in the sample.

4.4.10 Insulin and DNA content

An aliquot of the islet or islet cell aggregate suspension in EDTA was frozen, then thawed and diluted to a known volume with PBS. The samples were sonicated on ice. An aliquot was taken for insulin, immediately adding 2X high salt buffer (NaCl 2.15M, NaH_2PO_4 0.01M, Na_2HPO_4 0.04M, EDTA 0.002M), and then transferring to 4^{o}C for overnight insulin extraction. Thereafter the sample was stored at 20^{o}C until assayed using a rat insulin ELISA kit (ALPCO Diagnostics, Salem, NH) after appropriate dilution.

4.4.11 Alginate Content

The alginate content of samples were assayed by a method adapted from the literature using dimethyl methylene blue **(**DMMB) (Sigma Aldrich) dye which is a cation that binds to polyanions such as alginate (Chapter 2 and [72]). The ratio of the absorbance of a sample at the wavelengths of 520 nm and 650 nm increased linearly with increases in alginate concentration.

4.4.12 Glucose stimulated insulin secretion

Encapsulated islets or islet cell aggregates were suspended in Krebs Ringer buffer Hepes (KRBH) (NaCl 137 mM, KCl 4.8 mM, KH_2PO_4 1.2 mM, $MgSO_4.7H_20$ 1.2 mM, $CaCl_2.2H_20$ 2.5 mM, $NaHCO_3$ 5 mM, HEPES 16 mM, BSA 0.1% (w/v), pH 7.4) containing 2.8 mM glucose. The pre-culture and 20% O_2 culture samples were kept at 37^{o}C in humidified air and 5% CO_2 for the duration of the measurement. The low oxygen samples were kept in a controlled oxygen environment (Xvivo from Biospherix Ltd., Redfield, NY) throughout the duration of the measurement at 37^{o}C in humidified 2% or 0.5% oxygen, 5% CO_2, and balance N_2. The use of the Xvivo was critical to these measurements as they allowed for tissue collection, washes, and media changes without exposing the tissue to atmospheric oxygen allowing for static glucose stimulated insulin secretion measurements in low oxygen. Five 1-ml aliquots with approximately equal numbers of microcapsules containing islets or islet cell aggregates were pre-incubated for one hour. The *in vitro* insulin secretion was then assessed by consecutive incubations of one hour in KRBH containing 2.8mM glucose and 16.8mM glucose. At the end of each incubation 800 µl of the KRBH was removed and frozen for insulin assay. The tissue was collected and the DNA content was measured to normalize insulin secretion results.

4.4.13 Histology

Encapsulated islets or islet cell aggregates were fixed in 2.5% (w/v) glutaraldehyde in 0.1M phosphate buffer pH 7.4. Plastic 1-µm thick sections were generated and stained with toluidene blue (Thermo Fisher Scientific).

4.4.14 Immunohistochemistry

Encapsulated islet tissue was fixed in 4% paraformaldehyde for 2 hours then centrifuged in 2% agar before embedding in paraffin. 2 step sections from each block were stained in insulin and glucagon. Briefly sections were hydrated and guinea-pig anti-bovine insulin antibody (1:200) was added for 1 hr followed by washing in lamb serum before Texas red–conjugated anti–guinea pig antibody (1:200) was added for 1 hr After washing unconjugated Streptavidin was added for 1hr followed by biotin for 30 min. Then rabbit anti-goat glucagon antibody (1:3000) was added and sections were left in a humidity chamber overnight at 4^0C. After washing biotinylated anti-rabbit antibody (1:200) was added for one hour and finally Streptavidin-conjugated DTAF (dichlorotriazinyl amino fluorescein)(1:200). Coverslips were applied with DAPI (4',6-diamidino-2-phenylindole) containing mounting media (Vector laboratories). Stained sections were photographed in confocal mode of a LSM410 microscope. Insulin-positive (red) and glucagon-positive (green) cells were counted on one or two sections from each preparation to a total number 300 to 800 cells per preparation. Sections were prepared for encapsulated islets and islet cell aggregates from 3 separate experiments.

4.4.15 Syngeneic normoglycemic transplants

Encapsulated islets or islet cell aggregates were transplanted intraperitoneally to syngeneic (Lewis rat) recipients. Microcapsules were injected into the peritoneal cavity through a central midline 5-10 mm incision using a sterile plastic transfer pipette (Fisher Scientific). The incision was closed using 5/0 silk, the outer layers were stapled. The animals were anesthetized with Ketamine/Xylazine. Capsules were retrieved 2 weeks after transplantation by laparotomy and peritoneal lavage. Capsules were washed in PBS and prepared for Histology sections.

4.4.16 Xenogeneic hyperglycemic transplants

On day 2 post-isolation and shortly after encapsulation, islets and islet cell aggregate containing capsules were sampled in triplicate and total tissue volume was quantified by nuclei counting. The remaining tissue was cultured overnight in Ultraculture media (Cambrex Bioscience, Walkersville, MD) supplemented with glutamine (300mg/L) penicillin (100units/ml) and streptomycin (100ug/ml). On day 3 aliquots of 85 islet equivalents (IE) were prepared for each encapsulated tissue type, washed in KREBS buffer and transplanted intraperitoneally to diabetic BALB/c mice.

4.4.17 Intraperitoneal Glucose Tolerance Tests and blood glucose measurement

Transplant recipients were fasted overnight for 15 hours. They received 2g/kg of glucose by intraperitoneal injection using a 10% (w/v) glucose solution. Blood glucose was measured immediately prior to the injection (time 0) and at 15, 30, 60, 90 and 120 minutes thereafter. For determination of blood glucose concentrations blood was obtained from the tail vein and applied to a glucometer (One Touch).

4.4.18 Statistics

Data are expressed as average ± standard error of measurement (SEM). Statistical significance was determined by a two-way Student t-test or Fisher exact test as indicated for each data set.

4.5 RESULTS – *IN VITRO* EXPERIMENTS

4.5.1 Histology

Plastic sections (1-μm) were prepared for histological examination of encapsulated islets or aggregates following culture in 2% oxygen. Figure 4-4A is section of a microcapsule containing islets after 2 days of culture in 2% oxygen. The cells in the center or the islet are only stained lightly by toluidene blue indicating that the cells at the center of the islet are necrotic most likely due to a lack of oxygen. Figure 4-4B is a section of a microcapsule containing aggregates after 2 days of culture in 2% oxygen where the tissue looks healthy and there are not signs of necrosis. Qualitative observations of encapsulated tissue histological sections indicate that encapsulated aggregates survive better than encapsulated islets in low oxygen. Sections shown are representative of sections prepared from 3 separate experiments.

4.5.2 Oxygen Consumption Rate

Oxygen consumption rate (OCR) measurements of encapsulated tissue were performed on the day of encapsulation and again after two days of culture under normal (20%) or low (0.5% or 2%) oxygen conditions. The OCR is measured for a sample of capsules, and then the capsules are removed from the chamber and dissolved. The dissolved capsule tissue and alginate suspension can be analyzed to determine the insulin content, nuclei count, DNA content, or alginate content of the sample within the OCR chamber. The alginate content is measured in order to normalize the OCR results by the volume of capsules in the chamber. The capsule volume normalization is necessary due to the high variability of capsule sampling. In Figure 4-5 the results for OCR per ml capsule are shown for one experiment in which the encapsulated islets and aggregates are cultured in 20% and 2% oxygen. For all conditions in this experiment, the day of encapsulation or after two days of culture in 20% or 2% oxygen, the OCR per ml capsule is

higher for the aggregate containing capsules, indicating that the viable tissue density is higher in the aggregate capsules for all conditions. Even though the viable tissue density was higher for the aggregate capsules initially, there was less of a change in viable tissue density in capsules after culture in low oxygen for aggregate containing capsules (p=0.54) compared to islet containing capsules (p=0.062). The p-values compare OCR per ml capsules for either capsule type pre-culture to 2 days of culture in 2% oxygen.

OCR recovery, a measure of the fractional recovery of viability tissue from culture, is calculated from the measured values of OCR per ml capsule using the following equation:

$$\text{Fractional OCR Recovery} = \frac{\left(\text{OCR per ml capsule}\right)_{\text{After 2 Day Culture}}}{\left(\text{OCR per ml capsule}\right)_{\text{Pre-Culture}}} \qquad (4\text{-}9)$$

The fractional OCR recovery results are presented in Figure 4-6. Under normal culture conditions (20% O_2), all of the viable tissue was recovered for both aggregate and islet capsules because the measured fractional OCR recovery was greater than one. Culture in very low oxygen (0.5%) resulted in recovery of almost all viable tissue in aggregate capsules (fractional OCR Recovery = 0.94) but significantly less viable tissue from the islet capsules (fractional OCR Recovery = 0.59). Culture in low oxygen (2%) resulted in the recovery of all viable aggregate tissue (fractional OCR Recovery = 1.14) but only 61% of viable encapsulated islet tissue. Significantly less islet tissue was recovered after culture in low (0.5% or 2%) oxygen than after culture in 20% oxygen. There was only a small but significant loss of viable aggregate tissue after culture at 0.5% oxygen compared to the normal oxygen condition (20%), but the amount of aggregate tissue recovered after 0.5% oxygen culture was significantly higher than for encapsulated islets cultured at 0.5% oxygen. The measured fractional OCR recoveries

demonstrate that encapsulated aggregate survival is better than encapsulated islet survival in low oxygen.

4.5.3 Tissue Recovery

The tissue recovery from culture in normal (20%) and low (0.5% or 2%) oxygen is calculated by the following equation:

$$\text{Fractional Nuclei Recovery} = \frac{\left(\text{Nuclei per ml capsule}\right)_{\text{After 2 Day Culture}}}{\left(\text{Nuclei per ml capsule}\right)_{\text{Pre-Culture}}} \quad (4\text{-}10)$$

The alginate content of the sample is measured to normalize the nuclei count by the total volume of capsules in the sample due to the high variability of capsule sampling. The fractional nuclei recoveries after two days of culture in normal and low oxygen are presented in Figure 4-7. After culture in 20% or 2% oxygen there is no difference in tissue recovery between islet and aggregate capsules. There is also no difference in the tissue recovery for aggregate capsules between any of the culture conditions. There is a trend towards less tissue recovery in the islet capsules compare to the aggregate capsules cultured at 0.5% oxygen ($p=0.08$). The tissue recovery is significantly lower for islet capsules cultured at 0.5% oxygen compared to the islet capsules cultured at 20% oxygen. The measured losses in total tissue (nuclei recovery) are not as dramatic as those for viable tissue (OCR recovery) after culture in low oxygen. This is most likely due to the fact that although viable tissue has been lost the tissue has not yet been cleared from the capsules and is being detected by nuclei counts.

4.5.4 Insulin to DNA Ratio

The ratio of insulin to DNA is considered an index of beta cell viability because viable beta cells store insulin. This ratio decreased markedly in encapsulated islets cultured in 0.5% oxygen for 2 days, in contrast to no decline in encapsulated islet cell aggregates (Figure 4-8). This indicates an improved ability of islet tissue to withstand low oxygen tensions when islets are dispersed and reaggregated prior to encapsulation. The insulin to DNA ratio does not decline in either tissue type, and even increases in the encapsulated islets when cultured in 20% oxygen or 2% oxygen ($p<0.05$) indicating that these conditions are compatible with beta cell viability in both islets and islet cell aggregates. The improvement in insulin to DNA ratio in the encapsulated islets is in keeping with recovery of insulin stores and or loss of DNA through cell death in the islets following the encapsulation procedure [111].

4.5.5 Quantification of beta-cells versus non-beta cells

The increase in insulin to DNA ratio in the islets after culture in 20% oxygen may be somewhat explained by the beta cell counts which show a significant rise in the proportion of islet cells that are beta cells after culture in 20% oxygen (74±2% to 83±0%, $p<0.05$), indicating preferential survival of beta cells compared to non-beta cells in the islets (Table 4-2). This was not the case for islet cell aggregates in which the proportion of beta cells remained constant after normoxic culture (73±2%). Conversely after culture in 2% oxygen the proportion of beta cells in islets remained constant – presumably due to equal rates of death of beta and non-beta cells, whereas the proportion of beta-cells in the islet cell aggregates increased (73±2% to 84±5%, $p<0.05$) indicating preferential survival of beta cells compared to non-beta cells. It has previously been shown that on transplantation of non-encapsulated islets, over time there is preferential loss of non-beta cells [54]. It may be the case that when encapsulated, the normally

outermost non-beta cells are protected from the local stresses of handling (shearing forces for example), thereby preserving the normal beta to non-beta cell ratio. The rise in the ratio of beta to non-beta cells in the islet cell aggregates could be accounted for by a reduction in the rate of beta cell death compared to that which occurs due to central necrosis in the normal islet structure. The non-significant difference in cell composition after culture in 2% oxygen cannot however account for the marked difference in insulin to DNA ratio between the two tissue types – indicating that this difference truly indicates a greater islet tissue viability in the islet cell aggregates.

4.5.6 Glucose stimulated insulin secretion

Insulin secretion at basal glucose levels (2.8mmol/l) was appropriately low in both encapsulated tissue types on the day of encapsulation and a good response to high glucose concentration (16.8mmol/l) was demonstrated (Figure 4-9). Our results show that this normal pattern of insulin secretion was preserved in both tissue types after 2 days culture in 20% oxygen but became abnormal after 2 days culture in 2% or 0.5% oxygen. Basal insulin secretion was inappropriately high in both encapsulated islets and islet cell aggregates cultured in 2% or 0.5% oxygen. However in contrast to the islets, the islet cell aggregates continued to show a significant rise in insulin secretion in response to high glucose ($p<0.05$) after culture in 2% oxygen indicating a degree of preservation of regulated insulin secretion. Insulin secretion was significantly impaired for islets or aggregates cultured at 0.5% oxygen as the basal insulin secretion level was actually higher than the stimulated insulin secretion. The high basal insulin secretion rate that was observed could also have been from β cell degranulation or release of insulin from dead cells.

4.6 RESULTS – *IN VIVO* EXPERIMENTS

4.6.1 Histology

Encapsulated islets and islet cell aggregates were transplanted intraperitoneally to syngeneic (Lewis rat) recipients. Toluidene blue stained sections of the encapsulated tissue retrieved two weeks later were prepared (Figure 4-10). Large areas of central necrosis were apparent in many of the islets, and were especially prominent in the larger islets as demonstrated by pale stained cells, loss of nuclear staining and in some cases complete absence of tissue in the core. In contrast encapsulated aggregates remained healthy in appearance.

4.6.2 Hyperglycemic xenogeneic transplants

A volume of encapsulated rat islet tissue that would cure some but not all diabetic mouse recipients was determined in preliminary transplant experiments (data not shown). A marginal mass of 85IE (determined by nuclei counting) was chosen and this volume of encapsulated islets or islet cell aggregates was transplanted to diabetic BALB/c mice (n=10,12 respectively). Fed blood glucose concentrations were measured on day 1,3,7,10,and 13 post-transplantation (Figure 4-11). Transplanted encapsulated islet cell aggregates cured a greater proportion of recipients (83%) compared to encapsulated islets (30%) ($p<0.03$ Fisher exact test). IPGTTs performed on the cured transplant recipients showed a trend towards a better glucose clearance for the islet cell aggregate recipients than the islet recipients – a trend that was not significantly different due to the small number in the cured islet transplant recipient group (n=3) and comparable glucose clearance to the normoglycemic controls (Figure 4-12). This once again shows that the islet cell aggregates function effectively in response to glucose challenges, and indeed are more effective than islets in encapsulated intraperitoneal transplants at maintaining euglyemia in the fed state.

4.7 DISCUSSION

In this study we found that islet cell aggregates, as compared to intact islets, were superior in their ability to survive and function in a low oxygen culture and in the transplantation setting. Histological sections of capsules after culture in 2% oxygen or syngeneic transplantation showed signs of central necrosis in the islet tissue, but not for the aggregate tissue. OCR recovery, tissue recovery, the ratio of insulin to DNA content, and glucose stimulated insulin secretion measurements, the parameters that were measured to assess the ability of tissue to survive and function under low oxygen conditions, were all favorable towards the aggregates under at least one low oxygen condition. Since each of these measurements is an assessment of a slightly different but important parameter of islet tissue health it is to be expected that all of the results will not have the same degree of effect at a particular oxygen culture condition or all be effected at the same oxygen level. Results of OCR recovery are more dramatic than those for nuclei recovery because viable tissue is lost and then the nuclei are cleared from the capsule. Glucose stimulated insulin secretion is dysfunctional at 0.5% oxygen in both tissue types and for islets in microcapsules at 2% oxygen, but stimulation is observed for aggregates in capsules at 2% oxygen. It has been observed in previous work [44, 93] and is also consistent with the modeling results that insulin secretion is impaired at higher oxygen levels than is the case for tissue viability. The insulin to DNA ratio is considered to be a measure of tissue viability because a major function of healthy beta cells is to store insulin. However the ability of an islet to store insulin and normal mitochondrial function as measured by OCR are two very different parameters; exact agreement and response to low oxygen are not expected. The important conclusion from all of the measured viability parameters is that after culture in low oxygen, when oxygen causes detrimental effects on any of these parameters, it is always more severe for the intact islets as compared to the aggregates.

The modeling predictions proved to be a useful tool in guiding selection of oxygen levels at which to carry out experiments such that differences in aggregate and islet survival and function could be observed experimentally. The modeling predictions did not exactly agree with the experimental results, but the measured trends for OCR recovery are similar to the trends for predictions of fractional viability. After culture at 0.5% oxygen, a small amount of viable aggregate tissue was lost but significantly more was recovered than for encapsulated islets. After culture at 2% oxygen all viable aggregate tissue was recovered with a significant loss of islet tissue. There were similar amounts of viable islet tissue recovered in both low oxygen conditions even though there were predicted differences in fractional viability between the two low oxygen conditions. The predictions for fraction of normal insulin secretion do not exactly agree with the results for measurement of glucose stimulated insulin secretion, but the same trends were present in the predictions as in the actual experimental results. After culture in 0.5% oxygen the model predicted and the experimental results showed that insulin secretion was severely impaired for both tissue types. After encapsulated islet culture at 2% oxygen, theory predicted insulin secretion to be impaired and thus was found experimentally. Insulin secretion was predicted to be near normal for encapsulated aggregates cultured at 2% oxygen, and the experimental results agreed with the predictions as increased insulin secretion was measured after incubation at high glucose: however, insulin secretion was not completely normal as basal levels of insulin secretion were high.

Aggregate containing microcapsules can successfully reverse diabetes following xenogeneic transplantation. In fact the ability for the aggregate containing capsules to reverse diabetes, when a minimal mass of tissue is transplanted, was greater than for islet capsules. The reason for the aggregates' greater success rate is that tissue in the aggregate containing capsules

as a whole is exposed to higher oxygen levels such that less tissue dies after transplantation, and remaining viable tissue at the capsule interior is more likely to secrete insulin normally. Another potential reason for improved transplantation success rates is that because there is less tissue hypoxia and cell death, there are less pro-inflammatory cytokines and cell debris released from the capsules which means a lower risk of initiating a host immune response [107].

Limited oxygen transport to microencapsulated tissue is a major obstacle that has limited the success of microencapsulated islet transplantation to treat type 1 diabetes. In this study we have been able to show that the use of islet cell aggregates, which are smaller than intact islets, can significantly improve the ability of islet tissue to survive and function when cultured in low oxygen and to reverse diabetes in mice. The use of aggregates instead of intact islets has proven to be an effective strategy to reduce oxygen transport limitations and improve microencapsulated tissue transplants. This finding has great relevance to the future of insulin replacement therapy as a whole. To date, despite improved outcomes that came with the Edmonton protocol, clinical islet transplantation has met with limited success, and is an option only for patients with severe manifestations of type one diabetes [112, 113]. Finding a renewable source of beta cells is necessary to tackle the mismatch between supply and demand [114, 115]. Furthermore finding a means of transplanting those beta cells such that they remain viable and functional for longer, and do not require immunosuppressive drugs to evade rejection are key issues which are both addressed by the use of islet cell aggregates in microcapsules.

In conclusion, we found that encapsulated islet cell aggregates survive and function better in low oxygen environments compared to encapsulated whole islets. This has important implications for future developments in clinical islet tissue transplantation and beta cell replacement therapy as a whole.

Contributions: Islet isolations were performed with the assistance of Jennifer Hollister-Lock, Vaja Tchipasvilli, and Vassileios Kostaras from Joslin Diabetes Center. Histology sections were prepared by Chris Cahill (Joslin DERC). Abdulkadir Omer provided instruction on the preparation of microcapsules and assisted with the syngeneic transplantation experiments. Susan Bonner-Weir assisted in the evaluation of the histological sections.

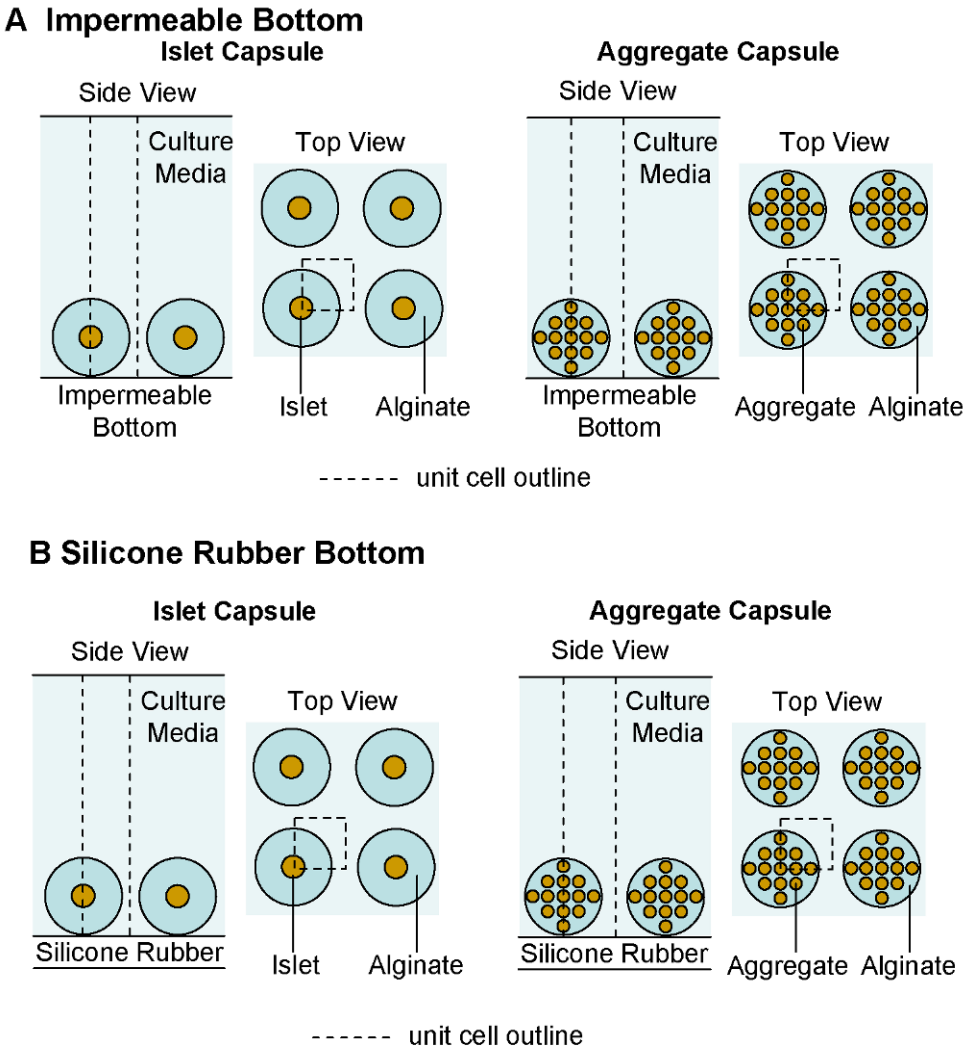

Figure 4-1: Sketches of example model geometries

For microcapsules containing one 150-µm islet or 1.2 IE of 50-µm aggregates in culture on either an oxygen impermeable bottom (A) or an oxygen permeable silicone rubber bottom culture dish (B). The dashed lines represent the unit cell in which the oxygen profile was calculated.

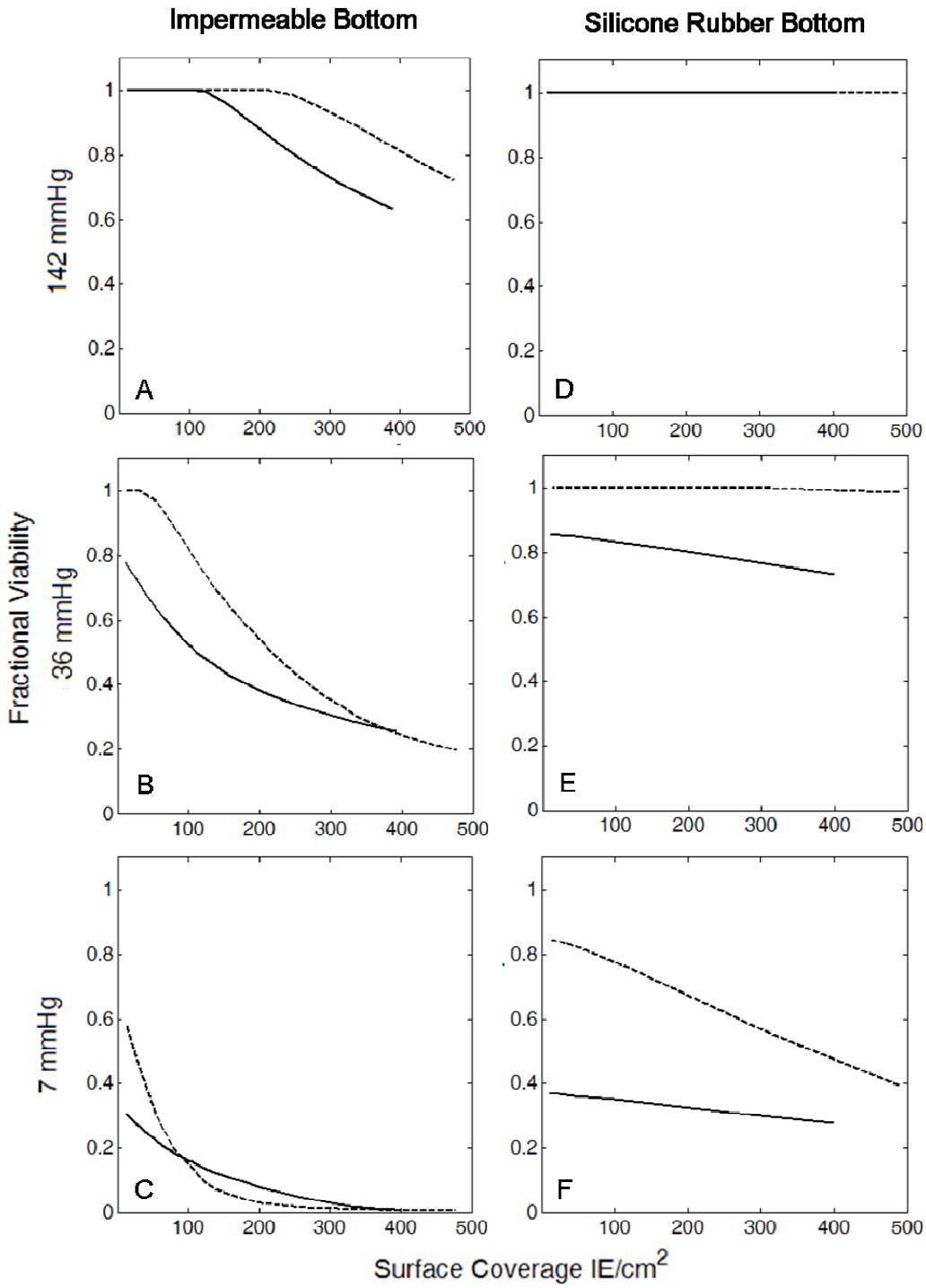

Figure 4-2: Predictions of fractional viability for islet (solid) and aggregate (dashed) capsules cultured on impermeable bottom dishes (A-C) or silicone rubber bottom dishes (D-F). At gas phase oxygen level of 142 mmHg (A,D), 36 mmHg (B,E) or 7 mmHg (C,F).

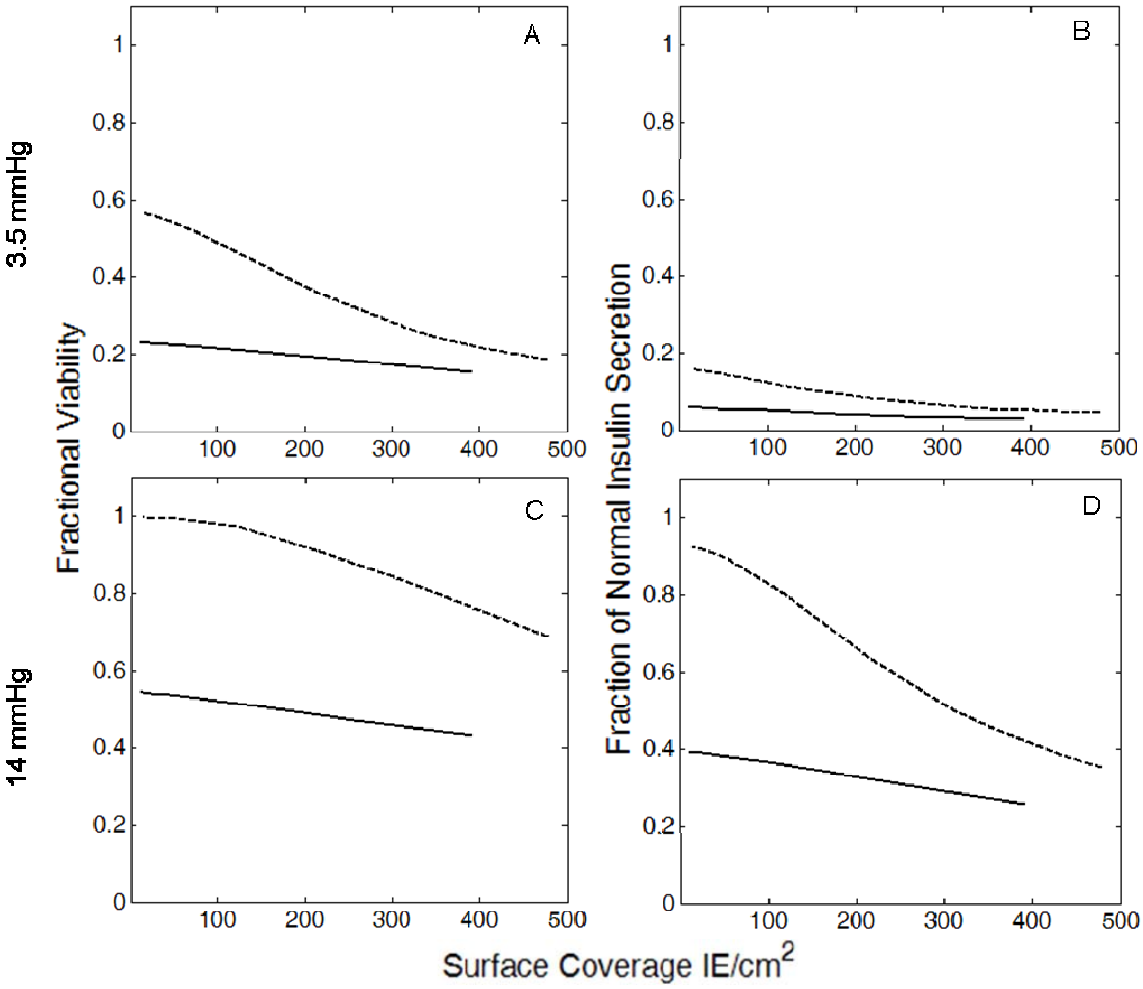

Figure 4-3: Comparison of predictions of fractional viability and insulin secretion for aggregate (dashed) and islet (solid) containing capsules cultured on silicon rubber in a gas phase oxygen partial pressure of 3.5 or 14 mmHg.

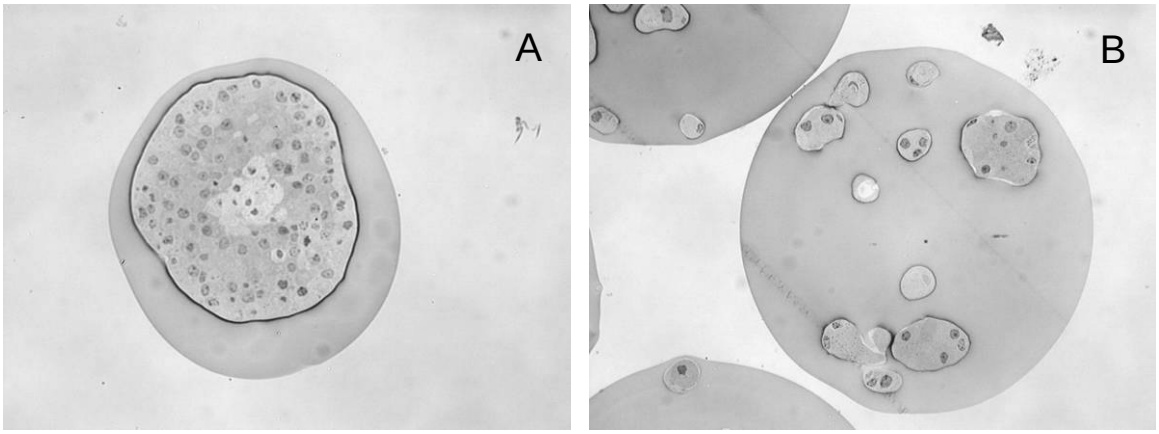

Figure 4-4: 1-µm plastic sections of microcapsules stained with toluidene blue after two day culture in 2% oxygen. (A) capsule containing an islet (B) capsule containing aggregates

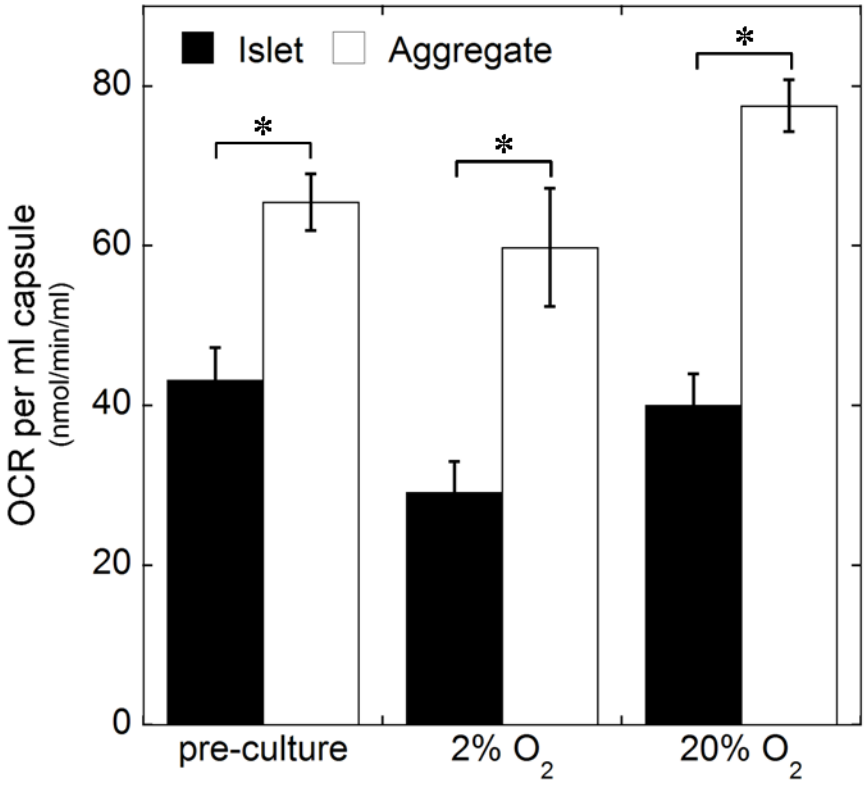

Figure 4-5: OCR per ml capsule for islet (black bars) and aggregates (white bars) on the day of encapsulation and after two days of culture in 20% or 2% oxygen.

In all conditions the measured OCR per ml capsule is higher for aggregate containing capsules than islet capsules (* = $p<0.05$ by unpaired student t-test). Results are presented for one representative experiment in which the measurements were made in triplicate (n=3).

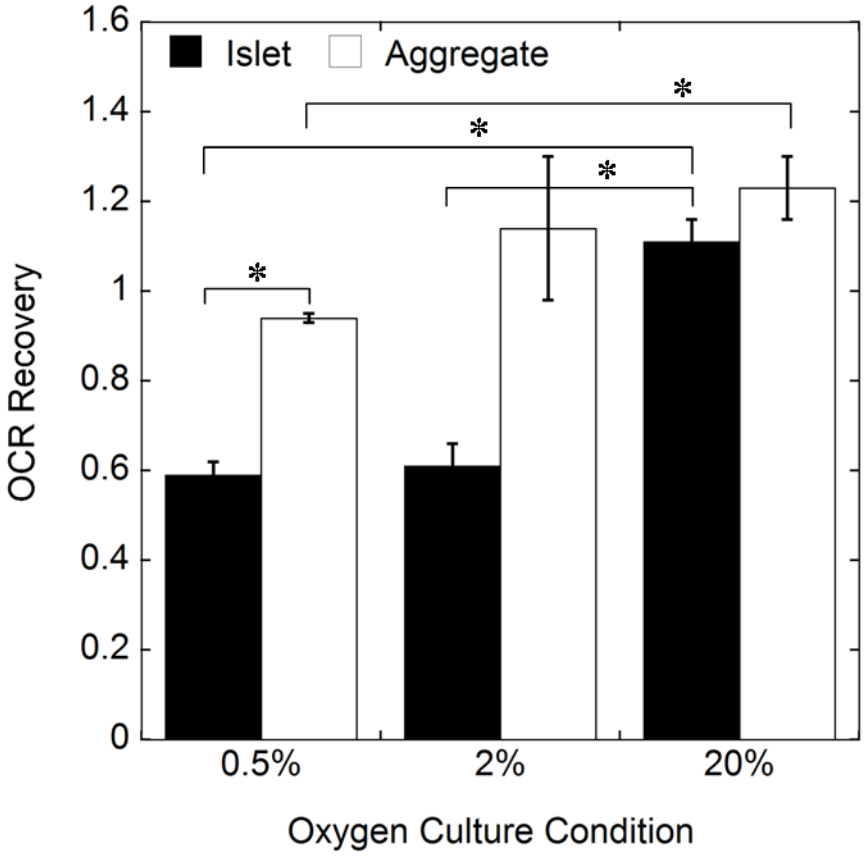

Figure 4-6: Fractional oxygen recovery of encapsulated islets (black bars) and aggregates (white bars) cultured for two days in 20% (n=5), 2% (n=3) or 0.5% (n=2) oxygen.

n is the number of independent experiments for which the OCR recovery was measured.

Statistical significance is represented by * which indicated $p<0.05$ by unpaired student t-test.

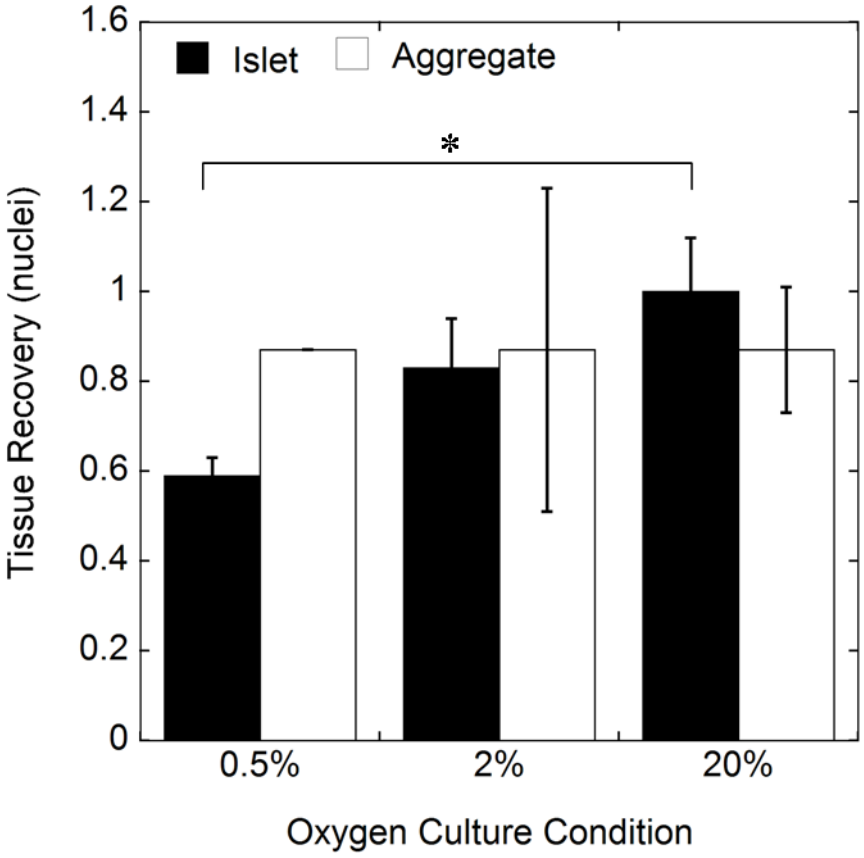

Figure 4-7: Fractional nuclei recovery of encapsulated islets (black bars) and aggregates (white bars) after two days of culture in 20% (n=5), 2% (n=3) or 0.5% (n=2) oxygen.

n is the number of independent experiments for which the nuclei recovery was measured.

Statistical significance is represented by * which indicated $p<0.05$ by unpaired student t-test.

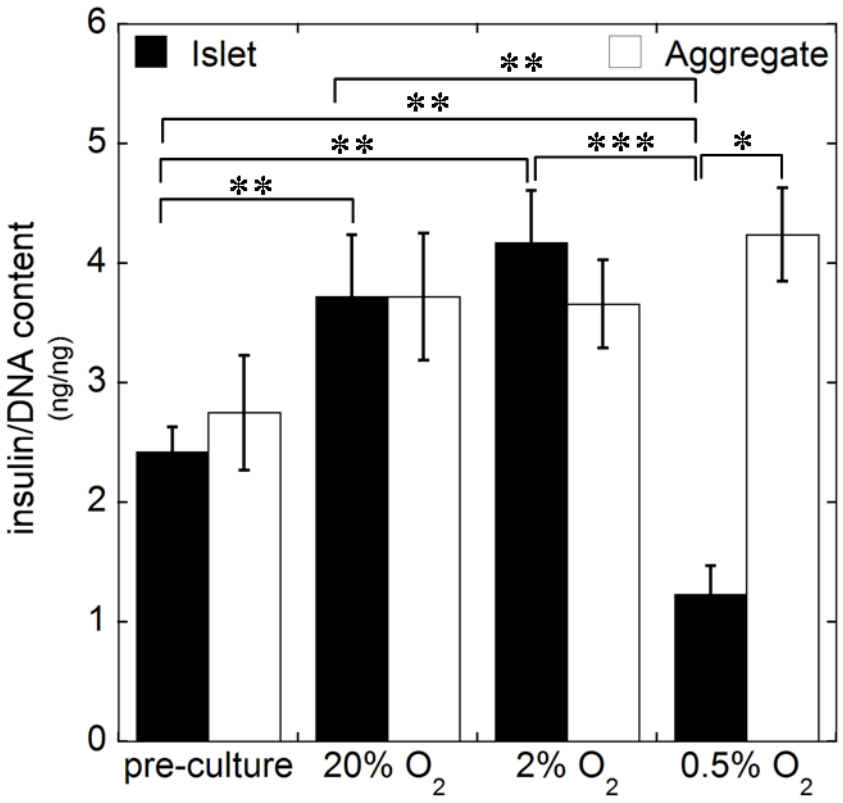

Figure 4-8: Ratio of insulin to DNA content in encapsulated islets (black bars) and aggregates (white bars) on the day of encapsulation (pre-culture) and after 2 days culture in 20%, 2% or 0.5% oxygen.

Pre-culture, 20% O_2: n=4, 2% O_2 n=1, 0.5% O_2 n=2. (n=3 replicates per experiment). * $p<0.0001$, ** $p<0.05$, *** $p<0.001$ (unpaired student t-test).

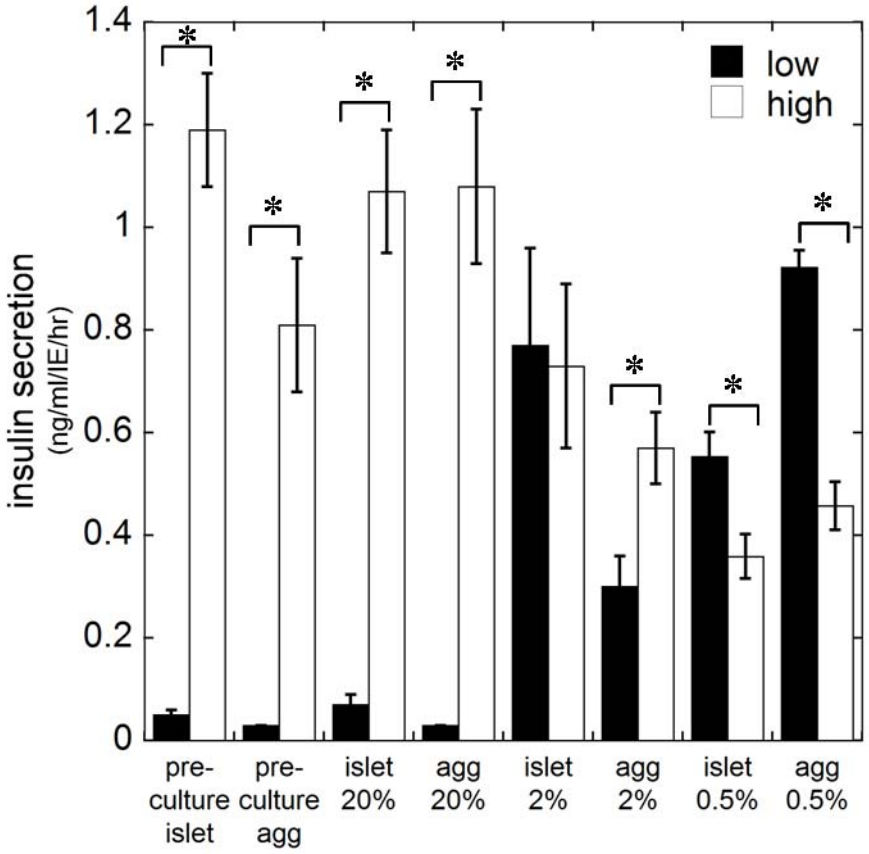

Figure 4-9: Glucose stimulated insulin secretion from encapsulated islets or aggregates (agg) in low glucose (2.8 mM, black bars) and high glucose (16.8 mM, white bars) KRBH. Measurements were made immediately after encapsulation prior to culture and then after two days of culture in 20%, 2%, or 0.5% oxygen. (n=2 experiments for 20% and 2%, 1 experiment for 0.5%, 5 replicates per experiment). * $p<0.05$ (paired student t-test).

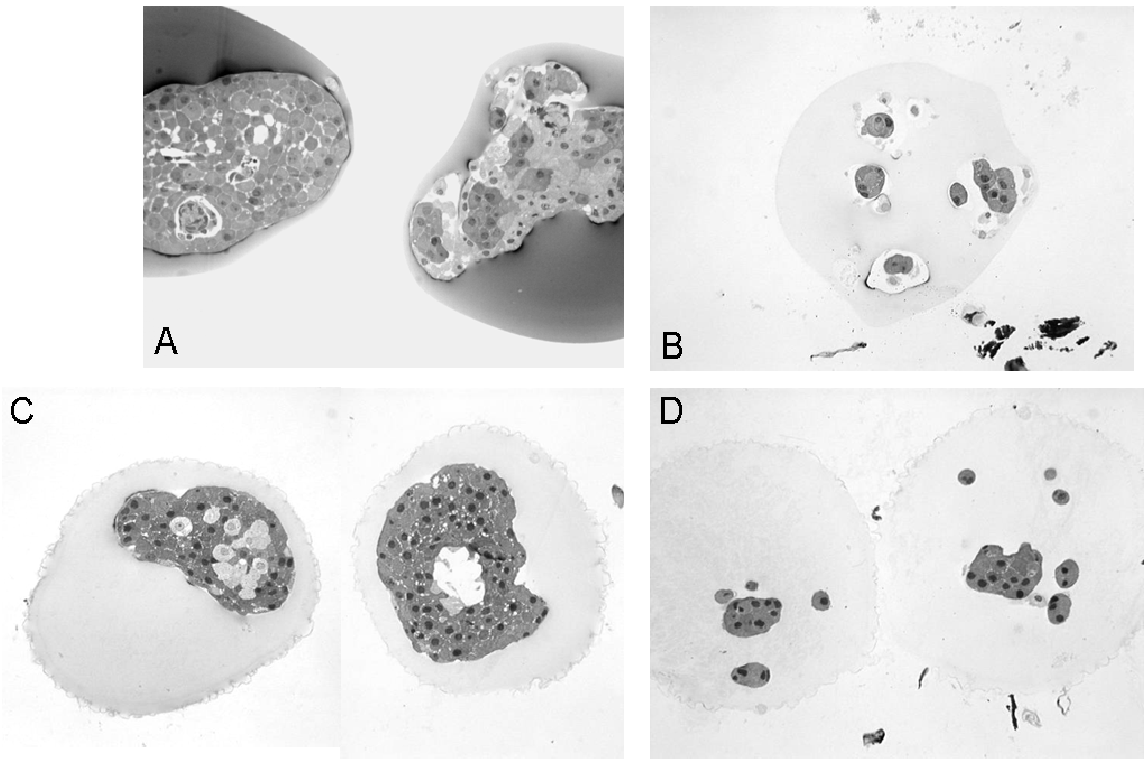

Figure 4-10: Plastic sections of capsules before and after two week syngeneic transplantation in non-diabetic rats.

(A) islet capsules pre-transplantation, (B) aggregate capsules pre-transplantation, (C) islet capsule post-transplantation, and (D) aggregate capsules post-transplantation.

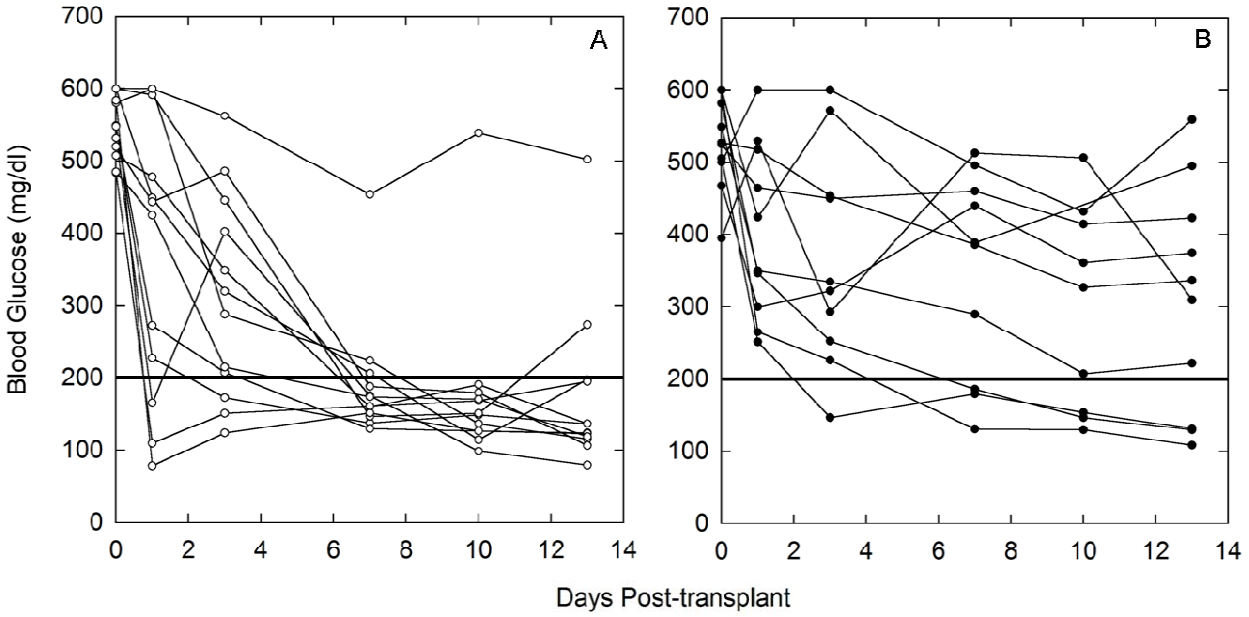

Figure 4-11: Blood glucose concentrations in diabetic BALB/c mice following intraperitoneal transplantation of encapsulated aggregates (A) or encapsulated islets (B).

(n=12, 10 respectively).

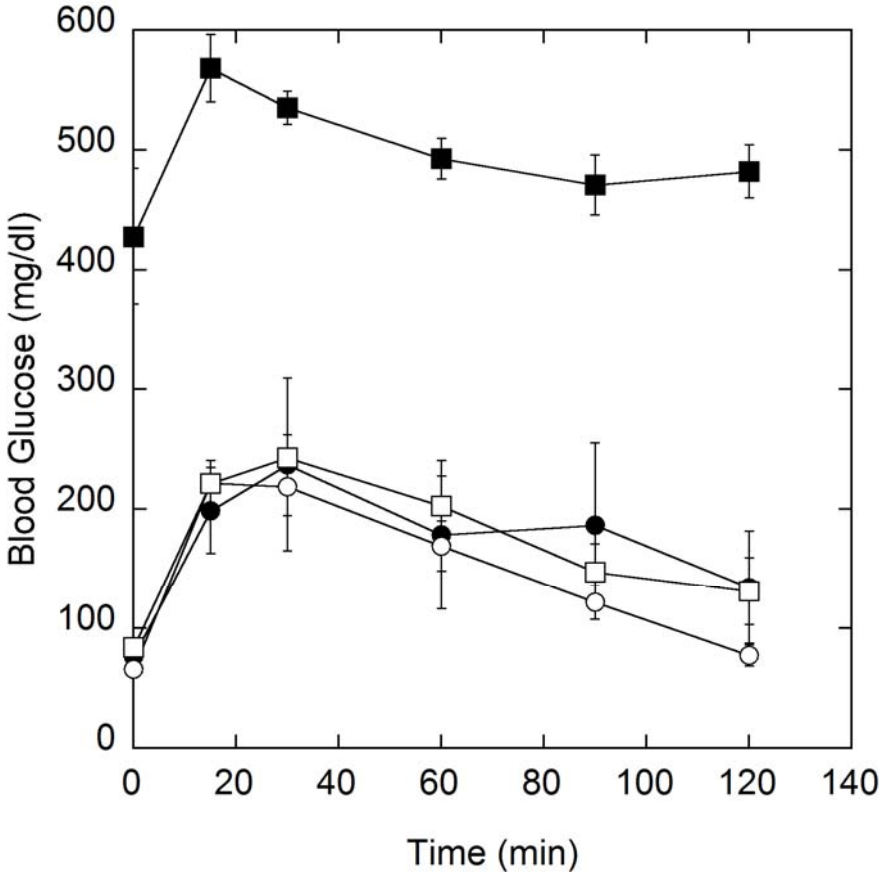

Figure 4-12: Intraperitoneal glucose tolerance test results

Blood glucose concentrations before (time 0) and after injection of glucose (2mg/g body weight) for encapsulated aggregates (○) or encapsulated islets (●), compared to normoglycemic (□) and hyperglycemic (■) controls. (n=12 10 3 and 2 respectively).

Table 4-1: Model parameters

Parameter	Symbol	Value	Units	Source
O_2 diffusivity in media	D_m	2.78×10^{-5}	cm^2/s	[23]
O_2 diffusivity in tissue	D_t	1.24×10^{-5}	cm^2/s	[23]
O_2 diffusivity in silicone rubber	D_{sr}	2.17×10^{-5}	cm^2/s	[116]
O_2 solubility in media	α_m	1.27×10^{-9}	mol/mmHg/ml	[23]
O_2 solubility in tissue	α_t	1.00×10^{-9}	mol/mmHg/ml	[23]
O_2 solubility in silicone rubber	α_{sr}	1.21×10^{-8}	mol/mmHg/ml	[116]
O_2 permeability in 2% (v/v) alginate	αD_{sr}	3.43×10^{-14}	mol/cm/mmHg/s	[23]
Maximum oxygen consumption rate	V_{max}	4×10^{-8}, 6×10^{-8}	$mol/cm^3/s$	[23], experiment
Michaelis-Menten Constant	K_m	0.44	mmHg	[23]
Insulin Secretion Model Parameter	P*	5.1, 1.1	mmHg	[93]

Table 4-2: Composition of islets and islet cell aggregates before and after hypoxic culture

Tissue type	Pre-culture β-cells (%)	20% O_2 β-cells (%)	2% O_2 β-cells (%)
Islet	74 ± 4 *	83 ± 0 *	76 ± 8
Islet cell aggregate	73 ± 1	73 ± 2 #	84 ± 5 #

Data are means +/- SE, n=3, *‡ $p<0.05$ by paired student t-test, †$p<0.02$ by unpaired student t-test.

Chapter 5 Evaluation of a perfluorocarbon emulsion within alginate capsules

5.1 INTRODUCTION

Microcapsules can be used to transplant islets to treat type 1 diabetes without the use of immunosuppressive drugs. Microcapsules are small spherical gels that range in size from 200 μm to 2 mm. Microcapsules are the most extensively studied encapsulation system and are the system that is under study in our lab. Microcapsules are hydrogels, most commonly made of alginate, that contain one to two islets. The tissue within a microcapsule relies on diffusion of nutrients through the hydrogel to the tissue and diffusion of waste products and secreted proteins of interest away from the tissue. The cells are protected from the immune system because the hydrogel keeps immune system effector cells, such as T cells and macrophages, from coming in contact with the transplanted tissue along with preventing or minimizing access of some large immune molecules such as antibodies and complement components.

Islets within the native pancreas are heavily vascularized, and during islet isolation procedures the vascular network of the islet is destroyed, collapses during culture and is never allowed to regenerate when the islets are transplanted within an immunoisolating device [89-91]. Tissue within a microcapsule must rely on delivery of oxygen and other nutrients by diffusion from the exterior of the device. Oxygen diffusion is much more limited than glucose diffusion because glucose concentrations *in vivo* are much higher than oxygen [92]. We will assume that the oxygen level is the critical component that determines encapsulated tissue survival and function. For oxygen to reach the encapsulated tissue it must diffuse from the vasculature to the device exterior, through the device to the tissue and through the islet while being consumed to

reach the cells at the center. Oxygen delivery is even further hampered when an immune reaction to the transplanted cells or immunoisolating material results in cells adhering to the outside of the device consuming oxygen before it is able to reach the cell in the device interior [23].

Reduced oxygen levels have been shown to reduce islet insulin secretion below what was observed under normoxic conditions [44, 47]. In the work by Dionne et al. [44] islets were perfused with media that was equilibrated with air at various oxygen levels, at gas phase P_{O2} values below 60 mmHg there was a reduction in insulin secretion. The ability of an islet to effectively secrete insulin following transplantation is essential for transplantation success. Thus, since reduced oxygen levels have been shown to decrease islet survival and function, effective oxygen delivery is critical for successful transplantation of immunoisolated islets to treat type 1 diabetes. Previous theoretical analysis of oxygen limitations to immunoisolated tissue have been studied and have shown that depending on the transplantation conditions these problems can be quite serious [23, 93].

In this study we will evaluate the use of a perfluorocarbon (PFC) emulsion as a permeability enhancer within the alginate matrix of a microcapsule to increase oxygen delivery to encapsulated islets. Perfluorocarbons are highly desirable materials for enhancing oxygen transport, due to their very high oxygen solubility, approximately 25 times that of water, on a volumetric basis. Enhanced solubility will lead to enhanced permeability because the permeability is a product of the solubility and diffusivity. Perfluorocarbon emulsions have been developed to be used as a blood substitute. There are reports in the literature that including a perfluorocarbon emulsion in islet culture enhances function [60]. Perfluorocarbons are also used during pancreas storage prior to islet isolation [61]. Culture of islets at the interface of a

perfluorocarbon and cell culture media (two layer method) has been studied and was not shown to be beneficial in improving islet survival [62]. There are two potential reasons for the lack of improvement (1) the culture system probably did not have any oxygen limitations for the islets cultured without PFC and (2) the two layer method is beneficial for short periods of time when the PFC can act as a source of oxygen, but as it is not exposed to the air directly it does not have an effect after its oxygen store has been depleted. All of these facts taken together indicate that the incorporation of perfluorocarbons into an encapsulating material is likely to be beneficial to enhancing islet survival in low oxygen. In Chapter 3 we determined based on theoretical predictions that perfluorocarbons can increase the oxygen levels experienced by encapsulated tissue and improve fractional viability and fraction of normal insulin secretion after transplantation. In this study we will expand the theoretical model in order predict encapsulated islet survival and function in culture in capsules with and without a perfluorocarbon emulsion. The modeling predictions will be used to select oxygen levels at which to carry out experiments. *In vitro* experiments were performed to determine if a PFC emulsion enhances islet survival in low oxygen. *In vivo* experiments were performed to evaluate the biocompatibility of PFC emulsion containing alginate microcapsules.

5.2 MODELING

To determine the culture conditions where the benefits of PFC containing microcapsules will be observed in terms of enhanced islet survival and function, a theoretical model has been developed to predict the local partial pressure of oxygen, which, in turn, is used to assess tissue viability and fraction of normal insulin secretion for encapsulated islets in culture. This model was adapted from the model for microcapsules containing islets discussed in Chapter 3 and quite similar to the model used in Chapter 4. For all calculations the microcapsules have a diameter of

500 μm, will contain one centrally located 150-μm diameter islet, and the microcapsule material will be 2% (v/v) alginate.

5.2.1 Model Geometry

Sketches of example geometries that were analyzed are presented in Figure 4-1A for microcapsules cultured on polystyrene which can be approximated as having an oxygen impermeable bottom and Figure 4-1B for microcapsules cultured in silicone rubber bottom plates which are oxygen permeable. All islet tissue is assumed to be spheres. An islet equivalent (IE) is a volume of tissue equal to that of a 150-μm sphere. The capsules are arranged in a monolayer on the bottom of the culture dish in a cubic array. For each capsule, with the origin placed at the center of the capsule, there are planes of symmetry perpendicular to the bottom of the culture dish, thus the model can be solved for only one quarter of the capsule in order to reduce the number of degrees of freedom.

5.2.2 Material and Tissue Properties

The effective permeability in subdomains containing several components was determined from theoretical relationships. The ratio of the effective permeability $(\alpha D)_{eff,i}$ for layer i consisting of a dispersed (d) phase and a continuous (c) phase (as occurs in the alginate subdomains of the model system) to the permeability of the continuous phase $(\alpha D)_c$ was calculated from Maxwell's relationship [75]

$$\frac{(\alpha D)_{eff,i}}{(\alpha D)_c} = \frac{2-2\phi+\rho(1+2\phi)}{2+\phi+\rho(1-\phi)} \tag{5-1}$$

where αD is the effective permeability of the material (mol/cm/mmHg/s), $\rho=(\alpha D)_d/(\alpha D)_c$ is the ratio of the permeability of the dispersed phase to the permeability of the continuous phase, and ϕ is the volume fraction of the dispersed phase. For the multiple dispersed phases employed in our model system, Maxwell's relationship was used sequentially, starting with the phase with the smallest particle size and ending with the phase with the largest particle size. For particle types of the same size, Maxwell's relationship was used for one particle, then the other (and in the reverse order), and the two results were averaged.

The perfluorocarbon emulsion that was studied consists of 70% (w/v) perfluorodecalin and 20% (w/v) Intralipid® (Baxter), a soybean oil emulsion and this emulsion will be what is used in all model simulations that contain PFC alginate [71]. In the final PFC alginate composite phase, there were perfluorodecalin and soybean oil droplets of approximately the same size; the alginate polymer itself was treated as an impermeable dispersed in water. The effective permeability of PFC emulsion was estimated by first using Maxwell's relationship for PFC droplets in water and then for soybean oil droplets in the PFC and water emulsion. Secondly, Maxwell's relationship was used for soybean oil droplets in water and then for PFC droplets in the soybean oil and water emulsion. The two calculated effective permeabilites were averaged. Finally, the effective permeability of PFC alginate was estimated with alginate as the dispersed phase and PFC emulsion as the continuous phase. The parameters used in the model are in Table 3-1.

5.2.3 Model Equations

The three-dimensional species conservation equation for reaction and diffusion at steady state was used to predict the oxygen profile within the different tissue, alginate, cell culture media, and silicone rubber subdomains of the culture system:

$$D_i \nabla^2 C_i = V_i \tag{5-2}$$

where D_i (cm^2/s) is the effective diffusivity of oxygen in subdomain i, C_i (mol/cm^3) is the concentration of oxygen in subdomain i, and V_i ($mol/cm^3/s$) is the local oxygen consumption rate per unit volume in subdomain i. For convenience, since partial pressures are equal across interfaces of different materials, we make use of oxygen partial pressure instead of concentration, which are related by

$$C = \alpha P \tag{5-3}$$

where α ($mol/cm^3/mmHg$) is the effective Bunsen solubility coefficient in subdomain i and P is the partial pressure of oxygen. Combining Eq. (1) and Eq. (2) gives

$$(\alpha D)_i \nabla^2 P_i = V_i \tag{5-4}$$

The oxygen consumption rate is assumed to follow Michaelis-Menten kinetics for all tissue,

$$V_i = \frac{V_{max} \varepsilon_i P_i}{K_m + P_i} \tag{5-5}$$

where V_{max} is the maximum oxygen consumption rate for the tissue, ε_i is the tissue volume fraction in subdomain i, and K_m is the Michaelis-Menten constant. No oxygen is consumed in the alginate, cell culture media, or silicone rubber subdomains; therefore V_i is equal to zero in those subdomains, and the tissue volume fraction in the islet or aggregate subdomains is equal to one.

The model was solved by the finite element method using the commercially available software package COMSOL Multiphysics in combination with MATLAB and using the model parameters in Table 3-1. (3-4) was solved simultaneously for all subdomains of the culture system subject to the following conditions. There are planes of symmetry on the sides of the unit cell where the media or capsule was cut and thus zero flux of oxygen across these boundaries. At the boundary between a tissue subdomain and the alginate subdomain or the alginate subdomain and culture media the partial pressure of oxygen and the flux of oxygen across the boundary are both equal. For the case of capsules cultured on polystyrene the bottom of the culture dish is assumed to be impermeable to oxygen and the flux across that boundary is zero. For the silicone rubber bottom culture condition, the oxygen partial pressure and flux of oxygen across the boundary are equal at the culture media and silicone rubber boundary. The bottom boundary of the silicone rubber membrane is at the partial pressure of oxygen in the gas phase. The external partial pressure of oxygen in the gas phase is specified and it is assumed that the top surface of the culture media is at the gas phase partial pressure of oxygen.

The fractional viability of the encapsulated tissue was estimated by determining the volume fraction of tissue where $P>P_C$. P_C is the critical oxygen partial pressure below which tissue dies and the value of P_C is assumed to be 0.1 mmHg [23]. The fractional viability was calculated using the following equation:

$$\text{Fractional Viability}=\frac{V_{Viable}}{V_{Tissue}} \qquad (5\text{-}6)$$

where V_{Viable} is the volume of tissue where P is greater that 0.1 mmHg and V_{Tissue} is the total encapsulated tissue volume.

The relationship used to predict the local fraction (F_I) of normal insulin secretion rate as a function of local oxygen partial pressure within the islet was developed from data on the effect of

hypoxia on islet insulin secretion, estimating the oxygen partial pressure profile within the islet in the experimental system, and then determining the simplest model type and parameter(s) that best predict the insulin secretion level [44, 93].

$$\begin{aligned} P < P^* \text{ mmHg} \quad & F_I = \frac{P}{P^*} \\ P \geq P^* \text{ mmHg} \quad & F_I = 1.0 \end{aligned} \tag{5-7}$$

When V_{max} equals $6x10^{-8}$ mol/cm^3/s, P* equals 1.1 mmHg [93]. A value of V_{max} of $6x10^{-8}$ mol/cm^3/s was used for the predictions of encapsulated tissue viability and function in culture because it corresponds to an OCR per cell of 4 fmol/min/cell which is within the range that was measured for rat islets used in these experiments. The fraction of normal insulin secretion averaged over all tissue within the microcapsule was determined by evaluating the volume integral of F_I in all tissue containing subdomains

$$F_S = \frac{\int_{\text{Viable}} F_I dV}{V_{\text{Tissue}}} \tag{5-8}$$

where F_S is the fraction of normal insulin secretion averaged over all of the encapsulate tissue.

5.3 MODELING RESULTS

Traditional cell culture is carried out in polystyrene dishes which have a bottom that can be assumed to be impermeable to oxygen. We performed calculations to predict the fractional viability for islet capsules with and without perfluorocarbon emulsion cultured on polystyrene dishes over a range of oxygen levels. We performed these calculations in order to determine what gas phase oxygen level should be used for *in vitro* culture experiments in order to show that islets survive better in PFC containing microcapsules. The predicted differences in fractional viability of islets were not as great between the normal alginate and PFC alginate capsules as we

would have hoped based on previous theoretical predictions with a specified capsule surface P_{O2} (Figure 5-2A-C). When cultured on polystyrene the prediction fractional viabilities were very dependent on tissue surface density. We also performed calculations in which the capsules were cultured in oxygen permeable silicone rubber bottom dishes (Figure 5-2D-F) which have been previously used to enhance oxygen transport to islets cultured at P_{O2} of 142 mmHg and for better oxygen control during embryonic stem cell differentiation at low oxygen [109, 110]. Calculations predicted greater differences in encapsulated islet survival, tissue could survive at lower gas phase oxygen levels for both capsule types, and the predicted viabilities had less of a dependence on surface density. The silicone rubber membranes allow for better oxygen control to the encapsulated islets and maximize the predicted differences in tissue survival. Silicone rubber membranes were therefore used for *in vitro* experiments to demonstrate that islets in PFC capsules will survive better than islets in normal alginate in low oxygen.

Calculations were performed to predict the fraction of normal insulin secretion and fractional viability of encapsulated islets with and without PFC emulsion in the microcapsule cultured on silicone rubber over at a gas phase oxygen level of 3.5 mmHg or 0.5% oxygen. These calculations were used to determine what gas phase oxygen level should be used during *in vitro* experiments to observe that islets in PFC alginate microcapsules function and survive better in low oxygen than islets in normal alginate microcapsules. At a gas phase oxygen level of 3.5 mmHg (0.5%) islet survival is predicted to be greater in PFC alginate capsules compared to normal alginate capsules (34% versus 23%) at low surface densities (Figure 4-3A). Insulin secretion is significantly impaired for both tissue types (<20%) (Figure 4-3B). We chose to culture tissue at a gas phase P_{O2} of 3.5 mmHg in order to ensure that there would be loss of tissue in the normal alginate capsules, but still greater survival rates in the PFC alginate capsules.

5.4 MATERIALS AND METHODS

5.4.1 Animals

Male Sprague-Dawley rats weighing 200-250 g (Harlan Sprague-Dawley, IN) were used as islet donors. Lewis rats were used as recipients of empty capsule transplants. Animals were kept in a conventional animal facility with free access to food and water. All animal experiments were approved by the Joslin Animal Care Committee.

5.4.2 Islet Isolation

Rat islets were isolated according to standard techniques [70]. Briefly a laparotomy was performed under anesthesia with Ketamine/Xylazine. The common bile duct was cannulated and 8-10 ml of rodent Liberase RI ((Roche) 0.33 mg/ml) in M199 media was injected. The pancreas was then removed and incubated in a circulating water bath at 37^{o}C for 24.5 minutes. The digested pancreatic tissue was washed with M199 containing 10% newborn calf serum (Mediatech) and then strained through 400 μm wire mesh (Thomas Scientific). Islets were purified by centrifugation at 1750xg for 17 minutes through a discontinuous Hisotpaque 1077 gradient (Sigma Aldrich). Islets were handpicked under a dissecting microscope, counted, and then cultured overnight at a density of up to 30 islets/cm^2 and a media height of 1.3 mm. Islet culture media was RPMI 1640 supplemented with 10% fetal bovine serum, penicillin 100 units/ml and 100 μg/ml streptomycin (Mediatech).

5.4.3 PFC Emulsion Preparation

A perfluorocarbon emulsion made from perfluorodecalin (Fluoromed, Round Rock, TX) and 20% (w/v) Intralipid® (Baxter, Deerfield, IL) (a soybean oil emulsion with composition 20% (w/v) soybean oil, 1.2% (w/v) egg yolk phospholipids, 2.3% (w/v) glycerin with balance water) was prepared similarly to a previously developed emulsion to be used a blood substitue

(Schweighardt and Kayhart 1990). 40 ml of Intralipid was added to the holding vessel of an M110Y Microfluidizer (Microfluidics, Newton, MA) and recirculated for 2 minutes at an operating pressure of 14,500 psi. Upon exit from the interaction chamber, before returning to the holding reservoir, the liquid was passed through a cooling coil during all instrument operation. 11.25 ml of perfluorodecalin was added dropwise over 3 minutes to the holding vessel while the emulsion was being recirculated. The instrument and contents sat without running for 5 minutes to cool and for the ice bath to be changed. The remainder of the perfluorodecalin (11.25 ml) was added dropwise to the holding vessel over three minutes while the emulsion was recirculated. After all of the emulsion components had been added the emulsion was recirculated for 5 minutes before being collected. The final PFC content of the emulsion was 70% (w/v).

5.4.4 Microencapsulation

Microcapsules were produced using highly purified sterile alginate. The exact concentrations and type of alginate varied depending on the experiment and if PFC emulsion was contained in the capsule. For normal alginate capsules a concentration of 1.5% (w/v) SLG100 (FMC Polymer, Norway) was used for *in vitro* experiments and a concentration of 1.9% (w/v) SLM100 (FMC Polymer, Norway) was used for transplant experiments both alginate types were dissolved in 0.9% (w/v) NaCl solution. For PFC alginate capsules a concentration of 0.5% (w/v) SLG100 was used for *in vitro* experiments and a concentration of 0.63% (w/v) SLM100 was used for transplant experiments both alginate types were dissolved in 70% (w/v) PFC emulsion. The final PFC concentration in the microcapsules was 70% (w/v). Islets were washed with calcium free Krebs buffer (135 mM NaCl, 4.7 mM KCl, 1.2 mM KH_2PO_4, 1.2 mM $MgSO_4$, 25 mM HEPES, pH 7.4) and then resuspended in alginate to form a tissue-alginate suspension. Microcapsules were produced by extrusion of the alginate-tissue suspension for *in vitro*

experiments or pure alginate solution for *in vivo* experiments through a needle using an electrostatic droplet generator (Pronova Polymer, Norway) into a stirred 20 mM $BaCl_2$ solution. Microcapsules ranged in size from 350 μm to 600 μm in diameter with an average for each batch between 400 μm and 500 μm. After sequential washes in HEPES buffer (132 mM NaCl, 4.7 mM KCl, 1.2mM $MgCl_2$, 25 mM HEPES, pH 7.4) and Krebs buffer (133 mM NaCl, 4.7 mM KCl, 1.2 mM KH_2PO_4, 1.2 mM $MgSO_4$, 25 mM HEPES, 2.5 mM $CaCl_2$, pH 7.4) the microcapsules were placed into culture. Some of the capsules used for the transplantation experiments were coated by two different methods. The coating of PFC alginate capsules with poly-L-lysine (PLL) and alginate used in the transplantation experiments were prepared as follows. After the wash with HEPES buffer the capsules were placed in a 0.1% PLL solution in calcium free Krebs buffer for 10 minutes, washed with calcium free Krebs buffer, placed in 0.19% (w/v) SLM100 alginate in calcium free Krebs buffer for 6 minutes, washed with calcium free Krebs buffer, and then with Krebs buffer. The second type of coated capsules had a pure alginate coating that was prepared after the HEPES buffer wash by placing the capsules in 0.19% (w/v) SLM100 in calcium free Krebs buffer for 6 minutes, washing the capsules with calcium free Krebs, transferring the capsules into 20 mM $BaCl_2$ for 5 minutes, washing the capsules with HEPES buffer, and finally with Krebs buffer.

5.4.5 Encapsulated Tissue Culture

Capsules that were cultured in 1% oxygen were placed in 100 cm^2 silicone rubber flasks (PR-AY-5-0017-5 from Wilson Wolf Manufacturing Inc., New Brighton, MN) in islet culture media at a depth of 2.5 mm, at a density of less than 30 IE/cm^2 The silicone rubber flasks were placed in a sealed humidified chamber within in an incubator at 37^oC that was continually flushed with 1% O_2, 5% CO_2, and balance N_2. Capsules to be cultured at 0.5% oxygen were

placed in 24 well plates that were custom made to contain silicone rubber bottoms (PR-AY-7-0004, from Wilson Wolf Manufacturing Inc., New Brighton, MN) in islet culture media at a depth of 10 mm at a density of 50-200 IE/cm^2 and then placed into a humidified incubator (Xvivo from Biospherix Ltd., Redfield, NY) where the gas levels were controlled to be at 5% CO_2, 0.5% O_2, and with balance N_2. Capsules were cultured for two days under these conditions for the *in vitro* experiments.

5.4.6 Oxygen Consumption Rate (OCR)

The oxygen consumption rate measurements were performed as previously described (Chapter 2 and [66]). Islet microcapsules were resuspended in DMEM without phenol red containing 4.5 g/l glucose supplemented with 0.6 g/l L-glutamine, 100 units/ml penicillin, 100 µg/ml streptomycin, 10 mM HEPES (all from Mediatech Inc., Herdon, VA) without serum for OCR measurements. Phenol red free media was required such that the media would be colorless as to not interfere with the absorbance measurements associated with the alginate or PFC emulsion content assays. The tissue microcapsule samples were added to a 200 µl stirred titanium chamber maintained (Micro Oxygen Uptake System FO/SYSZ-P250, Instech Laboratories, Plymouth Meeting, PA) at 37^{o}C [66]. After the samples equilibrated with air at 37^{o}C the chambers were sealed. The time dependent P_{O2} within the chamber was recorded with a fluorescence-based oxygen sensor (Ocean Optics, Dunedin, FL), and the data at high P_{O2} was fit to a straight line. The maximal OCR was evaluated from $OCR=V_{ch}\alpha(\Delta P_{O2}/\Delta t)$, where V_{ch} is the chamber volume and α is the effective Bunsen solubility coefficient for the contents of the OCR chamber and must be adjusted for the presence of PFC and soybean oil in the microcapsules.

5.4.7 Capsule Dissolution

Many of the quantitative measures of encapsulated tissue - nuclei counts, DNA content, alginate content, or insulin content require that the capsule first be dissolved. After OCR measurements were complete the tissue was collected from the chamber in order to determine the tissue and capsule quantity corresponding to each measurement. Tissue was removed from the microcapsules by adding 800 µl of 100 mM tetrasodium EDTA (pH=8) to approximately 300 µl of a capsule suspension. The samples were placed in an incubator at 37^{o}C for 1 and were vortex mixed every 30 minutes at which point the capsules had dissolved.

5.4.8 Nuclei Counts

Nuclei suspensions were prepared and quantified as described in Chapter 2. 200 µl aliquot of islet tissue from dissolved capsules (~ 2.5 x 10^6 cells/ml or 125 IEQ/ml) was resuspended in 100 µl of PBS and then incubated in a lysis solution (0.1 M citric acid and 10% (v/v) Triton X-100 (Sigma Aldrich)) for 15 min with vortex mixing every 5 minutes. Next the nuclei sample was sheared through a needle to liberate all nuclei. 100 µl of 100mM tetrasodium EDTA was added to the nuclei suspension to prevent alginate gelling prior to nuclei counting. The liberated nuclei were stained with 0.8 µM LDS 751 and 0.2 µM Sytox Orange (Invitrogen,) in D-PBS and counted using a benchtop flow cytometer (Guava Personal Cell Analyzer, Guava Technologies, Hayward, CA).

5.4.9 Alginate Content

The alginate content of samples were assayed by a method adapted from the literature using dimethyl methylene blue **(**DMMB) (Sigma Aldrich) dye which is a cation that binds to

polyanions such as alginate(Chapter 2, [72]). The ratio of the absorbance of a sample at the wavelengths of 520 nm and 650 nm increased linearly with increases in alginate concentration.

5.4.10 PFC Emulsion Content

The PFC emulsion content of samples were assayed by measuring the absorbance of diluted PFC emulsion samples. The emulsion content could be assessed by absorbance because due to the emulsion particle size (400 nm) the emulsion is opaque and thus at dilute concentrations the absorbance of a sample at any wavelength increases linearly with increasing emulsion content. We chose to measure the absorbance at 620 nm.

5.4.11 Histology

Encapsulated islets or islet cell aggregates were fixed in 2.5% (w/v) glutaraldehyde in 0.1M phosphate buffer pH 7.4. Plastic 1-μm thick sections were generated and stained with toluidene blue (Thermo Fisher Scientific).

5.4.12 Transplantation of Microcapsules into the Peritoneal Cavity

Microcapsules were injected into the peritoneal cavity of recipient rats through a central midline 5-10 mm incision using a sterile plastic transfer pipette (Fisher Scientific, Chicago, IL). The incision was closed using 5/0 silk, the outer layers were stapled. The animals were under anesthesia with Ketamine/Xylazine. Capsules were retrieved 2 weeks after transplantation by laparotomy and peritoneal lavage. Capsules were washed in PBS and prepared for paraffin sections.

5.4.13 Paraffin Sections

Capsules were fixed in buffered formalin for 1 hour. Capsules were embedded in 2% (w/v) agar, embedded in paraffin, sectioned, and stained with hematoxylin to label cells on the capsule exterior. Slides were then examined under a microscope and it was determined whether or not they elicited an immune reaction. It was necessary to look at the capsule sections to determine the degree of immune reactions because due to the complete opacity of the PFC containing capsules the cells on the capsule exterior could only clearly be observed after sectioning.

5.4.14 Statistics

Data are expressed as average ± standard deviation. Statistical significance was determined by a two-way Student t-test.

5.5 RESULTS

5.5.1 OCR and Tissue Recovery

Oxygen consumption rate (OCR) measurements of encapsulated islets were performed on the day of encapsulation and again after two days of culture under low (0.5% or 1%) oxygen conditions. The OCR is measured for a sample of capsules, and then the capsules are removed from the chamber and dissolved. The dissolved capsule tissue and alginate suspension can be analyzed to determine nuclei count, alginate content (normal alginate only), or PFC emulsion content of the sample within the OCR chamber. The alginate content or PFC emulsion content is measured in order to normalize the OCR results by the volume of capsules in the chamber. OCR recovery, a measure of the fractional recovery of viability tissue from culture, is calculated from the measured values of OCR per ml capsule using the following equation:

$$\text{Fractional OCR Recovery} = \frac{\left(\text{OCR per ml capsule}\right)_{\text{After 2 Day Culture}}}{\left(\text{OCR per ml capsule}\right)_{\text{After Encapsulation}}} \qquad (5\text{-}9)$$

OCR recovery was assessed for capsules containing islets with or without PFC emulsion cultured for two days in 0.5% oxygen in one experiment (Figure 5-4). The fractional OCR recovery in low oxygen for capsules containing islets and PFC was 0.91 indicating reduced oxygen limitations compared to an OCR recovery of 0.59 for the capsules containing islets without PFC. These results seem to indicate the PFC emulsion in the alginate microcapsule enhances tissue survival in low oxygen.

Prior to the one experiment at 0.5% oxygen many experiments (n=11) were performed in which islets were encapsulated in alginate with and without a PFC emulsion and cultured at 1% oxygen. The OCR and tissue recovery were then measured. Fractional tissue recovery from culture based on nuclei counts is calculated by the following equation:

$$\text{Fractional Tissue Recovery} = \frac{\left(\text{Nuclei per ml capsule}\right)_{\text{After 2 Day Culture}}}{\left(\text{Nuclei per ml capsule}\right)_{\text{After Encapsulation}}} \qquad (5\text{-}10)$$

The alginate or PFC emulsion content of the sample is measured to normalize the nuclei count by the total volume of capsules in the sample due to the high variability of capsule sampling. The results of the experiments at 1% oxygen were highly variable as can be seen by the large error bars even though the sample number is quite high and there was no difference in OCR recovery for either tissue type, but there was a significantly less tissue recovery in the PFC containing capsules compared to the normal alginate capsules (Figure 5-5). The loss of total tissue but not viable tissue indicated that something else was going on with the islets in the PFC emulsion containing capsules. There was a minimal loss of OCR recovery for either capsule type indicating that oxygen was not limiting enough to cause tissue death. Upon further analysis the

silicone rubber culture vessels used for 1% oxygen culture have a head space of about half a liter and no filter in cap for gas exchange. Potentially the large volume of air at atmospheric oxygen trapped in the flask initially continued to supply oxygen to the tissue throughout the two days of culture and thus limited the extent of tissue loss. The culture vessel was changed for the 0.5% experiments in order to not trap large amounts of atmospheric levels of oxygen in the culture system with the use of a 24 well plate with silicone rubber bottom wells that allows for gas exchange in the head space, a much smaller head space, and delivery of oxygen through the silicone rubber membrane at the bottom of the device.

From the measurements of OCR and nuclei one can also calculate the oxygen consumption rate per cell (Figure 5-6). The OCR per cell results were unusual for islets in PFC containing microcapsules. There was no change in OCR per cell for islets in normal alginate capsules between the two days of the experiment, but there was a significant increase in OCR per cell for islets in PFC containing capsules after two days of culture at 1% oxygen. At either experimental time point, pre-culture or after two days of culture at 1% oxygen the measured OCR per cell was significantly higher in the PFC containing capsules compared to the islets in the normal alginate capsules. The presence of PFC in the microcapsule appears to favorably influence oxygen consumption rates.

5.5.2 Histology

Histological sections of islet capsules with and without a perfluorocarbon emulsion cultured in 1% or 20% oxygen for two days were prepared to examine the health of the tissue following culture (Figure 5-7). In Figure 5-7A,D an islet in a normal alginate capsule shows signs of central necrosis as there is lighter toluidene blue staining at the center of the islet. In

Figure 5-7B,C,E,F a histological section of an islet in a PFC alginate capsulr the cells at the exterior of the islet, indicated by the arrow, are dead. In Figure 5-7F there appear to be reduced signs of central necrosis after culture in 1% oxygen as the capsules at the center are not lightly stained. In all section of islets in PFC capsules it was observed that cells that were in contact with the PFC alginate were dying leading us to believe that some component of the PFC emulsion is toxic to the islets.

In order to investigate further which component of the PFC emulsion was toxic to the islets, unencapsulated islets were cultured for two days in standard islet culture media (Figure 5-8A), at the interface between pure perfluorodecalin and islet culture media (Figure 5-8B), or islet culture media that contained Intralipid® (a soybean oil emulsion) (Figure 5-8C). The islets in standard islet culture media appear to be healthy. The islets cultured on top of perfluorodecalin also appear to be healthy with no signs of dead cells at the islet exterior. The islets tended to clump on top of the perfluorodecalin, but this could be due to the hydrophobic nature of perfluorodecalin. Islets cultured in media that contained Intralipid® do not look healthy and dead cells are present at the islet exterior. Based on histological analysis it seems that the toxic component of the PFC emulsion is the Intralipid®.

5.5.3 Empty PFC Capsule Transplants

Empty alginate capsules of four types: (1) no PFC emulsion 1.9% (w/v) alginate, (2) PFC emulsion 0.63% (w/v) alginate, (3) PFC emulsion 0.63% (w/v) alginate coated with pure alginate, and (4) PFC emulsion 0.63% (w/v) alginate coated with poly-L-lysine and alginate were transplanted into the peritoneal cavity of Lewis rats for 2 weeks. The PFC emulsion that was incorporated into the microcapsules was 70% (w/v) perfluorodecalin. At two weeks the

animals were sacrificed and the capsules were recovered from the peritoneal cavity. Alginate capsules that did not contain PFC emulsion caused no immune response *in vivo* as no cells were detected attached to the capsule surface after retrieval (Figure 5-9A). Capsules containing PFC emulsion with no additional coatings or only a pure alginate coating elicited a strong immune reaction as can be seen in the histological sections where the capsules are covered with many layers of cells (Figure 5-9B and C). Capsules containing PFC emulsion were biocompatible when a poly-L-lysine and pure alginate coatings were applied to the outside as again no cells were attached to the outside of the capsules after transplantation (Figure 5-9D). An effectively bound coating of the PFC capsules consisting of poly-L-lysine and alginate was necessary in order to make the capsules biocompatible.

5.6 DISCUSSION

The PFC emulsion that was incorporated into the alginate microcapsules proved to be toxic to encapsulated islets as observed by histology. Upon further examination by culturing naked islets in each of the emulsion components (perfluorodecalin or soybean oil emulsion) the component of the PFC emulsion that was toxic to islets was the soybean oil emulsion and not the PFC itself. The fact that we observed that a soybean oil emulsion was toxic to islets is not surprising as culture of islets in free fatty acids (the components of soybean oil) can induce apoptosis and reduces insulin secretion during long term culture [117-120]. The histology samples with islets cultured on top of perfluorodecalin showed that the islets tended to clump and in some cases there were no signs of central necrosis with very large tissue sizes. Potentially the presence of the perfluorodecalin in the culture flask was actually enhancing oxygen transport to the large tissue aggregates. This is only a general observation and was not quantified in any sort of systemic way, and there was some tissue that showed signs of central necrosis.

The OCR and nuclei recovery results for islets cultured in microcapsules with and without PFC emulsion at 1% oxygen were puzzling. There was no difference in OCR recovery for islets in the two capsule types, but there was a loss of tissue in the PFC containing microcapsules. The loss of tissue would be consistent with the fact that we observed cell death by histological analysis, but cell death was not detected by OCR recovery a proven method of measuring tissue loss due to oxygen transport limitations [110]. One potential explanation for a greater loss of tissue as compared to oxygen consumption is that the soybean oil emulsion in the microcapsule was stimulating insulin secretion. It has been reported that treatment of islets with free fatty acids, the components of soybean oil, for several hours can induce insulin or glucagon secretion [121]. The effect of free fatty acids on islets is complex as they are toxic in the long term, but stimulate insulin secretion in the short term. OCR has also been shown to increase with increases in insulin secretion in response to glucose [122]. Potentially the soybean oil emulsion is stimulating the islets to secrete insulin and thus increasing their oxygen consumption rate on a per cell basis in comparison to the islets in alginate microcapsules without PFC. The OCR recoveries presented at 0.5% oxygen look promising in that there is more tissue survival in capsules with PFC containing microcapsules, but all of these results are difficult to interpret as the effects of the soybean oil on the islets are complicating the interpretation of the data.

The experiment that was performed where encapsulated islets were cultured in 0.5% oxygen did show tissue death in the normal alginate capsules. We were able to actually induce death in the normal alginate capsules because a culture system was used that was not trapping large amounts of atmospheric oxygen levels in the culture system. It seems that this culture system is much better suited to carry out low oxygen culture experiments. The loss of tissue in

alginate capsules cultured at 0.5% oxygen is at least keeping with the theoretical predictions that the fractional viability should only be 20%; however the actual loss of tissue was not as severe.

In order to make the PFC emulsion containing microcapsules biocompatible after transplantation into the peritoneum of Lewis rats a poly-L-lysine and pure alginate coating needed to be applied to the capsules exterior. It is unknown whether with a new emulsion formulation that does not contain soybean oil whether this will be necessary. Potentially the soybean oil was toxic to tissue in the peritoneum and thus this is what caused the immune reaction. When a new formulation is developed the biocompatibility of capsules with and without coatings should be tested.

There is a potential for perfluorocarbons to be used to enhance oxygen transport to islets as pure perfluorocarbons do not appear to be toxic. A different PFC emulsion formulation needs to be developed which does not contain soybean oil. This new emulsion will likely be a suitable material to enhance the oxygen permeability of encapsulation materials. The theoretical predictions in Chapter 3 and this chapter have shown that a PFC emulsion can enhance the oxygen delivery to encapsulated tissue which in turn increases fractional viability and insulin secretion. Unfortunately due to the toxic side effects of the PFC emulsion we were not able to show that a PFC emulsion conclusively enhanced oxygen transport to encapsulated islets, but the approach warrants further investigation. When a non-toxic PFC emulsion is developed the experimental approach of culturing the encapsulated islets on silicone rubber and performing OCR and nuclei measurements should be performed to evaluate if the PFC emulsion can enhance islet survival in low oxygen.

Contributions: Islet isolations were performed with the assistance of Esther O'Sullivan, Jennifer Hollister-Lock, Vaja Tchipasvilli, and Vassileios Kostaras from Joslin Diabetes Center. Histology sections were prepared by Chris Cahill (Joslin DERC). Abdulkadir Omer provided instruction on the preparation of microcapsules and performed the empty capsule transplants with my assistance. Susan Bonner-Weir assisted in the evaluation of the histological sections.

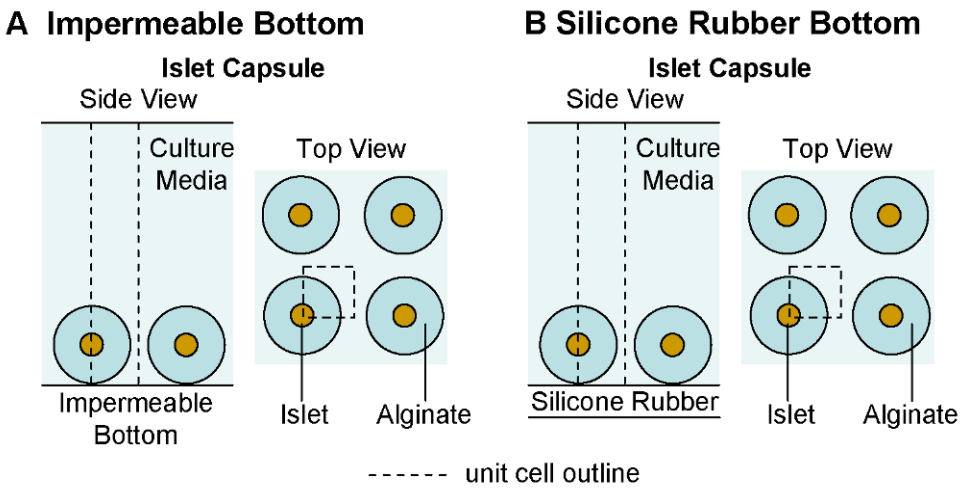

Figure 5-1: Sketches of example model geometries for microcapsules containing one 150-µm islet in culture on either an oxygen impermeable bottom (A) or an oxygen permeable silicone rubber bottom culture dish (B).

The dashed lines represent the unit cell in which the oxygen profile was calculated.

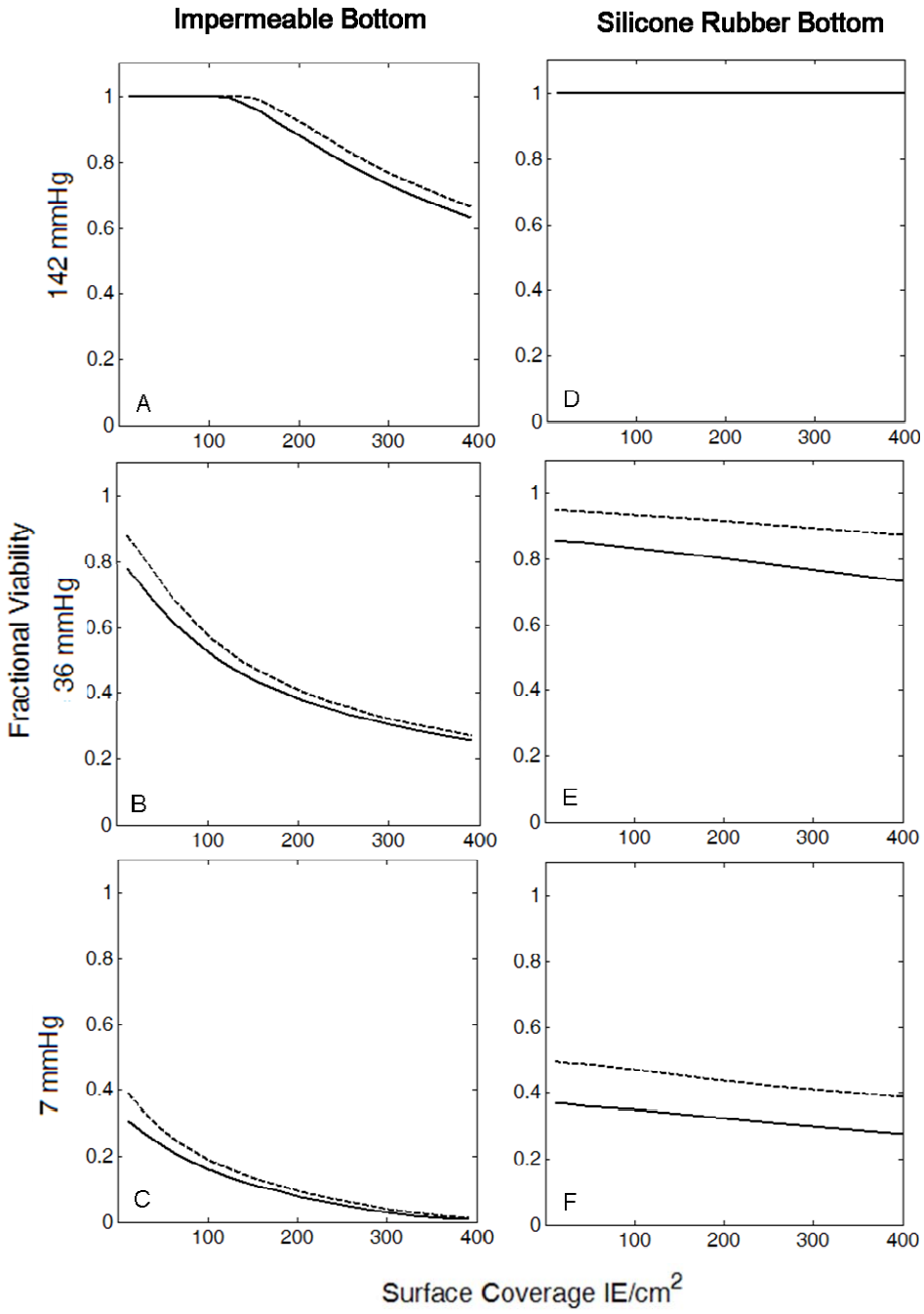

Figure 5-2: Comparison of predicted fractional viability for islets cultured in normal alginate (solid lines) or PFC alginate (dashed lines) capsules on polystyrene (A-C) or silicone rubber (D-F).

Predictions were made for a gas phase oxygen level of 142 (A,D), 36 (B,E), or 7 (C,F) mmHg.

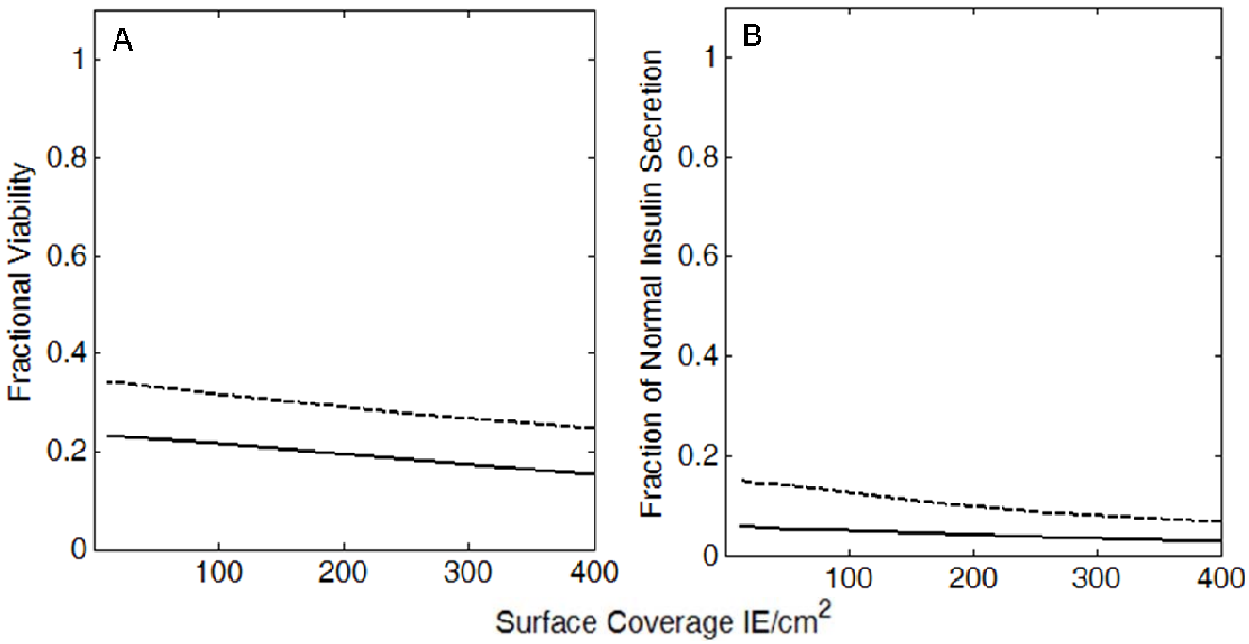

Figure 5-3: Comparison of predictions of fractional viability (A) and insulin secretion (B) for islets encapsulated in PFC alginate (dashed lines) and normal alginate (solid lines) cultured on silicon rubber at a gas phase oxygen partial pressure of 3.5 mmHg (0.5%).

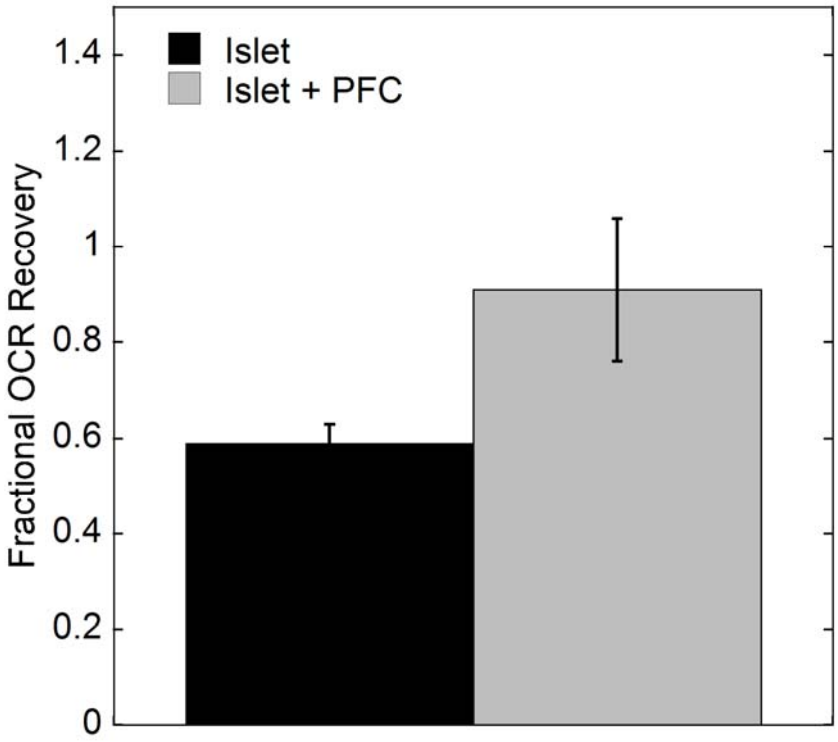

Figure 5-4: Measured fractional OCR recovery for islets in normal alginate or PFC alginate capsules cultured for two days at 0.5% oxygen from triplicate measurements in one experiment. The results were not statistically different based on a t-test $p>0.05$.

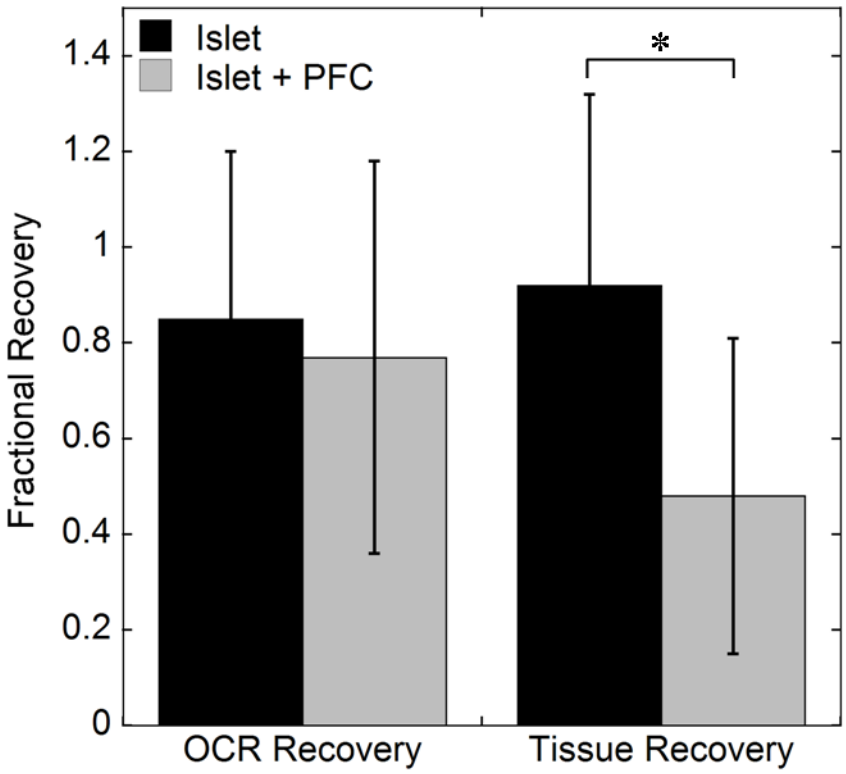

Figure 5-5: Measured fractional recoveries of oxygen consumption and tissue after culture for two days in 1% oxygen for islet capsules (black bars) or islet capsules with PFC (grey bars). There was no difference in OCR recoveries for either type of capsule ($p>0.05$ by unpaired student t-test), but there was a significant more loss of total tissue in the PFC containing capsules (* $p<0.05$ by unpaired student t-test).

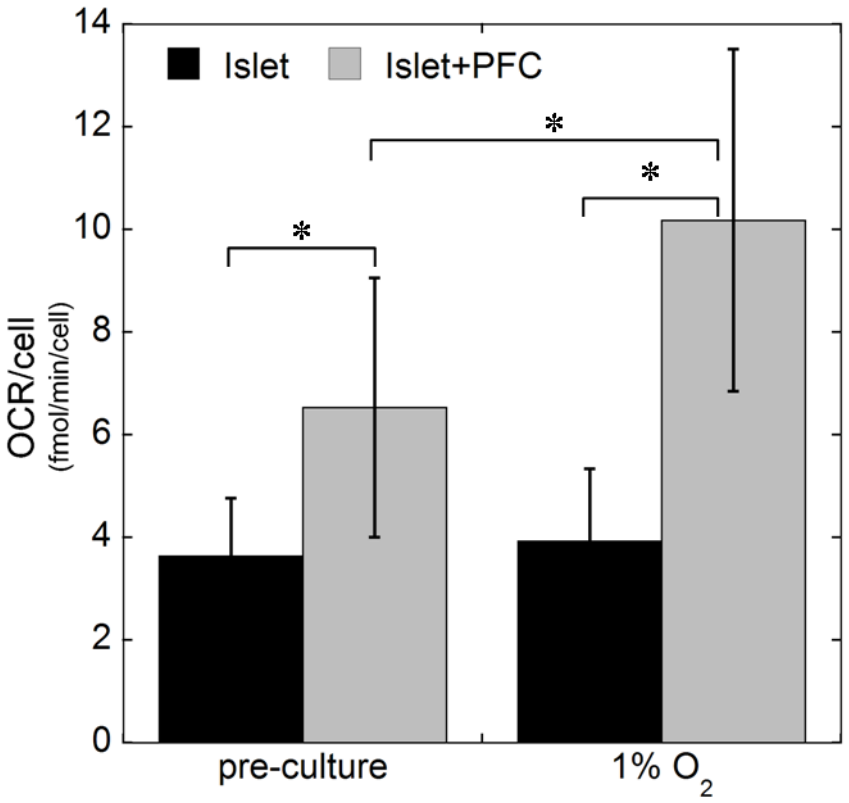

Figure 5-6: Measured oxygen consumption rater per cell before and after culture for two days in 1% oxygen for islet capsules (black bars) or islet capsules with PFC (grey bars).

There was no difference in OCR per cell for islet capsules between the two days ($p>0.05$ by unpaired student t-test), but there was a significant increase in OCR per cell in the PFC containing capsules (* $p<0.05$ by unpaired student t-test). Also at each experimental time point, prior to culture or after two days of culture at 1% oxygen the OCR per cell was significantly higher in the PFC containing capsules.

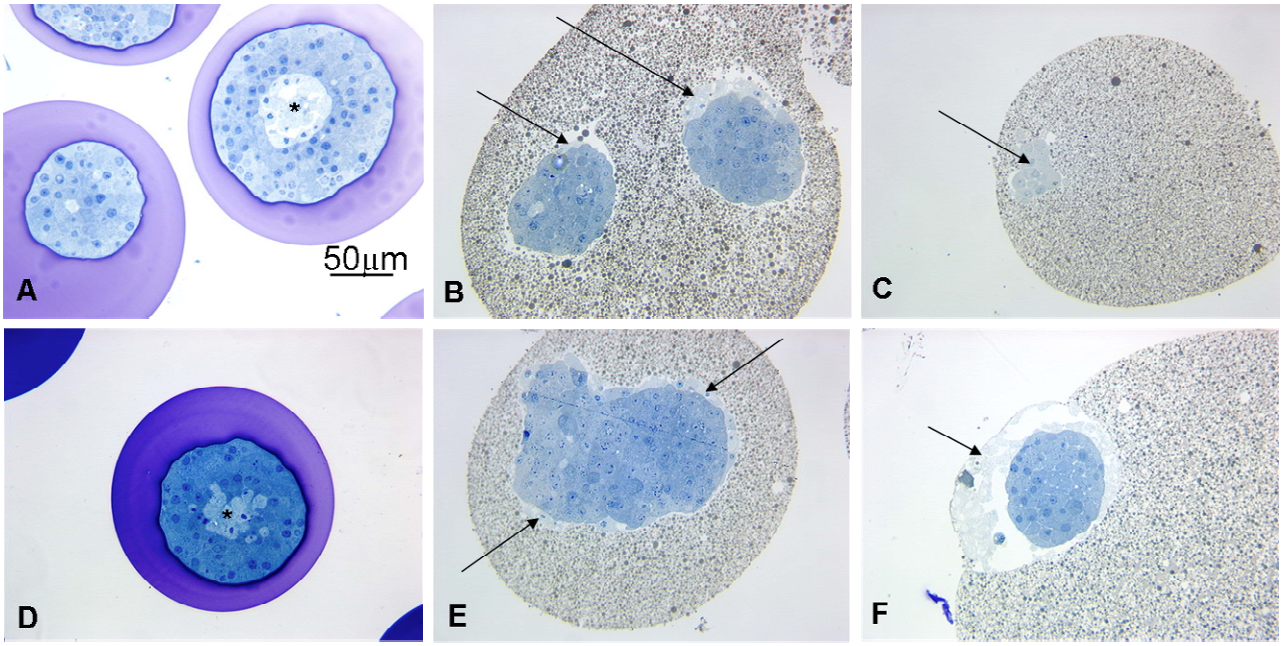

Figure 5-7: Histological sections of islets in microcapsules with and with PFC.

(A) normal alginate microcapsule after two days of culture 20 % oxygen– there are signs of central necrosis in the larger islet (*) as there is only light staining at the islet center. (B,E) 70% (w/v) PFC alginate microcapsule with islets on the day of encapsulation, there are already signs of toxicity as dead cells are found at the islet exterior. (C) 70% (w/v) PFC alginate microcapsule with an islet after two days of culture in 20% oxygen, there are signs of dead cells at the islet exterior. (D) normal alginate microcapsule after two days of culture in 1% oxygen there are signs of central necrosis. (F) 70% (w/v) PFC alginate microcapsule after two days of culture in 1% oxygen – there appear to be reduced signs of central necrosis as the tissue at the center of the islet appears healthy. The arrows indicate dead cells at the islet exterior due to toxic effects of the PFC alginate.

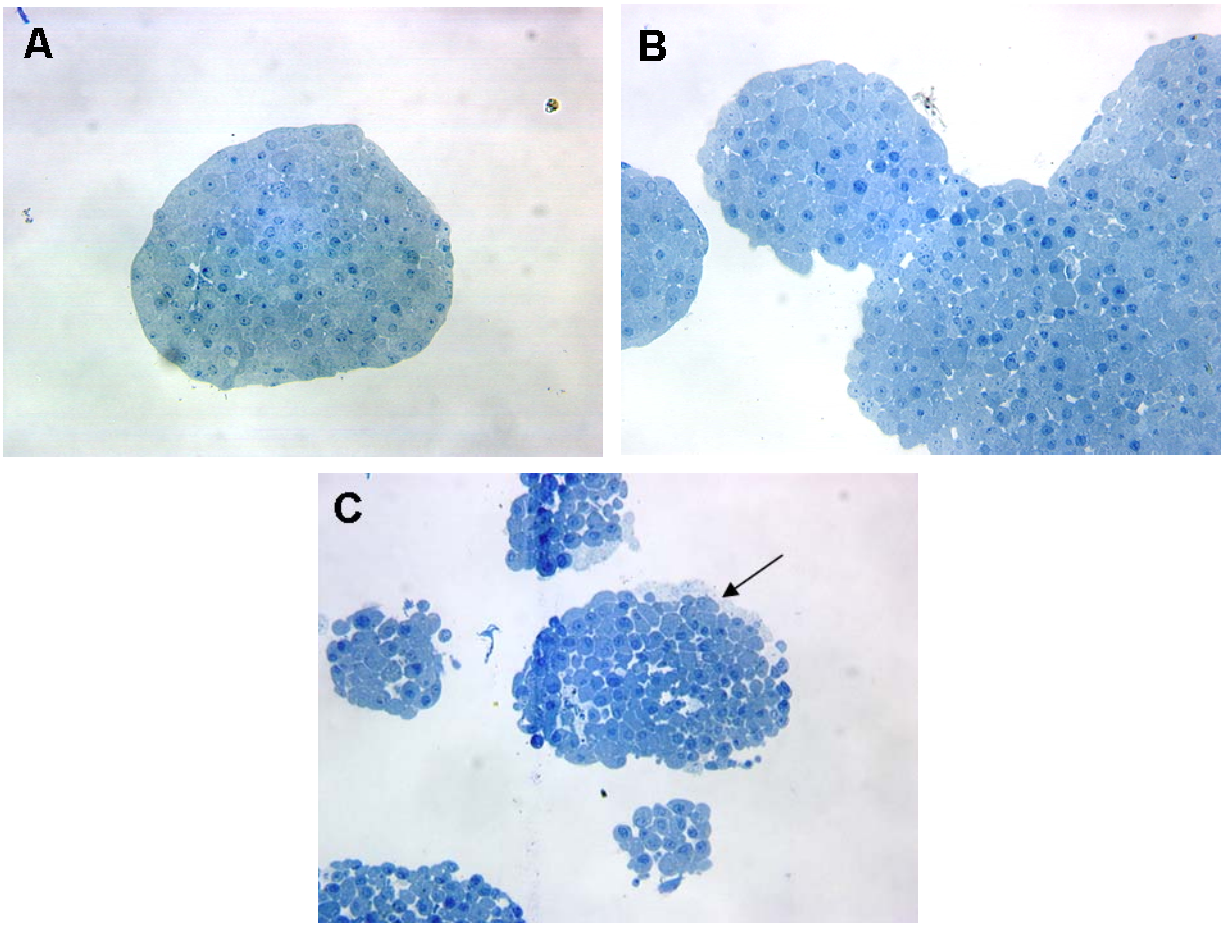

Figure 5-8: Histological sections of naked islets cultured under normal oxygen for two days. (A) naked islet in islet culture media – tissue appears healthy (B) naked islets cultured in islet culture media on top of pure perfluorodecalin – tissue appears healthy, but clumping occurred. (C) naked islets cultured in islet culture media containing Intralipid – arrow indicates dead cells most likely due to toxicity of Intralipid.

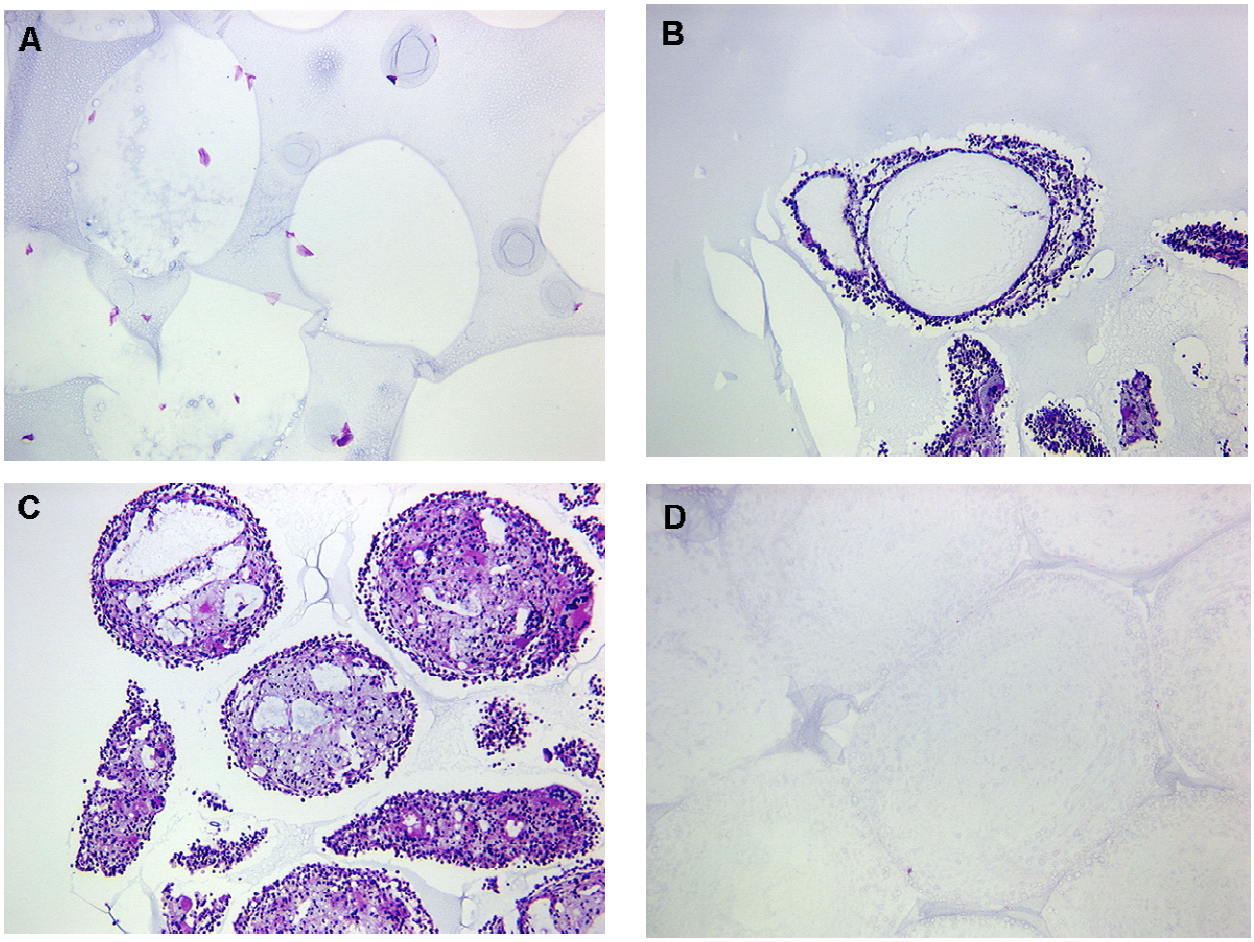

Figure 5-9: Paraffin sections of empty capsules transplanted into the peritoneal cavity of Lewis rats for two weeks stained with hematoxylin.

(A) 1.9% (w/v) Alginate (B) 70% (w/v) PFC 0.63% (w/v) Alginate (C) 70% (w/v) PFC 0.63% (w/v) Alginate coated with Alginate (D) 70% (w/v) PFC 0.63% (w/v) Alginate coated with PLL and Alginate.

Table 5-1: Model parameters

Parameter	Symbol	Value	Units	Source
O_2 diffusivity in media	D_m	$2.78x10^{-5}$	cm^2/s	[23]
O_2 diffusivity in tissue	D_t	$1.24x10^{-5}$	cm^2/s	[23]
O_2 diffusivity in silicone rubber	D_{sr}	$2.17x10^{-5}$	cm^2/s	[116]
O_2 solubility in media	α_m	$1.27x10^{-9}$	mol/mmHg/ml	[23]
O_2 solubility in tissue	α_t	$1.00x10^{-9}$	mol/mmHg/ml	[23]
O_2 solubility in silicone rubber	α_{sr}	$1.21x10^{-8}$	mol/mmHg/ml	[116]
O_2 permeability in 2% (v/v) alginate	αD_{Alg}	$3.43x10^{-14}$	mol/cm/mmHg/s	[23]
O_2 permeability in 70% (w/v) PFC 2% (v/v) alginate	$\alpha D_{PFC,Alg}$	$9.63x10^{-14}$	mol/cm/mmHg/s	[123]
Maximum oxygen consumption rate	V_{max}	$4x10^{-8}$, $6x10^{-8}$	$mol/cm^3/s$	[23], experiment
Michaelis-Menten Constant	K_m	0.44	mmHg	[23]
Insulin Secretion Model Parameter	P*	5.1, 1.1	mmHg	[93]

Chapter 6 Appendix

6.1 Effective Permeability and Solubility Calculations

The pure component solubility, diffusivity and permeability were found in the literature for each different type of material present in our model (Table 6-1). The effective solubility of each multicomponent phase modeled in the system was calculated by taking a volume average of the solubility of each pure component. The list of the volume fractions of each type of multiphase component are listed in Table 6-2 along with the volume averaged effective solubility.

The effective permeability in subdomains containing several components was determined from theoretical relationships. The ratio of the effective permeability $(\alpha D)_{eff,i}$ for subdomain i consisting of a dispersed (d) phase and a continuous (c) phase (as occurs in the alginate subdomains of the model system) to the permeability of the continuous phase $(\alpha D)_c$ was calculated from Maxwell's relationship [75]

$$\frac{(\alpha D)_{eff,i}}{(\alpha D)_c} = \frac{2-2\phi+\rho(1+2\phi)}{2+\phi+\rho(1-\phi)} \qquad (6\text{-}1)$$

where αD is the permeability of the material (mol/cm/mmHg/s), $\rho=(\alpha D)_d/(\alpha D)_c$ is the ratio of the permeability of the dispersed phase to the permeability of the continuous phase, and ϕ is the volume fraction of the dispersed phase. For the multiple dispersed phases employed in our model system, Maxwell's relationship was used sequentially, starting with the phase with the smallest particle size and ending with the phase with the largest particle size. For particle types of the same size, Maxwell's relationship was used for one particle, then the other (and in the reverse order), and the two results were averaged.

For the alginate capsules that contained PFC emulsion and cells Maxwell's relationship was used in the following order. The perfluorocarbon emulsion that we have been studying in the lab consists of 70% (w/v) perfluorodecalin and 20% (w/v) Intralipid® (Baxter), a soybean oil emulsion, and a PFC emulsion of this composition will be what is used in all model simulations that contain PFC alginate [71]. In the final PFC alginate composite phase, there were perfluorodecalin and soybean oil droplets of approximately the same size (0.4 μm mean diameter based on a volume average as measured by dynamic light scattering with Nanotrac, Microtrac Inc. Mongomeryville, PA); the alginate polymer itself was treated as an impermeable phase dispersed in water (Figure 6-1). The effective permeability of PFC emulsion was estimated by first using Maxwell's relationship for soybean oil droplets in water and then for PFC droplets in the soybean oil and water emulsion. Secondly, Maxwell's relationship was used for PFC droplets in water and then for soybean oil droplets in the PFC and water emulsion. The two calculated effective permeabilites were averaged (Figure 6-2). Finally, the effective permeability of PFC alginate was estimated with alginate as the dispersed phase and PFC emulsion as the continuous phase. For the case of single cells in normal alginate, Maxwell's relationship was first used to calculate the effective permeability of a dispersed tissue phase in water and then for alginate in the tissue and water emulsion. For single cells in PFC alginate, first the effective permeability of the PFC emulsion was calculated as described above, then the effective permeability of a dispersed tissue phase (diameter of a cell ~10 μm is greater than the emulsion particles 0.4 μm) in the PFC emulsion, and finally the overall effective permeability is calculated for a dispersed alginate phase in the PFC and tissue emulsion. The detailed description the calculations of effective permeability are contained in Table 6-3 through Table 6-6. The

effective diffusivities that were used in Chapter 2 were calculated by dividing the effective permeability by the effective solubility.

The enhancement of PFC emulsion permeability relative to that of water or to the Intralipid® emulsion that is used as the starting material is shown in Figure 6-3. A 70% (w/v) PFC emulsion has approximately 2.8 times the permeability of water and 2.1 times the permeability of Intralipid®. There is a smaller relative enhancement in the permeability of the emulsion when compared to Intralipid® because Intralipid® contains soybean oil, which has an enhanced permeability to oxygen as compared to water. In comparison, a 90% (w/v) PFC Emulsion (maximum PFC loading in our experimental system) has 3.6 times the permeability of water, and a 110% (w/v) PFC emulsion (maximum reported loading for a PFC emulsion in the literature) has 4.6 times the permeability of water.

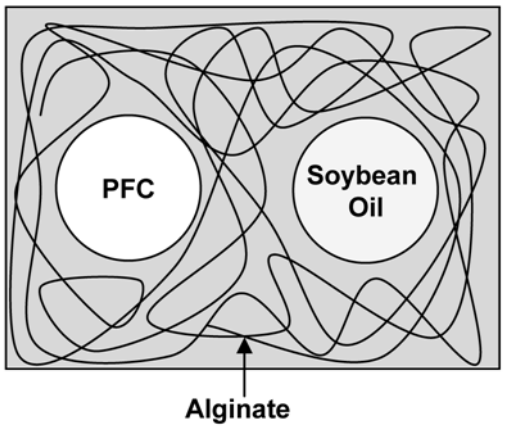

Figure 6-1: A schematic drawing of the components of PFC alginate which consists of PFC and soybean oil droplets suspended in an alginate matrix with a continuous water phase.

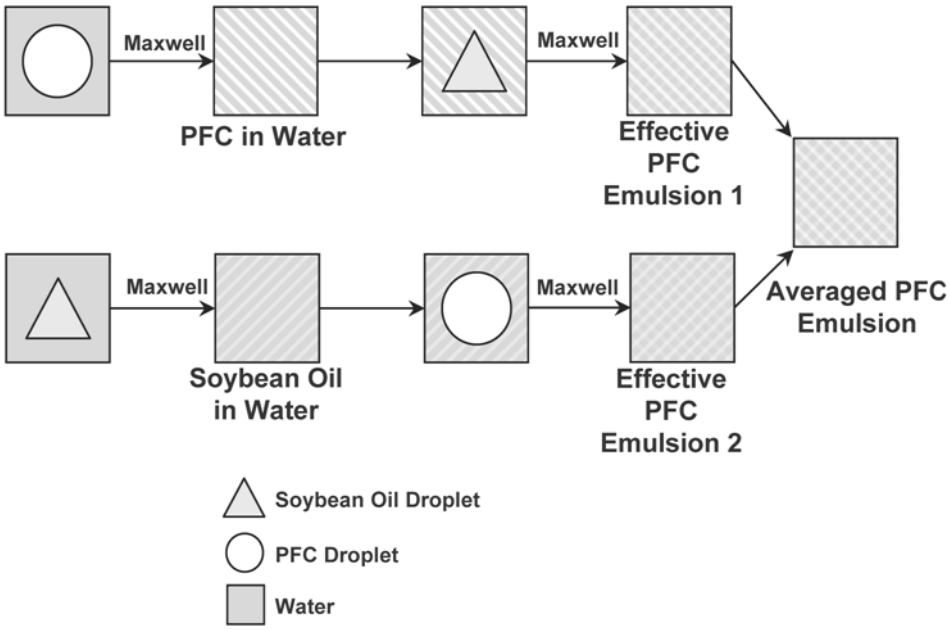

Figure 6-2: Sequence of calculations performed using Maxwell's relationship to calculate the effective permeability of PFC emulsion.

PFC emulsion consists of three phases: PFC droplets, soybean oil droplets, and water as the continuous phase.

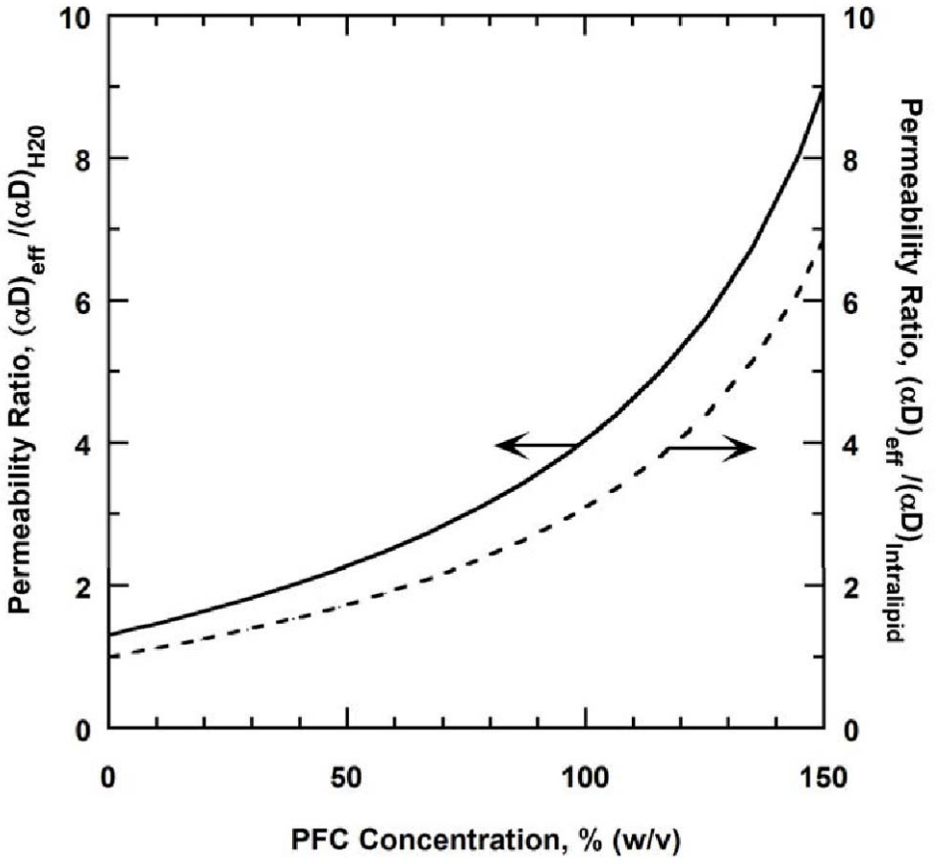

Figure 6-3: Permeability enhancement of PFC emulsion relative to water (left axis, solid line) or Intralipid® (right axis, dashed line)

Table 6-1: Diffusion coefficient (D), Bunsen solubility coefficient (α) or permeability coefficient for oxygen in all pure components in microcapsules.

Parameters are from the literature. The cell concentration in the microcapsules is 2.4×10^7 cells/ml.

	D (cm^2/s)	**α (mol/mmHg/ml)**	**α D (mol/cm/mmHg/s)**	**Source**
Tissue (t)	1.24×10^{-5}	1.00×10^{-9}	1.24×10^{-14}	[23]
Alginate (a)	0	0	0	[23]
PFC (pfc)	5.61×10^{-5}	2.54×10^{-8}	1.42×10^{-12}	[76]
Soybean Oil (soy)	2.13×10^{-5}	6.84×10^{-9}	1.46×10^{-13}	[77, 78]
Water (w)	2.78×10^{-5}	1.27×10^{-9}	3.53×10^{-14}	[23]

Table 6-2: Density of materials, volume fraction (ϕ) of phases in capsules and calculated effective solubilities (α_{eff}) .

Capsules contained 2% (v/v) alginate, pure PFC emulsion contained 70% (w/v) PFC, capsules with cells contained $2.4x10^7$ cells/ml.

$$\alpha_{eff} = \sum_{j=1}^{n} \alpha_j \phi_j \qquad (6\text{-}2)$$

Where n is the number of components in the system, α_j is the solubility of the jth component, and ϕ_j is the volume fraction of jth component. The calculations of effective permeability and solubility used in Chapter 3 employed a tissue volume fraction of 0.027 which only had effects on the parameters in the second decimal place. The effects of the different parameters would not be noticeable in the final calculations and thus the calculations were not updated with the parameter set.

			Volume fraction (ϕ) of phases in capsules				
Component	Density (g/ml)	α (mol/mmHg/ml)	Alginate	PFC Emulsion	PFC Emulsion + Alginate	Cells + Alginate	Cells + Alginate + PFC
Tissue (t)		$1.00x10^{-9}$	0	0	0	0.023	0.023
Alginate (a)		0	0.02	0	0.02	0.02	0.02
PFC (pfc)	1.93	$2.54x10^{-8}$	0	0.36	0.36	0	0.36
Soybean Oil (soy)	0.92	$6.84x10^{-9}$	0	0.12	0.12	0	0.12
Water (w)	1	$1.27x10^{-9}$	0.98	0.52	0.5	0.953	0.473
α_{eff} (mol/mmHg/ml)			$1.24x10^{-9}$	$1.06x10^{-8}$	$1.06x10^{-8}$	$1.23x10^{-9}$	$1.06x10^{-8}$

Table 6-3: Calculation sequence for effective permeability of 70% (w/v) PFC emulsion and 70% (w/v) PFC emulsion in 2% (v/v) alginate $(\alpha D)_{PFC\_alg}$.

Where soy is soybean oil, w is water, pfc is pure perfluorodecalin, a is alginate and the subscript numbers correspond to the effective permeability that was calculated in that step number. $(\alpha D)_5$ is the effective permeability of the PFC emulsion, and$(\alpha D)_6$ is the effective permeability of the PFC emulsion in alginate $(\alpha D)_{PFC\_alg}$.

Maxwell Step Number	ϕ	ρ	$(\alpha D)_{eff}$
1	0.12	$(\alpha D)_{soy}/(\alpha D)_w = 4.13$	4.21×10^{-14}
2	0.36	$(\alpha D)_{pfc}/(\alpha D)_1 = 33.85$	1.04×10^{-13}
3	0.36	$(\alpha D)_{pfc}/(\alpha D)_w = 40.34$	8.85×10^{-14}
4	0.12	$(\alpha D)_{soy}/(\alpha D)_3 = 1.65$	9.42×10^{-14}
5	average of $(\alpha D)_2$ and $(\alpha D)_4$		9.92×10^{-14}
6	0.02	$(\alpha D)_a/(\alpha D)_5 = 0$	9.63×10^{-14}

Table 6-4: Calculation sequence for effective permeability of 70% (w/v) PFC emulsion in 2% (v/v) alginate with 2.4×10^7 cells/ml $(\alpha D)_{cell\_PFC\_alg}$

Where soy is soybean oil, w is water, pfc is pure perfluorodecalin, t is tissue, a is pure alginate and any subscript numbers correspond to the effective permeability that was calculated in that step number. $(\alpha D)_7$ is the effective permeability of the PFC emulsion and cells in alginate $(\alpha D)_{cell\_PFC\_alg}$. Steps 1-5 are the same as in Table 6-3.

Maxwell Step Number	ϕ	ρ	$(\alpha D)_{eff}$
1	0.12	$(\alpha D)_{soy}/(\alpha D)_w = 4.13$	4.21×10^{-14}
2	0.36	$(\alpha D)_{pfc}/(\alpha D)_1 = 33.85$	1.04×10^{-13}
3	0.36	$(\alpha D)_{pfc}/(\alpha D)_w = 40.34$	8.85×10^{-14}
4	0.12	$(\alpha D)_{soy}/(\alpha D)_3 = 1.65$	9.42×10^{-14}
5	average of $(\alpha D)_2$ and $(\alpha D)_4$		9.92×10^{-14}
6	0.023	$(\alpha D)_t/(\alpha D)_5 = 0.125$	9.63×10^{-14}
7	0.02	$(\alpha D)_a/(\alpha D)_6 = 0$	9.36×10^{-14}

Table 6-5: Calculation sequence for effective permeability of 2% (v/v) alginate $(\alpha D)_{alg}$

Where a is pure alginate and any subscript numbers correspond to the effective permeability that was calculated in that step number. $(\alpha D)_1$ is the effective permeability of alginate $(\alpha D)_{alg}$.

Maxwell Step Number	ϕ	ρ	$(\alpha D)_{eff}$
1	0.02	$(\alpha D)_a/(\alpha D)_w = 0$	$3.43x10^{-14}$

Table 6-6: Calculation sequence for effective permeability 2% (v/v) alginate with $2.4x10^7$ cells/ml $(\alpha D)_{cell\_alg}$

Where t is tissue, a is pure alginate and any subscript numbers correspond to the effective permeability that was calculated in that step number. $(\alpha D)_2$ is the effective permeability of the PFC emulsion and cells in alginate $(\alpha D)_{cell\_alg}$.

Maxwell Step Number	ϕ	ρ	$(\alpha D)_{eff}$
1	0.023	$(\alpha D)_t/(\alpha D)_w = 0.35$	$3.46x10^{-14}$
2	0.02	$(\alpha D)_a/(\alpha D)_1 = 0$	$3.36x10^{-14}$

6.2 Model Equations

Equations ((3-4)) for the theoretical models solved in Chapter 3 are written out in detail for each subdomain type in this section. For the model geometries that contain discrete tissue subdomains for the islet and aggregate cases. The model equation in the tissue subdomain is:

$$(\alpha D)_t \nabla^2 P_t = \frac{V_{max} P_t}{K_m + P_t} \tag{6-3}$$

Where $(\alpha D)_t$ is the permeability of tissue, V_{max} is the maximum oxygen consumption rate of solid islet tissue, P_t is the partial pressure of oxygen within the tissue subdomain, and K_m is the Michaelis-Menten constant. The model equation in the alginate subdomain is given by:

$$(\alpha D)_{alg} \nabla^2 P_{alg} = 0 \tag{6-4}$$

Where $(\alpha D)_{alg}$ is the effective permeability of 2% (v/v) alginate that was calculated using Maxwell's relationship described above taking into account that there is water and a dispersed alginate phase in the alginate capsules. The model equation in the alginate subdomains that contain PFC emulsion is given by:

$$(\alpha D)_{PFC\_alg} \nabla^2 P_{PFC\_alg} = 0 \tag{6-5}$$

Where $(\alpha D)_{PFC\_alg}$ is the effective permeability of PFC alginate that was calculated using Maxwell's relationship sequentially as described above taking into account that there is water with dispersed alginate, PFC and soybean oil phases in the PFC alginate capsules.

There is only one subdomain in the cell containing capsules where the cells are considered to be a homogenous phase distributed throughout the entire capsule. The model equation for the cell containing alginate capsules is:

$$(\alpha D)_{cell\_alg} \nabla^2 P_{cell\_alg} = \frac{V_{max} \phi_t P_{cell\_alg}}{K_m + P_{cell\_alg}} \quad (6\text{-}6)$$

Where $(\alpha D)_{cell\_alg}$ is the effective permeability of alginate capsules containing cells that was calculated using Maxwell's relationship described above taking into account that there is water with a dispersed alginate and cell phase and ϕ_t is the volume fraction of tissue homogenously distributed throughout the capsule. The volume fraction (ϕ_t) of tissue for a 500-µm capsule containing one 150-µm is $(150/500)^3$=0.027 and also would correspond to a cell concentration of 2.4×10^7 cells/ml assuming 1560 cells per IE distributed throughout the capsule volume. This cell concentration and tissue volume fraction were used for calculations of capsules cells that contain one IE in a 500-µm capsule. The model equation for the cell and PFC emulsion containing alginate capsules is:

$$(\alpha D)_{cell\_PFC\_alg} \nabla^2 P_{cell\_PFC\_alg} = \frac{V_{max} \phi_t P_{cell\_PFC\_alg}}{K_m + P_{cell\_PFC\_alg}} \quad (6\text{-}7)$$

Where $(\alpha D)_{cell\_PFC\_alg}$ is the effective permeability of PFC alginate capsules containing cells that was calculated using Maxwell's relationship described above taking into account that there is water with dispersed alginate, cells, PFC and soybean oil phases.

6.3 Predictions of Actual Oxygen Level in 1% Experiments

For the experiments carried out in Chapter 5 at 1% oxygen they were not really at 1% oxygen as about a half liter of air at atmospheric oxygen was trapped within the head space of the culture vessel since the cap did not contain a filter. An order of magnitude estimate for the amount of time for the oxygen in the culture vessel head space to diffuse through the media and out of the device was on the order of 20 days over a surface area of 100 cm^2 and a media thickness of 2.5mm. Thus verifying that the experiments were not really carried out at 1% oxygen as the air at atmospheric oxygen was maintained within the vessel throughout the 2 day experiment. A reasonable assumption to model what conditions were experienced during culture would be to modify the models that were used in Chapter 5 and have the bottom of the silicone rubber at 1% oxygen or P_{O2} 7mmHg and the top of the media at atmospheric oxygen. The steady state oxygen profile was calculated at a surface density of 25 IE/cm^2 in normal alginate and PFC alginate capsules. The partial pressure of oxygen at the bottom of the islet in normal alginate was 4 mmHg and the top of the islet was at 10 mmHg for an average of 7 mmHg at the islet exterior. The partial pressure of oxygen at the bottom of the islet in PFC alginate was 9 mmHg and top was 15 mmHg for an average of 12 mmHg at the islet exterior. Similar oxygen levels at the islet exterior for normal alginate (7 mmHg) and PFC alginate (12 mmHg) are observed for culture on silicone rubber when the bottom of the silicone rubber and the top of the media are both at atmospheric oxygen for a gas phase oxygen level of 21 mmHg or about 3% oxygen.

6.4 Additional Figures from Calculations Performed in Chapter 3

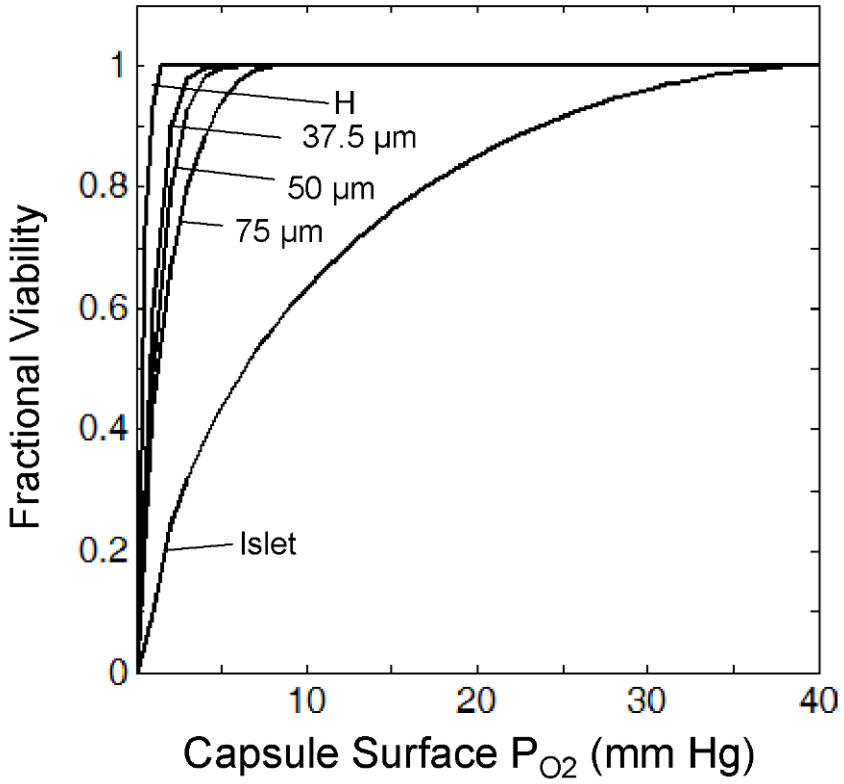

Figure 6-4: Predicted fractional viability as a function of capsule surface P_{O2} for a 500-µm capsule that contains one islet equivalent – homogeneously distributed throughout the capsule, as 64 37.5-µm aggregates, 27 50-µm aggregates, 8 75-µm aggregates, or 1 150-µm islet.

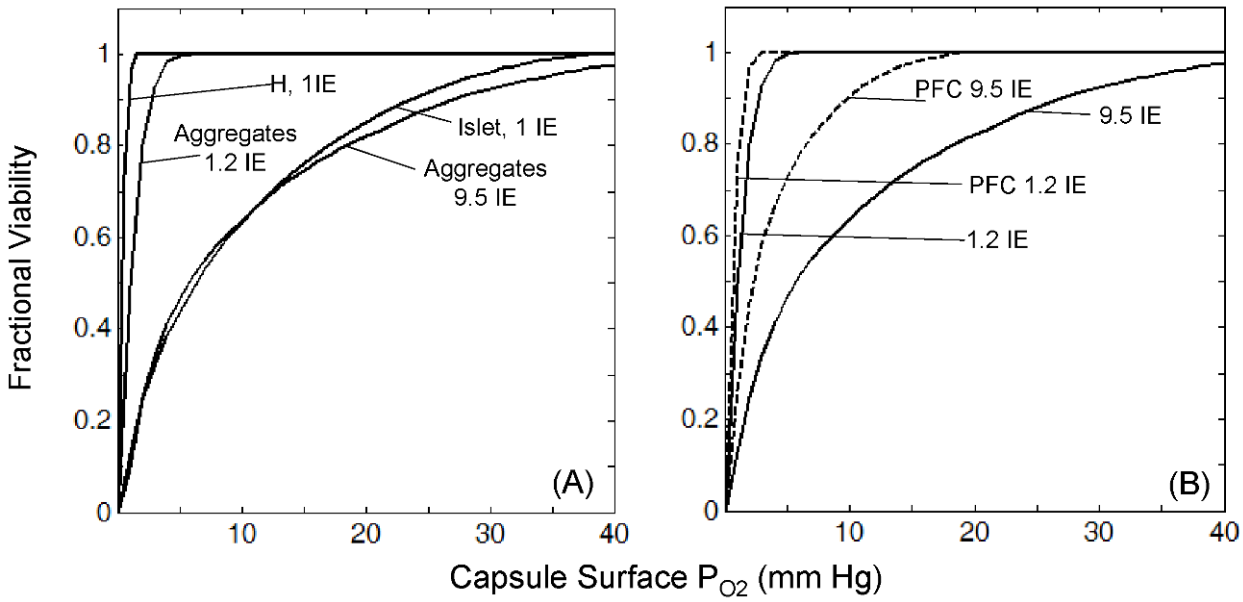

Figure 6-5: Predicted fractional viability for single cells, an islet, and 50-µm aggregates at various loadings in a 500-µm capsule.

(A) Alginate capsules (B) 50-µm aggregates at various loadings in a capsule containing 70% (w/v) PFC emulsion. IE=islet equivalent

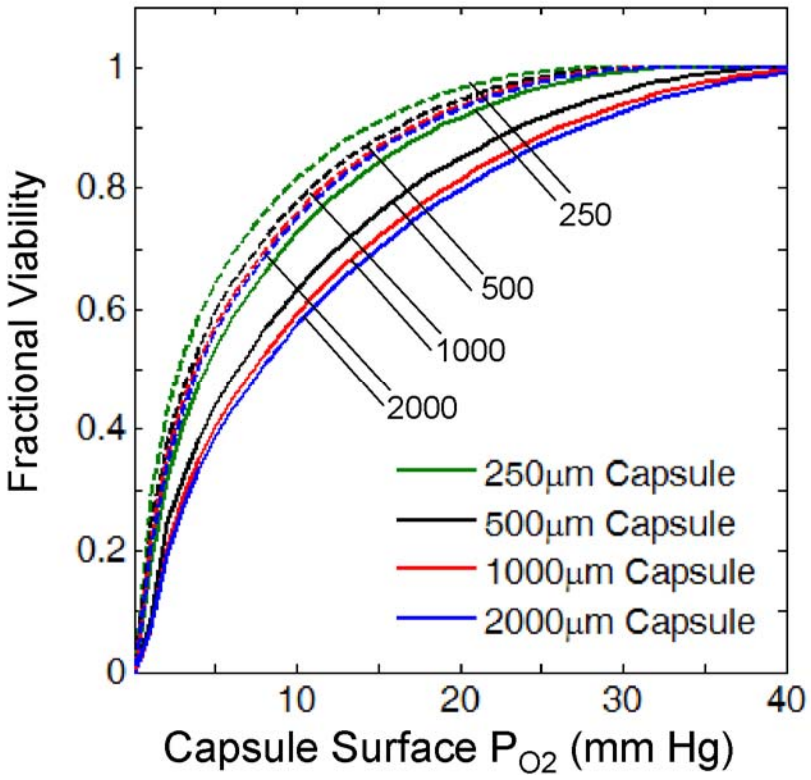

Figure 6-6: Predictions of fractional viability for one centrally located islet in a 250, 500, 1000, or 2000-μm capsule with (dashed lines) and without (solid lines) 70% (w/v) PFC emulsion.

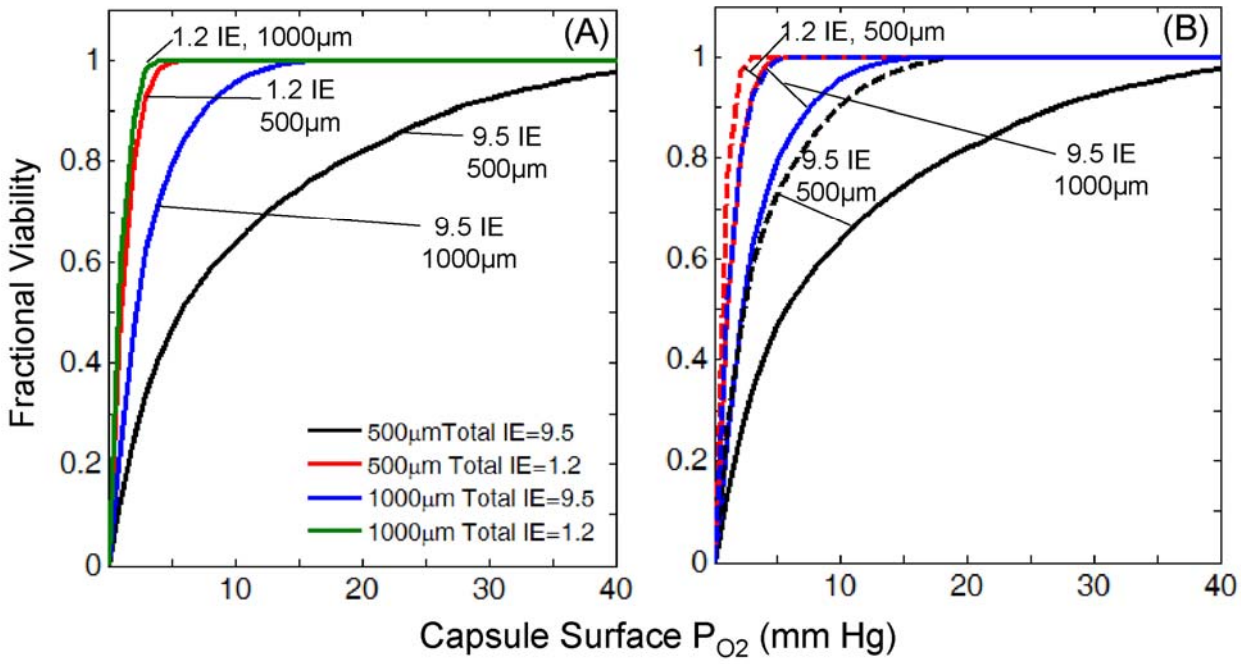

Figure 6-7: Predictions of fractional viability for 50-μm aggregates in either a 500-μm or 1000-μm diameter capsule.

(A) Normal alginate capsule (B) normal alginate (solid curves) and 70% (w/v) PFC alginate (dashed curves).

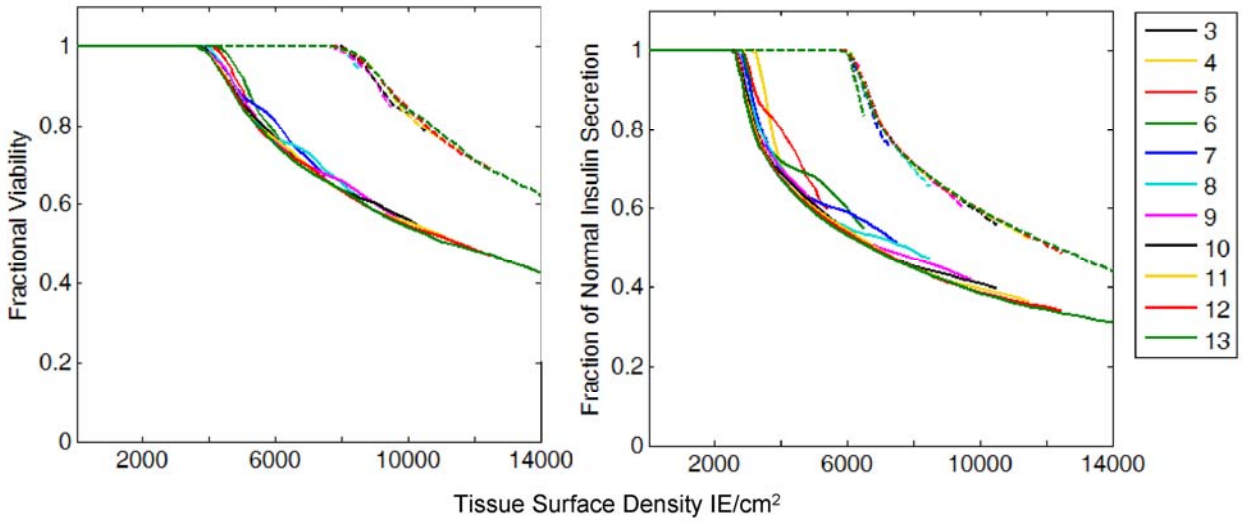

Figure 6-8: Predictions of fractional viability and fraction of normal insulin secretion for 37.5-µm aggregates in a 500-µm planar device.

The device surface oxygen level is 40 mmHg and the tissue within the device is arranged in 3-13 layers. The solid lines are for the predictions in normal alginate devices and the dashed lines are the predictions for 70% (w/v) PFC alginate devices.

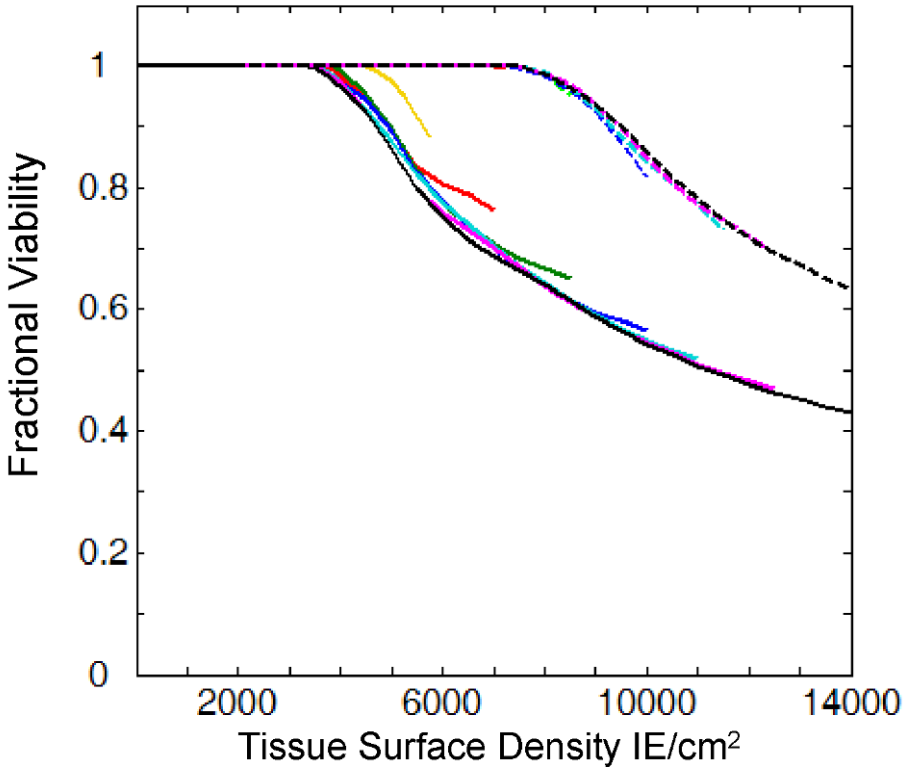

Figure 6-9: Predictions of fractional viability for 50-µm aggregates in a 500-µm planar device. The device surface oxygen level is 40 mmHg and the tissue within the device is arranged in 3-10 layers. The solid lines are for the predictions in normal alginate devices and the dashed lines are the predictions for 70% (w/v) PFC alginate devices.

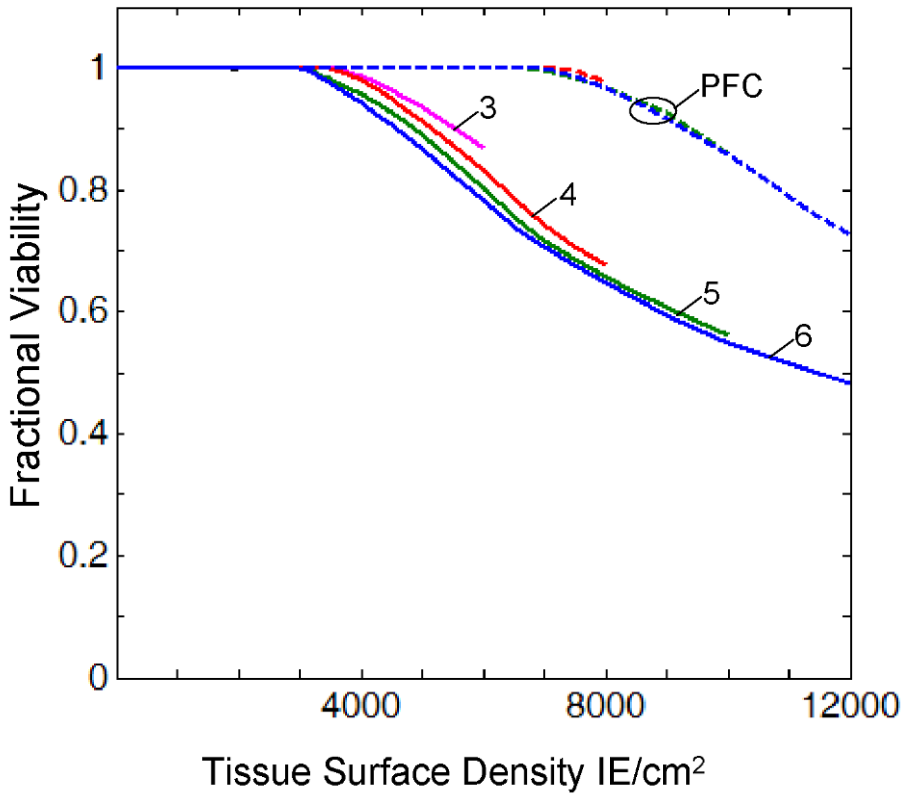

Figure 6-10: Predictions of fractional viability for 75-µm aggregates in a 500-µm planar device. The device surface oxygen level is 40 mmHg and the tissue within the device is arranged in 3-6 layers. The solid lines are for the predictions in normal alginate devices and the dashed lines are the predictions for 70% (w/v) PFC alginate devices.

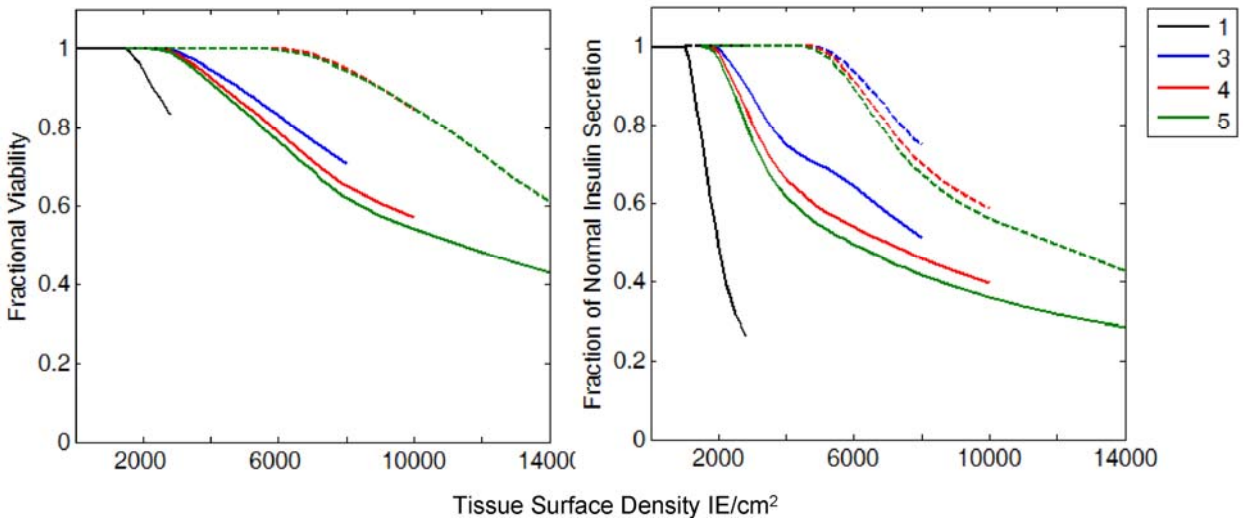

Figure 6-11: Predictions of fractional viability and fraction of normal insulin secretion for 100-µm aggregates in a 500-µm planar device.

The device surface oxygen level is 40 mmHg and the tissue within the device is arranged in 1, 3, 4, or 5 layers. The solid lines are for the predictions in normal alginate devices and the dashed lines are the predictions for 70% (w/v) PFC alginate devices.

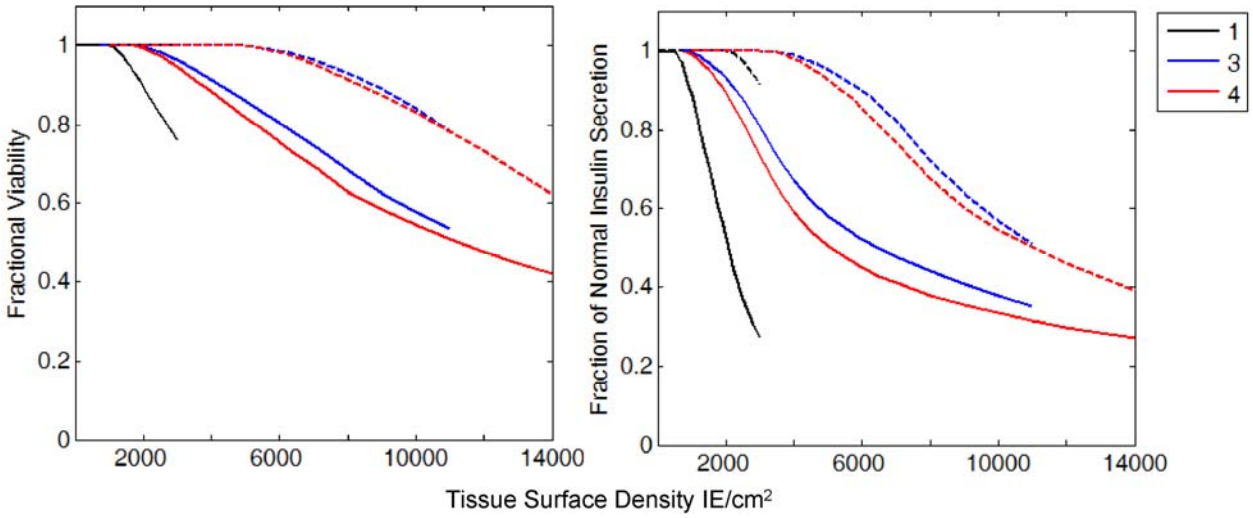

Figure 6-12: Predictions of fractional viability and fraction of normal insulin secretion for 125-µm aggregates in a 500-µm planar device.

The device surface oxygen level is 40 mmHg and the tissue within the device is arranged in 1,3 or 4 layers. The solid lines are for the predictions in normal alginate devices and the dashed lines are the predictions for 70% (w/v) PFC alginate devices.

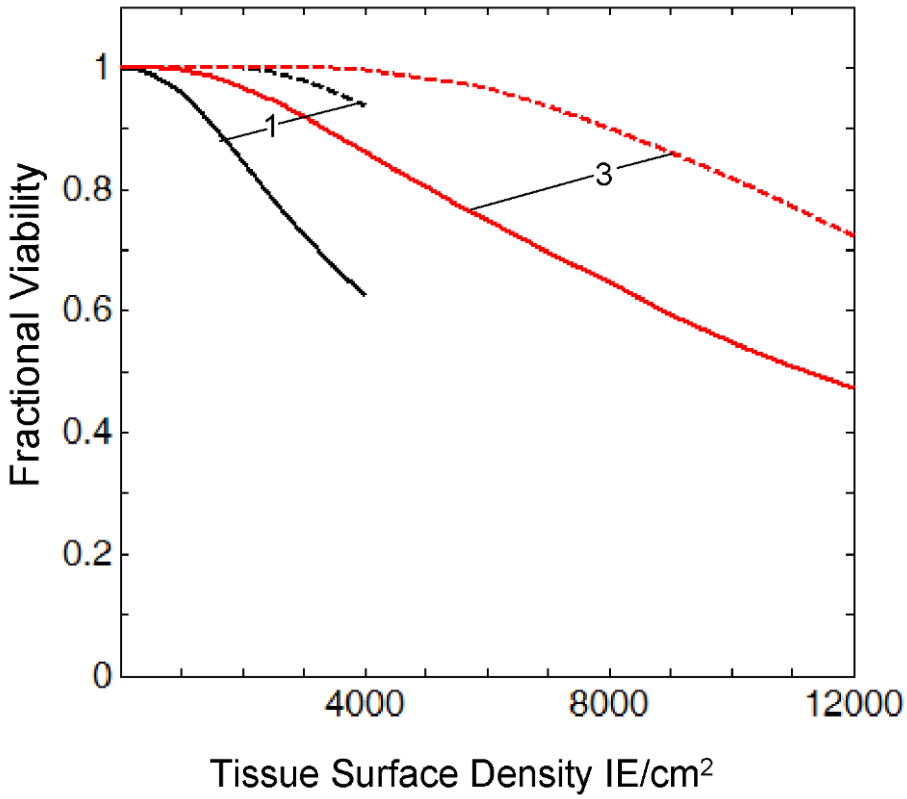

Figure 6-13: Predictions of fractional viability for 150-µm islets in a 500-µm planar device. The device surface oxygen level is 40 mmHg and the tissue within the device is arranged in 1 or 3 layers. The solid lines are for the predictions in normal alginate devices and the dashed lines are the predictions for 70% (w/v) PFC alginate devices.

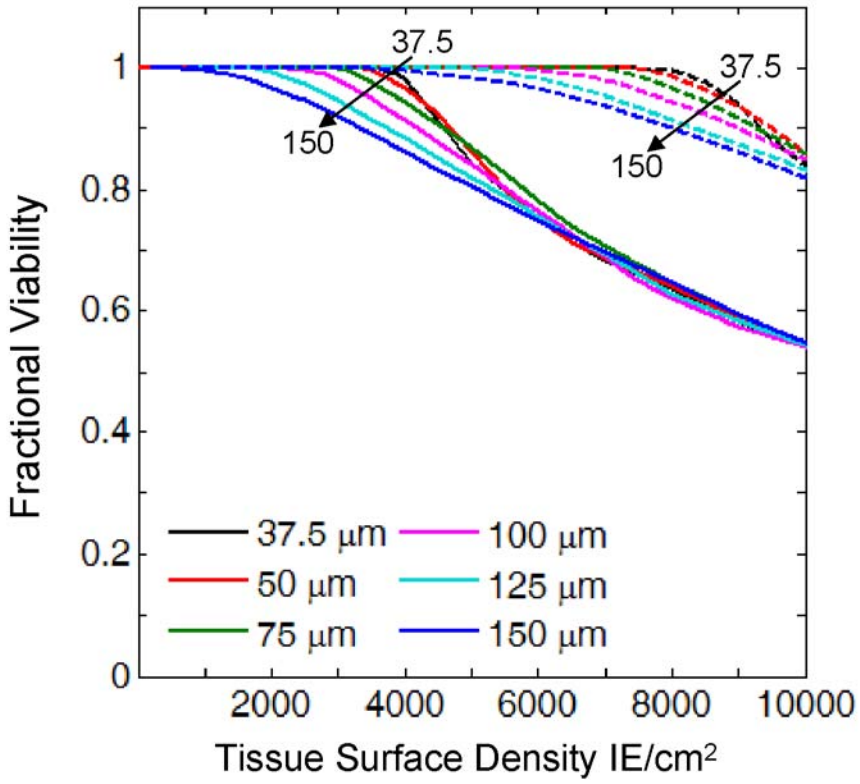

Figure 6-14: Fractional viability as a function of tissue surface density for tissue of a variety of sizes with tissue arranged in multiple layers throughout the device thickness the number of which being the maximum number that will fit for a particular size.

The device thickness is 500-µm. Device surface P_{O2} equals 40 mmHg. The solid lines are the predictions for normal alginate the dashed lines are the predictions for 70% (w/v) PFC alginate.

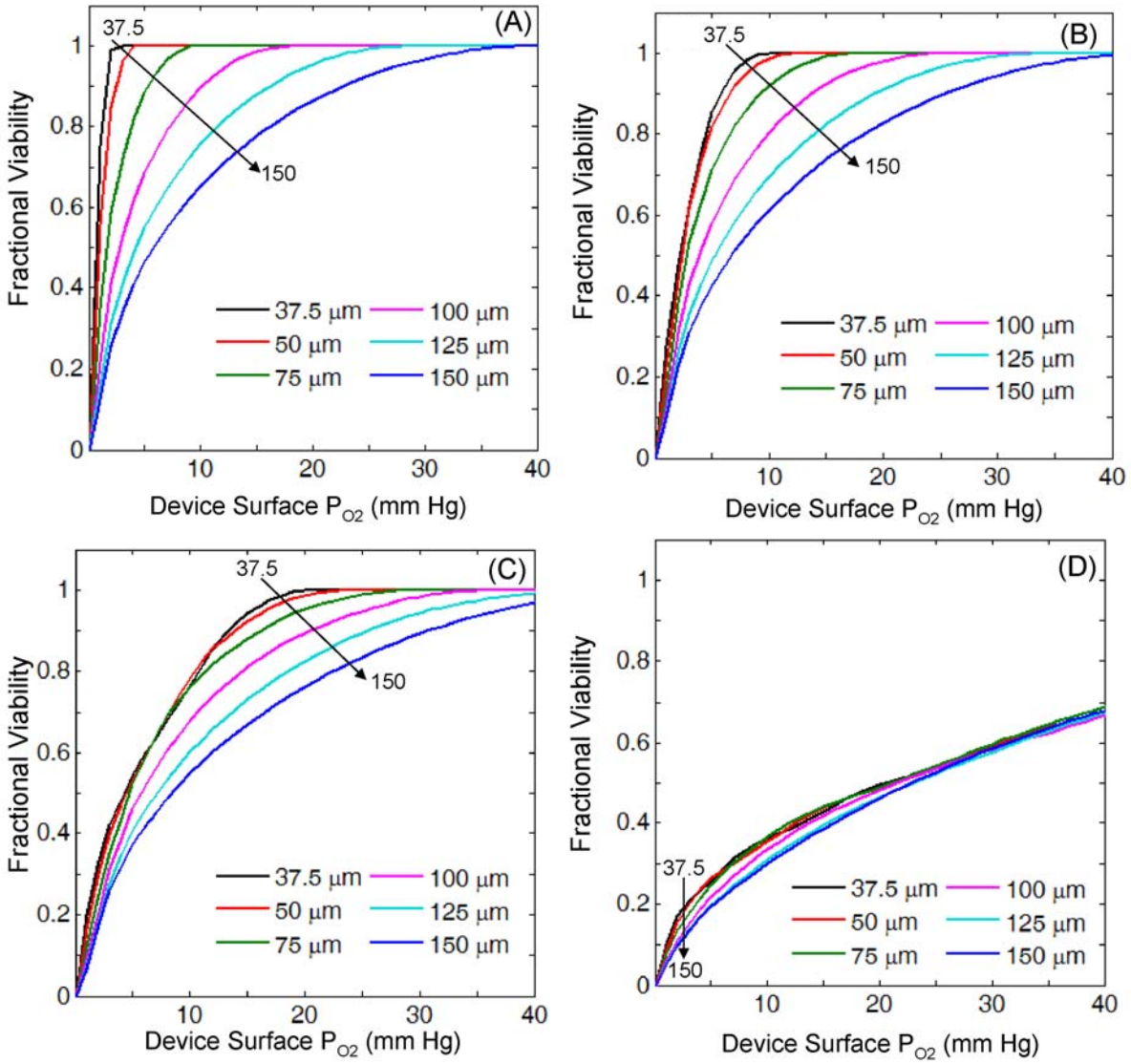

Figure 6-15: Predictions of fractional viability over a range of device surface P_{O2} for tissue of a variety of sizes arranged in multiple layers within a 500-µm planar diffusion chamber. The number of layers used is the maximum that would fit for a particular tissue size – 37.5-µm 13 layers, 50-µm 10 layers, 75-µm 6 layers, 100-µm 5 layers, 125-µm 4 layers, and 150-µm 3 layers. The device is 500-µm thick and made of normal alginate. The tissue device surface density was equal to (A) 150 IE/cm^2, (B) 1000 IE/cm^2, (C) 2000 IE/cm^2, and (D) 7272 IE/cm^2.

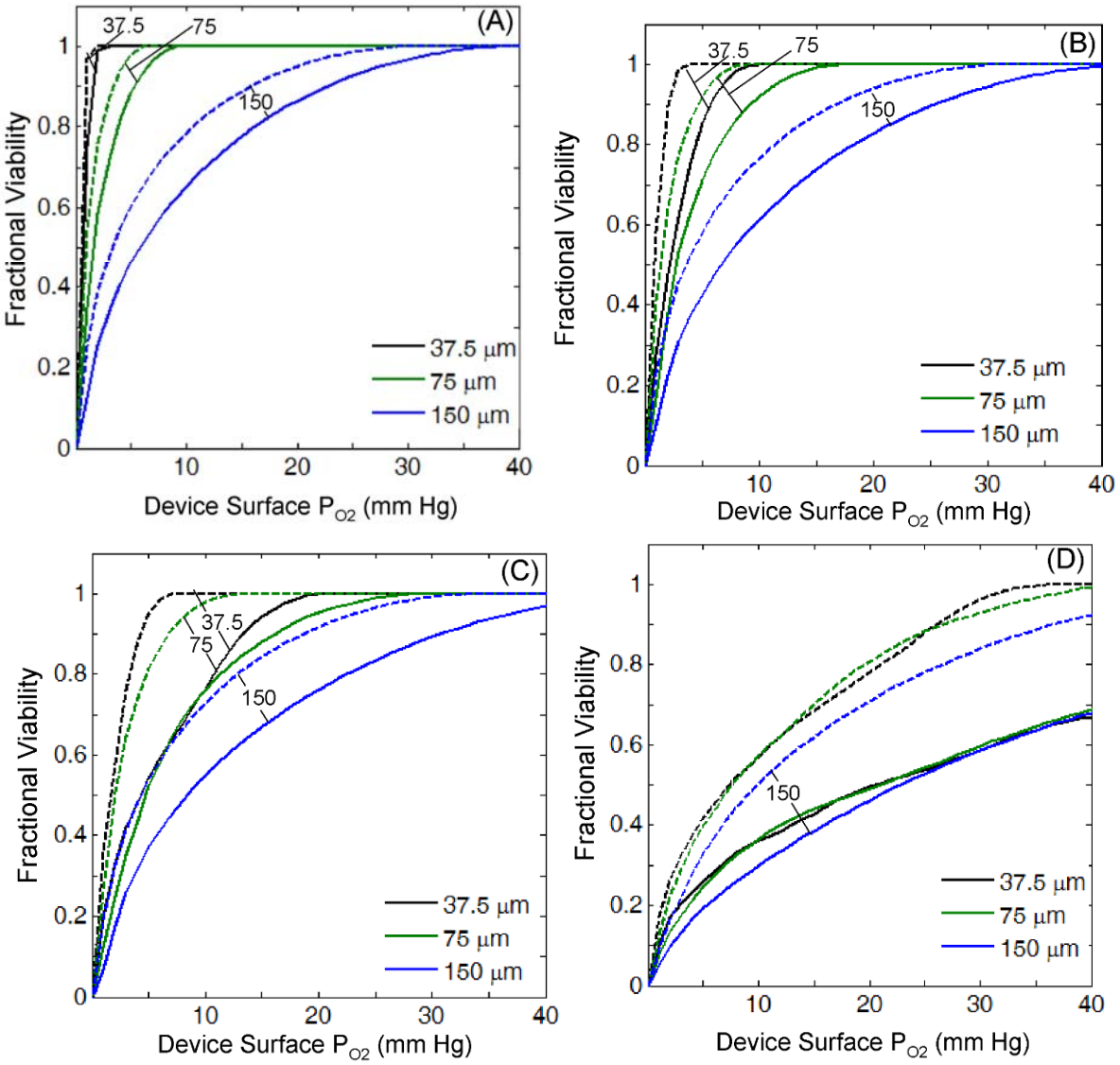

Figure 6-16: Predictions of fractional viability over a range of device surface P_{O2} for tissue of a variety of sizes arranged in multiple layers within a 500-µm planar diffusion chamber. The number of layers used is the maximum that would fit for a particular tissue size – 37.5-µm 13 layers, 75-µm 6 layers, and 150-µm 3 layers. The device is 500-µm thick and made of normal alginate (solid curves) and 70% (w/v) PFC alginate (dashed curves). The tissue device surface density was equal to (A) 150 IE/cm^2, (B) 1000 IE/cm^2, (C) 2000 IE/cm^2, and (D) 7272 IE/cm^2.

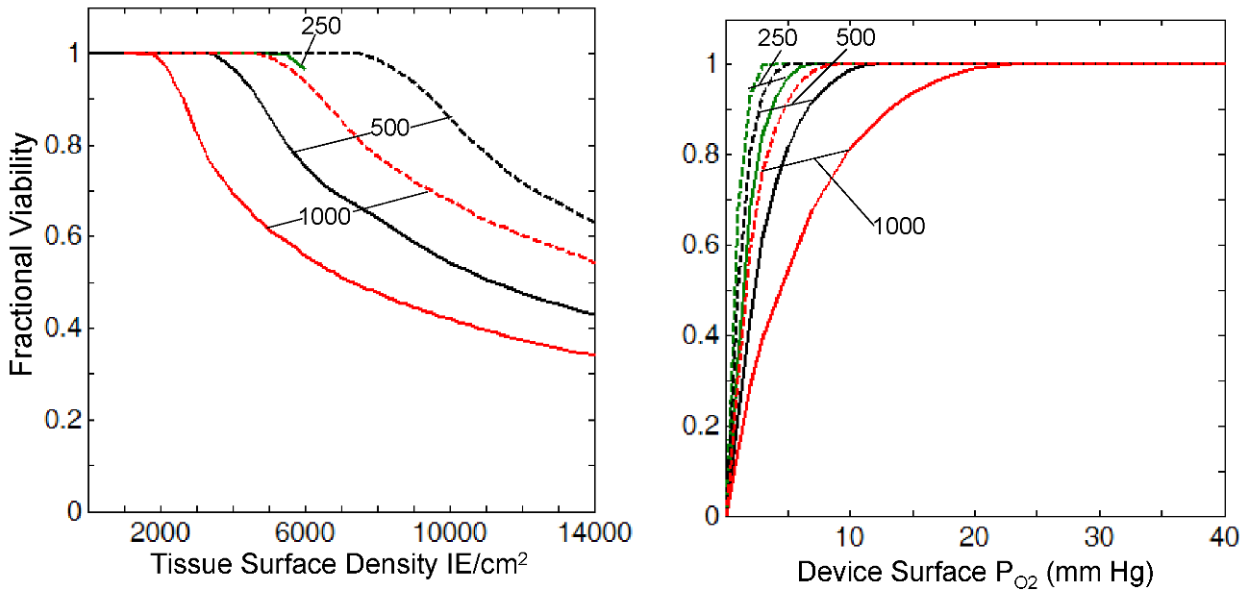

Figure 6-17: Effects of increasing device thickness on predictions of fractional viability for 50-µm aggregates arranged in multiple layers.

250-µm device 5 layers, 500-µm device 10 layers, and 1000-µm device 20 layers made from normal alginate (solid curves) or 70% (w/v) PFC alginate (dashed curves). (A) The effects of varying surface density for a device surface P_{O2} of 40mmHg were investigates and (B) the effects of reducing the device surface P_{O2} at a tissue loading of 1000 IE/cm^2.

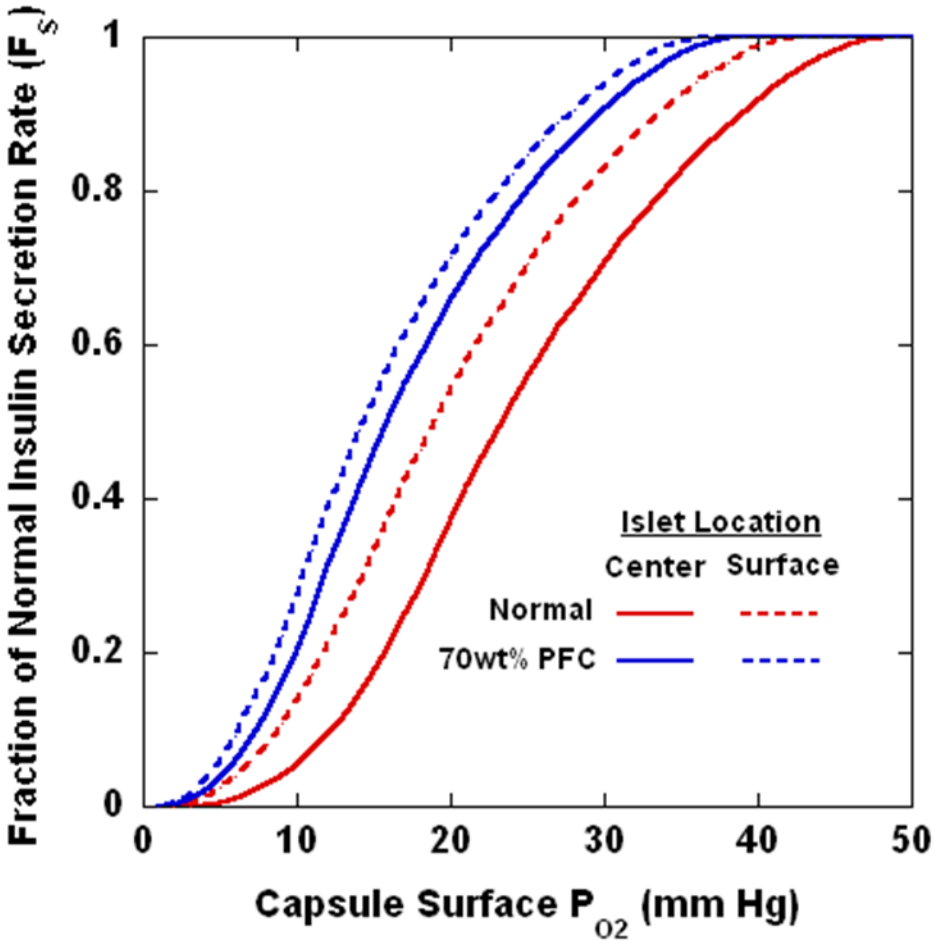

Figure 6-18: Predictions of fraction of normal insulin secretion for a 150-µm islet in a 500- µm capsule with and without PFC emulsion where the capsule is located at the center of the capsule or touching the surface of the capsule.

There are not large effects of the exact location of the islet for either microcapsule type.

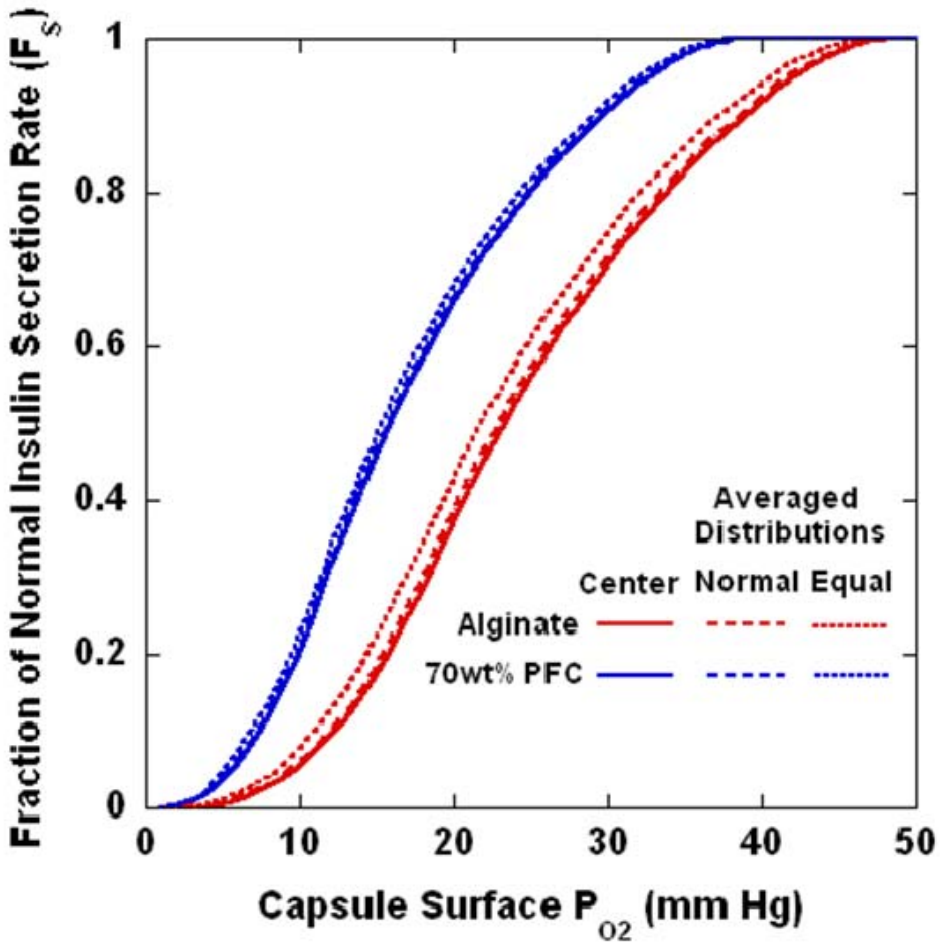

Figure 6-19: Volume averaged results for predicts of fraction of normal insulin secretion for 150-µm islets that are located through out the diameter of the 500-µm capsule.

The results are averaged either assuming an equal distribution of tissue throughout the capsule diameter or a normal distribution. The averaged results for the different distributions are all nearly identical to the results for an islet at the center. Thus in all calculations the results for a centrally located islet are only reported for the cases where a microcapsule contains one islet.

Calculations were also performed for encapsulated tissue in culture where a value of V_{max} = $4x10^{-8}$ nmol/cm^3/s was used for tissue oxygen consumption. The value of P* used in the insulin secretion model was 5.09 mmHg. The results are presented at 4 different oxygen levels in the following four figures. The data points represent the surface coverage at which the calculations were performed.

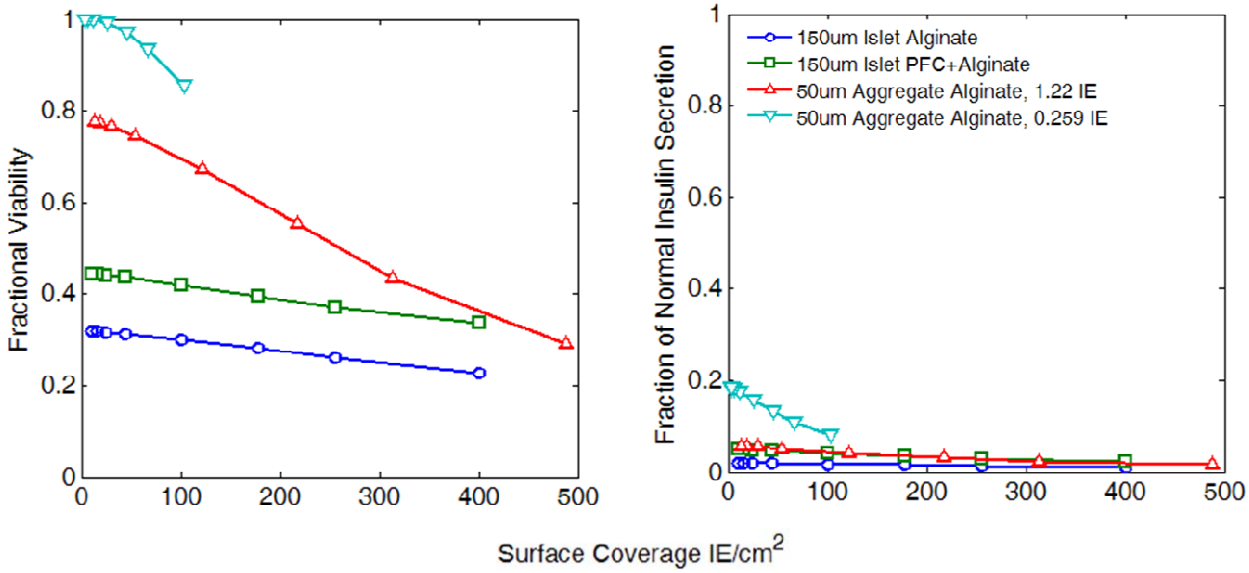

Figure 6-20: Predictions of viability and fraction of normal insulin secretion for tissue cultured in 500-µm capsules on silicone rubber at a gas phase P_{O2} of 3.5 mmHg.

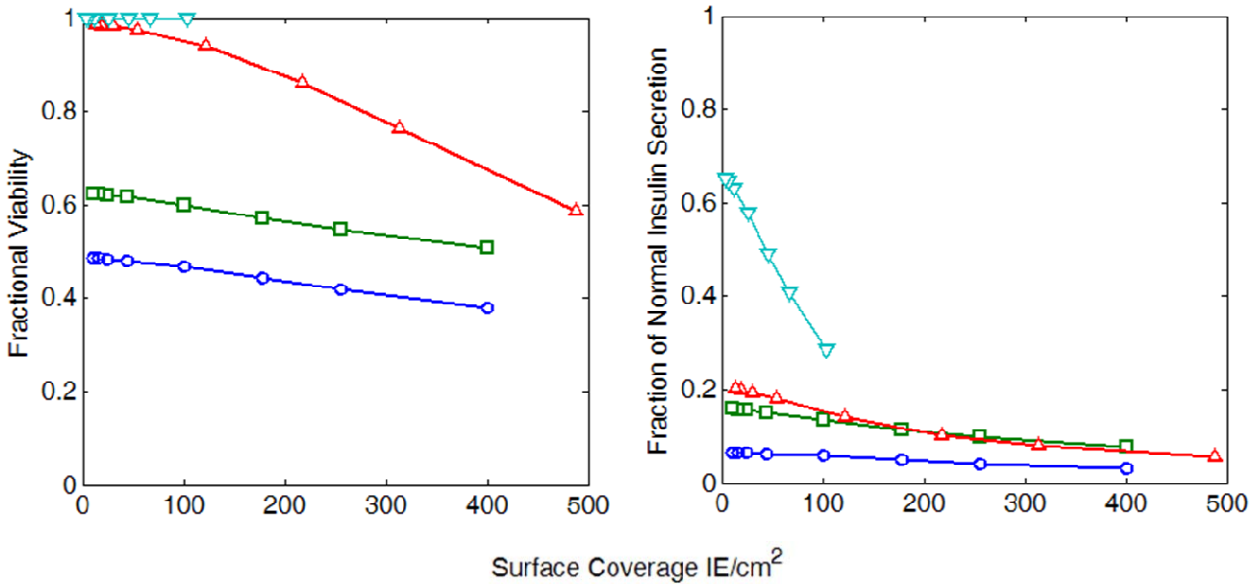

Figure 6-21: Predictions of viability and fraction of normal insulin secretion for tissue cultured in 500-µm capsules on silicone rubber at a gas phase P_{O2} of 7 mmHg.

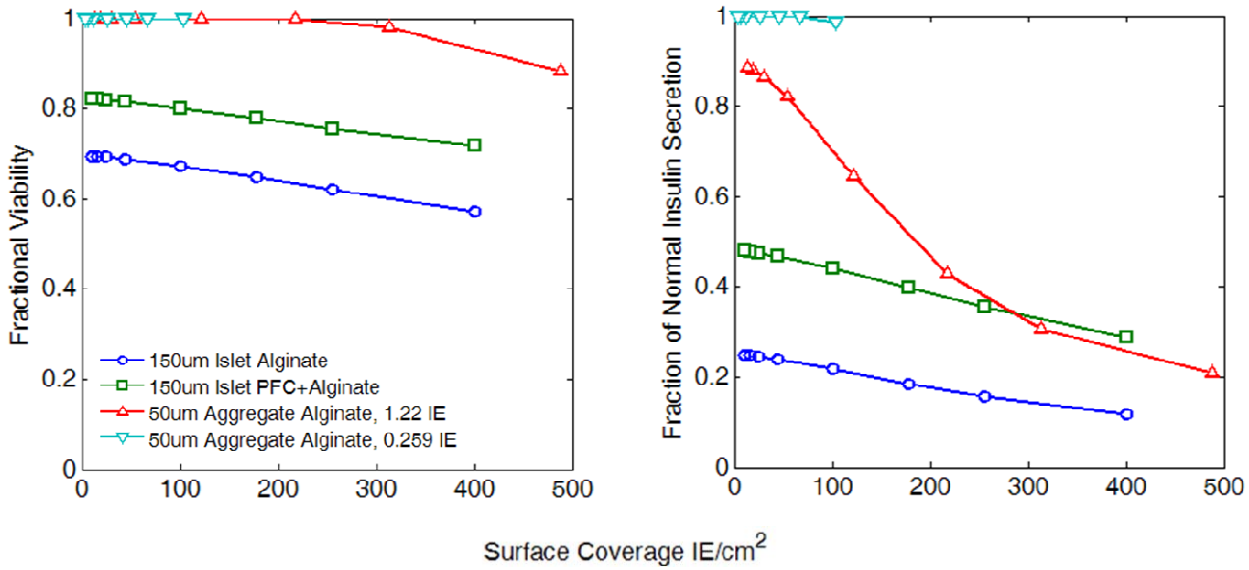

Figure 6-22: Predictions of viability and fraction of normal insulin secretion for tissue cultured in 500-µm capsules on silicone rubber at a gas phase P_{O2} of 14 mmHg.

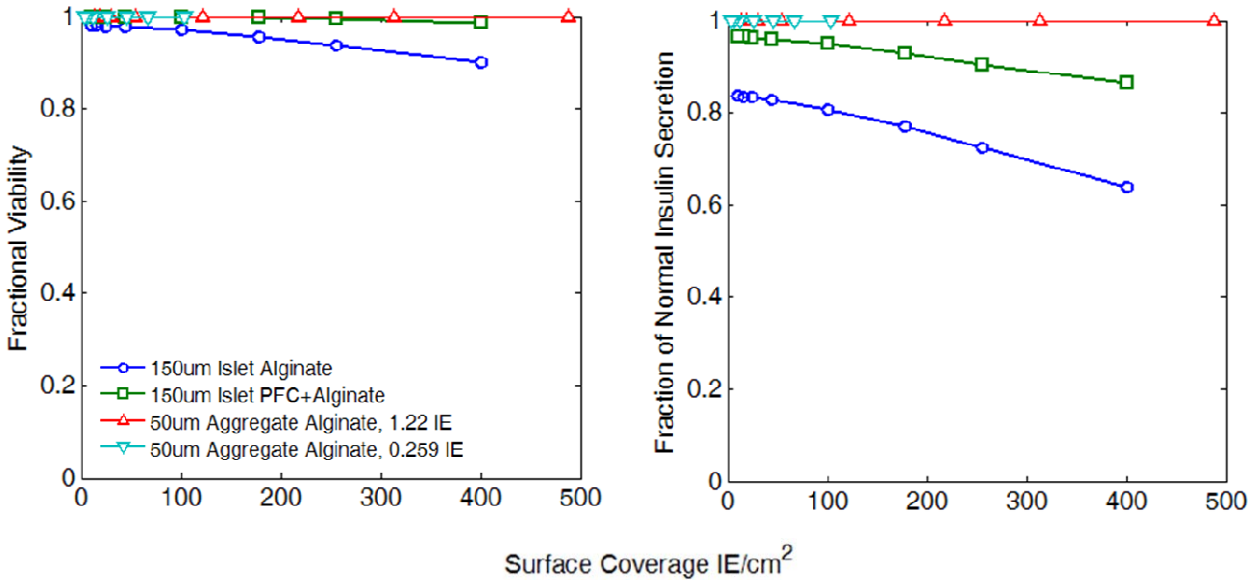

Figure 6-23: Predictions of viability and fraction of normal insulin secretion for tissue cultured in 500-µm capsules on silicone rubber at a gas phase P_{O2} of 36 mmHg.

REFERENCES

1. Center for Disease Control. National diabetes fact sheet, 2005. www.cdc.gov/diabetes/pubs/pdf/ndfs_2005.pdf
2. Center for Disease Control. Diabetes: Disabling disease to double by 2050, 2008. http://www.cdc.gov/nccdphp/publications/aag/pdf/diabetes.pdf
3. Sutherland, D.E.R., *Is immunosuppression justified for nonuremic diabetic patients to keep them insulin independent? (the argument for).* Transplantation Proceedings, 2002. 34: p. 1927-1928.
4. *The diabetes control and complications trial research group. The effect of intensive treatment of diabetes on the development and progression of long-term complications in insulin-dependent diabetes mellitus.* New England Journal of Medicine, 1993. 329(14): p. 977-986.
5. Plotnick, L.P., L.M. Clark, F.L. Brancati, and T. Erlinger, *Safety and effectiveness of insulin pump therapy in children and adolescents with type 1 diabetes.* Diabetes Care, 2003. 26(4): p. 1142-1146.
6. Kost, J., S. Mitragotri, R.A. Gabbay, M. Pishko, and R. Langer, *Transdermal monitoring of glucose and other analytes using ultrasound.* Nature Medicine, 2000. 6(3): p. 347-350.
7. Mitragori, S., M. Coleman, J. Kost, and R. Langer, *Analysis of ultrasonically extracted interstitial fluid as a predictor of blood glucose levels.* Journal of Applied Physiology, 2000. 89: p. 961-966.
8. Cefalu, W.T., *Evaluation of alternative strategies for optimizing glycemia: Progress to date.* American Journal of Medicine, 2002. 113(6A): p. 23S-35S.
9. Gough, D., J. Armour, and D. Baker, *Advances and prospects in glucose assay technologies.* Diabetologia, 1997. 40: p. S102-S107.
10. Gerritsen, M., J. Jansen, and J. Lutterman, *Performance of subcutaneously implanted sensors for continuous monitoring.* Netherlands Journal of Medicine, 1999. 54: p. 167-179.
11. Koschchinsky, T. and L. Heinemann, *Sensors for glucose monitoring: Technical and clinical aspects.* Diabetes Metabolism Research and Reviews, 2001. 17: p. 113-123.
12. Abel, P.U. and T. von Woedtke, *Biosensors for in vivo glucose measurement: Can we cross the experimental stage.* Biosensors and Bioelectronics, 2002. 17: p. 1059-1070.
13. Frost, M.C. and M.E. Meyerhoff, *Implantable chemical sensors for real-time clinical monitoring: Progress and challenges.* Current Opinion in Chemical Biology, 2002. 6: p. 633-641.
14. Galaev, I.Y. and B. Mattiasson, *'smart' polymers and what they could do in biotechnology and medicine.* Trends in Biotechnology, 1999. 17: p. 335-340.
15. Shapiro, A.M.J., J.R.T. Lakey, E.A. Ryan, G.S. Korbutt, E. Toth, G.L. Warnock, N.M. Kneteman, and R.V. Rajotte, *Islet transplantation in seven patients with type 1 diabetes mellitus using a glucocorticoid-free immunosuppressive regimen.* New England Journal of Medicine, 2000. 343(4): p. 230-238.
16. Burridge, P.W., A.M.J. Shapiro, E.A. Ryan, and J.R.T. Lakey, *Future trends in clinical islet transplantation.* Transplantation Proceedings, 2002. 34: p. 3347-3348.

17. Ryan, E.A., B.W. Paty, P.A. Senior, D. Bigam, E. Alfadhli, N.M. Kneteman, J.R.T. Lakey, and A.M.J. Shapiro, *Five-year follow-up after clinical islet transplantation.* Diabetes, 2005. 54: p. 2060-2069.
18. Weir, G.C. and S. Bonner-Weir, *Scientific and political impediments to successful islet transplantation.* Diabetes, 1997. 46(8): p. 1247-1256.
19. De Vos, P., J.F.M. Van Straaten, A.G. Nieuwenhuizen, M. de Groot, R.J. Ploeg, B.J. De Haan, and R. Van Schilfgaarde, *Why do microencapsulated islet grafts fail in the absence of fibrotic overgrowth?* Diabetes, 1999. 48(7): p. 1381-1388.
20. Rokstad, A.M., B. Kulseng, B.L. Strand, G. Skjark-Braek, and T. Espevik, *Transplantation of alginate microcapsules with proliferating cells in mice: Capsular overgrowth and survival of encapsulated cells of mice and human origin.* Annals of the New York Academy of Sciences, 2001. 944: p. 216-225.
21. Colton, C.K. and E.S. Avgoustiniatos, *Bioengineering in development of the hybrid artificial pancreas.* Transactions of ASME, 1991. 113: p. 152-170.
22. Colton, C.K., *Implantable biohybrid artificial organs.* Cell Transplantation, 1995. 4(4): p. 415-436.
23. Avgoustiniatos, E.S. and C.K. Colton, *Effect of external oxygen mass transfer resistance on viability of immunoisolated tissue.* Annals of the New York Academy of Sciences, 1997. 831: p. 145-167.
24. Trivedi, N., M. Keegan, G.M. Steil, J. Hollister-Lock, W.M. Hasenkamp, C.K. Colton, S. Bonner-Weir, and G.C. Weir, *Islets in alginate macrobeads reverse diabetes despite minimal acute insulin secretory responses.* Transplantation, 2001. 71(2): p. 203-211.
25. Renken, A. and D. Hunkeler, *Microencapsulation: A review of polymers and technologies with a focus on bioartificial organs.* Polimery, 1998. 43(9): p. 530-539.
26. Orive, G., R.M. Hernandez, A.R. Gascon, R. Calafiore, T.M.S. Chang, P. De Vos, G. Hortelano, D. Hunkeler, I. Lacik, A.M.J. Shapiro, and J.L. Pedraz, *Cell encapsulation: Promise and progress.* Nature Medicine, 2003. 9(1): p. 104-107.
27. Sakai, S., T. Ono, H. Ijima, and K. Kawakami, *Control of molecular weight cut-off for immunoisolation by multilayering glycol chitosan-alginate polyion complex on alginate-based microcapsules.* Journal of Microencapsulation, 2000. 17(6): p. 691-699.
28. Sakai, S., T. Ono, H. Ijima, and K. Kawakami, *Newly developed aminopropyl-silicate immunoisolation membrane for a microcapsule-shaped bioartificial pancreas.* Annals of the New York Academy of Sciences, 2001. 944: p. 277-283.
29. Bartkowiak, A., *Optimal conditions of transplantable binary polyelectrolyte microcapsules.* Annals of the New York Academy of Sciences, 2001. 944: p. 120-134.
30. Lim, F. and A.M. Sun, *Microencapsulated islets as bioartificial endocrine pancreas.* Science, 1980. 210(21): p. 908-910.
31. Strand, B.L., Y.A. Morch, T. Espevik, and G. Skjak-Braek, *Visualization of alginate-poly-l-lysine- alginate microcapsules by confocal laser scanning microscopy.* Biotechnology and Bioengineering, 2003. 82(4): p. 386-394.
32. Van Schilfgaarde, R. and P. De Vos, *Factors influencing the properties and performance of microcapsules for immunoprotection of pancreatic islets.* Journal of Molecular Medicine, 1999. 77: p. 199-205.
33. De Vos, P., B.J. De Haan, G.H.J. Wolters, J.H. Strubbe, and R. Van Schilfgaarde, *Improved biocompatibility but limited graft survival after purification of alginate for microencapsulation of pancreatic islets.* Diabetologia, 1997. 40: p. 262-270.

34. Wandrey, C. and D. Sainz Vidal, *Purification of polymeric biomaterials.* Annals of the New York Academy of Sciences, 2001. 944: p. 187-197.
35. Zimmermann, U., F. Thurmer, A. Jork, M. Weber, S. Mimietz, M. Hillgartner, F. Brunnenmeier, H. Zimmermann, I. Westphal, G. Fuhr, U. Noth, A. Hasse, A. Steinert, and C. Hendrich, *A novel class of amitogenic alginate microcapsules for long-term immunoisolated transplantation.* Annals of the New York Academy of Sciences, 2001. 944: p. 199-215.
36. De Vos, P., C.G. Hoogmoed, and H.J. Busscher, *Chemistry and biocompatibility of alginate-pll capsules for immunoprotection of mammalian cells.* Journal of Biomedical Material Research, 2002. 60: p. 252-259.
37. De Vos, P., C.G. van Hoogmoed, J. van Zanten, S. Netter, J.H. Strubbe, and H.J. Busscher, *Long-term biocompatibility, chemistry, and function of microencapsulated pancreatic islets.* Biomaterials, 2003. 24: p. 305-312.
38. Duvivier-Kali, V.F., A. Omer, R.J. Parent, J.J. O'Neil, and G.C. Weir, *Complete protection of islets against allorejection and autoimmunity by a simple barium-alginate membrane.* Diabetes, 2001. 50: p. 1698-1705.
39. Omer, A., M. Keegan, E. Czismadia, P. De Vos, N. Van Rooijen, S. Bonner-Weir, and G.C. Weir, *Macrophage depletion improves survival of porcine neonatal pancreatic cell clusters contained in alginate macrocapsules transplanted into rats.* Xenotransplantation, 2003. 10: p. 240-251.
40. Omer, A., V.F. Duvivier-Kali, N. Trivedi, K. Wilmot, S. Bonner-Weir, and G.C. Weir, *Survival and maturation of microencapsulated porcine neonatal pancreatic cell clusters transplanted into immunocompetent diabetic mice.* Diabetes, 2003. 52: p. 69-75.
41. Carlsson, P.-O., P. Liss, A. Andersson, and L. Jansson, *Measurements of oxygen tension in native and transplanted rat pancreatic islets.* Diabetes, 1998. 47(7): p. 1027-1032.
42. Schrezenmeir, J., L. Gero, C. Laue, J. Kirchgessner, A. Muller, A. Huls, R. Passmann, H.J. Hahn, L. Kunz, W. Mueller-Klieser, and J.J. Altman, *The role of oxygen supply in islet transplantation.* Transplantation Proceedings, 1992. 24(6): p. 2925-2929.
43. Dionne, K.E., C.K. Colton, and M.L. Yarmush, *Effect of oxygen on isolated pancreatic tissue.* Transactions of the American Society of Artificial and Internal Organs, 1989. 35(3): p. 739-741.
44. Dionne, K.E., C.K. Colton, and M.L. Yarmush, *Effect of hypoxia on insulin secretion by isolated rat and canine islets of langerhans.* Diabetes, 1993. 42: p. 12-21.
45. Ohta, M., D. Nelson, J. Nelson, M.D. Meglasson, and M. Erecinska, *Oxygen and temperature dependence of stimulated insulin secretion in isolated rat islets of langerhans.* Journal of Biological Chemistry, 1990. 265(29): p. 17525-17532.
46. Schrezenmeir, J., L. Gero, M. Solhdju, J. Kirchgessner, C. Laue, J. Beyer, H. Stier, and W. Muller-Klieser, *Relation between secretory function and oxygen supply in isolated islet organs.* Transplantation Proceedings, 1994. 26(2): p. 809-813.
47. De Groot, M., T.A. Schuurs, P.P.M. Keizer, S. Fekken, H.G.D. Leuvenink, and R. Van Schilfgaarde, *Response of encapsulated rat pancreatic islets to hypoxia.* Cell Transplantation, 2003. 12: p. 867-875.
48. Brauker, J., V. Carr-Brendel, L. Martinson, J. Crudele, W. Johnston, and R.C. Johnson, *Neovascularization of synthetic membranes directed by membrane microarchitecture.* J. Biomed. Mat. Res., 1995. 29(12): p. 1517-1524.

49. Rafael, E., G.S. Wu, K. Hultenby, A. Tibell, and A. Wernerson, *Improved survival of macroencapsulated islets of langerhans by preimplantation of the immunoisolating device: A morphometric study.* Cell Transplantation, 2003. 12: p. 407-412.
50. Bloch, K., E. Papismedov, K. Yavriyants, M. Vorobeychik, S. Beer, and P. Vardi, *Photosynthetic oxygen generator for bioartificial pancreas.* Tissue Engineering, 2006. 12(2): p. 337-344.
51. Wu, H., E.S. Avgoustiniatos, L. Swette, S. Bonner-Weir, G.C. Weir, and C.K. Colton, *In situ electrochemical oxygen generation with an immunoisolated device.* Annals of the New York Academy of Sciences, 1999. 875: p. 105-125.
52. Leung, A., Y. Ramaswamy, P. Munro, G. Lawrie, L. Nielsen, and M. Trau, *Emulsion strategies in the microencapsulation of cells: Pathways to thin coherent membranes.* Biotechnology and Bioengineering, 2005. 92(1): p. 45-53.
53. Zekorn, T., U. Siebers, A. Horcher, R. Schnettler, U. Zimmermann, R.G. Bretzel, and K. Federlin, *Alginate coating of islets of langerhans: In vitro studies on a new method for microencapsulation for immuno-isolated transplantation.* Acta Diabetologia, 1992. 29: p. 41-45.
54. King, A.J.F., J.R. Fernandes, J. Hollister-Lock, C.E. Nienaber, S. Bonner-Weir, and G.C. Weir, *Normal relationship of beta- and non-beta-cells not needed for successful islet transplantation.* Diabetes, 2007. 56: p. 2312-2318.
55. Dionne, K.E., *Effect of hypoxia on insulin secretion and viability of pancreatic islet tissue*, in *Chemical Engineering*. 1989, M.I.T.: Cambridge, MA. p. 461.
56. MacGregor, R.R., S.J. Williams, P.Y. Tong, K. Kover, W.V. Moore, and L. Stehno-Bittel, *Small rat islets are superior to large islets in in vitro function and in transplantation outcomes.* American Journal of Physiology-Endocrinology and Metabolism, 2006. 290(5): p. E771-E779.
57. Lehmann, R., R.A. Zuellig, P. Kugelmeier, P.B. Baenninger, W. Moritz, A. Perren, P.A. Clavien, M. Weber, and G.A. Spinas, *Superiority of small islets in human islet transplantation.* Diabetes, 2007. 56(3): p. 594-603.
58. McMillan, J.D. and D.I.C. Wang, *Mechanisms of oxygen transfer enhancement during submerged cultivation in perfluorochemical-in-water dispersions.* Annals of the New York Academy of Sciences, 1990. 589: p. 283-300.
59. Poncelet, D., R. Leung, L. Centomo, and R.J. Neufeld, *Microencapsulation of silicone oils within polyacrylamide-polyethylene membranes as oxygen carriers for bioreactor oxygenation.* Journal Of Chemical Technology and Biotechnology, 1993. 57: p. 253-263.
60. Zekorn, T., U. Siebers, R.G. Bretzel, S. Heller, U. Meder, H. Ruttkay, U. Zimmermann, and K. Federlin, *Impact of the perfluorochemical fc43 on function of isolated islets.* Hormone Metabolism Research, 1991. 23: p. 302-303.
61. Matsumoto, S. and Y. Kuroda, *Perfluorocarbon for organ preservation before transplantation.* Transplantation, 2002. 74(12): p. 1804-1809.
62. Bergert, H., K.-P. Knoch, R. Meisterfeld, M. Jager, J. Ouwendijk, S. Kersting, H.D. Saeger, and M. Solimena, *Effect of oxygenated perfluorocarbons on isolated rat pancreatic islets in culture.* Cell Transplantation, 2005. 14: p. 441-448.
63. Chae, S.Y., Y.Y. Kim, S.W. Kim, and Y.H. Bae, *Prolonged glucose normalization of streptozotocin-induced diabetic mice by transplantation of rat islets co-encapsulated with crosslinked hemoglobin.* Transplantation, 2004. 78(3): p. 392-397.

64. Colton, C.K., K.K. Papas, A. Pisania, M.J. Rappel, D.E. Powers, J.J. O'Neil, A. Omer, G.C. Weir, and S. Bonner-Weir, *Characterization of islet preparations*, in *Cellular transplantation: From laboratory to clinic*, C. Halberstadt and D.F. Emerich, Editors. 2007, Elseveir, Inc.: New York.
65. Pisania, A., *Development of quantitative methods of quality assessment of islets of langerhans*, in *Chemical Engineering*. 2007, M. I. T.: Cambridge, MA. p. 257.
66. Papas, K.K., A. Pisania, H. Wu, G.C. Weir, and C.K. Colton, *A stirred microchamber for oxygen consumption rater measurements with pancreatic islets.* Biotechnology and Bioengineering, 2007. 98(5): p. 1071-1082.
67. Khattak, S.F., K.-s. Chin, S.R. Bhatia, and S.C. Roberts, *Enhancing oxygen tension and cellular function in alginate cell encapsulation devices through the use of perfluorocarbons.* Biotechnology and Bioengineering, 2007. 96(1): p. 156-166.
68. Weber, L.M., J. He, B. Bradley, K. Haskins, and K.S. Anseth, *Peg-based hydrogels as an in vitro encapsulation platform for testing controlled beta-cell microenvironments.* Acta Biomaterialia, 2006. 2: p. 1-8.
69. Papas, K.K., R. Long, A. Sambanis, and I. Constantinidis, *Development of a bioartificial pancreas: I. Long-term propagation and basal and induced secretion from entrapped betatc3 cell cultures.* Biotechnology and Bioengineering, 1999. 66(4): p. 219-230.
70. Gotoh, M., T. Maki, T. Kiyoizumi, S. Satomi, and A.P. Monaco, *An improved method for isolation of mouse pancreatic islets.* Transplantation, 1985. 40: p. 437-438.
71. Schweighardt, F.K. and C.R. Kayhart, *Concentrated stable fluorochemical aqueous emulsions containing triglycerides*. 1990, Air Products and Chemicals, Inc.: United States.
72. Halle, J.-P., D. Landry, A. Fournier, M. Beaudry, and F.A. Leblond, *Method for the quantification of alginate in microcapsules.* Cell Transplantation, 1993. 2: p. 429-436.
73. Morch, Y.A., I. Donati, B.L. Strand, and G. Skjak-Braek, *Effect of ca2+, ba2+ and sr2+ on alginate microbeads.* Biomacromolecules, 2006. 7: p. 1471-1480.
74. Avgoustiniatos, E.S., K.E. Dionne, D.F. Wilson, M.L. Yarmush, and C.K. Colton, *Measurements of effective diffusion coefficient of oxygen in pancreatic islets.* Industrial and Engineering Chemistry Resesarch, 2007. 46(19): p. 6157-6163.
75. Maxwell, J.C., *A treatise on electricity and magnetism*. Vol. 1. 1881, London, UK: Clarendon Press. 440.
76. Tham, M.K., R.D. Walker, and J.H. Modell, *Diffusion coefficients of o_2, n_2 and co_2 in fluorinated ethers.* J Chem Eng Data, 1973. 18: p. 411-412.
77. Bailey, A.E., *Bailey's industrial oil and fat products*. 4 ed, ed. D. Swern. Vol. 1. 1979, New York: Wiley.
78. Fillion, B. and B.I. Morsi, *Gas-liquid mass-transfer and hydrodynamic parameters in a soybean oil hydrogenation process under industrial conditions.* Ind. Eng. Chem. Res., 2000. 39: p. 2157-2168.
79. Omer, A., V. Duvivier-Kali, J. Fernandes, V. Tchipashvili, C.K. Colton, and G.C. Weir, *Long-term normoglycemia in rats receiving transplants with encapsulated islets.* Transplantation, 2005. 79(1): p. 52-58.
80. Brauker, J., G.H. Frost, V. Dwarki, T. Nijjar, R. Chin, V. Carr-Brendel, C. Jasunas, D. Hodgett, W. Stone, L.K. Cohen, and R.C. Johnson, *Sustained expression of high levels of human factor ix from human cells implanted within an immunoisolation device into athymic rodents.* Human Gene Therapy, 1998. 9: p. 879-888.

81. Schwenter, F., B.L. Schneider, W.F. Pralong, N. Deglon, and P. Aebischer, *Survival of encapsulated human primary fibroblasts and erythropoietin expression under xenogeneic conditions.* Human Gene Therapy, 2004. 15: p. 669-689.
82. Hasse, C., G. Klock, A. Schlosser, U. Zimmermann, and M. Rothmund, *Parathyroid allotransplantation without immunosuppression.* The Lancet, 1997. 350: p. 1296-1297.
83. Buchser, E., M. Goddard, B. Heyd, J.M. Joseph, J. Favre, N. de Tribolet, M. Lysaght, and P. Aebischer, *Immunoisolated xenogeneic chromaffin cell therapy for chronic pain: Initial clinical experience.* Anesthesiology, 1996. 85(5): p. 1005-1012.
84. Kishima, H., T. Poyot, J. Bloch, J. Dauguet, F. Conde, F. Dolle, F. Hinnen, W. Pralong, S. Palfi, N. Deglon, P. Aebischer, and P. Hantraye, *Encapsulated gdnf-producing c2c12 cells for parkinson's disease: A pre-clinical study in chronic mptp-treated baboons.* Neurobiology of Disease, 2004. 16: p. 428-439.
85. Bloch, J., A.C. Bachoud-Levi, N. Deglon, J.P. Lefaucheur, L. Winkel, S. Palfi, J.P. Nguyen, C. Bourdet, V. Gaura, P. Remy, P. Brugieres, M.-F. Boisse, S. Baudic, P. Cesaro, P. Hantraye, P. Aebischer, and M. Peschanski, *Neuroprotective gene therapy for huntington's disease, using polymer-encapsulated cells engineered to secrete ciliary neurotrophic factor: Results of a phase i study.* Human Gene Therapy, 2004. 15: p. 968-975.
86. Aebischer, P., M. Schluep, N. Deglon, J.-M. Joseph, L. Hirt, B. Heyd, M. Goddard, J.P. Hammang, A.D. Zurn, A.C. Kato, F. Regli, and E.E. Baetge, *Intrathecal delivery of cntf using encapsulated genetically modified xenogeneic cells in amyotrophic lateral sclerosis patients.* Nature Medicine, 1996. 2(6): p. 696-699.
87. Avgoustiniatos, E.S. and C.K. Colton, *Design considerations in immunoisolation*, in *Principles of tissue engineering*, R. Lanza, R. Langer, and W. Chick, Editors. 1997, R.G. Landes Co.: Austin. p. 333-346.
88. Gianello, P. and D. Dufrane, *Encapsulation of pig islets by alginate matrix to correct streptozotocin-induced diabetes in primates without immunosuppression.* Xenotransplantation, 2007. 14(5): p. 441.
89. Nyqvist, D., M. Kohler, H. Wahlstedt, and P. Berggren, *Donor islet endothelial cells participate in formation of functional vessels within pancreatic islet grafts.* Diabetes, 2005. 54(8): p. 2287-2293.
90. Parr, E.L., K.M. Bowen, and K.J. Lafferty, *Cellular-changes in cultured mouse thyroid-glands and islets of langerhans.* Transplantation, 1980. 30(2): p. 135-141.
91. Mendola, J.F., C. Goity, J. Fernandezalvarez, A. Saenz, G. Benarroch, L. Fernandezcruz, and R. Gomis, *Immunocytochemical study of pancreatic-islet revascularization in islet isograft - effect of hyperflycemia of the recipient and of in vitro culture of islets.* Transplantation, 1994. 57(5): p. 725-730.
92. Tannock, I.F., *Oxygen diffusion and the distribution of cellular radiosensitivity in tumors.* Br. J. Radiol., 1972. 45: p. 515-524.
93. Avgoustiniatos, E.S., *Oxygen diffusion limitations in pancreatic islet culture and immunoisolation*, in *Chemical Engineering*. 2001, M.I.T.: Cambridge, MA. p. 647.
94. Zimmermann, U., U. Noth, P. Grohn, A. Jork, K. Ulrichs, J. Lutz, and A. Haase, *Non-invasive evaluation of the location, the functional integrity, and the oxygen supply of implants: ^{19}f nuclear magnetic resonance imaging of perfluorocarbon-loaded ba^{2+}-alginate beads.* Artificial Cells Blood Substitutes Immobilization Biotechnology, 2000. 28(2): p. 129-146.

95. Duvivier-Kali, V.F., A. Omer, M.D. Lopez-Avalos, J.J. O'Neil, and G.C. Weir, *Survival of microencapsulated adult pig islets in mice in spite of an antibody response.* American Journal of Transplantation, 2004. 4: p. 1991-2000.
96. Nir, T., D.A. Melton, and Y. Dor, *Recovery from diabetes in mice by beta cell regeneration.* J Clin Invest, 2007. 117(9): p. 2553-61.
97. Bonner-Weir, S., M. Taneja, G.C. Weir, K. Tatarkiewicz, K.-H. Song, A. Sharma, and J.J. O'Neil, *In vitro cultivation of human islets from expanded ductal tissue.* Proceedings of the National Academy of Sciences, 2000. 97(14): p. 7999-8004.
98. Ramiya, V.K., M. Maraist, K.E. Arfors, D.A. Schatz, A.B. Peck, and J.G. Cornelius, *Reversal of insulin-dependent diabetes using islets generated in vitro form pancreatic stem cells.* Nature Medicine, 2000. 6(3): p. 278-282.
99. Dor, Y., J. Brown, O.I. Martinez, and D.A. Melton, *Adult pancreatic beta-cells are formed by self-duplication rather than stem-cell differentiation.* Nature, 2004. 429(6987): p. 41-6.
100. Weir, G.C., *Can we make surrogate beta-cells better than the original?* Semin Cell Dev Biol, 2004. 15(3): p. 347-57.
101. Bonner-Weir, S. and G.C. Weir, *New sources of pancreatic beta-cells.* Nature Biotechnology, 2005. 23(7): p. 857-61.
102. Narushima, M., N. Kobayashi, T. Okitsu, Y. Tanaka, S.-A. Li, Y. Chen, A. Miki, K. Tanaka, S. Nakaji, K. Takei, A.S. Guitierrez, J.D. Rivas-Carrillo, N. Navarro-Alvarex, H.-S. Jun, K.A. Westerman, H. Noguchi, J.R.T. Lakey, P. Leboulch, N. Tanaka, and J.-W. Yoon, *A human beta-cell line for transplantation therapy to control type 1 diabetes.* Nature Biotechnology, 2005. 23(10): p. 1274-82.
103. Kroon, E., L.A. Martinson, K. Kadoya, A.G. Bang, O.G. Kelly, S. Eliazer, H. Young, M. Richardson, N.G. Smart, J. Cunningham, A.D. Agulnick, K.A. D'Amour, M.K. Carpenter, and E.E. Baetge, *Pancreatic endoderm derived from human embryonic stem cells generates glucose-responsive insulin-secreting cells in vivo.* Nature Biotechnology, 2008. 26(4): p. 443-52.
104. Lifson, N., C.V. Lassa, and P.K. Dixit, *Relation between blood flow and morphology in islet organ of rat pancreas.* Am J Physiol, 1985. 249(1 Pt 1): p. E43-8.
105. Ritz-Laser, B., J. Oberholzer, C. Toso, M.C. Brulhart, K. Zakrzewska, F. Ris, P. Bucher, P. Morel, and J. Philippe, *Molecular detection of circulating beta-cells after islet transplantation.* Diabetes, 2002. 51(3): p. 557-61.
106. Davalli, A.M., Y. Ogawa, C. Ricordi, D.W. Scharp, S. Bonner-Weir, and G.C. Weir, *A selective decrease in the beta cell mass of human islets transplanted into diabetic nude mice.* Transplantation, 1995. 59(6): p. 817-20.
107. Bertuzzi, F. and C. Ricordi, *Prediction of clinical outcome in islet allotransplantation.* Diabetes Care, 2007. 30(2): p. 410-7.
108. Weir, G.C., P.A. Halban, P. Meda, C.B. Wollheim, L. Ocri, and A.E. Renold, *Dispersed adult rat pancreatic islet cells in culture: A, b, and d cell function.* Metabolism, 1984. 33(447-453).
109. Powers, D.E., *Effects of oxygen on embryonic stem cell proliferation, energetics, and differentiation into cardiomyocytes*, in *Chemical Engineering*. 2007, M.I.T.: Cambridge, MA. p. 114.
110. Rappel, M.J., *Maintaining islet quality during culture*, in *Chemical Engineering*. 2007, M.I.T.: Cambridge, MA. p. 274.

111. Sandler, S., A. Andersson, D.L. Eizirik, C. Hellerstron, T. Espevik, B. Kulseng, B. Thu, D.G. Pipeleers, and G. Skjak-Braek, *Assessment of insulin secretion in vitro from microencapsulated fetal porcine islet-like cell clusters and rat, mouse, and human pancreatic islets.* Transplantation, 1997. 63(12): p. 1712-1718.
112. Shapiro, A.M., J.R. Lakey, E.A. Ryan, G.S. Korbutt, E. Toth, G.L. Warnock, N.M. Kneteman, and R.V. Rajotte, *Islet transplantation in seven patients with type 1 diabetes mellitus using a glucocorticoid-free immunosuppressive regimen*, in *N Engl J Med*. 2000. p. 230-8.
113. Ryan, E.A., B.W. Paty, P.A. Senior, D. Bigam, E. Alfadhli, N.M. Kneteman, J.R. Lakey, and A.M. Shapiro, *Five-year follow-up after clinical islet transplantation*, in *Diabetes*. 2005. p. 2060-9.
114. Ricordi, C. and H. Edlund, *Toward a renewable source of pancreatic beta-cells*, in *Nat Biotechnol*. 2008. p. 397-8.
115. Bonner-Weir, S. and G.C. Weir, *New sources of pancreatic beta-cells*, in *Nat Biotechnol*. 2005. p. 857-61.
116. Colton, C.K. and R.F. Drake, *Effect of boundary conditions on oxygen transport to blood flowing in a tube.* Chemical Engineering Progress Symposium Series, 1971. 67(114): p. 88-95.
117. Shimabukuro, M., Y.-T. Zhou, M. Levi, and R.H. Unger, *Fatty acid-induced beta cell apoptosis: A link between obesity and diabetes.* Proceedings of the National Academy of Sciences, 1998. 95: p. 2498-2502.
118. Kharroubi, I., L. Ladriere, A.K. Cardozo, Z. Dogusan, M. Cnop, and D.L. Eizirik, *Free fatty acids and cytokines induce pancreatic beta-cell apoptosis by different mechanisms: Role of nuclear factor-kappab and endoplasmic reticulum stress.* Endocrinology, 2004. 145(11): p. 5087-5096.
119. Oprescu, A.I., G. Bikopoulos, A. Naassan, E.M. Allister, C. Tang, E. Park, H. Uchino, G.F. Lewis, I.G. Fantus, M. Rozakis-Adcock, M.B. Wheeler, and A. Giacca, *Free fatty-acid-induced reduction in glucose-stimulated insulin secretion - evidence for a role of oxidative stress in vitro and in vivo.* Diabetes, 2007. 56: p. 2927-2937.
120. Nunes, E., F. Peixoto, T. Louro, C.M. Sena, M.S. Santos, P. Matafome, P.I. Moreira, and R. Seica, *Soybean oil treatment impairs glucose-stimulated insulin secretion and changes fatty acid composition of normal and diabetic islets.* Acta Diabetologia, 2007. 44: p. 121-130.
121. Wrede, C.E., R. Buettner, H. Wobser, I. Ottinger, and L.C. Bollheimer, *Systemic analysis of the insulinotropic and glucagonotropic potency of saturated and monounsaturated fatty acid mixtures in rat pancreatic islets.* Hormone Metabolism Research, 2007. 39: p. 482-488.
122. Sweet, I.R., M. Gilbert, R. Jensen, O. Sabek, D.W. Fraga, A.O. Gaber, and J. Reems, *Glucose stimulation of cytochrome c reduction and oxygen consumption as assessment of human islet quality.* Transplantation, 2005. 80(8): p. 1003-1011.
123. Lewis, A.S. and C.K. Colton, *Engineering challenges in immunobarrier device development*, in *Principles of tissue engineering*, R.P. Lanza, R. Langer, and J. Vacanti, Editors. 2007, Elsevier. p. 405-418.